Sustainability in Organic Synthesis -

Bidentate Lewis Acid Inverse Electron-Demand Diels-Alder Reactions and the Synthesis of Organic Redox Flow Battery Electrolyte Materials

Inauguraldissertation zur Erlangung des Doktorgrades der Naturwissenschaftlichen Fachbereiche im Fachgebiet Organische Chemie der Justus-Liebig-Universität Gießen

vorgelegt von

Sebastian Schmalisch

aus Berlin

Betreuer: Prof. Dr. Hermann A. Wegner

Gießen 2021

Table of Content

Versicherung nach §17 der Promotionsordnung

Ich erkläre: Ich habe die vorgelegte Dissertation selbstständig und ohne unerlaubte fremde Hilfe und nur mit den Hilfen angefertigt, die ich in der Dissertation angegeben habe. Alle Textstellen, die wörtlich oder sinngemäß aus veröffentlichten Schriften entnommen sind, und alle Angaben, die auf mündlichen Auskünften beruhen, sind als solche kenntlich gemacht. Ich stimme einer evtl. Überprüfung meiner Dissertation durch eine Antiplagiat-Software zu. Bei den von mir durchgeführten und in der Dissertation erwähnten Untersuchungen habe ich die Grundsätze guter wissenschaftlicher Praxis, wie sie in der „Satzung der Justus-Liebig-Universität Gießen zur Sicherung guter wissenschaftlicher Praxis" niedergelegt sind, eingehalten.

Sebastian Schmalisch   Ort, Datum

Dekan: Prof. Dr. Thomas Wilke

Erstgutachter: Prof. Dr. Hermann A. Wegner

Zweitgutachter: Prof. Dr. Richard Göttlich

Abstract

Sustainable development in organic chemistry is driven by limited fossil raw materials, waste production and environmental pollution. The waste issue can be solved by catalysed one-step reactions, which are more sustainable than waste-producing multistep reactions. Since 2011, the Wegner group develops such reactions: the bidentate boron Lewis acid catalysed inverse electron-demand Diels-Alder (IEDDA) reaction of 1,2-diazines. In this thesis, the bidentate boron Lewis acid catalysed IEDDA reaction of phthalazines with substituted 2,3-dihydrofurans and 5-thioalkyl-2,3-dihydrofurans was investigated in an explorative study. The substitution pattern determined the subsequent rearrangement or elimination reaction to dihydronaphthalines or naphthofurans.
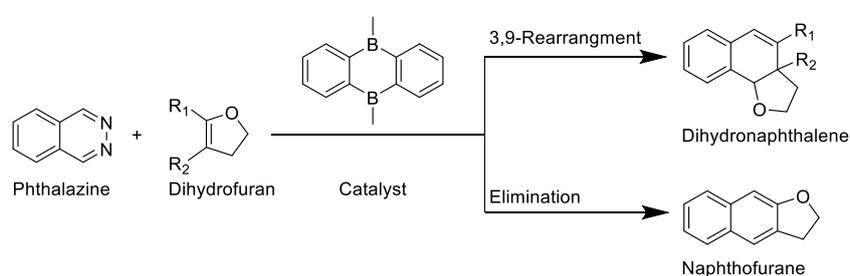
In the second part of this thesis, the catalysed IEDDA reaction was used to synthesize organic redox material for organic redox flow batteries, which could store the generated energy of renewable power plants, and thus, circumvent carbon dioxide production from limited carbon feedstocks. To bypass these fossil raw materials as starting material, wood-derived vanillin was investigated as renewable and, thus, sustainable precursor for the synthesis of redox materials. The obtained vanillin-derived material and the diazaanthraquinones and 5,8-dihydroxyphthalazines, synthesized in the IEDDA reaction of 1,2,4,5-tetrazine and naphthoquinone/benzoquinone, were analysed via cyclic voltammetry regarding their electrochemical potentials and their stability. The vanillin-derived redox material showed the feasibility of synthesizing redox material from renewable sources. The diazaanthraquinones and 5,8-dihydroxyphthalazines were demonstrated as potential battery material. The 5,8-dihydroxyphthalazines surpassed the diazaanthraquinones with regard to their higher potentials and increased stability.
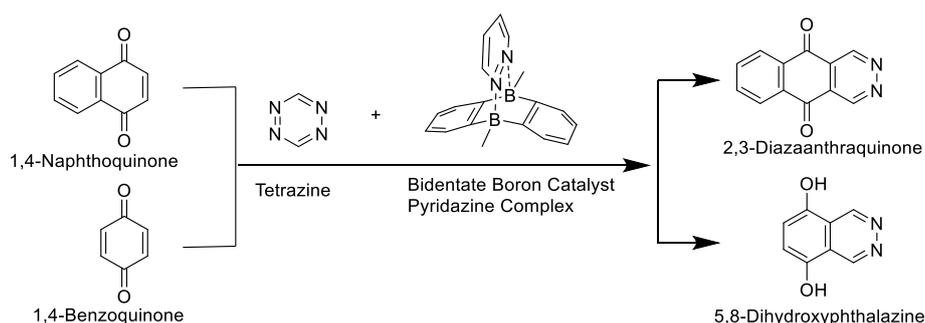
Zusammenfassung

Die nachhaltige Entwicklung in der organischen Chemie wird angetrieben von begrenzten fossilen Rohstoffen, der Abfallproduktion und Umweltverschmutzung. Das Abfallproblem kann durch katalysierte und einstufige Reaktionen gelöst werden, die nachhaltiger sind als Abfall produzierende Mehrschrittreaktionen. Seit 2011 entwickelt die Arbeitsgruppe Wegner solche Reaktionen: Die bidentate Bor-Lewis-Säure katalysierte Diels-Alder Reaktion mit inversen Elektronenbedarf (engl. Abk.: IEDDA) von 1,2-Diazinen. Diese Arbeit untersucht explorativ bidentate Bor-Lewis-Säure katalysierte IEDDA Reaktionen von substituierten 2,3-Dihydrofuranen und 5-thioalkyldihydrofuranen. Das Subsitutionsmuster bestimmte die darauffolgende Umlagerungs- oder Eliminierungsreaktion zu Dihydronaphthalinen oder Naphthofuranen.
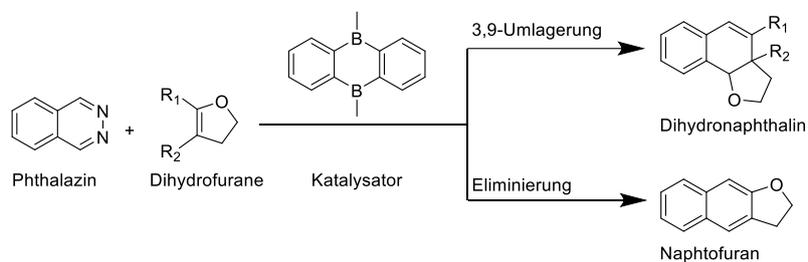
Im zweiten Teil dieser Arbeit wurden katalysierte IEDDA Reaktionen zur Synthese von organischen Redoxmaterial für Redox-Flow-Batterien verwendet, welche die Energie aus erneuerbarer Energiequellen speichern können und somit die Kohlenstoffdioxidproduktion aus fossilen Quellen umgeht. Um fossile Rohstoffe als Ausgangsmaterial zu vermeiden, wurde mit aus Holz hergelltem Vanillin ein erneuerbares, und somit nachhaltiges Edukt für die Synthese von Redoxmaterial untersucht. Die Vanillin-basierten Redoxmaterialien und die aus der IEDDA Reaktion von 1,2,4,5-Tetrazin und Naphthochinonen bzw. Benzochinonen synthetisierten Diazaanthrachinone und 5,8-Dihydroxyphthalazine wurden hinsichtlich ihrer elektrochemischen Potentiale und ihrer Stabilität analysiert. Die Vanillin-basierten Redoxmaterialien demonstrieren die Synthetisierbarkeit von Batteriematerial aus nachwachsenden Rohstoffen. Die Diazaanthrachinone und 5,8-Dihydroxyphthalazine stellten sich als potenzielles Batteriematerial heraus, wobei die 5,8-Dihydroxyphthalazine höherer Potentiale und eine bessere Stabilität aufwiesen.
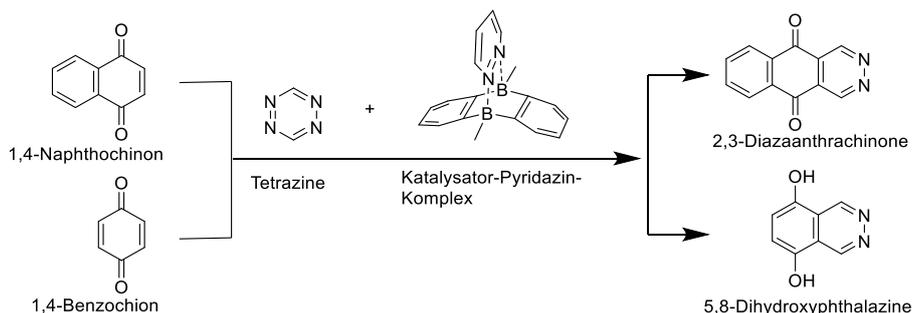
1. Introduction

Organic chemistry must face the challenge of sustainability: The limited availability of fossil carbon feedstocks as main resource of chemical industry, waste production, and environmental pollution forces chemists to change synthesis to reach the sustainable development goals (SDGs) of the United Nations.[1,2] One approach to tackle these aims is the reduction of multistep waste-producing reactions with equimolar reagents and the rise of catalysed one-step reactions. One of these very powerful transformations is the well-studied Diels-Alder reaction, which creates up to four stereocenters in one step.[2] This reaction becomes even more fruitful if it is integrated in a catalysed domino reaction. A catalysed domino Diels-Alder reaction has the advantage of sustainability by saving material, energy, time, and costs compared to stepwise procedures. Such a reaction was developed by Wegner and colleagues[3–9]: An inverse electron-demand Diels-Alder (IEDDA) reaction of 1,2-diazine, catalysed by a bidentate boron Lewis acid, generates a reactive *o*-quinodimethane which underwent subsequent substrate-dependent domino reactions. The results of substituted 2,3-dihydrofurans as dienophiles in these catalysed IEDDA/domino reactions have not been studied entirely yet. Therefore, this thesis set out to examine the catalysed domino Diels-Alder reactions of phthalazines with substituted-2,3-dihydrofurans in an explorative study. The influence of the sterical and electronic properties of the dihydrofurans on the thermodynamics and kinetics of the reaction should be investigated. Beside these developments of a new sustained synthetic methodology, the change from restrictedly available fossil carbon reserves to renewable resources challenges the energy production and the chemical industry. Compared to continuously energy-producing fossil-based powerplants, non-continuous renewable energies, e. g. sun and wind powerplants, require an energy storage system to compensate fluctuations regarding the continuous demand of energy. Such energy storage systems demand a fast change between charging/discharging, a sufficient capacity and lifespan. Redox flow batteries (RFB) provide a fast response to charging/discharging, a scalable capacity, and a long lifetime.[10] Compared to metal-based materials for RFBs, organic redox flow battery (ORFB) materials would reduce the costs, decrease the risk of environmental hazards and bypass geopolitical and socio-economic problems linked to mining, production, and disposing of metals.[10–12] Moreover, even the fossil carbon reserves are finite, and replacement is needed by the chemical industry.[1] Such a sustainable resource is wood that can be industrially disassembled into cellulose, mainly used in paper industry, and lignin. The latter material can be further converted in the sulphite process into vanillin, a potential starting material for the chemical industry, e.g. for polymers or dyes.[13] Therefore, organic redox materials, ideally from renewable resources, are necessary. ORFB material should be synthesized and investigated in cooperation with the research group of Prof. Dr. J. Janek and

Prof. Dr. D. Mollenhauer of the Justus Liebig University, and the CMBlu Energy AG company. This thesis focuses on the synthesis of organic redox material, which should be electrochemically investigated by Jonas D. Hofmann of the Janek group. These investigations of the redox material should be supported by computational studies by the Mollenhauer group. In the first part of the ORFB section of this thesis, vanillin was studied as a starting material for organic redox materials The development of ORFB materials was challenged by the major issues of organic redox materials: sufficient solubility in water, long-term stability and large potential, and thus higher cell voltage, were needed for a competitive and durable energy storage compared to metal-based RFBs. Second, the powerful bidentate boron Lewis acid catalysed IEDDA reaction should be studied to give access to ORFB Material. The successful synthesis of 2,3-diazaanthraquinones by Hong et al.[9] should be extended to 2,3-diazanapthoquinones. Electrochemical properties of both diaza materials should be investigated according to applications as ORFB material.

2. Fundamentals of Diels-Alder Reaction, Lewis Acid Catalysis and Redox Flow Battery: A Review of Literature

2.1 Diels-Alder Reaction

2.1.1 Mechanism and Application

Investigations on cycloadditions started before Diels' and Alder's important contribution in 1928 which later came to be known as Diels-Alder reaction.[14] As early as in 1906 Albrecht[15] isolated a product from the reaction of cyclopentadiene (**1**) and 1,4-benzoquinone (**2**) but he struggled to elucidate the structure (Scheme 1). Later in 1920, Josephson and v. Euler[16] investigated the reaction of isoprene (**5**) and **2** (Scheme 2). They concluded that a cycloaddition occurred due to their assumed hydrogenated anthraquinones **6a**, **6b** products.
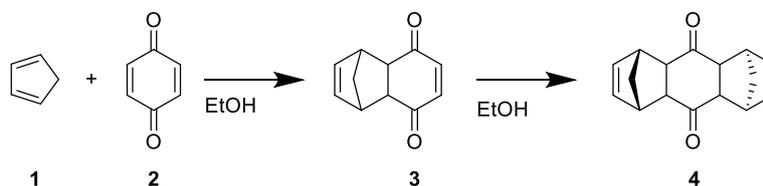
Scheme 1: Albrecht's reaction of cyclopentadiene and benzoquinone and Diels' and Alder's structural elucidation.[15,17]
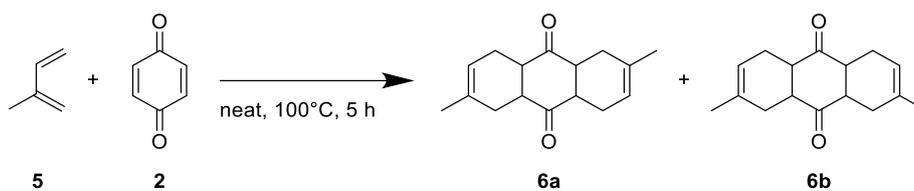
Scheme 2: First cycloaddition of isoprene on benzoquinone reported by v. Euler and Josephson.[16]

Finally, Kurt Alder and Otto Diels elucidated the correct structures of Albrecht's products and generalised the cycloaddition concept.[15,17] Their efforts in the field of cycloadditions were honoured by naming this reaction Diels-Alder (DA) reaction and by awarding them the Nobel Prize in 1950.[18]
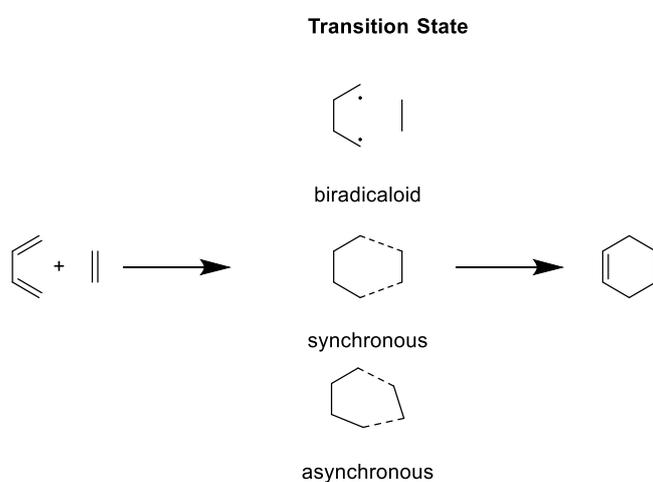
Transition State

Scheme 3: Postulated transition states in Diels-Alder reactions.

After multiple investigations and intense discussions on the mechanism including asynchronous, synchronous, concerted and biradicaloid transition states summarized by Houk et al.[19], a concerted process, already proposed by Wassermann[20] in 1935, was accepted to describe the Diels-Alder reaction (Scheme 3).
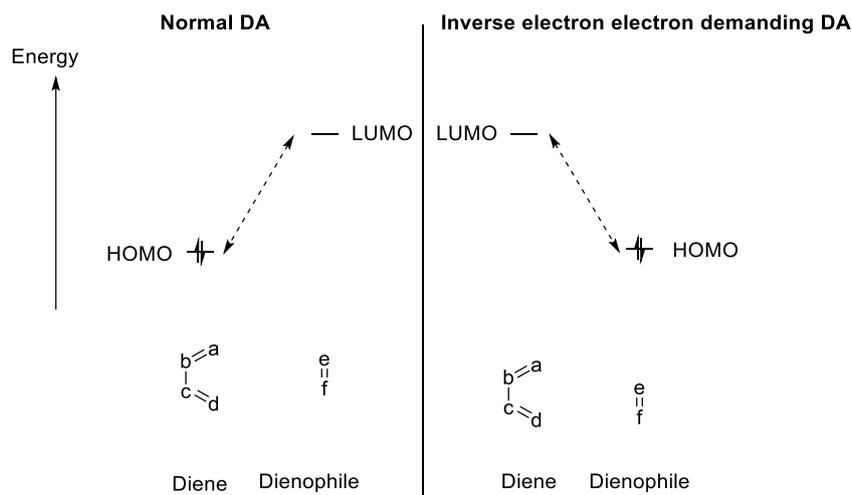
Figure 1: Orbital interactions of Diels-Alder reactions.[21,22]

Substantial contributions for a deeper understanding of the Diels-Alder mechanism reaction were provided by the frontier molecular orbital (FMO) theory by Fukui[21] and by Woodward-Hoffmann (Scheme 4).[22,23] As a consequence of these concepts, the strongest interaction in the DA reaction is between the highest occupied molecular orbital HOMO and lowest occupied molecular orbital LUMO. In a normal DA reaction, the HOMO of the Diene interacts with the LUMO of the dienophile. By contrast, in an inverse electron-demand DA (IEDDA) reaction, the LUMO of the diene interacts with the HOMO of the diene. According to the Woodward-Hoffmann rules, the DA reaction was classified as a symmetry and thermally allowed $[_{\pi}4_s+_{\pi}2_s]$ cycloaddition.
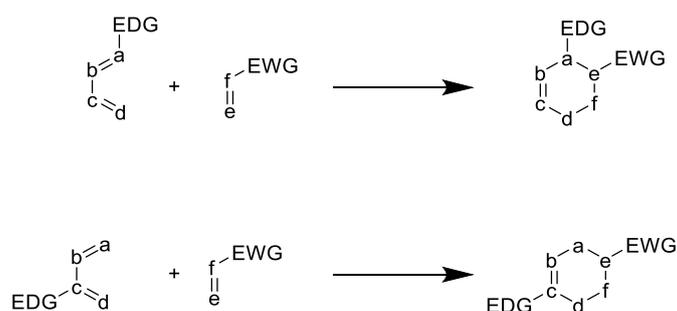
Scheme 4: Regioselectivity in Normal DA reactions.[24,25]

The electronic properties of the HOMO/LUMO orbitals influence the regioselectivity of the DA reaction. A molecular orbital (MO) of the dienophile with a high orbital coefficient interacts with the MO with the highest orbital coefficient of the diene, and the MOs with the lowest orbital coefficients interact with each other, respectively. A normal DA reaction would be enhanced by a Diene with electron-donating groups EDG increasing the HOMO energy level and a dienophile with electron-withdrawing groups EWG decreasing the LUMO energy (Scheme 4, 5).[24–27]

6

Scheme 5: Regioselectivity in IEDDA reactions.[25,26]

s-trans *s-cis* *s-trans* *s-trans*

Scheme 6: Locking reasons for *s-trans* conformation.[28,29]

exo TS   secondary orbital interactions   *endo* TS

Scheme 7: *Exo*- vs. *endo*-transition state.[30,31]
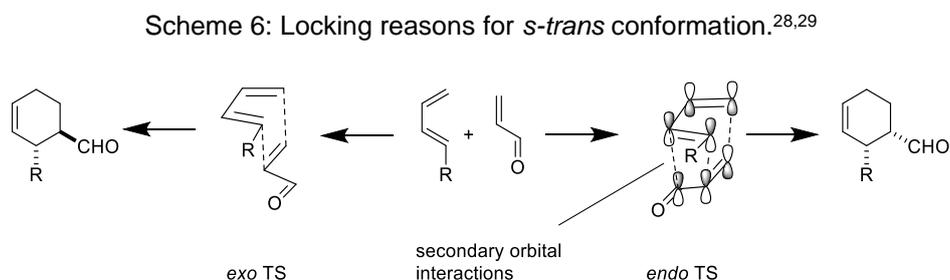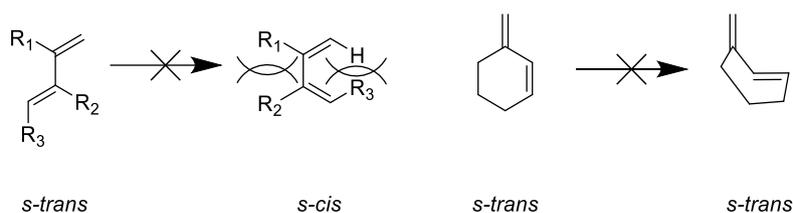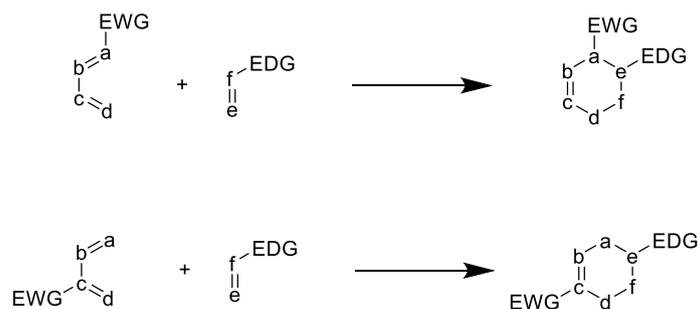
The *s-cis* conformation is preferred for the DA reaction. Steric or ring geometry reasons locking the diene in the s-trans conformation hinder the DA reaction from occurring or decrease the reaction rate (Scheme 6).[28] Alder and Stein[30] investigated the stereoselectivity of the products of the DA reaction. In their results, the *endo*-transition state is preferred to the *exo*-transition state. Although the *exo*-transition state is often the more sterically demanding, the *endo*-transition state was preferred due to secondary orbital interactions (Scheme 7). This so-called '*endo*-rule' was explained by Woodward and Hoffmann and was further confirmed by Wannere et al.[31] with computations. Alder's '*endo*-rule' is limited because sterical hindrance and the solvent have an influence on the *exo*/*endo* selectivity. The *E*/*Z*-stereoinformation of the dienophile and the diene was preserved due to their *syn*-addition (Scheme 8).[32]
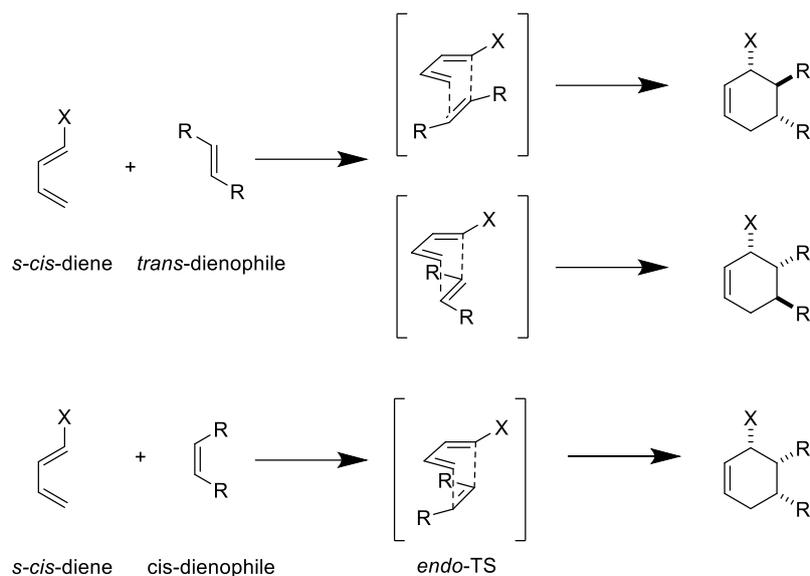
Scheme 8: Preservation of the stereoinformation during cycloaddition.

Woodward, one of the inventors of the Woodward-Hoffman-rules, showed how the total synthesis of natural products benefits from a DA reaction with the first synthesis of cortisone (**10**) in 1952 (Scheme 9). Quinone **7** reacted in a DA reaction with buta-1,3-diene (**8**) yielding naphthoquinone, which was further transformed into **10**.[33]
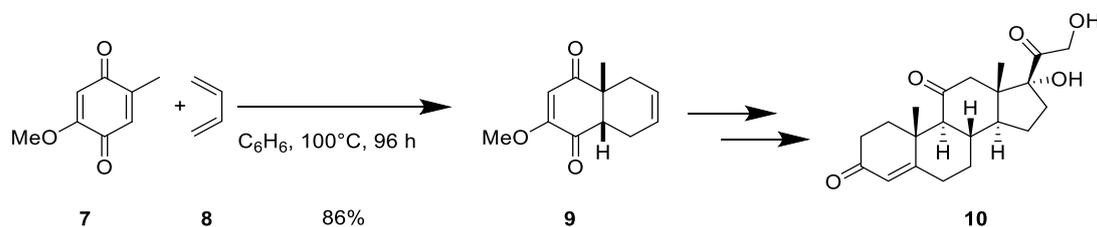
Scheme 9: Woodward's synthesis of cortisone.[33]

These examples showed the applicability of the Diels-Alder reaction. Although this addition reaction is highly atom-efficient because minimal waste is produced, it is rarely used in large-scale industrial processes. Safety issues and the necessary batch process are supposed to be reasons for using other reactions. Further problems might be the instability of the dienes and/or dienophiles and their technical or economical availability. Despite these issues, DA reactions were successfully applied in industrial ton-scale synthesis.[34]
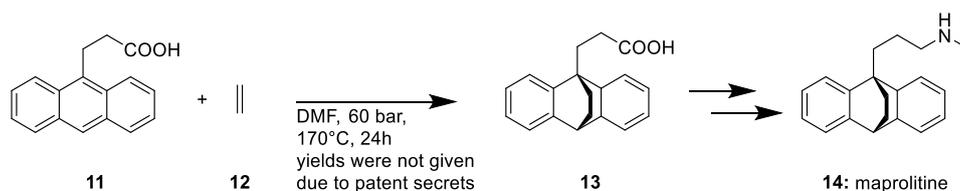
Scheme 10: Synthesis of maprolitine.[35]

For instance, the psychotropic drug maprolitine (**14**) vis synthesized at 170°C and 60 bars through a DA Reaction of anthracene derivative **11** and ethylene (**12**) (Scheme 10). Distinct safety arrangements are required due to high pressure and temperature reaction and ethylene's polymerisation tendency and high flammability.[35,36] Similar issues were solved in the Bayer-Kawasaki process: 1,3-Butadiene (**8**) reacts at 220°C with 1,4-naphthoquinone (**15**) and oxygen to the dye precursor anthraquinone (**16**), which is produced on a 3000 ton-scale (Scheme 11).[37–40]
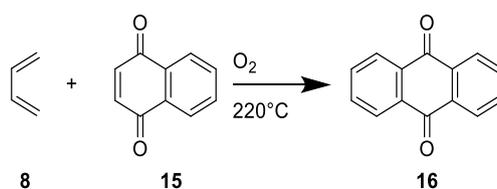
Scheme 11: Bayer-Kawasaki process for the synthesis of anthraquinone.[38,39]

A synthesis of anthraquinone via DA reaction also played an important role in the discovery of the Retro-Diels-Alder reaction: the thermally induced disassembly of bicyclic **17** to anthraquinone (**16**) and ethylene (**12**) by Diels and Alder showed the reversibility of the DA reaction (Scheme 12).[41]
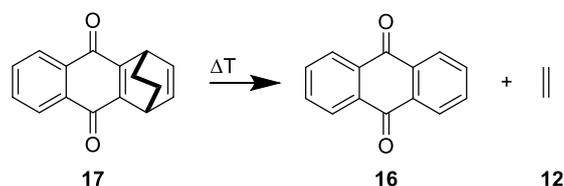
Scheme 12: Retro-Diels-Alder reaction to anthraquinone and ethylene.[17]

DA- and Retro-DA reactions are useful tools to implement and remove protecting groups in synthesis. For instance, in the ubiquinone **21** synthesis of Rüttimann and Lorenz[42], the quinone moiety of **18** was protected by cycloaddition and -revision of cyclopentadiene (**1**) (Scheme 13).
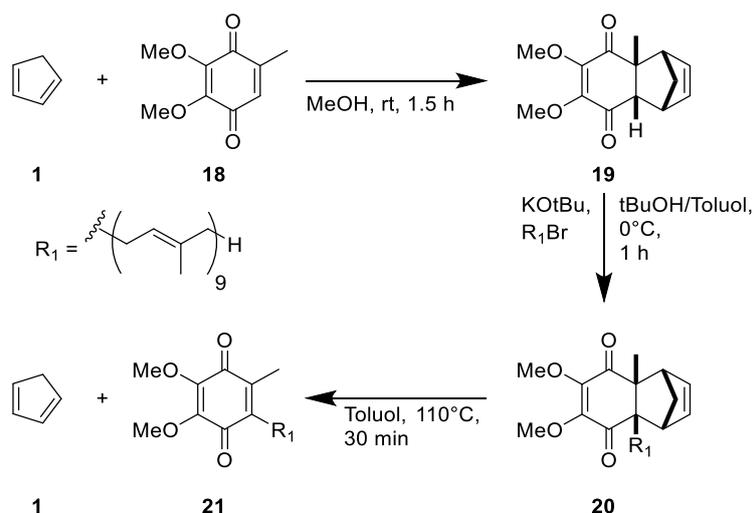
Scheme 13: Protection via Da/retro-DA reaction with cyclopentadiene.[42]

2.1.2 Hetero Diels-Alder Reactions

In 1925, Diels[43] found that cyclopentadiene (**1**) and diethyl azodicarboxylate (**22**) underwent a cycloaddition (Scheme 14). This reaction exemplifies Hetero Diels-Alder (HDA) reactions with dienophiles and/or dienes containing heteroatoms that give access to heterocycles.
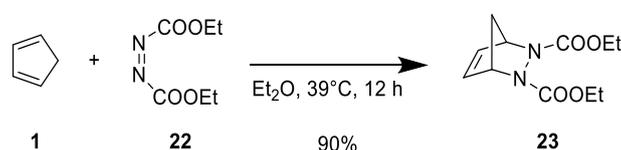
Scheme 14: Cycloaddition of cyclopentadiene and diethyl azodicarboxylate.[43]
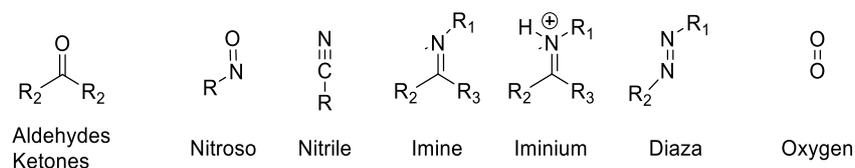
Scheme 15: Selection of heteroatom containing dienophiles.[44–46]
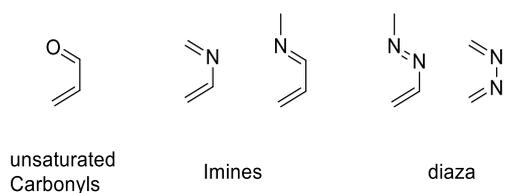
Scheme 16: Selection of heteroatom containing dienes.[44–46]

Dienophiles with electronegative heteroatoms, e. g. O- and N-atoms, lower the LUMO energy which enhances the orbital overlap to the HOMO of the diene promoting the normal Diels-Alder reaction. Carbonyl, nitroso, nitrile, iminium, diaza compounds and even oxygen were used as dienophiles (Scheme 15). The IEDDA reaction benefits from an electronegative heteroatom located at the diene decreasing the $LUMO_{diene}$-$HOMO_{dienophile}$ difference. Dienes as α,β-unsaturated carbonyls, vinyl-imines or diaza compounds were used (Scheme 16).[44–46] The heteroatoms in the dienes and/or dienophiles induce with their inhomogeneous electronic structure an asynchronous transition state of HDA reactions.[47] The decrease of the $LUMO_{dienophil}$-$HOMO_{diene}$ difference facilitates the normal reaction. The application of the HAD reaction already started after the Second World War in the production of the anthelmintic ascaridol (**25**) from *Dysphania ambrosioides* (Scheme 17). Based on the results of Schenck and Ziegler[48] in 1944, **25** was synthesized in an HDA reaction of *α*-terpinene (**24**) with singlet oxygen generated from oxygen, light and chlorophyll. This simple approach was even used in industrial-scale production which used ethanolic solutions of **24** and chlorophyll containing stinging nettle extract exposed to sunlight in glass carboys.[49]
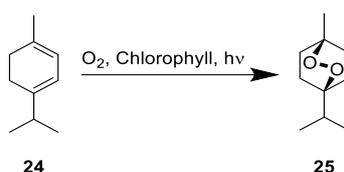
Scheme 17: Synthesis of Ascaridol.[48]
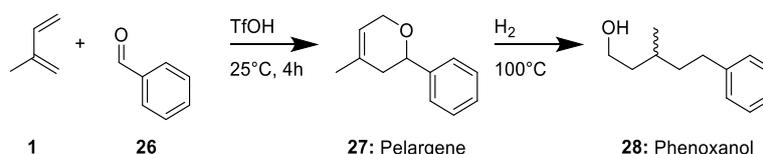
Scheme 18: Synthesis of fragrances via DA reaction.[50,51]

Another example of the HAD reaction is the synthesis of the fragrance Phenoxanol (**28**) starting with an oxa-HDA reaction (Scheme 18). Isoprene (**1**) and benzaldehyde (**26**) were reacted to pelargene (**27**), followed by an hydrogenative ring-opening to **28**, which is produced in ton-scale.[50–52]
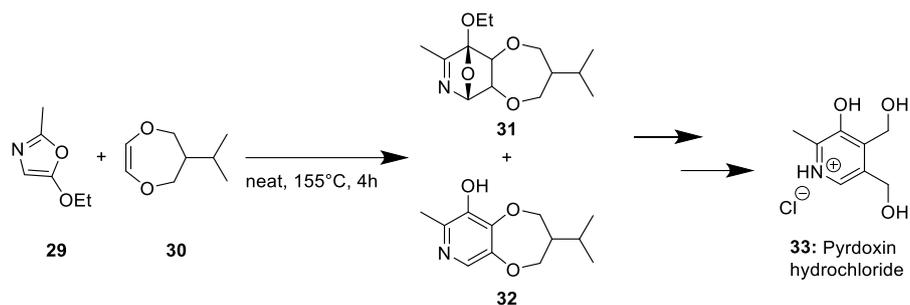
Scheme 19: Vitamin B$_6$ synthesis of DSM.[53]

An imine-type HDA reaction was applied by DSM in the production of pyridoxin, also named vitamin B$_6$, starting from oxazole **29** and enol ether **30** (Scheme 19). A mixture of acetal **31**, which partially eliminates to pyridine **32**, was obtained. Several further steps led to the pyridoxin hydrochloride (**33**) (Scheme 20).[53]
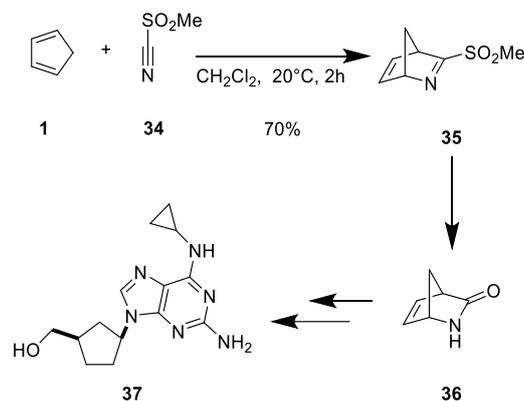
Scheme 20: Synthesis of abacavir.[54]

A nitrile-HDA reaction is used in the industrial synthesis of the reverse transcriptase inhibitor anti-HIV drug abacavir (**37**) (Scheme 20). Nitrile **34** reacted with cyclopentadiene (**1**) to **35**, which was transformed into the so-called Vince lactam **36**. The targeted *C*-nucleoside analogue **37** was obtained after further necessary transformations.[54]
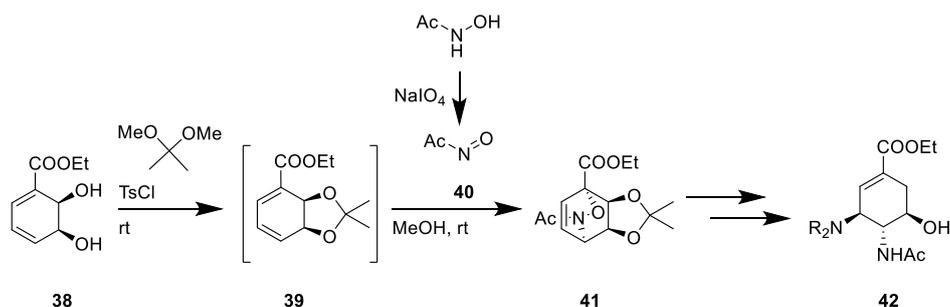
Scheme 21: Synthesis of oseltamivir.[55]

An example of an HDA reaction with a nitrosyl dienophilie was Sullivan's et al.[55] synthesis of the antiviral drug oseltamivir derivative **42** (Scheme 21). Nitrosyl **40** was generated via oxidation of acetyl hydroxylamine with sodium periodate. Diene **38** was acetonide protected with 1,1-dimethoxypropane catalysed by toluenesulfonyl chloride. Direct HDA reaction with diene **39** and nitrosyl **40** led to bicyclic **41**, which is transformed in further steps into oseltamivir derivative **42**.
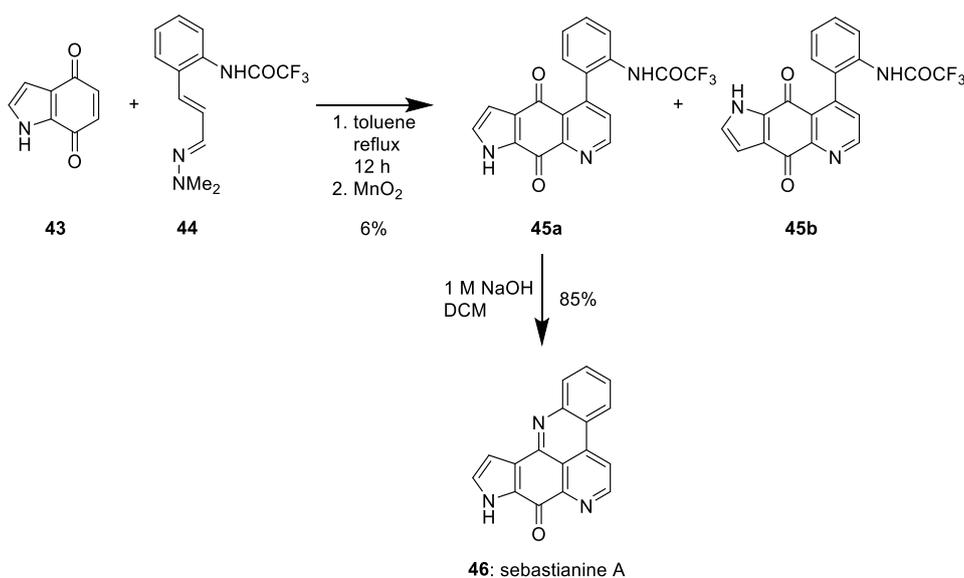
Scheme 22: Synthesis of sebastianine A.[56]

The synthesis of marine pyridoacridine alkaloid sebastianine A (**46**) by Legentil et al.[56] is an example of an HDA reaction with an 1-aza-diene (Scheme 22). The *α,β*-unsaturated hydrazine **44** underwent with quinone **43** a cycloaddition and subsequent oxidation to quinone **45a** and **45b**. Further treatment with base yielded **46**. As in the carbon-based DA reactions, there also retro-HDA cyclorevisions. Such transformations turned out to be a useful tool in the industrial purification of sterols. The isolation of sterol **47** out of a mixture of sterols started with the HDA reaction with 4-phenyl-1,2,4-triazoline-3,5-dione **48** to **49**, which was separable via extraction and chromatography. After a retro-HDA reaction supported by LiAlH4 in the cold or thermally in DMI, sterol **47** was obtained (Scheme 23).[57,58]
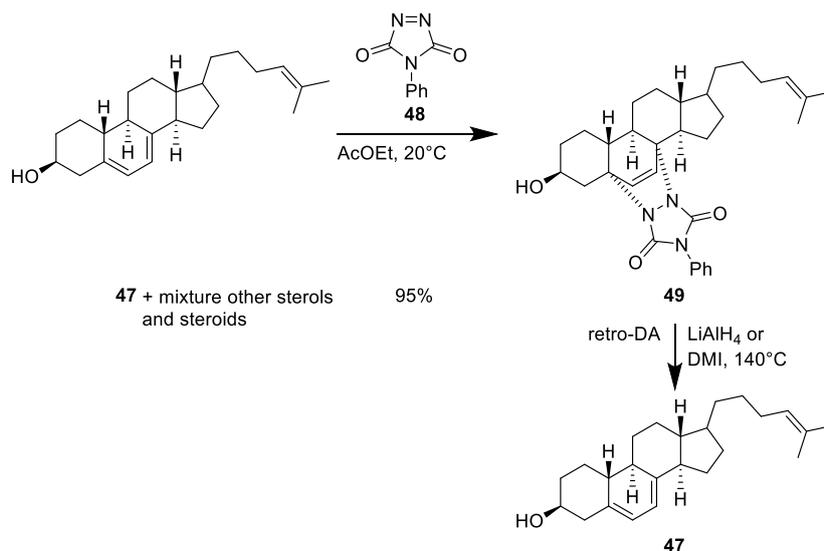
Scheme 23: Purification of sterols via HDA/retro-HDA reaction.[57,58]
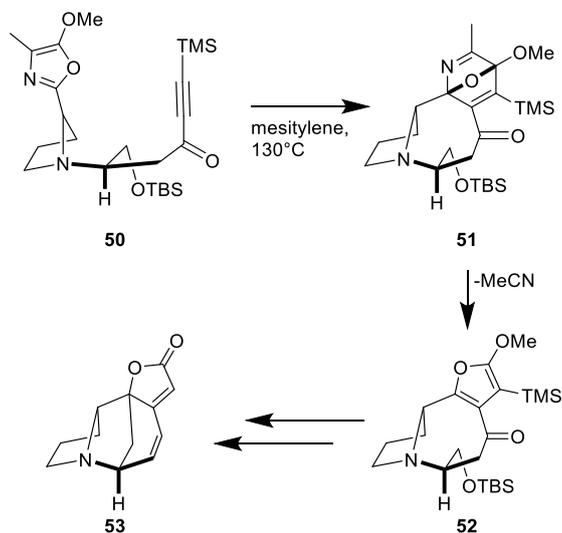
Scheme 24: Synthesis of norsecurinine with HDA/retro-HAD sequence.[59]

The strategy of a (H)DA- and a retro-(H)DA reaction series allows the creation of new structures by combining two molecules and expelling a different one. Jacobi et al.[59] applied this method in the synthesis of norsecurinine (**53**) by the intramolecular reaction of an oxazole with an alkyne **50** (Scheme 24). After the cycloaddition, **51** expelled in a retro-HDA reaction acetonitrile yielding furan **52**. Target compound **53** was obtained after further transformations.

14

2.1.3 Inverse Electron-Demand Diels-Alder Reaction

First IEDDA reactions were observed by Bachmann and Deno[60] as well as Carboni and Lindsey[61]. They discovered the reaction of 1-vinyl-naphthalene (**54**) with butadiene carboxylic-acid derivatives **55** to cyclohexene acids **56a**-**56c**, and tetrazines **57** with alkenes **58** with subsequent oxidation to pyridazines **60** with potassium chromate, respectively (Scheme 25, 26).
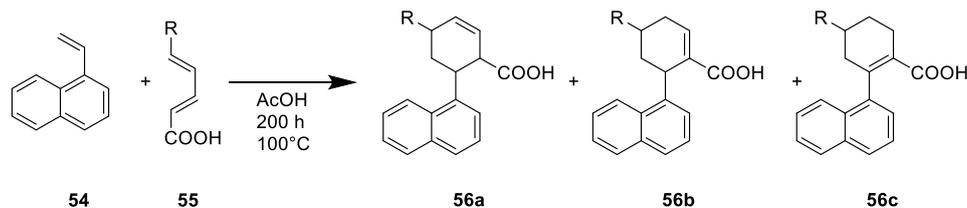
Scheme 25: Reaction vinyl naphthalene and butadiene acid.[60]
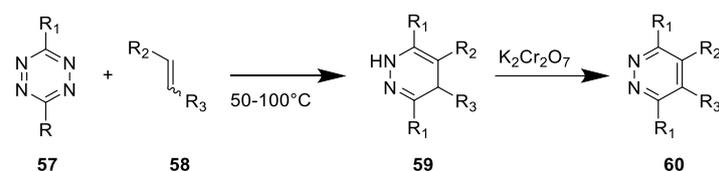
Scheme 26: Reaction of tetrazine and alkene.[61]
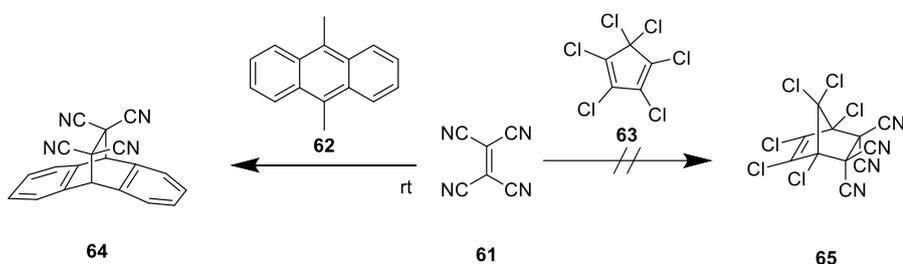
Scheme 27: Borderline case for normal DA reactions.[27]
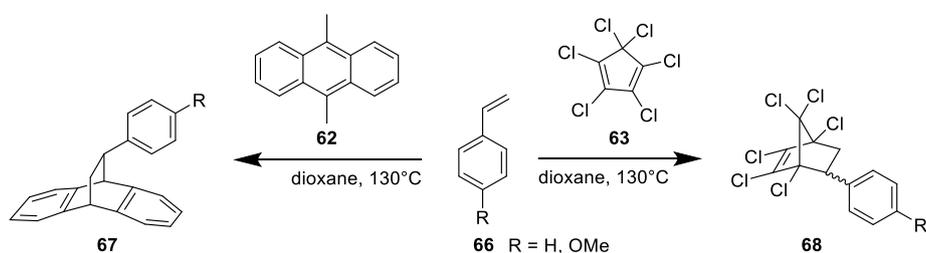
Scheme 28: Cycloadditions of styrenes.[27]

In 1962, the concept of IEDDA reactions was clarified by Sauer, Wiest, and Wiemer[27] by investigating the reaction kinetics of alkenes and 9,10-dimethylanthracene (**62**) and the hexachlorocyclopentene (**63**) (Scheme 27, 28). Their example of a very electron-poor

dienophile tetracycanoethylene (**61**) readily underwent a DA reaction with electron-rich **62** to **64** but not with electron-poor **67**. On the other hand, the electron donating styrene dienophiles **66** reacted slowly with the electron-rich diene 9,10-dimethylanthracene (**62**) to **67** but underwent a fast cycloaddition reaction with the electron-poor diene hexachlorocyclopentene (**63**) to **68**. Therefore, they defined the reaction of an electron-rich dienophile and an electron poor diene as a DA reaction with inverse electron-demand.
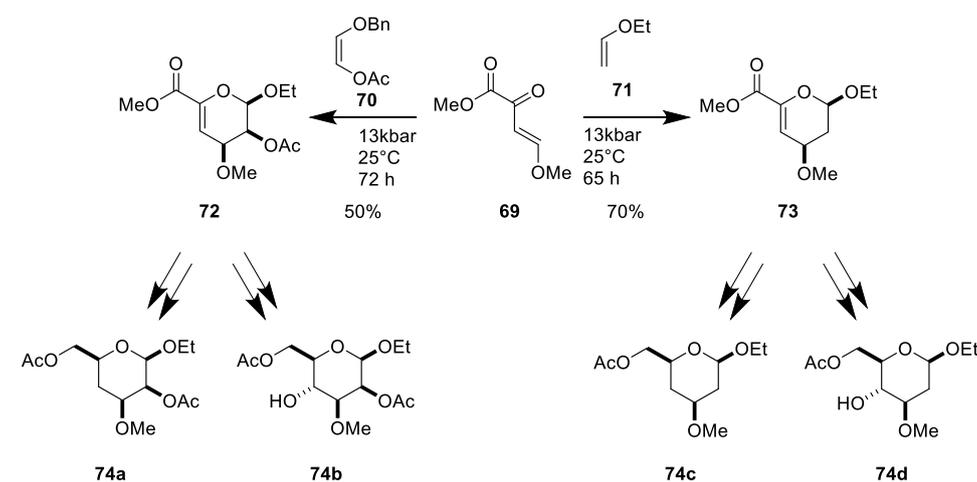
Scheme 29: Synthesis of mannoside derivatives.[62]

Alongside full-carbon based dienes, heteroatomic ones were also used due to the LUMO-energy lowering effect. This effect was applied in the synthesis of mannoside derivatives **74a** - **74d** (Scheme 29). Boger and Robarge[62] exemplified an oxa-IEDDA reaction transforming unsaturated α-keto ester **69** with the vinyl ethers **70** and **71** into the pyranoids **72** and **73**, respectively. The mannoside derivatives **74a** - **74d** were obtained after additional transformations.
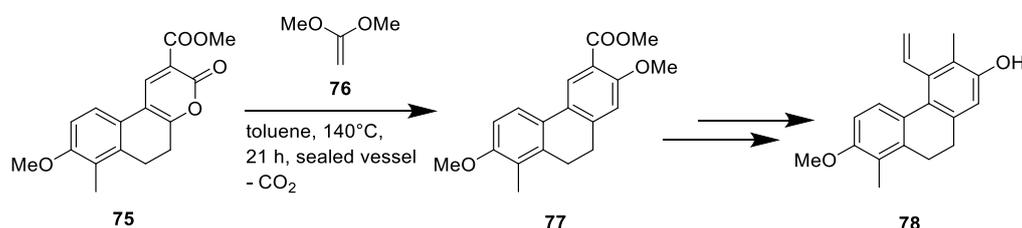
Scheme 30: Synthesis of juncusol via carbon dioxide driven IEDDA/retro-DA reaction.[63]

IEDDA/retro-DA reactions are driven thermodynamically by the expulsion of volatile compounds, e. g. carbon dioxide or nitrogen forcing the equilibrium to generate the targeted product. For instance, the production of carbon dioxide in the IEDDA/retro-DA reaction of 2-pyrone **75** with 1,1-dimethoxy ethene (**76**) is the thermodynamic propulsion to synthesize **77**,

a precursor in the synthesis of the natural compound juncusol (**78**) by Boger and Mullican (Scheme 30).[64] In the field of heteroatom IEDDA reactions, many important contributions to aza-dienes made by Sauer et al.[65] and Boger and et al.[66,67]. In kinetic studies, Sauer et al.[65] investigated the rates of tetrazines and dienophiles in IEDDA reactions determining rate-enhancing dienophile properties (Scheme 31, 32). Their results indicated that alkene dienophiles reacted faster than alkyne dienophiles. Furthermore, cyclic strain and EDG substituents accelerate the reaction rates of dienophiles.
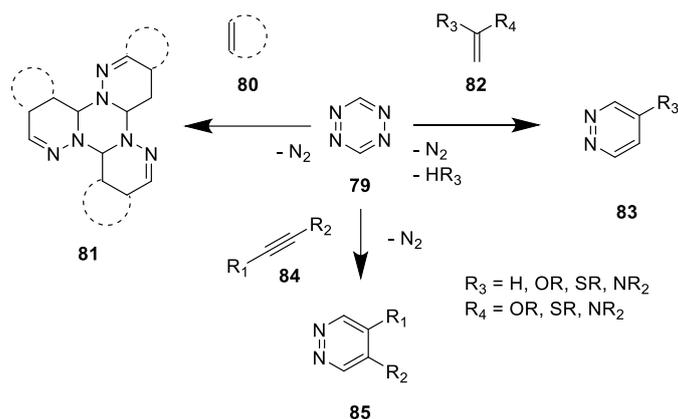
Scheme 31: IEDDA reactions of 1,2,4,5-tetrazine and alkenes and alkynes.[65]

The 1,2,4,5-tetrazine (**79**) underwent a cycloaddition/nitrogen expulsion with cyclic alkenes **80** and trimerized to **81**, whereas enamines or enol ethers yielded pyridazines (Scheme 31). Ketene (thio-)aminales or (thio-)acetals **82** led to mixtures of pyridazines via elimination of a substituent. Thiomethyl-substituents showed the maximum tendency to eliminate. Alkynes **84** and tetrazines yielded pyridazines **85**.[65]
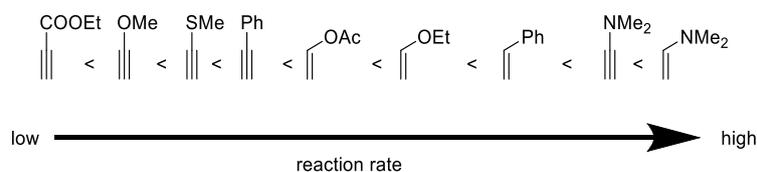
Scheme 32: Reaction acceleration of dienophiles.[65,67,68]

These rate-accelerating substituents and multiple bond effects of the dienophile were also investigated by Boger et al[67] and condensed by Oliveira et al.[68] in a reactivity series (Scheme 32). Further investigations focused on tuning the reactivity of aza-dienes. Sauer et al.[69] found that an increasing number of nitrogen atoms in the diene also increases the reaction rate (Scheme 33).These series were complemented with 1,2,4-triazenes by Müller and Sauer[65,70], Houk et al.[71], Gruseck and Heuschmann[72] and Horner et al.[73] The 1,2,4-triazenes showed faster kinetics than 1,2,3-triazene but slower ones than 1,2,4,5-tetrazine.[71]
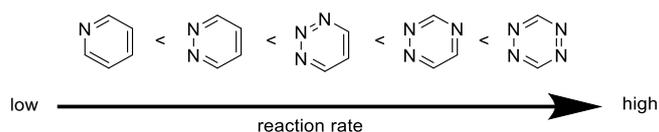
Scheme 33: Influence of the aza-atom pattern on reaction rates.[65,70–73]
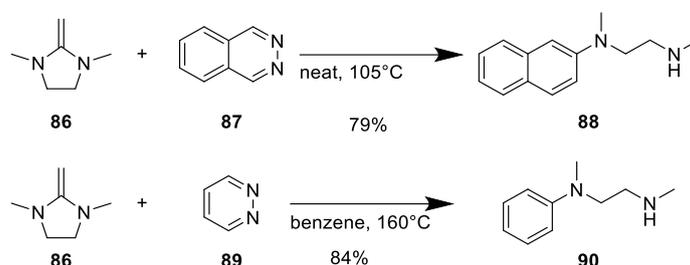
Scheme 34: Reactivity of pyridazine and phthalazine.[72]

The diazine phthalazine (**87**) may be located in the aza-series according to the results of Gruseck and Heuschmann[72]. They found a higher reactivity of (**87**) towards methylidene imidazolidine **86** than pyridazine (**89**), yielding naphthyl amine **88** or phenyl amine **90,** respectively (Scheme 34).[72] A thorough search of the relevant literature applying phthalazines in uncatalyzed IEDDA reactions yielded barely this work and a publication by Oishi et al.[74]
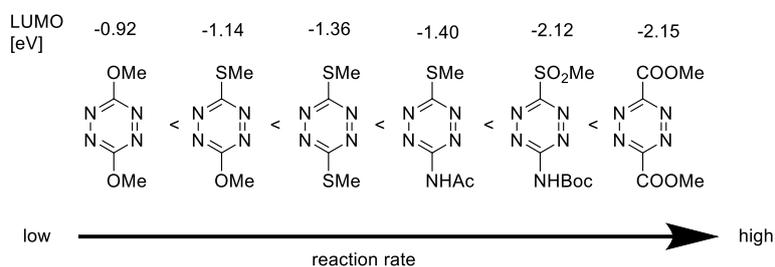
Scheme 35: Dependency of the substituents and LUMO-energy levels on the reaction rates.[66]

Moreover, the influence on the reactivity of the 3,6-substituents of tetrazines were investigated by Boger et al.[66] (Scheme 35). The rates were enhanced by changing from electron donating groups as methoxy ethers to electron-withdrawing groups as methyl esters. This increase in reaction rates corresponds to the substituent dependent decrease in LUMO energy which was further supported by computations on AM1-level.[66]
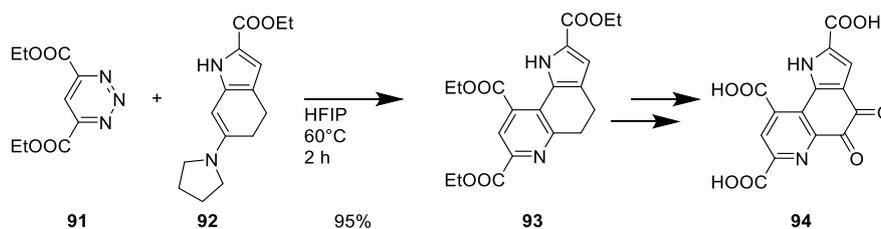
Scheme 36: Synthesis of methoxatin.[75]

Glinkerman and Boger[75] applied their expertise in IEDDA reactions of 1,2,3-triazenes in the synthesis of the redox cofactor methoxatin (**94**) (Scheme 36). The key step is the cycloaddition of 4,5-diethylcarboxylate-1,2,3-triazene (**91**) and pyrrolidinyl enamine **92** to substituted pyridine **93** as precursor of **94**. As another diene, a 1,2-diazine was used in the synthesis of vindoline (**97**), a precursor of the anticancer drug vinblastine (Scheme 37). The synthesis of Ishikawa et al[76] contains an intramolecular domino reaction of an oxadiazole with an indole **95** yielding **96** via an [4+2]/[3+2] cycloaddition cascade. Vindolin (**97**) was obtained after further steps.
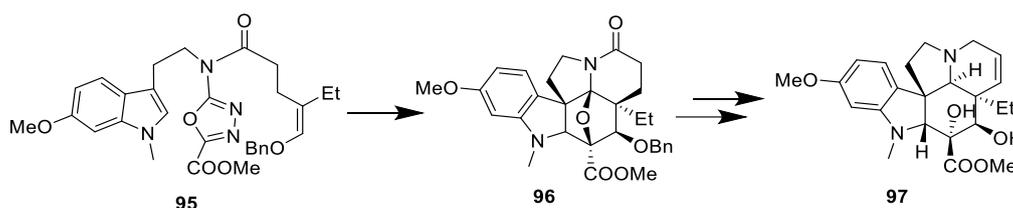
Scheme 37: Synthesis of vindoline.[76]

Besides the investigations on scope and optimisations and total synthesis applications, Sauer and Boger paved the way for the application of IEDDA reactions of tetrazines in biorthogonal chemistry, summarized in a review by Oliveira et al.[68] Compared to other biorthogonal reactions, such as copper-catalysed and non-catalysed azide cycloadditions, tetrazine-based reactions benefit from high reaction rates even in low concentrations, the slow reactivity towards biomolecules and the low toxicity of tetrazine and strained dienophiles. These advantages allow selective IEEDA reactions *in vitro* and *in vivo*, which allows higher resolution imaging and the elucidation of fast bioorganic reactions. Attached fluorescent dyes or radioisotopes are common tracers to observe the reactions and resulting products and structures.[68] The IEDDA reagents are valuable alternatives to fluorescent protein conjugates because their small size overcomes image resolution and photophysical issues resulting from the huge size and higher photostability of fluorescent proteins.[68]
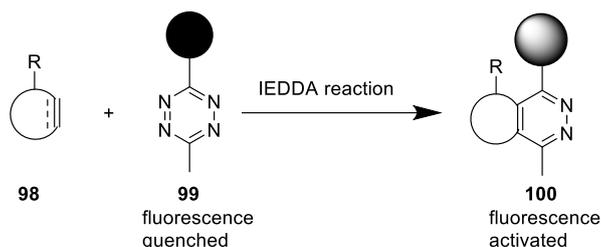
Scheme 38: Activating the fluorescent probe.[68,77]

The fluorescence-quenching ability of tetrazines on fluorescent dyes was applied in fluorescent probes for imaging. A tetrazine attached to a fluorescent dye **98** quenches the fluorescence. After IEDDA reaction, e.g. with an cycloalkene **98**, the fluorescent dye is enabled **100** and allows imaging (Scheme 38).[68,77]
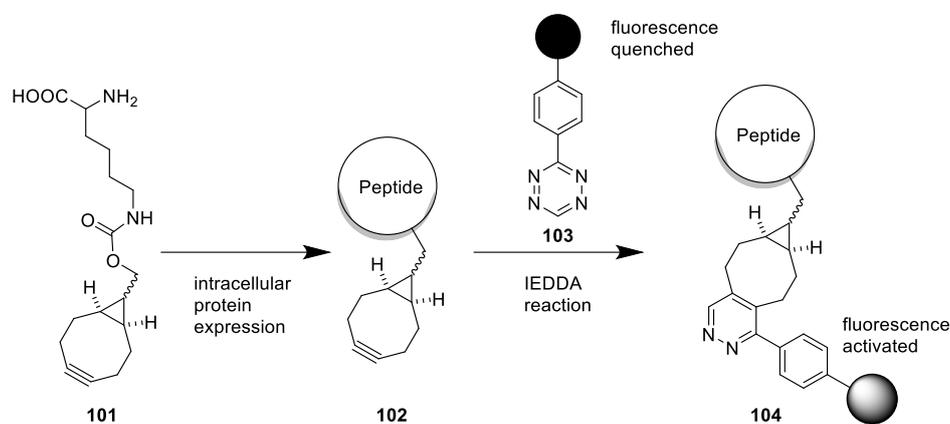
Scheme 39: Application of IEDDA cycloaddition in protein imaging.[78]

For instance, the high resolution of IEDDA-fluorescent probes allowed Uttamapinant et al.[78] to image the cytoskeletal ultrastructures in living cells (Scheme 39). After intracellular protein expression with artificial amico acids equipped with a cyclooctyne (**101**), dienophiles were spread in the peptides **102** of the cytoskeletal structures. The IEEDA reaction with the added tetrazine fluorescent dye probes **103** generated fluorogen-active cytoskeleton **104**.[78] In summary, the IEDDA reaction of tetrazines with dienophiles transformed from a laboratory curiosity to a useful tool in biochemistry.

2.2 Lewis Acid Catalysis

2.2.1 Diels-Alder Reactions Catalysed by Lewis Acids

Lewis acids, defined by G.N. Lewis in 1923, are electron-pair acceptors which interact with electron-pair donors, defined as Lewis bases.[79] This Lewis acid - Lewis base interaction is crucial for understanding the widespread Lewis acid/base catalysis.[80] The rate-accelerating

effect of Lewis acids on DA reactions was observed by Yates[81] in 1960 in the reaction of dimethyl fumarate (**105**) and anthracene (**106**) with and without the Lewis acid aluminium-(III)-chloride to bicyclic **107** (Scheme 40). Without Lewis acid, the reaction needed refluxing conditions for 2-3 days, whereas the aluminium-(III)-chloride catalysed reaction only needed two hours at room temperature.[81]
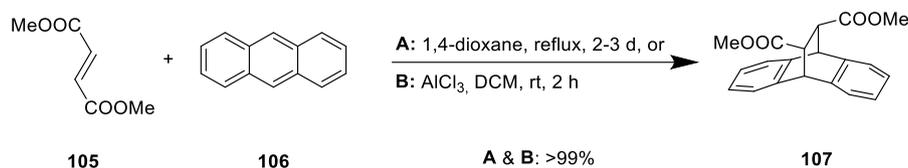
Scheme 40: Rate acceleration by Lewis acid catalysed DA reaction of dimethyl fumarate and anthracene.[81]
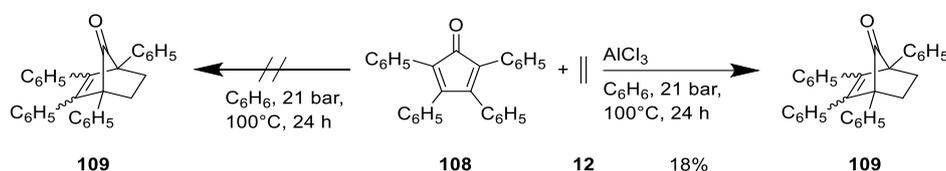
Scheme 41: Effect of Lewis acid catalysis on IEDDA reaction by Allan et al.[82]

Shortly after Yates, Allan et al.[82] noticed in 1962 that the IEDDA reaction between tetraphenylcyclopentadienone (**108**) and ethylene (**12**) to bicyclic **109** only occurred with the addition of aluminium(III)-chloride (Scheme 41). Without Lewis acid, no reaction was observed. Therefore, Lewis acids also enabled overcoming thermodynamical barriers in (IED-)DA-reactions.
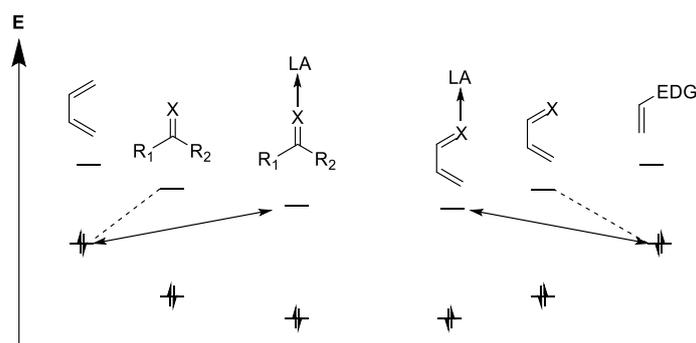
Scheme 42: Influence of the Lewis acid on DA/IEDDA reactions.[44]

These effects were further rationalized by applying the FMO-theory on Lewis acid catalysed Diels-Alder reactions (Scheme 42). The free electron pairs of hetero atoms coordinate with the Lewis acid. The resulting decrease of the HOMO-LUMO energy gap between the dienophile/diene enhances the DA/IEDDA reaction.[44]

21
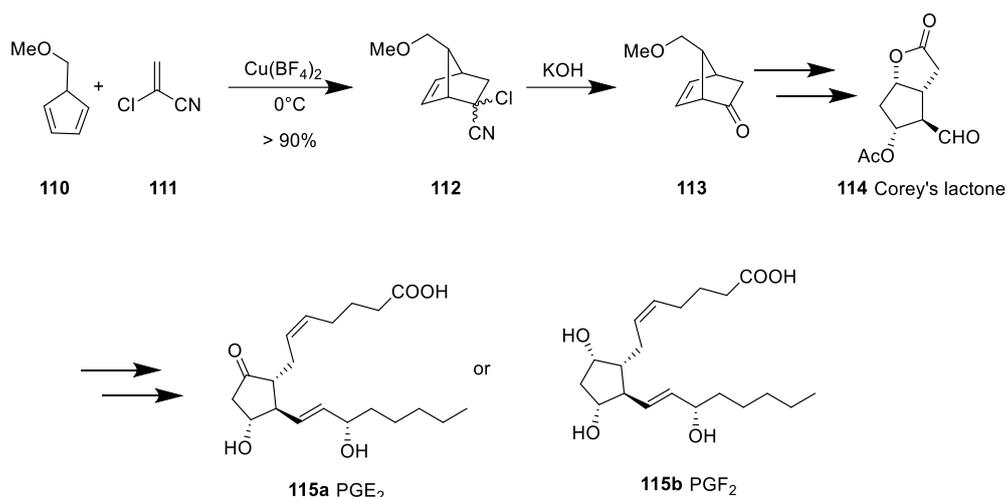
Scheme 43: Corey's prostaglandine synthesis.[83]

A Lewis acid catalysed DA reaction was applied in total synthesis by Corey in 1962 in the first stereoselective prostaglandine synthesis of PGE_2 **115a** and PGF_2 **115b** (Scheme 43).[83] The DA reaction of methoxymethyl cyclopentadiene **110** and 1,1-chloro-cyano-ethylene (**111**) generated the precursor **112** for Corey's lactone **114** which gives access to different prostaglandins **115a** and **115b** in further steps.
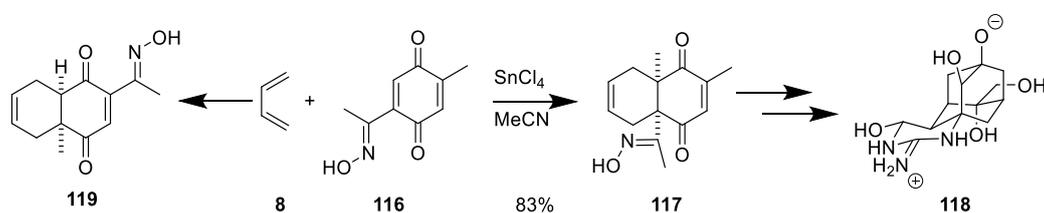
Scheme 44: Chemoselective DA reaction induced by Lewis acid.[84,85]

Furthermore, the chemoselectivity of DA reactions can be also influenced by Lewis acids. The Lewis acid tin(IV)-chloride determined in the synthesis of Tetrodotoxin (**118**) of Kishi et al.[84,85] from 1972 the outcome of the reaction between benzoquinone **116** and 1,3-butadiene (**8**) (Scheme 44): the electron-withdrawing effect of the Lewis acid on the oxime/carbonyl conjugated double bond resulted in a preferred reaction to precursor **117** in 83% yield. Without Lewis acid non-oxime conjugated double bond was electron-poorer and reacted primarily to **119**.[84,85]

22
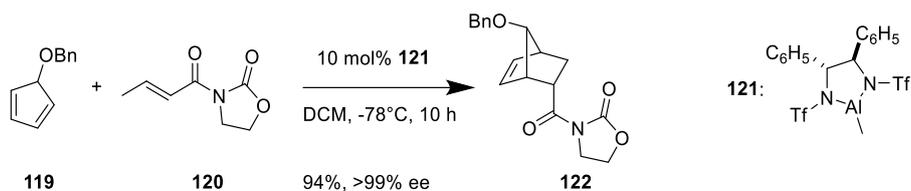
Scheme 45: Corey's enantioselective approach.[86]

The progress in the field of DA reactions led to increased enantioselectivity accessible via appropriate chiral Lewis acids which controlled the transition state. The approach to prostaglandin was improved by Corey et al.[86] in 1989 with an enantioselective DA reaction between cyclopentadiene **119** and dienophile **120** via a chiral aluminium Lewis acid **121** (Scheme 45). Product **122** was obtained in 94% yield and with ee of >99%.
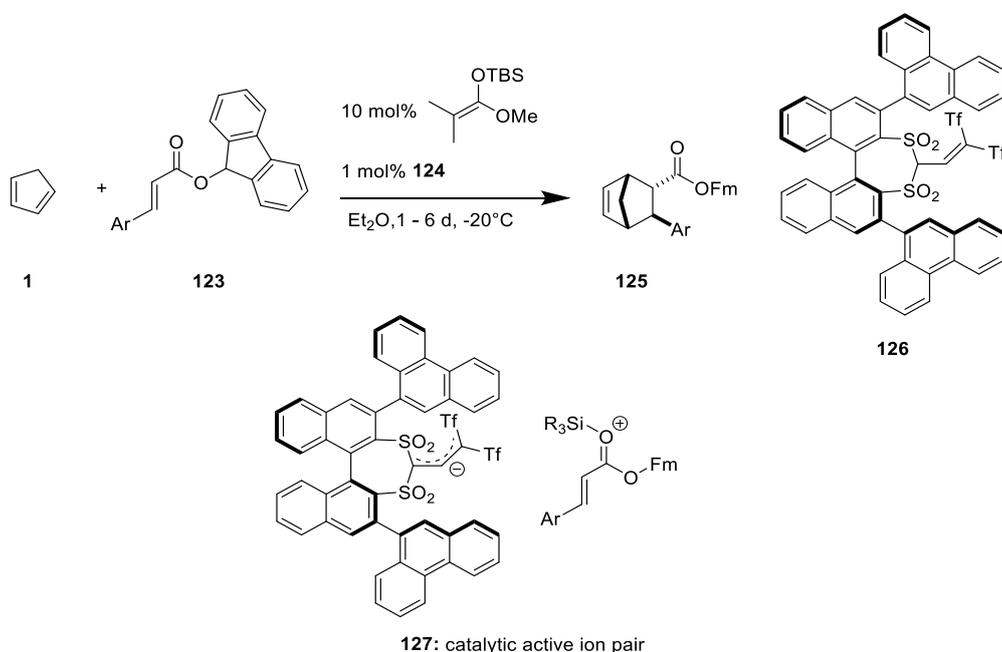
Scheme 46: Gatzenmeier's enantioselective silyl ion lewis acid ion pair.[87]

Further investigations by Gatzenmeier et al.[87], published in Science in 2018, revealed that even ion pairs of chiral anions with silyl Lewis acid cations were sufficient for maintaining an enantioselectivity of more than 92% ee in DA reactions (Scheme 46). In the silyl cation catalysed DA reaction of cyclopentadiene (**1**) with α,β-unsaturated ester **123** the generated chiral anion **127** of **126** controlled the stereochemistry of the product **125**.
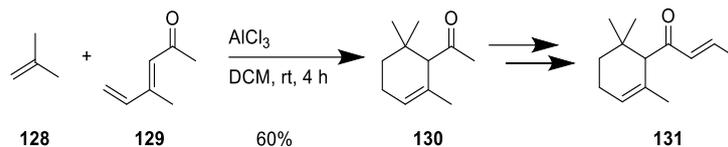
Scheme 47: Synthesis of α-damascone.[88]

Moreover, Lewis acid support was also applied in IEDDA reactions. The synthesis of natural fragrance compound α-Damascone (**131**) by Cookson et al.[88] started with a Lewis acid assisted IEDDA reaction of 2-methylprop-1-ene (**128**) and ketone **129** yielding **130**, which was converted into **131** by following reactions. (Scheme 47)
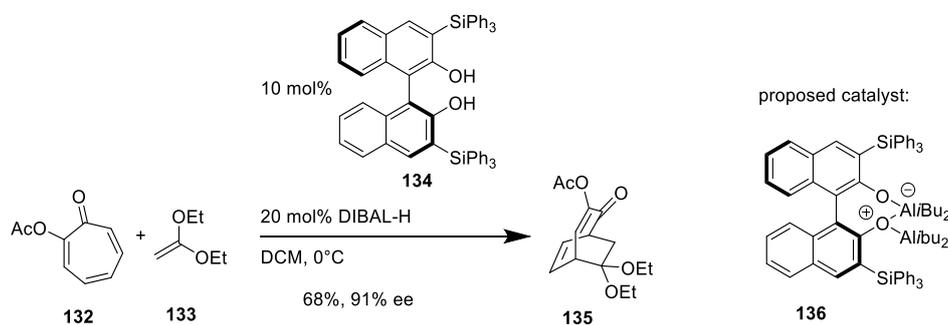
Scheme 48: Chiral Lewis acid assisted IEDDA reaction of Tropones.[89]

Enantioselectivity in Lewis acid catalysed IEDDA reactions can be achieved by chiral Lewis acids. Li et al.[89] applied this approach in the reaction of Tropone **132** with 1,1-diethyl vinyl ether **133**, using a chiral catalyst **136** generated from BINOL-derivative **134** and di*iso*butylaluminium hydride DIBAL-H (Scheme 48). Bicyclic **135** was obtained 68% and 91% ee.
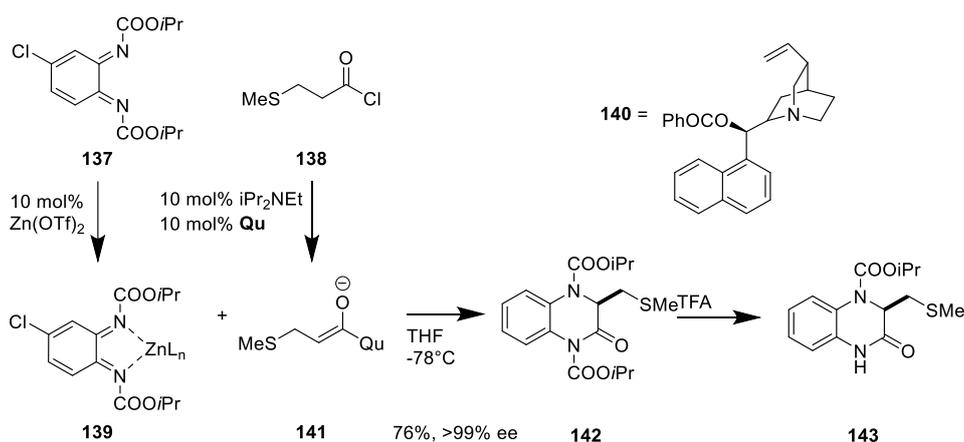
Scheme 49: Chiral auxiliary assisted IEDDA reaction for product with HIV antiviral activity.[90]

Only a few examples of Lewis acid catalysed IEDDA reactions of 1,2-diazine were found in literature. For instance, in the IEDDA reaction of benzoquinone 1,2-diimine **137** Abraham et

al.[90] utilized quinine **140** as auxiliary to generate a chiral enolate **141** to direct the enantioselectivity (Scheme 49). An activation of **137** with zinc triflate **139** was necessary to perform the cycloaddition with enolate **141** to **142**. Further deprotonation with TFA gave access to the anti-HIV virus active compound **143**.
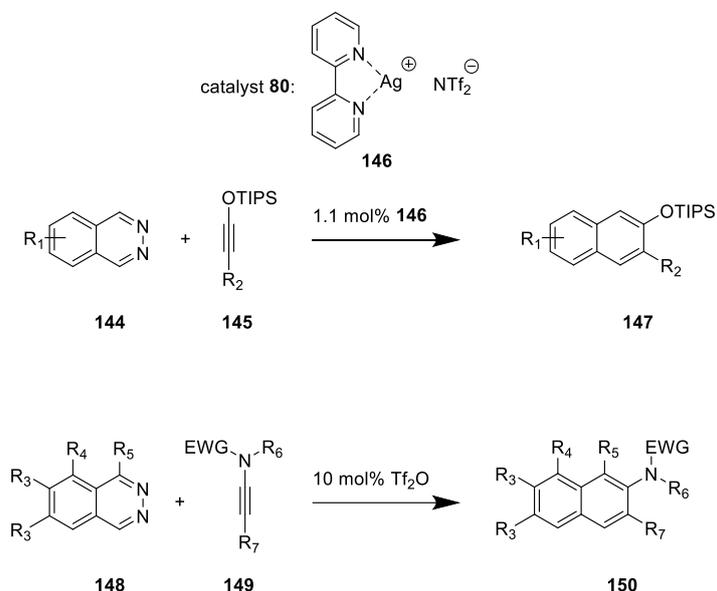
Scheme 50: Silver and triflate anhydride catalysed diaza-IEDDA reaction.[91,92]

Furthermore, Türkmen et al.[91] and Xue et al.[92] reported Lewis acid catalysed IEDDA reactions of phthalazines with alkynes (Scheme 50). A silver catalyst **146** was applied by Türkmen et al.[91] on **144** and oxo-alkynes **145** yielding naphthol derivatives **147**. Organic Lewis acid triflate anhydride was used by Xue et al.[92] on **148** and amino-alkynes **149** generating amino naphthyl amins **150**.[91,92] These rare 1,2-diazine cycloadditions contributed to the wide field of applied Lewis acid assistance or catalysis of IEDDA and DA reactions.

2.2.2. Bifunctional Lewis Acid Activation

Many Lewis acid activated reactions are based on a monodentate interference between the electron acceptor and donator **120** (Scheme 51). Even bidentate Lewis acids often coordinate in monodentate single fashion **121** due to strong monodentate coordination and a transient character of the di-σ-bonding. Additionally, the difficult synthesis of these bifunctional compounds often hampered further studies.[93]

151　　**152**　　**153**　　**154**
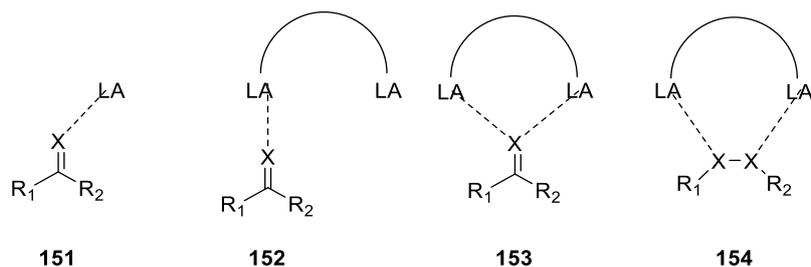
Scheme 51: Coordination of monodentate and bidentate Lewis acids.

Nevertheless, a few examples of bidentate coordination to monodentate **152** and **153** or bifunctional Lewis bases **123** can be found in literature.[93] A thorough search of the relevant literature yielded the result that the coordination behaviour of bidentate Lewis acid was investigated by Biallas and Shriver for the first time. In 1966, the authors studied the 1,2-bis-(difluoroboryl)-ethane (**156**) and its reaction on trityl ethers (Scheme 52). For instance, the fluoroborane **156** cleaved the trityl oxygen bond of bis(trityl)-ether **155** forming adduct **157**.[94]

155　　　**156**　　　　　　　　**157**
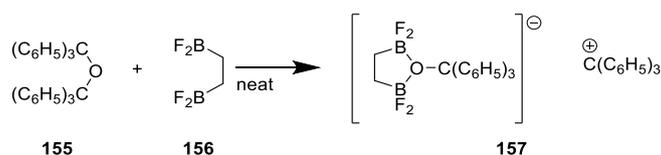
Scheme 52: Boron bidentate Lewis acid coordination experiments.[94]

159　　　　　　**158**　　　　　　　**160**
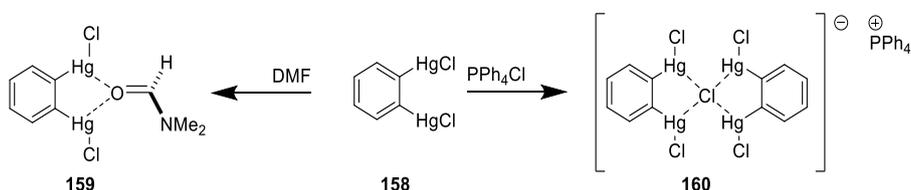
Scheme 53: Bidentate mercury Lewis acid coordination.[95–97]

In 1986, the bidentate coordination of 1,2-phenylenedimercury dichloride (**158)** on *N,N*-dimethylformamide DMF **159** and chloride anions **160** was observed by Wuest et al.[95,96] (Scheme 53). They published further coordination experiments with hydroxides and amide carbonyls in 1999.[97]

26
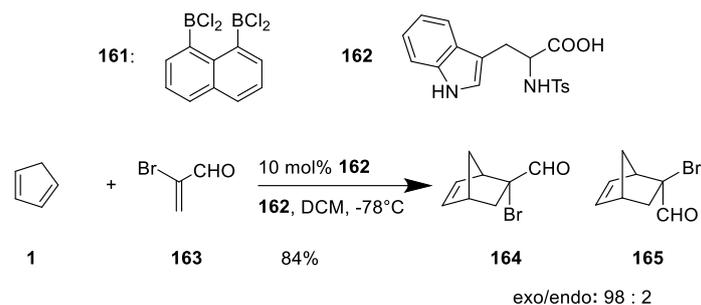
Scheme 54: Bis(dichloroboryl)naphthalene catalyzed DA reaction.[98]

In 1995, Reilly and Oh applied a bidentate Lewis acid in organic chemistry: the borane 1,8-bis-(dichloroboryl)-naphthalene (**161**) catalysed the DA reaction of cyclopentadiene (**1**) and 2-bromoacrolein **163** to bicyclic **164** and **165** supported by the tryptophan derivative **162** (Scheme 54).[98] The authors proposed a higher selectivity of bidentate Lewis acids due to a more rigid transition state, but they did not compare their results to a monodentate catalyst.
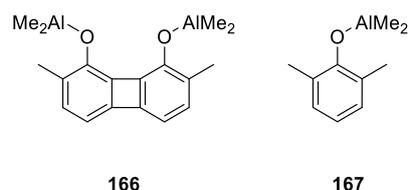
Scheme 55: Bidentate and monodentate aluminium Lewis acids of Maruoka.[93]

A deeper insight into monodentate and bidentate Lews acids was contributed by Maruoka et al.[93] in 2001 due to comparison of the bidentate aluminium Lewis acid **166** with monodentate Lewis acids such as **167** (Scheme 55). In the Mukaiyama-Aldol reaction between **168** and **169**, the bidentate Lewis acid **166** surpassed the monodentate Lewis acid **167** by reaching a yield of 87% of product **170** compared to a yield of 0% and no reaction at all, respectively (Scheme 56).
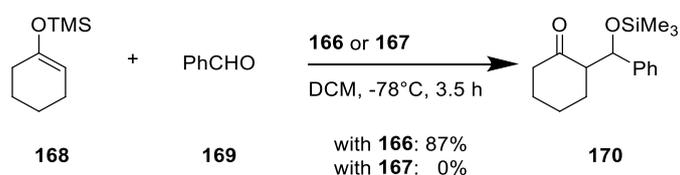
Scheme 56: Mukaiyama aldol reaction with bidentate and monodentate Lewis acid.[93]
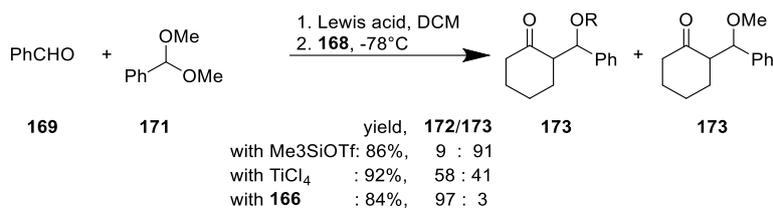
Scheme 57: Selectivity change in Mukaiyama aldol reaction.[93]

Slight modifications by adding benzaldehyde dimethyl acetal (**171**) and by testing different Lewis acids also showed the ability of bidentate Lewis acids to change the ratios between the products **172** and **173** (Scheme 57).[93] Monodentate Lewis acids increased the formation of **172**, whereas bidentate **166** preferentially yielded **173**.
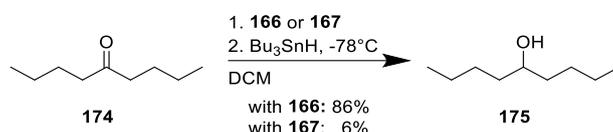
Scheme 58: Ketone reduction with Maruoka's Lewis acid.[93]

The bidentate **166** caused a higher yield of 96% compared to monodentate **167** with a yield of 6% in carbonyl reduction of 5-nonanone (**174**) with tributyl tin hydride to 5-nonanol (**175**) (Scheme 58).[93] The higher yields and the selectivity control of **166** highlighted the advantage of a bidentate Lewis acid over a monodentate one.

2.3 Redox Flow Battery

2.3.1 Electrochemistry of the Redox Flow Battery

A redox flow battery (RFB) consists of two Nernst half-cells divided by a separator, two electrodes connected with the electrical circuit, pumps and two tanks (Figure 2). The main difference to normal solid redox material-based batteries is that the redox-active material is dissolved in a liquid electrolyte. Hence, the anode redox active material is designated as anolyte, whereas the cathode redox-active material is designated as catholyte.[10] The separator is not permeable to the anolyte or catholyte, but it is permeable to the electrolyte.

28
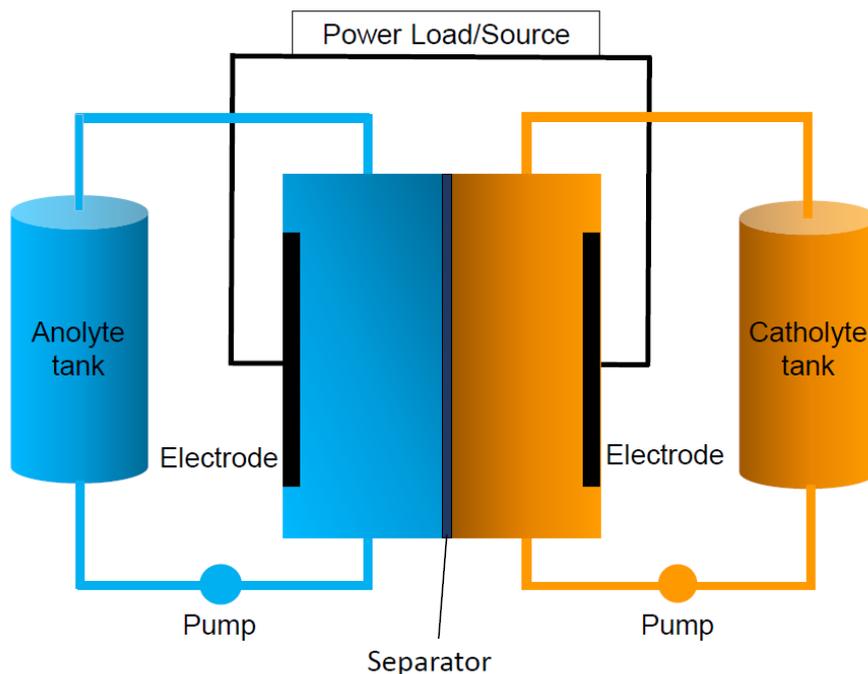
Figure 2: Redox flow battery.[10]

Compared to a solid material battery, the design of an RFB enables to scale the capacity and the power separately. The capacity depends on the volume of the material reservoirs, the concentrations, and the potential difference between the redox materials. The power scales with the size of the active electrode surface, the number of electrodes and/or stacks of the system. In hybrid redox flow batteries HRFB with non-flow/flow redox materials, for example Zn/Zn^{2+}, power and capacity are dependent on each other because the cell electroplating surface determines the capacity, rather than the size of the material reservoir. Designing efficient RFBs requires continuous research in the technology of the separators, electrodes and pumps. However, these technical details exceed the range of this study which is focused on the organic redox active material for RFBs. Therefore, only the necessary key facts are summarized here. A low resistance, mechanical stability as well as a high and durable selectivity for the electrolyte are essential criteria for a separator to maintain the efficiency of the RFB. Deposition phenomena of materials on the surface cause blocking of the pores, which deactivates the flow of the separator. Most separator materials are based on non-perfluorinated and perfluorinated ion exchange membranes or even simple microporous filters for larger redox active materials. The materials used for electrodes are graphite felt, carbon paper or metal mesh/foam doped or coated with additives or nanoparticles. They should provide a high electrical conductivity, a large surface, fast reaction kinetics and stability towards the electrolyte in the potential window. Furthermore, electrodes should cause a minimum of side reactions, such as the water-splitting reaction to hydrogen and oxygen in

aqueous electrolytes, which decreases the efficiency. The performance of RFBs and materials can be evaluated with the following physical parameters. The cell voltage is defined as the difference of the electrode potentials (Equation 1) which can be described with the Nernst equation (Equation 2). The cell voltage U (unit V) depends on the standard electrochemical potential $E°$ and the activity a of the anolyte and catholyte material. The activity can be approximated with the concentration of the redox material.

$$U = \Delta E = E_{cathode} - E_{anode}$$

Equation 1: U = cell voltage, $E_{cathode}$ = electrode potential of the cathode, E_{Anode} = electrode potential of the anode.

$$E = E^0 - \frac{RT}{zF} \ln \left(\frac{a_{Red}}{a_{Ox}} \right)$$

Equation 2: E = potential, $E°$ = standard potential, R = gas constant, T = Temperature, z = number of electrons during redox process, F = Faraday constant, a = activity of the redox material

A large difference between cathode and low anode standard potential is favoured to increase the cell voltage. The current density J (A/cm^2) influences the rate of charging/discharging and depends on the area of the membrane (Equation 3).

$$J = \frac{I}{A}$$

Equation 3: J = current density, I = current, A = area.

The capacity of RFBs is determined by the amount of stored redox material (Equation 5). The energy density ED (Wh/dm^3 or Wh/l) describes the energy amount stored in the battery per volume (Equation 5).

$$C = nzF$$

Equation 4: C = Capacity, n = amount of material, z = number of electrons, F = Faraday's constant.

$$ED = \frac{m \cdot z \cdot F \cdot U}{M \cdot V}$$

Equation 5: ED = energy density, m = mass of redox material, z = number of electrons, R = Faraday's constant, U = voltage, M = molar mass, V = Volume.

The coulombic efficiency *CE* is the ratio between the charges during charging and discharging from the same loading cycle (Equation 6). A *CE* value less than <99% is a sign for side reactions of the redox active material or a crossing of the material through the membrane. The capacity retention describes the amount of preserved capacity from the initial capacity over time. The capacity retention *CR* can also be given as a percentage of the initial capacity (Equation 7). The capacity fade can be related to the number of charge/discharge cycles or to time measured in days. Kwabi et al.[99] pointed out that the capacity fade rate per day should preferably be considered by the evaluation of the long-term stability of redox materials. The authors emphasized that the capacity decay is more related to the time than to the number of cycles.

$$CE = \eta_C = \frac{Q_D}{Q_C}$$

Equation 6: CE = η_C = coulombic efficiency, Q_D = discharging charge, Q_C = charging charge.

$$CR = \frac{C_p}{C_i} \cdot 100\%$$

Equation 7: *CR* = Capacity retention, C_p = preserved capacity, C_i = initial capacity.

The voltage efficiency VE relates the mean discharging voltage to the mean charging voltage (Equation 8). The discrepancy of these voltage values results from overpotentials due to diffusion, polarisation and ohmic overpotentials. The energy efficiency EE is obtained through the multiplication of CE and VE and gives a value for applied and retained energy (Equation 9).

$$VE = \eta_V = \frac{\frac{\int_0^{T_D} E_D(t)dt}{T_D}}{\frac{\int_0^{T_C} E_C(t)dt}{T_C}} = \frac{\bar{E}_D}{\bar{E}_C}$$

Equation 8: VE = η_V = voltage efficiency, *C* = charging, *D* = discharging, *E* = potential, *T* = time during discharging/charging.

$$EE = \eta_{EE} = \eta_C \cdot \eta_V$$

Equation 9: EE = η_{EE} = energy efficiency, η_V = voltage efficiency η_C = coulomb efficiency.

RFBs provide values between about 50 to 90% varying according to the material and current density. These physical parameters are affected by the applied electrolyte, which is either aqueous or organic. Organic solvents overcome the voltage limitation of the water-splitting side

reaction and enable the use of redox materials with higher potentials. As a result, higher cell voltages and energy densities can be obtained. The drawback of organic solvents is the lower ion conductivity and accessible current densities compared to water. Moreover, water is less hazardous than organic solvents with regard to flammability and the environment.[10]

Table 1: Metal-based redox material.

Entry	Redox material	Ref.
1	$CrSO_4/Cr_2(SO_4)_3//Cr_2(SO_4)_3/H_2Cr_2O_7$	[100,101]
2	$TiCl_4//FeCl_3$	[102]
3	$Ti(SO_4)_2//FeSO_4$	[102]
4	$Fe^{3+}/Fe^{2+}//Cr^{3+}Cr^{2+}$	[103]
5	$VO_2^+/VO^+//V^{2+}/V^{3+}$	[104,105]
6	$Zn/Zn^{2+}//Br_2/2Br^-$	[106,107]

The development of RFBs started with aqueous electrolytes and metal-based redox materials (Table 1). The first RFB were set up by Kangro[100] in a patent in 1957 utilizing chromium sulfate solutions as redox material (Table 1, Entry 2).[100] In 1962, Kangro and Pieper demonstrated alternative materials based on titanium and iron (Table 1, Entry 2,3).[102] The concept of an RFB was then further pursued by the National Aeronautics and Space Administration (NASA) which led to an iron/chromium RFB (Table 1, Entry 4). The low selectivity of the membranes available at that time decreased the capacity. The first successful all-vanadium utilizing RFB (VRFB) was reported by Skyllas-Kazacos (Table 1, Entry 5).[104,105] Furthermore, the first zinc/bromine HRFB was developed by Exxon and Gould Inc. in the 1970's (Table 1, Entry 6). The VRFB is the state-of-the-art metal-based system on the market used to benchmark other redox materials with its cell voltage of 1.25 V and an energy density of 15-40 Wh/l. The variety of investigated metal or inorganic redox material exceeds the range of this study, which is focused on organic redox materials. In context of this research interest, the drawbacks of metal-based batteries are more important. The mining, production and disposal of metals related to their geoconcentration result in geopolitical issues as well as socio-economic and environmental problems.[10] The corrosive electrolyte solutions and the toxicity of the redox materials (e.g. vanadium salts, bromine) are potential hazards for the environment.[10] The system costs of metal-based batteries should not be underestimated, for instance, the costs of VRFBs with $320 kW/h exceed the target costs of the U.S. Department of Energy which amount to

$100 kW/h.[108] Therefore, cheaper and less hazardous alternative redox materials which are more independent of restricted local and natural resources are needed.

2.3.2 Materials for Non-Aqueous Organic Redox Flow Battery

Organic charge-storage materials arose as an alternative to inorganic redox active materials. They should ideally be cheaper than metal-based materials. Wei et al.[108] pointed out that the costs for vanadium-(VI)-oxide exceed the costs for organic materials or their precursors. From a geopolitical point of view, their abundancy and availability depend on chemical production rather than local access to ore deposits. Moreover, organic redox materials offer manifold options to adjust the potential, the solubility, and the chemical reversibility via modifications of the redox moiety and substituents.[10] The following charge-carrier materials illustrate the diversity of the organic redox materials in organic and aqueous solvents.

176a   **176b**
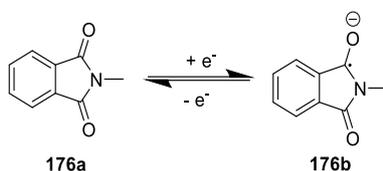
Scheme 59: Redox chemistry of phthalimide.[109]

177a   **177b**
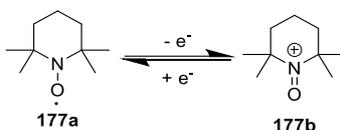
Scheme 60: Reduction and oxidation of TEMPO and its derivatives.[110]

The development of all-organic redox material in nonaqueous RFBs started with Li et al.[111] in 2011 when they investigated a *N*-methylphthalimide MePhth(**176a**)/TEMPO (2,2,6,6-tetramethylpiperidin-1-yl)-oxyl (**177b**) battery (Scheme 59, 60, Table 2, Entry 1). Both materials provide a single radical electron redox step. The gap between the potentials of phthalimide at -0.88 V, and TEMPO at -0.72 V increased the cell voltage to 1.6 V, which is even higher than the cell voltage of the benchmark VRFB with only 1.25 V. On the other hand, the energy density of 1.7 Wh/L is lower than in the case of VRFB with 15 – 40 Wh/L, and the coulombic efficiency of 90% over 20 cycles indicated side reactions and/or membrane crossings.

Table 2: Materials for non-aqueous ORFBs (NAORFBs).

Entry	Anolyte	Catholyte	E^0_{Anode}|$E^0_{cathode}$| Cell voltage in [V]	Cycles	Concentration of Redox material and Electrolyte	Capacity retention Coulombic efficiency	Ref.
1	**176**	**177**	-0.88| 0.72| 1.6	20	0.1 M in MeCN, 1 M NaClO₄	N/A, > 90%	[111]
2	**178a**	**177**	-1.64| 0.48ᵃ| 2.1-2.3	N/A	0.2 M in PC, 1 M TEABF₄	N/A, > 80%	[112]
3	**179**	**180**	2.48| 4ᵇ| 1.4-2.4	30	0.05 M in PC, 0.2 M LiBF₄	N/A 70%	[113,114]
4	**179**	**181**	-0.54| 0.86| N/A	60	0.05 – 0.035 M in PC, 0.2 M LiBF₄	N/A, > 80%	[115]
5	**182**	**183**	-0.9| 1.34| > 2	100	0.5 M in MeCN, 1 M TEANTFSI	N/A, 86%	[116]
6	**176**	**183**	-1.79| 0.51ᵃ| 2.0-2.4	50	0.3 M, 1 M LiTFSI in DME	N/A 90%	[117]
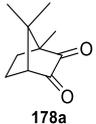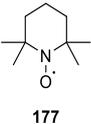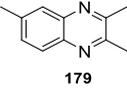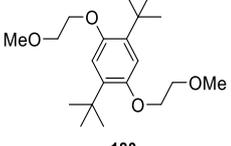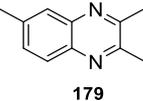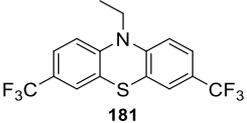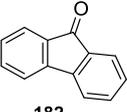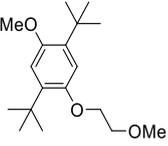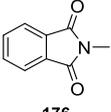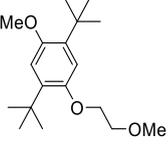
N/A: no data available; ᵃ vs. Ag/Ag+; ᵇ vs. Li/Li+
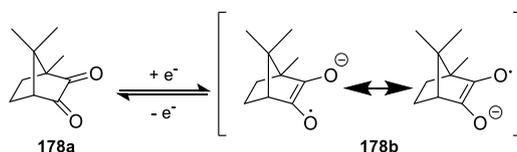
Scheme 61: Reduction and oxidation of camphorquinone.[112]

TEMPO was also used as catholyte by Park et al.[112] in a 'proof-of-concept'-battery with camphorquinone (**178a**) as anolyte (Scheme 61, Table 2, Entry 2). This battery was only investigated in a stationary state without flowing electrolytes. Camphorquinone (**178a**) underwent a single electron reduction/oxidation step between the diketone to a mesomeric

stabilised radical anion **178b** with a potential of -1.64 V (vs. Ag/AgCl). The camphorquinone/TEMPO battery reached a high cell voltage of 2.1 - 2.3 V but only a low coulombic efficiency of 80% after the third cycle. The authors attributed the capacity decay to membrane crossing and low mass transport due to the stationary state set-up without pumping. Finally, Park et al.[112] showed the utilisation of camphorquinone and TEMPO as redox materials, but the membrane permeability limited the performance of the battery. Apart from the nitroxide- and carbonyl-based materials, Brushett et al.[113,114] tested 2,5-di-tert-butyl-1,4-bis(4-methoxyethoxy) benzene DBBB (**180**) and 2,3,6-trimethylquinoxaline TMeQ (**179**) as alternative redox-active battery materials (Table 2. Entry 3). The authors used a 'coin cell' battery set-up originally designed to investigate lithium-ion/thin films. A low solubility of 0.05 M DBBB propylene carbonate/0.2 M LiBF$_4$ limited the capacity to 0.6 Ah/l. A coulombic efficiency of around 70% over 30 cycles was achieved. Brushett et al.[113,114] demonstrated that DBBB and TMeQ can be used as redox material for RFBs. However, the performance of the battery was restricted by the low solubility of the redox material. Kaur et al.[115] adopted TMeQ **179** and combined it in a NAORFB with 3,7-bis(trifluoromethyl)-*N*-ethylphenazine BCF3EPT (**181**) with propylene carbonate/LiBF$_4$ as supporting electrolyte (Table 2, Entry 4). A redox material concentration of 0.05 M provided an energy density of 0.84 Wh/L, but most of the capacity was lost after 100 cycles. A higher concentration of charge-carrier material of 0.15 M led to a coulombic efficiency of 89% and an energy density of 2.5 Wh/L over 60 cycles, which indicated a capacity decay. A higher capacity fade was observed after only 20 cycles when a higher concentration of 0.35 M was applied. The capacity loss resulted from the crossover of the material, which was due to a non-optimized membrane and an irreversible side reaction of the catholyte BCF3EPT **181**. Moreover, the low solubility of TMeQ **179** in propylene carbonate limited the overall capacity. As an alternative organic anolyte, Wei et al.[117] used 9-fluorenone FL (**182**) to exploit the single electron redox reaction between the ketone and the ketyl-radical as anolyte (Table 2, Entry 5). The catholyte was 2,5-di-*tert*-butyl-1-methoxy-4-(2-methoxyethoxy)-benzene DBMMB (**183**). The FL/DBMMB materials reached in acetonitrile/tetraethylammonium bis-(trifluoromethane)-sulfonimide TEANFTSI a concentration of 0.5 M which is the highest solubility in organic solvents presented in this study. A high cell voltage of 2.37 V and a theoretical energy density of 15 Wh/L were estimated, which are comparable to the values of a VRFB with 1.25 V and 15-40 Wh/L. Unfortunately, only 73% of the energy density was reached. Furthermore, a coulombic efficiency of 86% and a capacity loss of 80% were observed over 100 cycles, which indicated a membrane crossing of the material or side reactions. Wei et al.[117] suspected the ketyl-radical of FL of dimerizing or deprotonating and/or adding to the solvent acetonitrile. The same group exchanged FL with N-methylphthalimide MePhth (**176**) and developed a MePhth/DBMMB battery with DME/LiTFSI as electrolyte (Table 2, Entry 6). A cell voltage of 2.0 - 2.4 V was achieved at a material

concentration of 0.3 M. Over the 50 charge/discharge cycles a coulombic efficiency of 90% was achieved. Therefore, the MePhth/DBMMB battery was more stable than the aforementioned NAORB materials. To sum up the physical parameters and the performances of the mentioned NAORFBs (Table 2), organic redox materials in organic solvents can provide higher cell voltages than aqueous ORFBs. Drawbacks are the observed capacity decay induced by side reactions or membrane crossings. Moreover, the limited solubilities of the materials resulted in lower energy densities.

2.3.3 Quinone derived Aqueous Organic Redox Flow Battery Materials

The redox cores investigated for aqueous organic redox flow batteries (AORFBs) were mostly based on quinones, viologen, TEMPO, ferrocenes, and aza-aromatics. With regard to the quinones, Aspuru-Guzik et al.[118] made a noteworthy contribution in 2015 with a comprehensive and systematic computational study. The authors screened the dependence of the electrochemical potential on the benzo-, naphtho-, and anthraquinone core pattern and on the substituents on the *ortho*-, *meta*- and *para*-position. Concerning the quinone moiety, they proposed that *ortho*-substituted (1,2-benzo-, 2,3-naphtho-, 2,3-anthra-) quinones have a higher potential than the *para*-substituted (1,4-benzo-, 1,4-naphtho-, 9,10-anthra) quinones. Additional benzo-functionalities decreased the potentials as observed in the descending calculated potentials from 1,4-benzoquinone via 1,4-naphthoquinone to 9,10-anthraquinone. This decay was an example of the calculated substituent effect: electron-donating substituents, such as the benzo-functionality, ($-OH$, $-NH_2$, $-NR_2$) decreased the potential, whereas electron-withdrawing functionalities (e.g. $-CN$, $-NO_2$, $-SO_3H$, $-PO_3H_2$, $-COOH$, $-CF_3$) increased the potential. These combined results were immensely helpful to predict potentials of quinone-based materials. Even before this systematic study, AORFBs had been developed. Xu et al.[119] demonstrated in 2009 a chloranil (**184a**)/cadmium HRFB (Table 3, Entry 1).

Table 3: Quinone based redox materials.

Entry	Anolyte (potential)	Catholyte (potential)	E^0_{Anode}| $E^0_{cathode}$| Cell voltage in [V]	Cycles	Concentration of Redox material and Electrolyte	Capacity retention Coulombic efficiency	Ref.
1	Cd/Cd^{2+}	chloranil **184**	-0.40| 0.71| 0.97	100	0.5 M $CdSO_4$ 0.5 M H_2SO_4 1 M $(NH_4)_2SO_4$	99%	119
2	$Pb/PbSO_4$	**185**	-0.35| 0.72| N/A	9	N/A 3 M H_2SO_4	N/A 93%	120
3	**186**	**187**	0.09| 0.85| N/A	12	0.2 M in 1 M H_2SO_4	> 90% N/A	121
4	**188**	**189**	0.19| 0.82| N/A	25	2 M in 1 M H_2SO_4	N/A >99%	122
5	**190**	$[Fe(CN)_6]^{4-}/[Fe(CN)_6]^{3-}$	-0.72| 0.51| 1.21	150	8 M in 1 M KOH	99.8% per cycle 99%	123
6	**191**	$[Fe(CN)_6]^{4-}/[Fe(CN)_6]^{3-}$	N/A| 0.51| N/A	400	N/A	>99% 99.9%	123
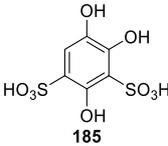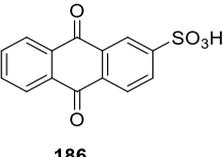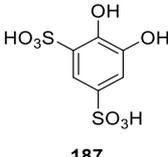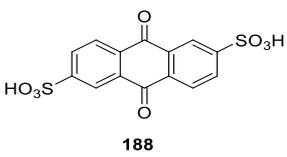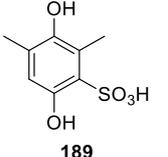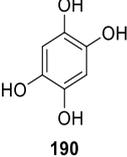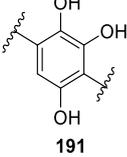
N/A: no data available.
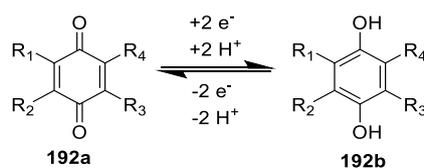
Scheme 62: Common reduction/oxidation of quinones.

Chloranil (**184**) provides a two electron/two proton reduction/oxidation process, which is common to all quinones (Scheme 62). A membrane was not needed in this battery setup

because chloranil (**184**) along with its reduced benzenediol form and the cadmium metal were insoluble in the electrolyte. A discharge cell voltage of 0.97 V and a good coulombic efficiency of 99% were achieved over 100 charge/discharge cycles. Nevertheless, the toxic and carcinogenic cadmium metal and the acidic electrolyte were disadvantages with regard to environmental, health and construction issues.[119] As further development of this group, tiron (disodium 4,5-hydroxybenzene-1,3-disulfonate) (**185)** was tested in combination with lead/lead(II)-sulfate as further HRFB material (Table 3, Entry 2).[120] The tiron reached a potential of 0.72 V. The low coulombic efficiency of 38% in first cycle indicated an irreversible side reaction which diminished the capacity of the battery. Furthermore, a low *p*H value of 4 was necessary for the electrolyte and the redox material, lead, was toxic. Therefore, the lead/tiron battery does not meet the proposed criteria of a non-toxic and less hazardous ORFB.
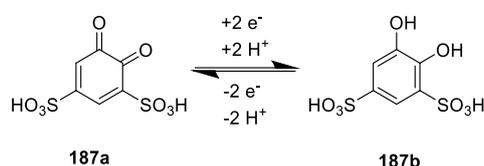
Scheme 63: ORFB with *ortho*-BQDS form Yang et al.[121]

In 2014, Yang et al.[121] improved the redox potential of benzoquinone-based catholytes by switching to the *ortho*-quinone 4,5-dihydroxybenzene-1,3-disulfonic acid BQDS (**187**), which achieved a high potential of 1.1 V vs. NHE (normal hydrogen electrode) (Scheme 63, Table 3, Entry 3). In combination with the anthraquinone 2-sulfonic acid AQS (**186**) as anolyte, the authors developed one of the first fully organic RFBs with a cell voltage of 0.76 V. The low solubility of 0.2 M for both materials in 1 M H_2SO_4 as electrolyte limited the energy density to 1.25 Wh/L. Furthermore, a capacity retention of 90% was achieved after 12 cycles, which indicated side reactions of the charge-carrier material BQDS **187**.
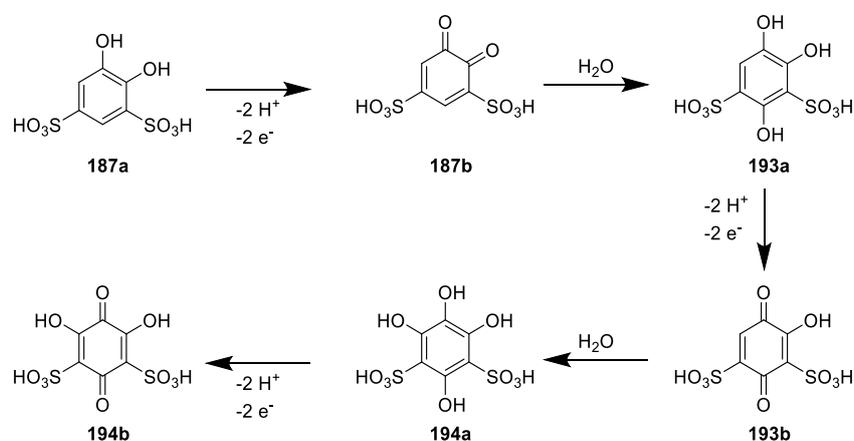
Scheme 64: Michael-type side reactions of benzoquinone materials.[122]

In 2017, Hoober-Burkhardt et al.[122] proposed that the side reaction of the BQDS (**187**) resulted from multiple Michael-type-additions of water and subsequent electrochemical oxidations to **194b** (Scheme 64). These side reactions generated hydroxylated 1,4-benzoquinone species with lower potential, which decreased the overall cell voltage by 100 mV for each hydroxylation. In addition to the BQDS oxidations, the anolyte AQS material was reduced as well and persisted in reduced form after the first charge. Therefore, the usable amount of charge-carrier material decreased and diminished the overall capacity. To overcome these material issues, Hoober-Burkhardt et al.[122] developed 3,6-dihydoxy-2,4-dimethylbenzenesulfonic acid DHDMBS (**189**) as Michael-type attack resistant catholyte with a potential of 0.82 V vs. NHE (Table 3, Entry 4).
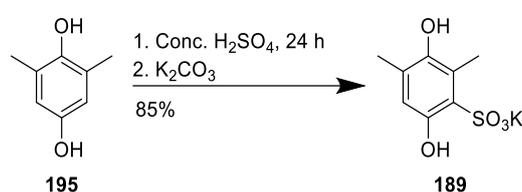
Scheme 65: Synthesis of DHDMBS.[122]

The treatment of commercially available 2,6-dimethyl-1,4-benzoquinone (**195**) with sulfuric acid and the neutralisation with potassium carbonate yielded **189** (Scheme 65). The methyl substituent and the *para*-positioned quinone decreased the potential to 0.82 V vs. NHE compared to BQDS **187**. Unfortunately, after 25 cycles, ^{1}H-NMR-studies revealed a crossing of DHDMBS through the membrane into the anolyte chamber, which effected a capacity fading. Murali et al.[124] and Kwabi et al.[99] estimated the capacity decay with 1% per cycle and 5.5% per day. A membrane optimisation decreased the capacity loss to only 0.5% per day. Basic electrolytes provided increased potential and solubility of hydroxylated quinoid redox materials.[123,125,126] Therefore, Yang et al.[123] switched to 2,5-dihydroxy-1,4-benzoquinone DHBQ (**190**) in alkaline media (Table 3, Entry 5). The deprotonated hydroxyl functions of DHBQ in basic 1 M KOH increased the solubility to 8 M. Moreover, the additional negative charges should prevent Michael-additions of nucleophiles such as water. The increased negative charge at the benzoquinone shifted the potential of -0.72 V to the negative anolyte area. Aqueous potassium hexacyanoferrate(II)/hexacyanoferrate(III) was used as catholyte providing a potential of 0.51 V. Both materials combined achieved a high cell voltage of 1.2 V. The membrane crossing of **190** was prevented by switching to thicker membranes. A capacity decay depending on the pH height was observed. Higher pH values increased the capacity loss. An analysis via NMR and LC-MS indicated side reactions of DHBQ including Michael-additions with hydroxide anions. Yang et al.[123] and Kwabi et al.[99] estimated the capacity loss of 0.24% per cycle but 9% per day. To suppress the Michel-additions, Yang et al.[123]

polymerised the BQ material to polyHBQ **191** to sterically hinder nucleophile attacks (Table 3, Entry 6). The polyHBQ material led to a CE of 96% and a capacity retention of 99.62% over 400 cycles which indicated a more stable material. As only 25% of the theoretical capacity was reached, the polymerisation diminished the amount of effective charge-carrier material. To summarize the benzoquinone materials, the general drawbacks consisted in the intermembrane crossing and the instability due to Michael additions, which caused a capacity decay that may hamper long-term applications in AORFBs.

Table 4: Anthraquinones utilized as redox material in AORFBs.

Entry	Anolyte (potential)	Catholyte (potential)	E^0_{Anode}|$E^0_{cathode}$ cell voltage in [V]	Cycles	Concentration of Redox material and Electrolyte	Capacity retention Coulombic efficiency	Ref.
1	**186**	**187**	0.09|0.85 0.76	12	0.2 M in 1 M H_2SO_4	> 90% N/A	121
2	**188a**	**189**	0.19|0.82|N/A	25	1 M in 1 M H_2SO_4	N/A > 99%	122
3	**188b**	HBr/Br$_2$	0.21|1.07|0.86	10-15	> 1 M in 1 M H_2SO_4	>99& per cycle N/A	127
4	**197**	$[Fe(CN)_6]^{4-}$/$[Fe(CN)_6]^{3-}$	-0.70|0.51|1.2	100	>0.6 M in 1 M KOH	>99& per cycle 99%	126
5	R = (CH$_2$)$_4$COOH **198**	$[Fe(CN)_6]^{4-}$/$[Fe(CN)_6]^{3-}$	-0.52|0.51|1.05	250	>1 M in 1.2 M KOH	>99& per cycle >99%	128
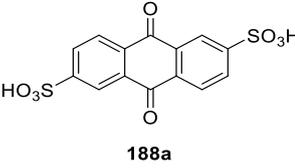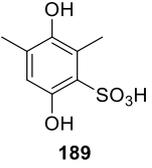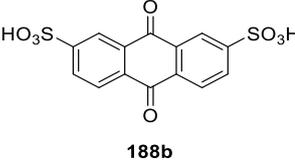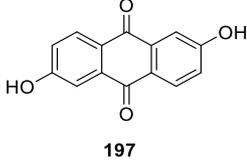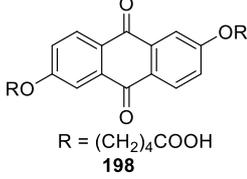
N/A: no data available

Compared to benzoquinones, the additional benzo-functionalities of 9,10-anthraquinones hinder Michael additions but decrease their potential. Their relatively low potential paved their way as anolytes in AORFBs. Yates et al.[81] and Hoober-Burkhardt et al.[122] already used anthraquinone-2-sulfonate AQS (**186F** with a potential of 0.15 V and anthraquinone-2,6-disulfonic acid 2,6-AQDS (**188a**) with potential of 0.19 V as anolytes but focused more on the benzoquinone materials (Table 4, Entry 1, 2). Anthraquinone-2,7-disulfonic acid 2,7-AQDS was investigated by Huskinson et al.[127] in 2014 as anolyte in a HBr/bromine//AQDS/H$_2$AQDS metal-free aqueous inorganic/organic RFB (Table 4, Entry 3). The 2,7-AQDS (**188b**) reached a solubility of over 1 M and achieved a coulombic efficiency of 99% over 10 cycles. The energy density of over 50 Wh/L for 2,7-AQDS outcompetes vanadium as charge-carrier material in VRFBs with only 15 – 40 Wh/L. The capacity fading rate of the HBr/AQDS battery with 0.014% per cycle and 0.19% per cycle was calculated by Kwabi et al.[99], which indicated that AQDS is more stable than DHDMBS. The observed capacity loss was attributed mainly to the membrane crossing of bromine. Disadvantageously, the anthraquinone/bromine battery had a low cell voltage of 0.86 V. The limiting factor was the high potential of 2,7-AQDS of 0.21 V, which is due to the electron density withdrawing effect of the sulfonic acid groups. The cell voltage of anthraquinone containing RFBs was increased to 1.2 V by Lin et al.[126] by utilizing 2,6-hydroxyanthraquinone DHAQ (**197**) in a basic electrolyte of 1 M KOH (Table 4, Entry 4). This voltage enhancement originated from the lower potential of -0.65 V due to the more electron donating effects of the hydroxyl groups. The solubility of DHAQ reached moderate 0.6 M. Combined with potassium ferrocyanide as catholyte, a flow battery with a CE of over 99%, an energy efficiency of 84%, and a capacity fading of 0.01% per cycle over 100 cycles was achieved. Lin et al.[126] and Kwabi et al.[99] estimated the capacity fade of 0.1% per cycle and 8% per day. The capacity loss was attributed to leakage of the battery system and degradation reactions of the DHAQ material.
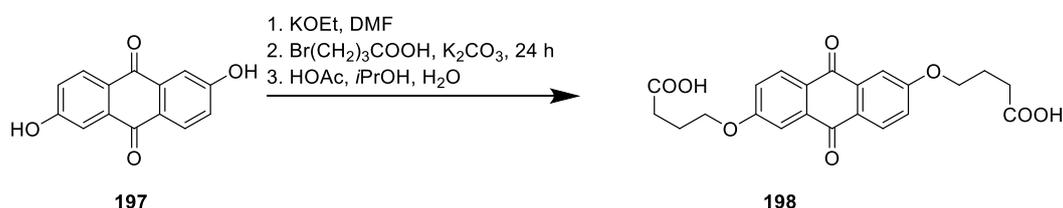
Scheme 66: Synthesis of DBEAQ.[128]

Kwabi et al.[128] improved the Fe(CN)$_6$/DHAQ battery by substituting the anolyte with 4,4'-((9,10-anthraquinone-2,6-diyl)-dioxy)dibutyrate DBEAQ (**198**) (Scheme 66, Table 4, Entry 5). It was synthesized via Williamson ether synthesis of the potassium salt of DHAQ with 4-bromo-butyric acid followed by acidification with acetic acid (Scheme 66). The additional carboxy butyrate

substituents increased the solubility of DBEAQ to 1 M, compared to DHAQ with only 0.6 M at pH 14. Hence, the achieved energy density of 12 – 17 Wh/L reached the value of the benchmark VRFB with 15 – 40 Wh/L. Moreover, the capacity fade rate of DBEAQ/Fe(CN)$_6$ RFB with 0.001% per cycle was ten times slower than DHAQ/Fe(CN)$_6$ with 0.01% per cycle. Kwabi et al.[99,128] estimated a lower capacity fade rate of DBEAQ of 0.04% per day compared to DHAQ with 8% per day. Thus, DBEAQ had the slowest capacity decay of all quinone-based materials. Unfortunately, the butyric acid substituents lowered the potential to 0.52 V, which decreased the cell voltage to 1.05 V.
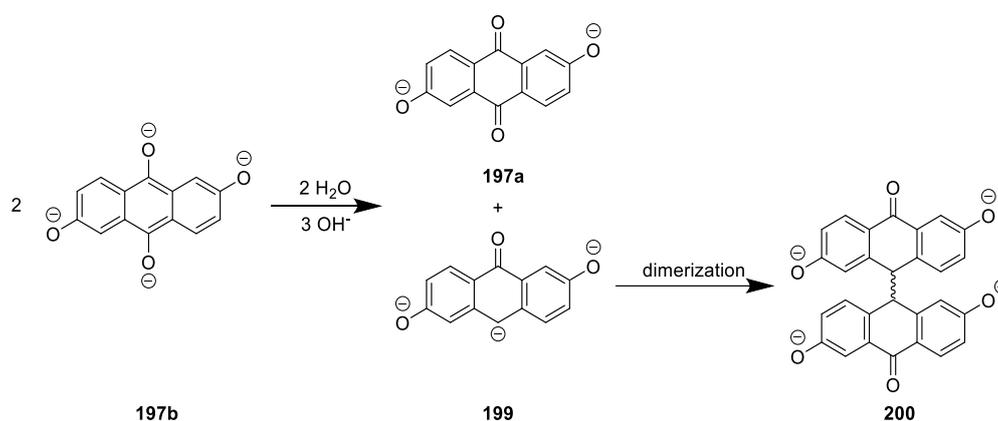
Scheme 67: Disproportionation and dimerization degradation process of Anthraquinones.

In 2019, Goulet et al.[129] elucidated a degradation process of DHAQ redox material. They proposed a disproportionation of the reduced anthraquinone **197b** with water to anthraquinone **197a** and a negative charged anthrone **199** followed by dimerization to **200** (Scheme 67). NMR and HPLC-MS analysis of the anolyte exposed to charge/discharge cycles over several days confirmed the generation of **199** and **200**. Goulet et al.[129] pointed out that a degradation of DAHQ can be supressed by circumventing high states of charge and aeration of the electrolyte enhancing the reoxidation of the anthrone **199** back to the anthraquinone **197**. Therefore, the capacity fade rate of DHAQ with 8% per day was decreased to 0.14% per day. In summary, it can be stated that anthraquinones provide a stable redox material predestined for anolyte applications in ORFBs, preferentially in basic electrolytes.[125]

2.3.4 TEMPO- and Viologen-derived Aqueous Organic Redox Flow Battery Materials

Simultaneously to the investigations on quinone redox materials for flow batteries, TEMPO derivatives **211** and viologen (1,1'-substituted 4,4'-bipyridinium) derivatives **212** were developed and investigated as alternative charge-carrier materials for ORFBs (Scheme 68-70).[10,110,125]
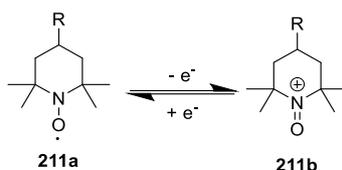
Scheme 68: Reduction and oxidation of TEMPO and its derivatives.[110]
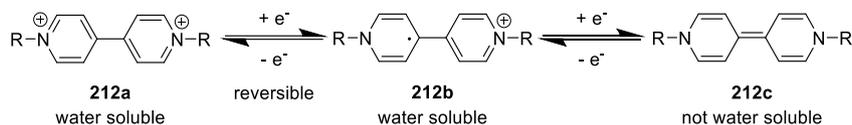
Scheme 69: Oxidation and reduction of viologen derivatives.[110]

Both materials provide a reversible radical redox reaction.[110] TEMPO **211a** is persistent and stable due to the steric hindrance of the methyl groups and the delocalized radical in the N-O bond, and it can be oxidised to **211b**. Delocalisation is also the reason for the stability of the water-soluble viologen radical **212b** generated from dication **212a**.[125] The second reduction step of radical **212b** generating **212c** was often not exploited because **212c** is less water-soluble and tends to undergo side-reactions (Scheme 69).[125,130]
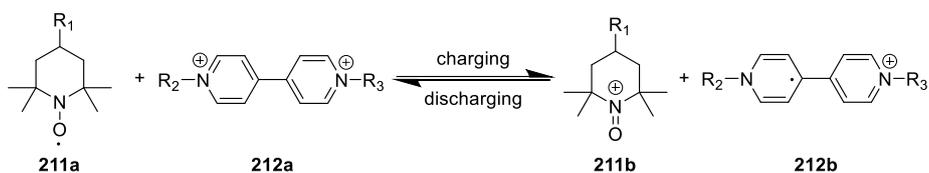
Scheme 70: Overall redox reaction of TEMPO and viologen derivatives.

In 2015, viologen and TEMPO were implemented in separate water-soluble polymers **201** and **202** by Janoschka et al.[131] in an AORFB (Table 5, Entry 1). This setup prevented the intermembrane crossing of the charge-carrier materials and decisively reduced the cost of the battery. The huge size of the polymer bond charge carrier materials required only simple and low-cost microporous filters instead of ion-selective membranes, which are often account for 40% of the price of the battery.

Table 5: Aqueous TEMPO and viologen based ORFB materials.

Entry	Anolyte (potential)	Catholyte (potential)	E^0_{Anode} | $E^0_{cathode}$ | cell voltage in [V]	Cycles	Redox material Concentration and Electrolyte	Capacity retention Coulombic efficiency	Ref.
1	**201**	**202**	-0.4| 0.7| 1.1	10000	N/A in 2 M NaCl	80% 70.5%	131
2	**203**	**204**	-0.45| 0.80| 1.25	100	0.5 M in 1 M NaCl	99% 89%	110
3	**203**	**205**	-0.45| 1.25| 1.40	100	2.0 M in 0.1 M NaCl		132
4	R = (CH₂)₃NMe₃Cl **206**	**205**	-0.38| 1.25| 1.38	500	0.5 M in 0.5 M NaCl	99%/ 97.5%	133
5	Zn/Zn²⁺	**207**	-1.08| 0.8| 1.70	100	1 M in 2 M ZnCl₂ and 2 M NH₄Cl	93.6% 98.1%	134
6	**203**	**208**	-0.45| 0.61| 1.05	100	0.5 M in 2.0 M NaCl	81% 99%	135
7	R = (CH₂)₃NMe₃Cl **206**	**209**	-0.36| 0.39| 0.75	250	1.3 M	98.6% 99.95%	136
8	R = -(CH₂)₃SO₃⁻ **210**	I₃⁻/I⁻	-0.43| 0.57| 1.0	300	0.5 M in 2 M KCl	94.1% 99%	137
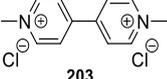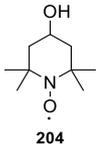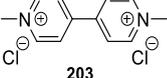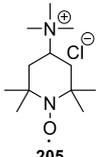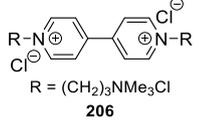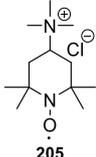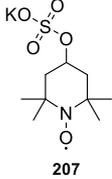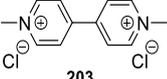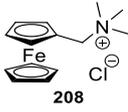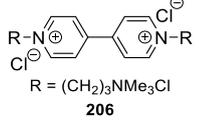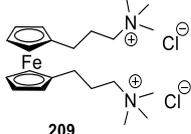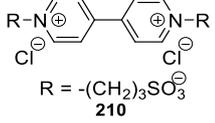
N/A: no data available, [a] vs. Ag/AgCl
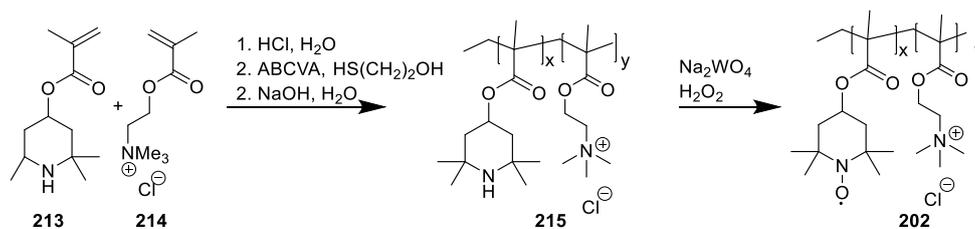
Scheme 71: Synthesis of the water-soluble TEMPO-polymer.[131]

The TEMPO-polymer was synthesized by the acidification of (2,2,6,6-tetramethylpiperidin)-4-yl-methacrylate (**213**) and [2-(metharcyloyloxy)ethyl]trimethylammonium chloride (**214**) in water and the polymerisation with 4,4-azobis(4-cyano valeric acid) ABCVA as a starter (Scheme 71). After the treatment of the base, amine **215** was obtained, and the following oxidation with sodium tungstate and hydrogen peroxide yielded **202**.
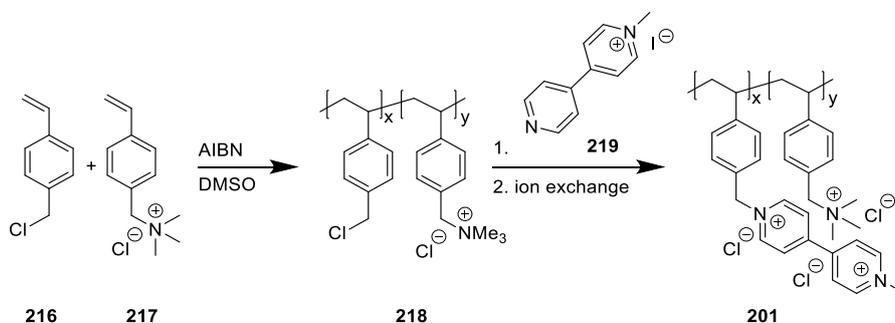
Scheme 72: Synthesis of the water-soluble viologen polymer.[131]

The synthesis of the viologen polymer was started by the polymerisation of 4-vinyl benzyl chloride (**216**) and (4-vinylbenzyl)-trimethylammonium chloride (**217**) with AIBN as radical starter (Scheme 72). Nucleophilic substitution with 1-methyl-4,4'-(bipyridin)-1-ium iodide (**219**) and subsequent anion exchange yielded **201**. These materials required only sodium chloride solution as electrolyte instead of corrosive acids or bases, which eased the technical set-up and decreased safety issues. The polymer-based flow battery reached a cell voltage of 1.1 V and an energy density of 8.0 Wh/L; thus, it approached the values of VRFB with 1.25 V and 15-40 Wh/L.[109] A capacity retention of 80% over 10,000 cycles was achieved. A capacity fade of 0.25% per cycle and 7.5% per day rate was estimated by Janoschka et al.[131] and Kwabi et al.[99] The authors attributed this significant capacity fading to side reactions of the methylviologen material.[131] Furthermore, only 75% of the theoretical capacity of the polymer redox material was accessible for charging/discharging leaving 25% unused. Thus, the polymerisation decreased the available capacity of the inserted material. To sum up, the polymerisation of the charge carrier material lowered the costs and hindered the intermembrane crossing but the capacity preservation suffered from material instability. The disadvantages of the catholyte polyTEMPO became apparent in a zinc/polyTEMPO HRFB

demonstrated by Winsberg et al[138]. Although this battery reached a high cell voltage of 1.7 V and an energy density of 8.1 Wh/L, polyTEMPO limited the current densities to low 20 mA/cm^2, and thus, slowing down the charging/discharging. Moreover, the capacity was restricted to low 2.4 Ah/L.

Another AORFB utilizing the water-soluble TEMPO derivative 4-hydroxy-2,2,6,6-tetramethylpiperidin-1yl)-oxyl TEMPOL (**204**) as catholyte with a potential 0.8 V vs. SHE (standard hydrogen potential electrode) and methylviologen (**203**) as anolyte with a potentials of -0.45 V was demonstrated by Liu et al[110] (Table 5, Entry 2). This battery was tested with a redox material loading of 0.5 M in 1 M NaCl solution and achieved a high cell voltage of 1.25 V and a CE >99% over 100 cycles. The capacity fade rates reached 0.1% per cycle but a tremendous 28% per day according to Liu et al.[110] and Kwabi et al.[99] This decay indicated the instability and/or the intermembrane crossing of the redox materials. Janoschka et al.[132] pointed out that the solubility of TEMPOL is limited to 0.5 M. Moreover, the hydroxy substituent of TEMPOL might be oxidized by TEMPOL itself in a side reaction yielding the ketone.
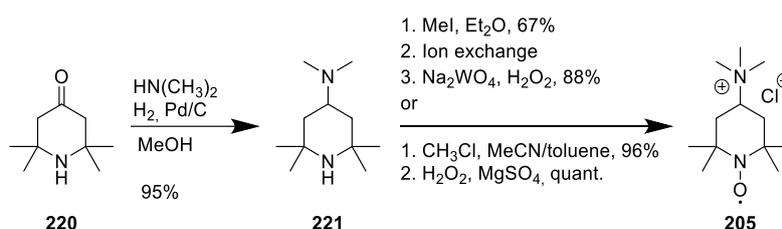
Scheme 73. Synthesis of TEMPTMA.[132]

Janoschka et al.[132] reduced the capacity decay to 0.02% per cycle, and 0.27% per day according to Janoschka et al.[132] and Kwabi et al.[99], by replacing TEMPOL with trimethyl *N,N,N,N*-2,2,6,6-heptamethylpiperidyloxy-4-ammonium chloride TEMPTMA (**205**) (Scheme 73, Table 5, Entry 3).[132] TEMPTMA was synthesized starting with the reductive amination of 2,2,6,6-tetramethyl-piperidin-4-one (**220**) with dimethylamine, hydrogen and palladium on charcoal as catalyst to **221**. Alkylation with methyl iodide, ion exchange and oxidation with sodium tungstate and hydrogen peroxide yielded TEMPTMA. The synthesis can be shortened to a two-step procedure by alkylation of **221** with methyl chloride under pressure and oxidation with hydrogen peroxide with magnesium sulfate. Compared to TEMPOL, the non-oxidizable trimmethylammonium group increased the stability, quadrupled the solubility, and increased the potential by about 150 mV to 1.00 V vs. SHE due to their electron-withdrawing effect.
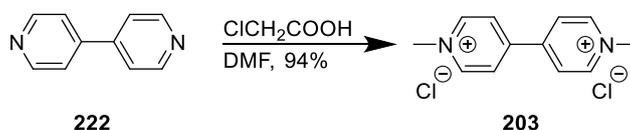
Scheme 74: Synthesis of methyl viologen.[139]

Methyl viologen (**203**) was synthesized via a the procedure published by Yang et al.[139] Treatment of 4,4'-bipyridine (**222**) with 2-chloroacetic acid in DMF yielded **203** (Scheme 74). The TEMPTMA/methyl viologen battery reached – with a solubility of 2 M of each charge-carrier material – a cell voltage of 1.4 V and an energy density of 38 Wh/L, which was in the range of VRFBs with 1.25 V and 15-40 Wh/L. The chloride anions of the anolyte and catholyte working as electrolytes even made an additional electrolyte dispensable. As the investigations only cover 100 charge/discharge cycles, the long-time stability of the materials remains unclear. DeBruler et al.[133] tried to benefit from the TEMPTMA and applied it together with 1,1'[(3-trimethylammonio)propyl]-4,4'-bipyridine (NPr)$_2$Vi (**206**) in an AORFB (Table 5, Entry 4). The additional ammonium groups should provide a higher water solubility of the viologen (NPr)$_2$Vi giving access to the second oxidation state with higher potential (E_1 = 0.35 V, E_2 = 0.72 V) during charging/discharging. This purpose was approved by measuring a high cell voltage of 1.7 V, which outcompete other AORFBs. However, the TEMPTMA/(NPr)$_2$Vi suffered from a capacity fade rate of 0.45% per day. Hu et al.[140] decreased the capacity fade rate to 0.2% by using only the (NPr)$_2$Vi radical and avoiding the unstable double reduced quinoid form of (NPr)$_2$Vi.

Subsequently in 2017, Winsberg et al.[99,134] improved the capacity fade rate of TEMPO derivatives with TEMPO-4-sulfate potassium salt (**207**) to low 0.0058% per cycle in a zinc/TEMPO-4-sulfate HRFB (Table 5, Entry 5).
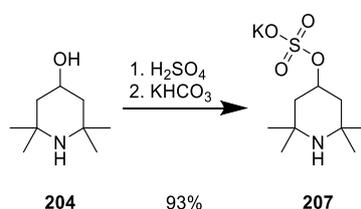
Scheme 75: Synthesis of TEMPO-4-sulfate.[134]

The switch to anionic TEMPO-4-sulfate was necessary because the zinc anolyte is not compatible with membranes used for cationic TEMPTMA. TEMPO-4-sulfate **207** was obtained after the treatment of TEMPOL **204** with sulfuric acid and potassium bicarbonate (Scheme 75). A potential of 0.8 V was achieved for TEMPO-4-sulfate. The zinc/TEMPO-4-sulfate battery reached a cell voltage of 1.7 V, a higher capacity of 26.7 Ah/L, a larger current density of 80 mA/cm^2 and a higher energy density of 20.4 Wh/L than the zinc/polyTEMPO battery. These physical parameters matched or even surpassed the energy density and cell voltage of the VRFB with 15-40 Wh/L and 1.25 V, respectively. Unfortunately, the capacity fade rate per day reached 1.38% according to Winsberg et al.[134] and Kwabi et al.[99], indicating material stability issues or membrane crossings of the TEMPO-4-sulfate.[99]
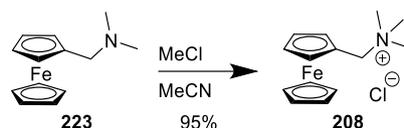
Scheme 76: Synthesis of FcNCl.[135]

As an alternative to TEMPO derivatives, Hu et al.[135] implemented (ferrocenylmethyl)trimethylammonium chloride FcNCl (**208**) with a potential of 0.61 V in an AORFB with methyl viologen (Table 5, Entry 6). This ferrocene derivative was synthesized via alkylation of (ferrocenylmethyl)dimethylamine with methyl chloride (Scheme 76).[135] This battery achieved a cell voltage of 1.05 V and an energy density of 7.0 Wh/L with a methyl viologen concentration of 0.5 M. A capacity retention of 91% over 700 cycles was reached at this concentration of methyl viologen.[135] The capacity fading rate was improved to of 0.01% per cycle and 0.22% per day according to Hu et al.[135] and Kwabi et al.[99]
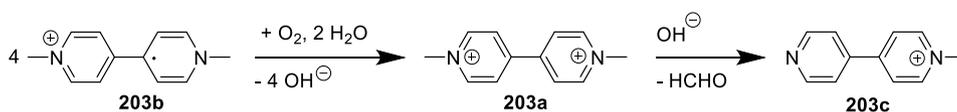
Scheme 77: Disproportionation of methylviologen under oxygen.[136]
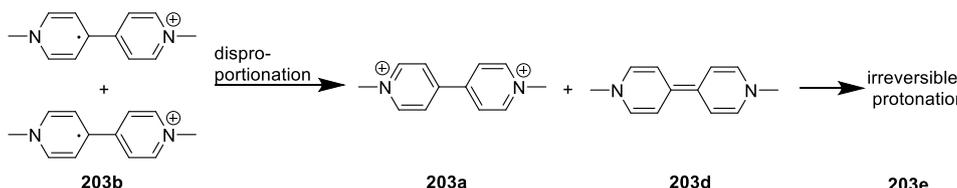
Scheme 78: Disproportionation of methylviologen without oxygen.[136]

Viologen concentrations higher than 0.5 M induced a greater capacity decay. For instance, at a methyl viologen concentration of 0.7 M, a capacity loss of 0.04% per cycle was observed. Investigations on ferrocenium, TEMPO and viologen redox material by Beh et al.[136] considered side reactions to be the reason for the capacity decay. In the case of viologens, a disproportionation reaction of the radical viologen during charging was proposed. In the presence of oxygen, four equivalents of the viologen radical **203b** reacted to hydroxide anions and four equivalents of **203a**, decreasing the amount of reduced viologen, and consequently, the capacity (Scheme 77). Further hydroxide anions demethylate **203a** in an irreversible reaction to formaldehyde and redox inactive 1-methyl-4,4'-(bipyridin)-1-ium chloride (**203c**) inducing further capacity loss. In the absence of oxygen, two radicals **203b** can dimerize and disproportionate to **203a** and water insoluble **203d**, which can further undergo irreversible reactions with protons to redox-inactive species **203e** (Scheme 78). The overall depopulation of active charge-carrier material resulted in a capacity decay.
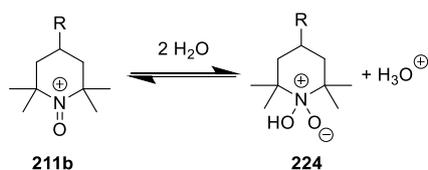
Scheme 79: Water splitting of oxidized TEMPO.[136,141]
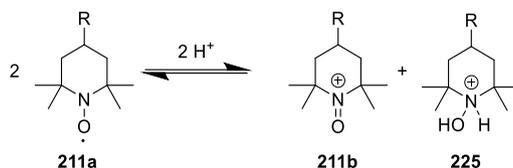
Scheme 80: Disproportionation reaction of TEMPO.[136,141]

The capacity decay was not limited to viologen, because TEMPO based materials also contributed charge-carrier material loss due to side reactions. Oxidized TEMPO and its derivates **211b** can split water, yielding **224** and an oxonium ion. This acid can react with TEMPO **211a** to oxidised derivatives **211b** and **225**. These side reactions decreased the overall catholyte amount and thus the capacity (Scheme 79 and 80). Furthermore, Singh et al.[125] pointed out that the membrane crossing of TEMPO derivatives is still an issue. In the case of ferrocenium-based redox materials, side reactions of two ferrocenium molecules with oxygen may occur. Alkyl substituents should stabilize ferrocene materials towards oxygen. The methyl trimethylammmonium substituted ferrocenes can be attacked by nucleophiles expelling trimethylamine. Beh et al.[136] considered the side reactions for ferrocene and viologen based materials and added trimethylpropyl ammonium chloride substituents (Table 5, Entry 7). In the case of the viologen derivative 4,4'-bis-(3-(trimethylammonio)propyl-bipyridinium tetrachloride BTMAP-Vi (**206**), the additional charges should supress the dimerization and following disproportionation due to repulsion. The same effect was proposed to protect the ferrocene derivative 1,1'-bis-((trimethylammonio)propyl) ferrocene BTMAP-Fc (**209**). These modifications of the materials led to a low capacity fading rate of 0.0057% per cycle and 0.1% per day of the BTMAP-Fc/BTMAP-Vi battery according to Beh et al.[136] and Kwabi et al.[99], which indicated a higher stability compared to previous viologen and ferrocene materials.
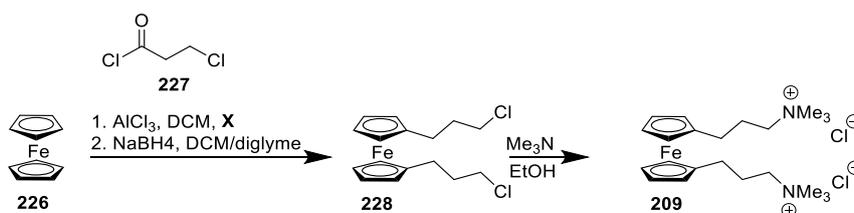
Scheme 81: Synthesis of BTMAP-Fc.
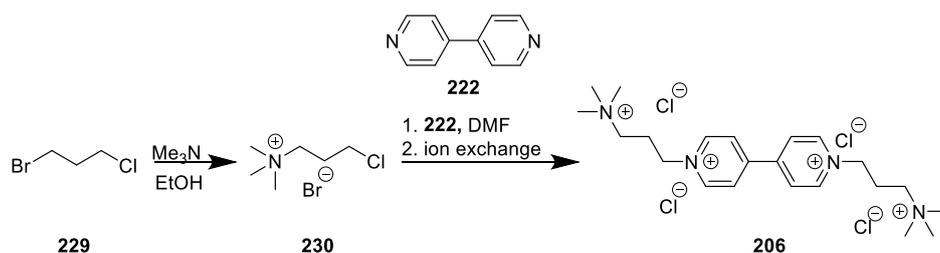
Scheme 82: Synthesis of BTMAP-Vi.

The synthesis of BTMAP-Fc started from ferrocene (**226**), which was subjected to a Friedel-Crafts-acylation with 3-chloro-propionyl chloride (**227**) and aluminium(III)-chloride as catalyst (Scheme 81). After subsequent reduction with sodium borohydride, the 1,1'-bis-(3-chloro)propyl ferrocene (**228**) was obtained. Nucleophilic substitution with trimethylamine yielded BTMAP-Fc **209**. Same reaction was used for starting the synthesis of BTMAP-Vi, as 3-bromo-1-chloropropane (**229**) was treated with trimethylamine yielding (3-chloropropyl)-trimethyl ammonium chloride (**230**) (Scheme 82). A further reaction with 4,4'-bipyridine (**222**) and further ion exchange yielded BTMAP-Vi **206**. The small difference between the potentials of BTMAP-Fc with 0.39 V vs. SHE and BTMAP-Vi with -0.36 V vs. SHE restricted the cell-voltage to 0.75 V. Moreover, the energy density only reached 13-20 Wh/L. In conclusion, the BTMAP-Fc/BTMAP-Vi was a stable material which did not match the cell voltage of 1.25 V, but which can reach the energy density of 15-40 Wh/L of the VRFB.
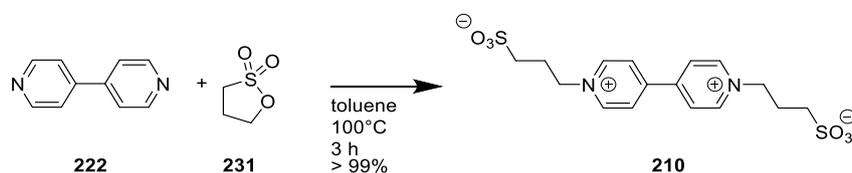
Scheme 83: Synthesis of (SPr)₂V.

DeBruler et al.[137] demonstrated 1,1'-(3-sulfonatopropyl)-4,4'-biypridinium (SPr)₂Vi (**210**) as anolyte and potassium triiodine/iodide as catholyte in an AORFB (Table 5, Entry 8). These anionic materials permitted the application of cation-selective membranes with higher conductivity instead of anion-selective membranes required for cationic viologen species. Therefore, higher current densities of up to 100 mA/cm² were achieved. The (SPr)₂Vi **210** was obtained by heating 4,4-bipyridin (**222**) with propane-1,3-sultone (**231**), and it and offered a potential of -0.43 V (Scheme 83). Potassium iodide/triiodide offered a potential of 0.57 V. The battery reached a cell voltage 1.0 V, which is lower than the parameter of VRFB with 1.25 V. A capacity retention of 94.1% over 300 cycles was obtained. A low capacity fade rate of 0.1% per cycle or 0.45% per day was estimated by DeBruler et al.[137] and Kwabi et al.[99] Side reactions of the materials were not observed. Therefore, these materials showed promising results which need to be investigated further. In summary, it can be stated that derivatives of viologen,

TEMPO and ferrocene offered redox materials in neutral pH electrolytes compared to the acidic or basic media of the quinone materials. As non-corrosive electrolytes were determined as the ideal goal in ORFB material development by Schubert et al.[10], viologen, TEMPO, and ferrocene outcompete quinone charge-carrier materials in terms of supporting electrolytes.

2.3.5 Aza-aromatics as Organic Redox Flow Battery Materials

Table 6: Bioinspired and other *N*-containing aromatic redox materials.

Entry	Anolyte material	Catholyte material	E^0_{Anode}|$E^0_{cathode}$ Cell voltage in [V]	Cycles	Concentration of Redox material and Electrolyte	Capacity retention Coulombic efficiency	Ref.
1	**232**	$[Fe(CN)_6]^{4-}/$ $[Fe(CN)_6]^{3-}$	-0.53| 0.40| 1.03	200	0.06 M in 1 M KOH/1.5 M nicotinamide	99.98% 99.7%	142
2	**233**	$[Fe(CN)_6]^{4-}/$ $[Fe(CN)_6]^{3-}$	-0.60| 0.40| 1.2	400	1 M in 1 M KOH	99% 99%	143
3	**234**	$[Fe(CN)_6]^{4-}/$ $[Fe(CN)_6]^{3-}$	-0.78| 0.40| N/A	N/A	N/A in 1 M KOH	N/A	113
4	**234**	$O_2/2OH^-$	-0.78| 0.40| 0.95	20	N/A in 2 M NaOH	N/A	144
5	**235**	$[Fe(CN)_6]^{4-}/$ $[Fe(CN)_6]^{3-}$	-0.82| 0.50| 1.4	500	2.8 in 1 M NaOH	N/A 99.98%	145
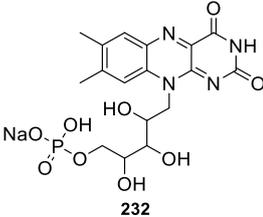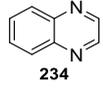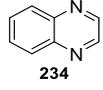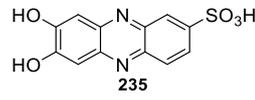
N/A: No Data available
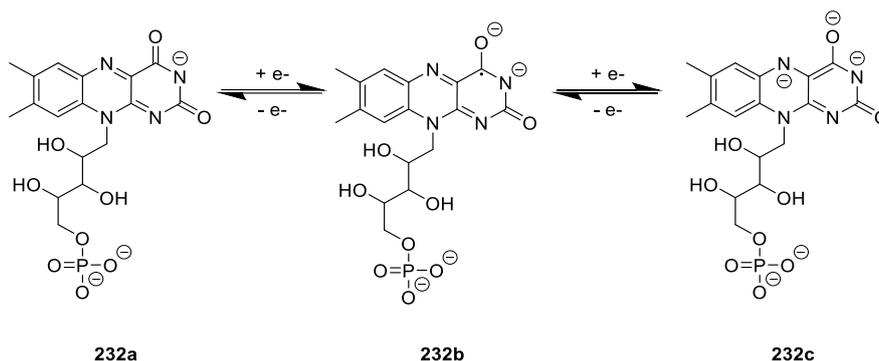
Scheme. 84: Redox chemistry of flavin mononucleotide.[142]

Alongside viologen derivatives, the class of aza-aromatics used in ORFBs were extended to alloxazines, quinoxalines and phenazines (Table 6).[113,142–145] The redox activity of the isoalloxazine moiety, widespread in enzyme cofactors such as flavins, inspired Orita et al.[142] to investigate flavin mononucleotide FMN (**232**) as redox material (Table 6, Entry 1). This charge-carrier material showed a potential of -0.5 V and provided a two-step redox process at a pH 14 in a 1 M KOH solution (Scheme 84). Nicotinamide, also known as Vitamin B$_3$, was necessarily added to increase the solubility of FMN. AORFB was developed with the FMN sodium salt as anolyte and potassium hexacyanoferrate as catholyte. At a FMN concentration of 0.24 M and 1 M of the additive, the battery reached a capacity retention of 99% over 200 cycles, a cell voltage of 0.96 V and an energy density of 4.83 Wh/L. The last two values are low compared to VRFB with 1.25 V and 15-40 Wh/L. The capacity fade rate of 0.02% per cycle and 0.6% per day, according to Orita et al.[142] and Kwabi et al.[99], were attributed to side reactions, which were not further investigated, rather than to membrane crossovers. As analogues to the battery of Orita et al.[142], Lin et al.[143] used 7/8-carboxy alloxazine ACA (**233**) as anolyte and iron hexacyanoferrate in an AORFB (Table 6, Entry 2). The ACA material provided a slightly lower redox potential of 0.62 V and a higher solubility of 0.5 M in 1 M KOH compared to FMN. This battery provided a cell voltage of 1.2 V and a capacity retention of 99.98% per cycle. In comparison to FMN, the capacity fade rate per cycle of 0.013% was lower, but the rate per day doubled to 1.2% according to Lin et al.[143] and Kwabi et al.[99] As an analysis of the material with ^{1}H-NMR spectroscopy supported the proposed hydroxide-induced ring-opening degradation reaction to redox-inactive species. To sum up, FMN and ACA redox material are examples of bioinspired AORFB materials that reached the cell voltage of VRFB. However, the FMN and ACA showed a moderate long-term stability and a low solubility. Stability was also the major problem of quinoxalines as redox materials. Milshtein et al.[146] suggested quinoxaline (**234**) as charge-carrier in AORFBs because of its low reduction potential of -0.78 V at pH 14, it seemed to be a promising anolyte candidate (Table 6, Entry 3). Unfortunately, a patent application using quinoxaline together with potassium hexacyanido

ferrate revealed a capacity fade of 100% per day according to Kwabi et al[99], which indicated a material degradation or membrane crossovers.[113] A later study of Leung et al.[144] demonstrated a quinoxaline/oxygen battery with 2 M NaOH as electrolyte (Table 6, Entry 4). The average coulombic efficiency of 81% over 20 cycles already indicated a capacity fade rate of 10% per day corresponding to Leung et al.[144] and Kwabi et al.[99] Side reactions and degradations or membrane crossing of the material might cause this capacity decay.[99,144] A smaller capacity fade rate was reached by Hollas et al.[145] with a battery using 7,8-dihydroxyphenazine-2-sulfonic acid DHPS (235) as anolyte and potassium hexacyanido ferrate as catholyte (Table 6, Entry 5). Hollas et al.[145] and Kwabi et al.[99] estimated a capacity fade of 0.02% per cycle and 0.68% per day.

Table 7: Bipolar materials in NAORFB.

Entry	Bipolar material	E^0_{Anode}| $E^0_{cathode}$| Cell voltage in [V]	Cycles	Redox material Concentration and Electrolyte	Capacity retention Coulombic efficiency	Ref.
1	236	0.5[a]| -2.0[a]| 2.5	20	8.41 g/dm³, PC, 1 M TBABF₄	N/A 78%	147
2	237	-1.98[a]| 0.74[a]| 1.3-2.3	3	0.05 M in MeCN/ Toluene, 0.1 M TBAClO₄	N/A 60-80%	148
3	238	-1.76[a]| 0.46[a]| 1.5 – 2	15	0.5 M in MeCN, 1 M TBAPF₆	N/A	149
4	239	-1.25| 0.37|[a] 1.62	75	PC, 0.5 M TBAPF₆	N/A/ 90%	150
5	240	N/A| N/A| 1.28	100	PC, 0.5 M TBAClO₄	N/A 89	151
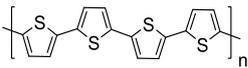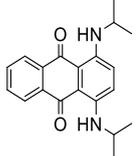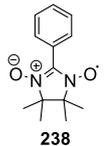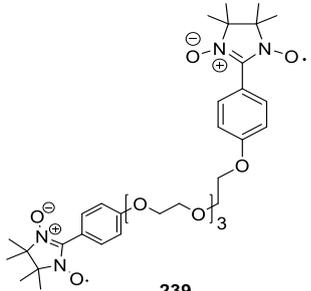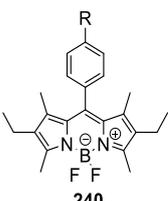
N/A: no data available; [a] vs. Ag/Ag⁺

The anolyte DHPS provided a high solubility of 1.8 M and a low potential of -0.81 V at pH 14. A capacity retention of 99.98% over 500 cycles and a voltage of 1.4 V were achieved with the DHPS/ potassium hexacyanoferrate battery. The capacity loss was attributed to membrane crossing of the material. The high voltage and the low capacity fade rates made DHPS a promising anolyte.

2.3.6 Bipolar Redox Flow Battery Materials

Bipolar materials provide at least two different redox potentials which can be utilised as catholyte or anolyte. Combining both functions in one material overcomes the crossing through the membrane, only inducing a coulombic efficiency decay and not a capacity loss during charging/discharging. In 2014, Oh et al.[147] investigated polythiophene polymer particles PT (**236**) as a biploar material in an NAORFB using propylene carbonate/tetraethylammonium tetrafluoroborate as electrolyte (Table 7, Enty 1). The cell voltage of 2.5 V was higher than the1.25 V of a VRFB, but the energy density of 2.7 Wh/L was lower than that of the VRFB with 15-40 Wh/L. A coulombic efficiency of 78% over 20 cycles was achieved. The PT/PT battery suffered from decreasing inner resistance and particle cluster formation blocking the channels. As another NAORB bipolar material, Potash et al.[148] implemented 1,4-di*iso*propylaminoanthraquinone (**237**), also known as Disperse Blue 134 (DB 134) (Table 7, Entry 2). This anthraquinone possesses four redox potentials at -1.98 V, -1.51 V, 0.25 V and 0.74 V vs Ag/AgCl expanding the theoretical cell voltage to 2.72 V, and consequently, also enlarging the capacity of the battery. Unfortunately, the accessible capacity of the battery was limited by the low solubility of DB 134 of 0.1 M in the electrolyte toluene/acetonitrile/TBAClO₄. The coulomb efficiency of 65% – 81% may indicate side reactions of DB-134. The battery reached a cell voltage of 1.3 V and a low energy density of 0.94 Wh/L. Compared to a VRFB with 1.25V and 15-40 Wh/L, the cell voltage was matched but the energy density was far too low.
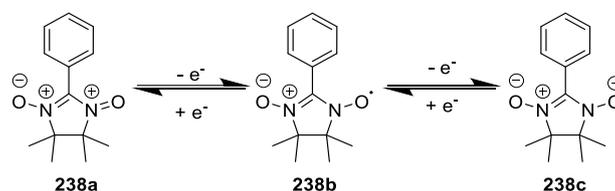
Scheme 85: Redox chemistry of PTIO.

A bipolar material with higher solubility in acetonitrile of up to 2.6 M provided 2-phenyl-4,4,5,5-tetramethyl-imidazolin-1-oxyl-3-oxide PTIO (**238**) (Table 7, Entry 3). This stable radical was suggested by Duan et al.[149] as bipolar material because it offers a reversible single electron reduction or oxidation step (Scheme 85). Despite the high solubility of PTIO in acetonitrile, a

low concentration of 0.5 M in acetonitrile/TBAPF$_6$ was used in a PTIO/PTIO battery setup. An energy density of 9 Wh/L during charge and 5 Wh/L during discharge was achieved and the coulombic efficiency reached 90% over 15 cycles. The capacity decay was attributed to side reactions of PTIO or material crossover while charging/discharging. The electric density and efficiency were better than the parameters of DB-134, but it still not matches the values of VRFB. Hagemann et al.[150] adopted the bipolar PTIO and linked two molecules of it with a polyethylene glycol chain NN/NN **239** to increase the solubility and the theoretical capacity (Table 7, Entry 4). Compared to single PTIO, the solubility of NN/NN in acetonitrile rose from 2.6 M to 3.8 M and it can store twice the number of electrons. The low concentrations of 0.1 M in acetonitrile/TBAPF$_6$ of NN/NN during the battery testing led to a low energy density of 4.1 Wh/L. High concentrations of up to 3.8 M were prohibited by the low solubility of the double-charged species of NN/NN. The NN/NN provided a catholyte potential of 0.37 V vs. AgNO$_3$ and an anolyte potential of -1.25 V vs. Ag/AgNO$_3$ generating a cell voltage of 1.62 V. This high voltage even outcompetes the VRFB with only 1.25 V. A coulombic efficiency up to 95% was reached. One major drawback was the low solubility of NN/NN which should be improved according to the authors.
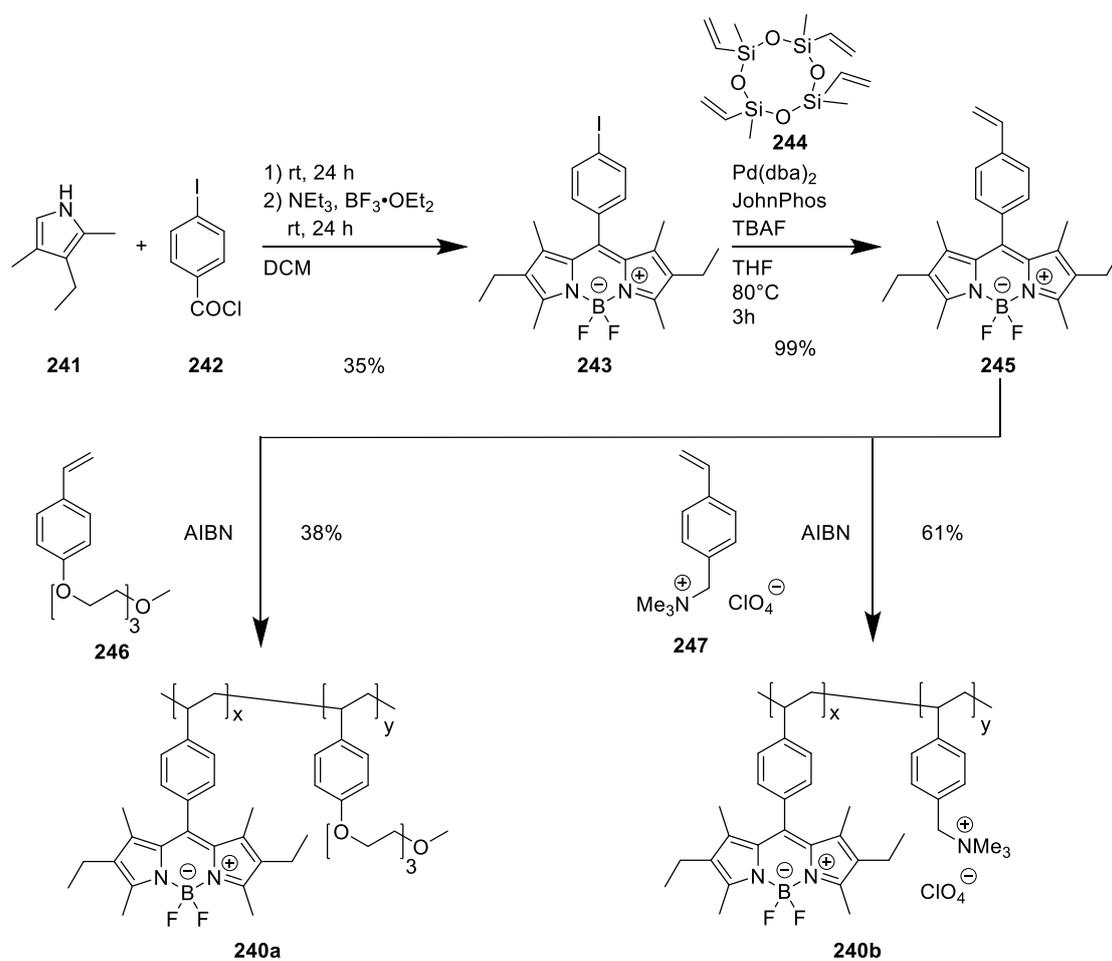
Scheme 86: Syntheses of poly-BODIPY materials.

A new and boron-based bipolar NAORFB was demonstrated by Winsberg et al.[151] with polymer linked boron-dipyrromethenes polyBODIPY **240**, offering potentials of -1.51 V and 0.69 V vs. AgNO₃ in propylene carbonate/0.1 M TBAClO₄, respectively (Scheme 86, Table 7, Entry 5).[151] The BODIPY core **243** structure was synthesized via the reaction of 3-ethyl-2,4-dimethylpyrrol (**241**) with 4-iodo benzoic acid chloride (**242**) and subsequent treatment with boron trifluoride etherate and triethylamine. The vinyl functionality of **245** was installed via palladium catalysed Hiyama cross coupling with vinyl siloxane **244**. After the copolymerisation of **245** with 4-vinylphenol triethylene glycol monomethyl ether (**246**) and (4-vinylbenzyl) trimethylammonium perchlorate (**247**), the materials **240a** and **240b** were obtained. In the final battery setup, **240a** was the anolyte, and **240b** was the catholyte. The **240a/240b** battery reached a discharge voltage of 1.28 V on average and an overall coulombic efficiency of 89%. Unfortunately, a capacity decay of more than 30% over the first 10 cycles of 100 charging/discharging cycles was observed, which needs to be investigated further.

Table 8. Bipolar material in AORFB.

Entry	Bioplar material	E^0_{Anode}|$E^0_{cathode}$ in [V]	Cycles	Concentration of Redox material and Electrolyte	Capacity retention Coulombic efficiency	Ref.
1	**248**	-0.6|0.8|1.2	1800	0.5 M NaCl + 10% diglyme	80% 98.3%	152
2	**249**	-0.49|0.7|1.16		0.1 M in 0.3 M NaCl + 20% EDC	N/A	153
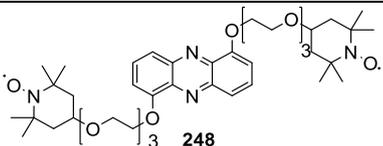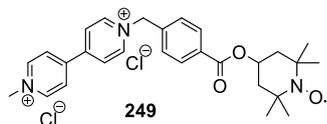
Beside the non-aqueous bipolar material, Schubert et al.[152,153] developed water-soluble bipolar redox materials in order to minimize the costs and environmental hazards. Winsberg et al.[152] started by connecting phenazine anolyte and TEMPO catholyte via a triethylene glycol TEG linker in charge-carrier **248** (Table 8, Entry 1). This redox material offered a reversible two electron reduction or oxidation step at a potential of -0.39 V and 0.81 V vs. SHE (Scheme 87).
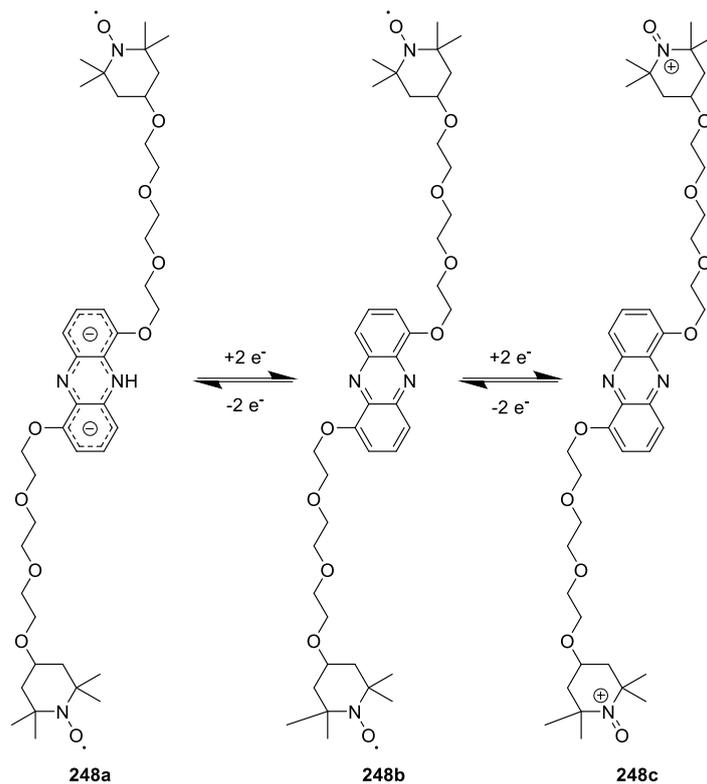
Scheme 87: Redox chemistry of phenazine-TEG-TEMPO material.
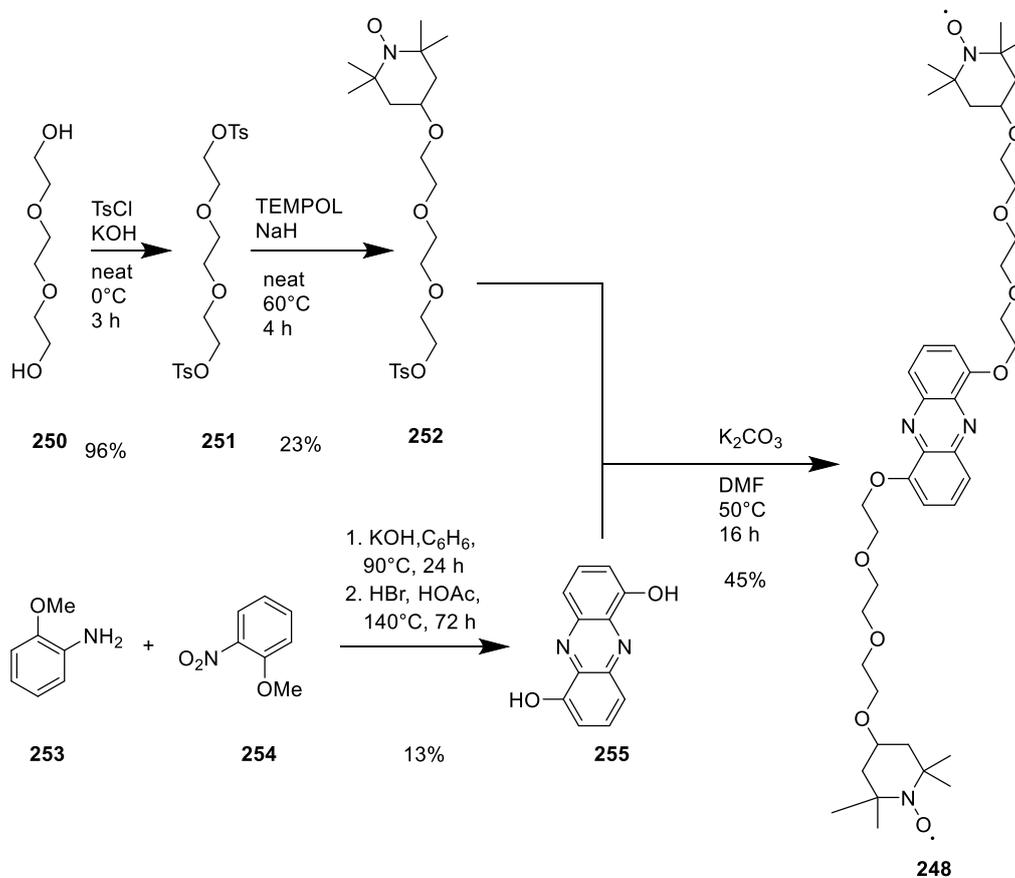
Scheme 88: Synthesis of phenazine-TEG-TEMPO material.

Material **248** was produced in a convergent synthesis in which the TEMPO-TEG-linker **252** and the dihydroxyphenazine **255** were connected in the last step (Scheme 88). TEMPO-TEG-linker synthesis **252** started with the tosylation of triethylene glycol (**250**) to **251** and the treatment with deprotonated TEMPOL. A Wohl-Aue reaction[154] of 2-methoxyanilin (**253**) and 1-methoxy-2-nitrobenzene (**254**) and a subsequent demethylation with hydrobromic acid yielded the 1,6-dihydroxy phenazine (**255**). After the nucleophilic substitution of **252** and **255**, material **248** was obtained. A battery charged with 10 mM **248** in 0.5 M NaCl solution with 10% diglyme as solubility-enhancing additive underwent 1,851 charge/discharge cycles. A cell voltage of 1.2 V and a coulomb efficiency of 98.3% were achieved.[125] A drawback of the **248** material is the low energy efficiency less than 50% resulting from the slow phenazine kinetics. A capacity fade rate of 0.011% per cycle and 0.62% per day according to Winsberg et al.[152] and Kwabi et al[99] may have resulted from a continuous degradation of the redox material previously described for TEMPO based materials.
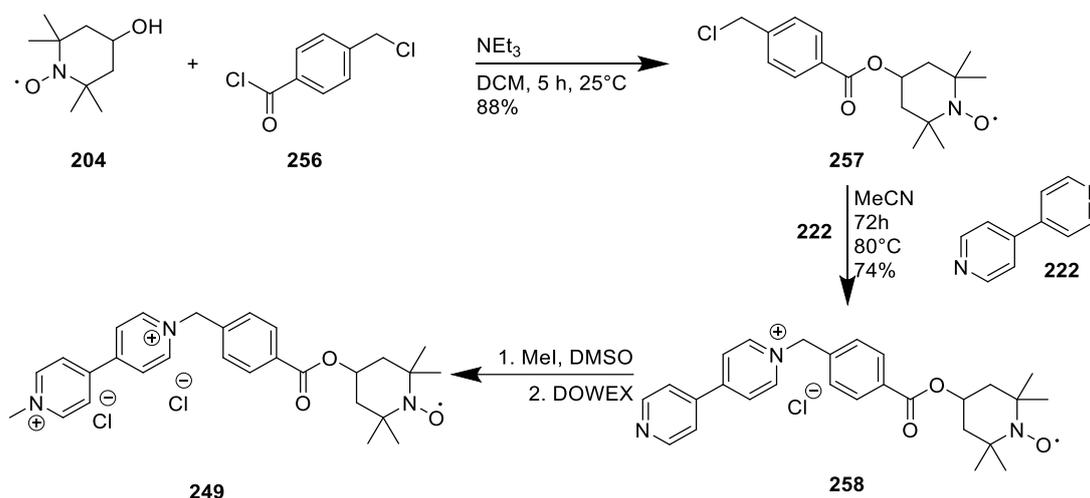
Scheme 89: Synthesis of VIOTEMP.[153]

As another water-soluble bipolar redox material, Janoschka et al.[153] developed 1-(4-(((1-oxyl-2,2,6,6-tetramethylpiperidin-4-yl)oxy)carbonyl)benzyl)-1′-methyl-[4,4′-bipyridine]-1,1′-diium-chloride VIOTEMP **249** by combining viologen and TEMPO with a linker (Table 8, Entry 2). The synthesis of VIOTEMP started with the esterification of TEMPOL (**204**) and 4-(chloromethyl)-benzoyl chloride (**256**) yielding **257** (Scheme 89). Viologen was installed by adding 4,4'-bipyridin (**222**) to **257** and subsequent treatment with methyl chloride followed by ion-exchange. The low solubility of the radical viologen species of VIOTEMP required ethylene carbonate as solubility enhancer. VIOTEMP was investigated with 0.1 M in phosphate or acetate buffer and showed a potential of 0.67 V and -0.49 V. Unfortunately, during the charge/discharge cycling, a capacity decay was observed, which indicates side reactions of VIOTEMP. Therefore, VIOTEMP is not suitable as an ORFB material.

2.4 Previous Research in the Wegner Group

2.4.1 Bidentate Boron Catalysis with Phthalazines

The foundation of the bidentate boron Lewis acid catalysis was set up by Siebert et al.[155–157], who synthesized the 9,10-dihydroboraanthracene moiety and conducted metal coordination studies. Later, Kaufmann and et al.[158,159] optimized the synthesis of 9,10-dihydoboraanthracenes via *ipso*-subsitution of an organosilanes with boron trichlorides. This preparation was simplified to a three-step synthesis by Kessler et al.[4,160,161]: A silylation of 1,2-dibromobenzene (**259**) via Grignard reaction to 1,2-bis-(trimethylsilyl)-benzene followed by the insertion of boron trichloride led to 9,10-dichloro-9,10-dihydro-9,10-boraanthracene (**261**), which was converted into Lewis acid 9,10-dimethyl-9,10-dihydro-9,10-boraanthracene (**262**) via methylation with trimethylaluminium (Scheme 90).
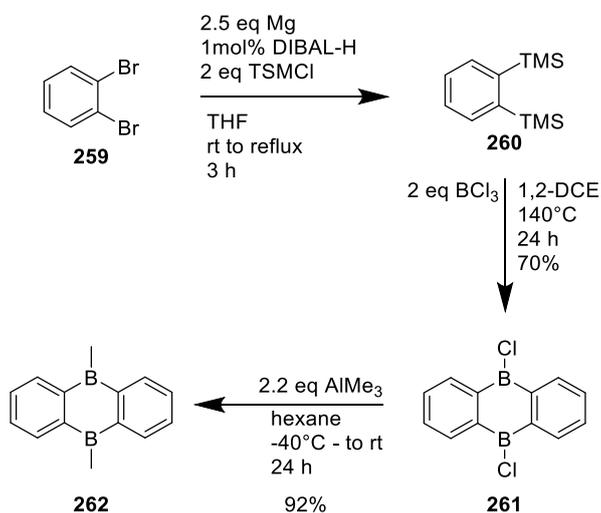
Scheme 90: The optimized bidentate boron Lewis acid synthesis by Kessler et al..[4,160]
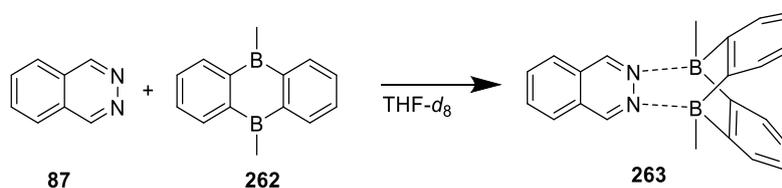
Scheme 91: Coordination between phthalazine and bidentate boron Lewis acid.[160]
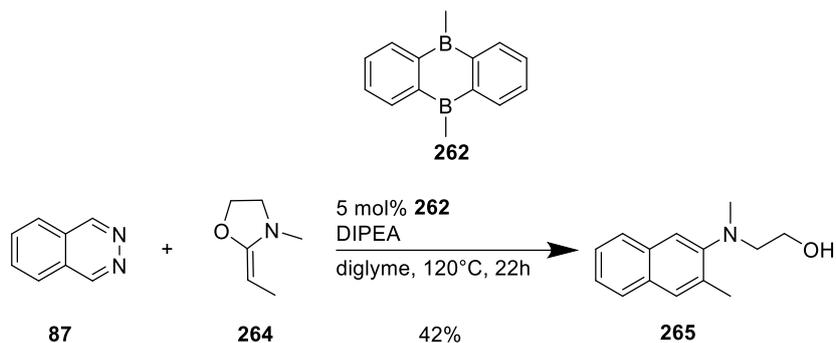
Scheme 92: Lewis acid catalysed IEEDA reaction of phthalazine and oxazolidine.[3]

The coordination of this bidentate boron Lewis acid **262** with phthalazine (**87**) was observed in ^{1}H-NMR, which had been predicted by computational studies (Scheme 91). As the computational studies indicated a decrease of the LUMO energy of the boron Lewis acid coordinated phthalazine, an IEDDA reaction with an electron-rich dienophile should occur. Therefore, the Lewis acid catalysed IEDDA reaction of oxazolidine (**264**) and phthalazine (**87**) was investigated. As a successful result of this reaction the IEDDA product naphthalene **265** was obtained (Scheme 92).[3]
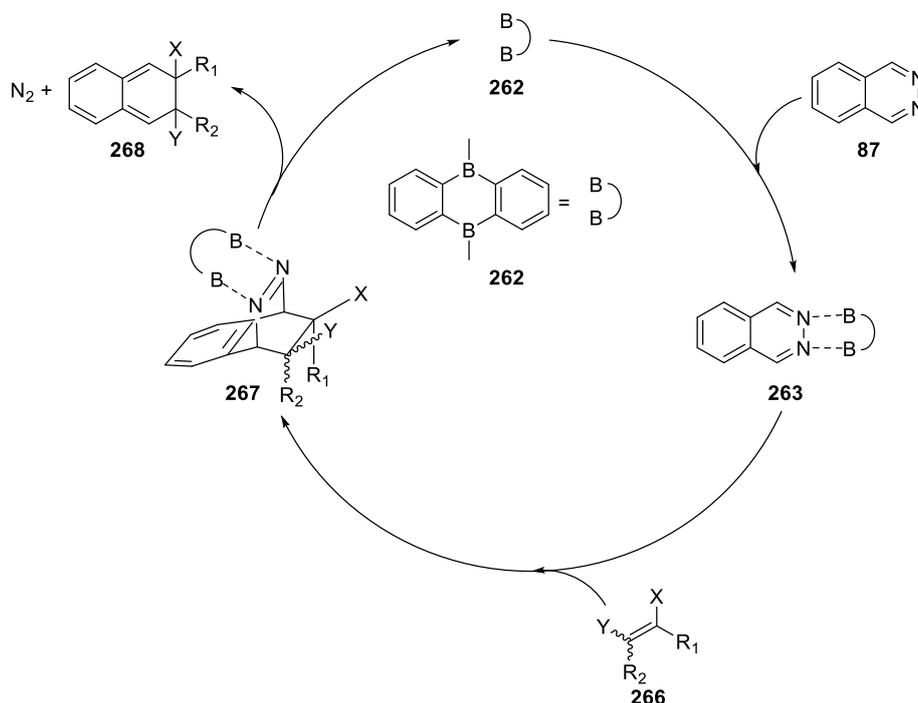
Scheme 93: Reaction mechanism of the bidentate boron Lewis acid catalysed IEDDA reaction.[3]

The mechanism proposed for this catalysed IEDDA reaction started with the complexation of phthalazine (**87**) bidentate boron Lewis acid **262** (Scheme 93). The decreased LUMO energy of the **87** enabled dienophile **266** to undergo a cycloaddition to **267**. The subsequent expulsion of nitrogen is the thermodynamic reason for obtaining **262** back, enabling the catalytic cycle, and the reactive *o*-quinodimethane **268**.
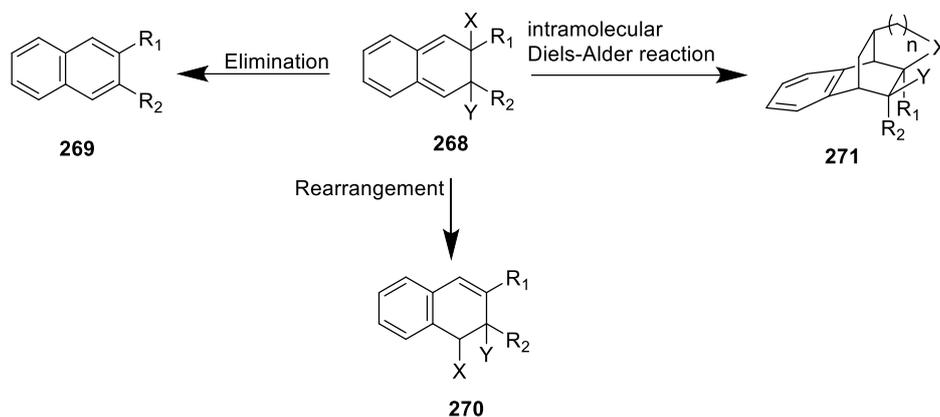
Scheme 94: Stabilization reactions of the *o*-quinodimethane.[3–6]

Depending on the substrate, this highly reactive species **268** undergoes elimination to naphthalene **269**, rearrangements to styrenes **270**, or intramolecular Diels-Alder reactions to multicycles **271**, to gain aromaticity for stabilisation (Scheme 94). The substituents of the *o*-quinodimethane determine which reaction occurs.
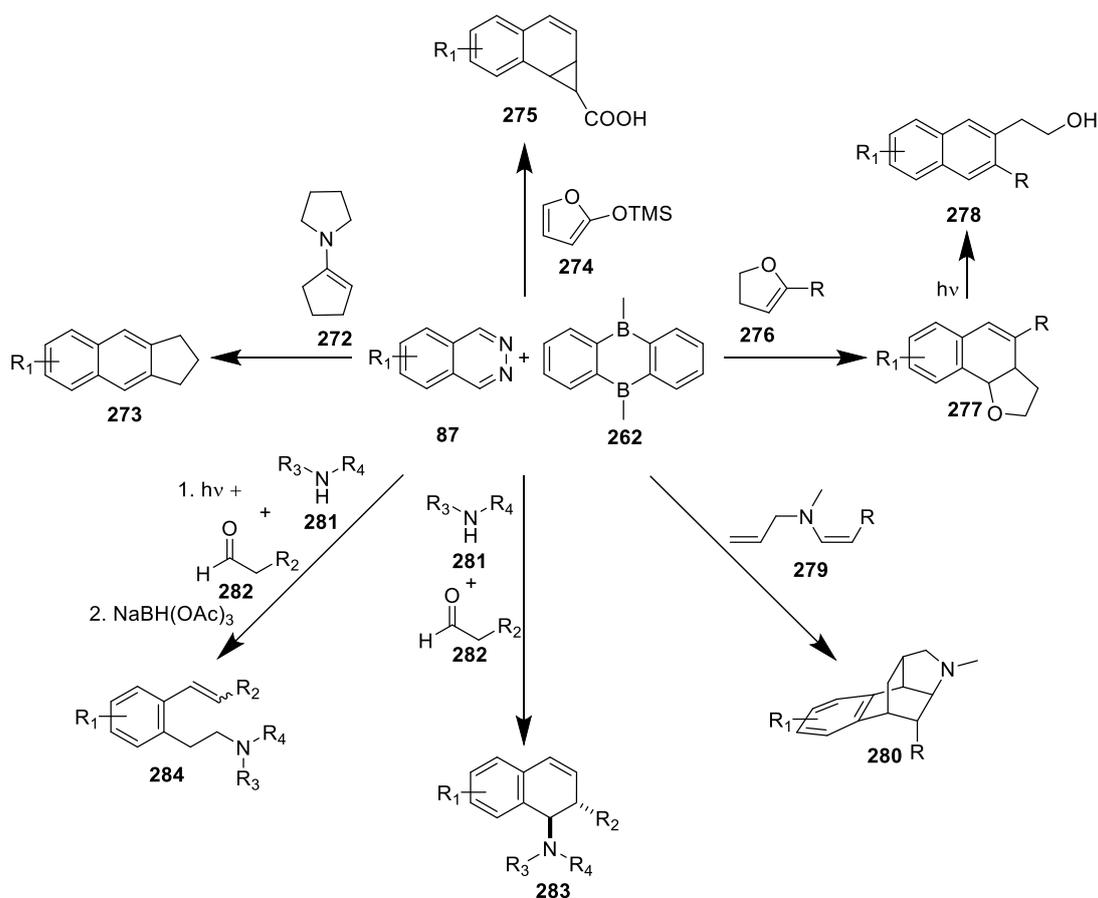
Scheme 95: Diversity of the bidentate Lewis acid catalysed IEEDA reaction of phthalazine.[3–8]

Kessler et al.[3–5,160] studied the reaction of **87** and **262** with enamines, e. g. **272**, 2-siloxy-furans **274**, and 5-alkyl-2,3-dihydrofurans **276** (Scheme 95). In the case of enamines, naphthalenes **273** were obtained after elimination. The 2-siloxy-furans **274** and 5-alkyl-2,3-dihydrofurans **276** underwent rearrangements to cyclopropanes **275** and furans **276**, which can be converted via *UV*-light into (2-hydroxyethyl)-naphthalenes **278**.
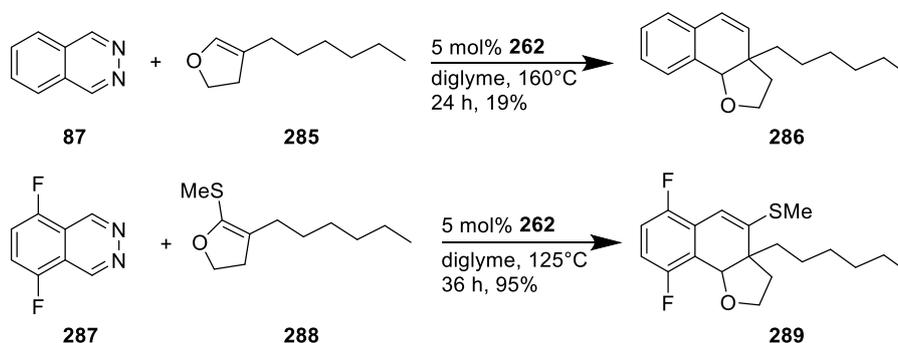
Scheme 96: IEDDA/domino reactions of 4-hexyl-2,3-dihydrofuran.

First experiments with 4-hexyl-2,3-dihydrofuran (**285**) and 4-hexyl-5-thiomethyl-2,3-dihydrofuran (**288**), and **87** and 5,8-difluorophthalazine (**287**) yielded the rearrangement

products **286** and **289** (Scheme 96). Schweigerhauser et al.[6] showed that enamines with additional alkenes **279** reacted to multicycles **280** via intramolecular DA reaction of *o*-quinodimethane (Scheme 95). More refined reaction parameters in the reaction with enamines generated *in situ*, generated from amine **281** and aldehydes **282**, allowed Ahles et al.[7] to favour the rearrangement over elimination, obtaining styrene amine **283**. Additional UV-light opened the *o*-quinodimethane, and subsequent treatment with sodium triacetoxy borohydride led to amines **284**.[8]

2.4.2 Synthesis of Diazaanthraquinones via catalysed IEDDA reaction

As widespread biological substances[162], drugs[163], and dyes[164], anthraquinones offer electrochemical redox capabilities that make them suitable as organic redox materials for RFBs.[127] In this compound class, especially the 2,3-diazaanthraquinones were only accessible via a multistep synthesis by Krapcho et al.[165] and Hassan et al.[166] Hong et al.[9] simplified their synthesis to a one-step procedure by applying the bidentate boron Lewis acid catalysed IEDDA reaction. Exposing 1,2,4,5-tetrazine (**79**) and 1,4-naphthoquinones **290** to the bidentate boron Lewis acid as pyridazine complex yielded 2,3-diazaanthraquinones **292** (Scheme 97).
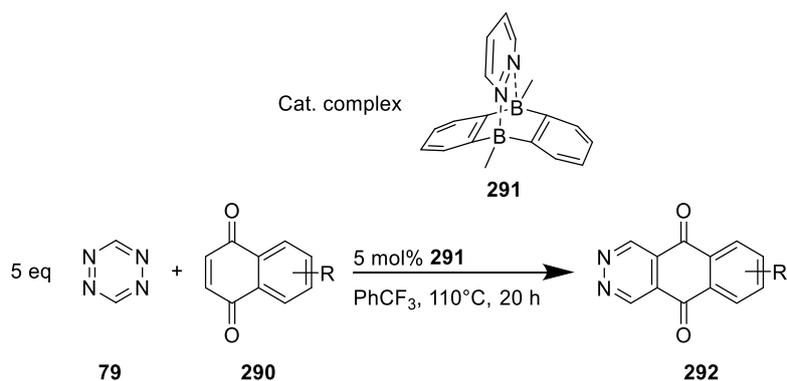
Scheme 97: Synthesis of diazaanthraquinones via IEDDA reaction.[9]
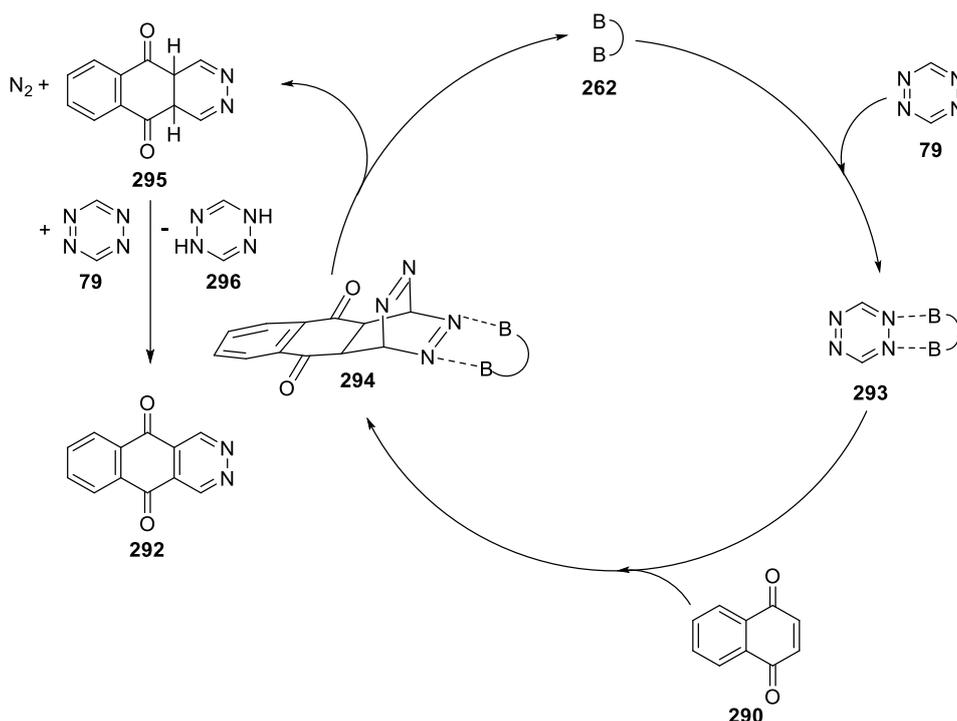
Scheme 98: Mechanism of the 2,3-diazaanthraquinone IEEDA Lewis acid catalysis.[9]

The reaction mechanism is proposed analogously to the phthalazine based catalysis: the bidentate boron Lewis acid **262** coordinated to the 1,2,4,5-tetrazine (**79**) and decrease its LUMO energy level (Scheme 98). Therefore, this complex **293** was enabled to undergo cycloaddition with naphthoquinone. The following expulsion of nitrogen was the thermodynamic driving force of the reaction. The generated dihydro-diazaanthraquinone **295** was oxidized by excess tetrazine (**79**) to diazaanthraquinone **292**. The 1,2-diazine functionality of the 2,3-diazanthraquinones **292** was exploited to perform another bidentate boron Lewis acid catalysed IEDDA reaction with electron-rich dienophiles **297**. This procedure enabled the synthesis of substituted anthraquinones **298** (Scheme 99).[9]
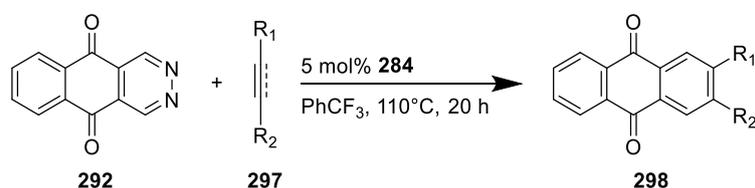
Scheme 99: Anthraquinone synthesis starting from 2,3-diazaanthraquinone via catalysed IEDDA reaction.[9]

64

3. Objectives of the Thesis

3.1 Domino IEDDA Reaction of Phthalazines and Dihydrofurans

Kessler et al.[4] reported the bidentate boron Lewis acid catalysed IEDDA reaction of phthalazine (**87**) and 5-alkyl-2,3-dihydrofurans **276** (Scheme 100). After the domino rearrangement of *o*-quinodimethane **299**, the tetrahydrofurans **300** were exposed to UV-light, and thus, converted into the naphthalene product **301** via elimination. This subsequent rearomatization reaction should be prevented by a non-hydrogen substituent R_2 from dihydrofuran **302**, because the generated quaternary carbon atom cannot form an aromatic bond. Therefore, the *o*-quinodimethane **303** should only rearrange to styrene **304**.
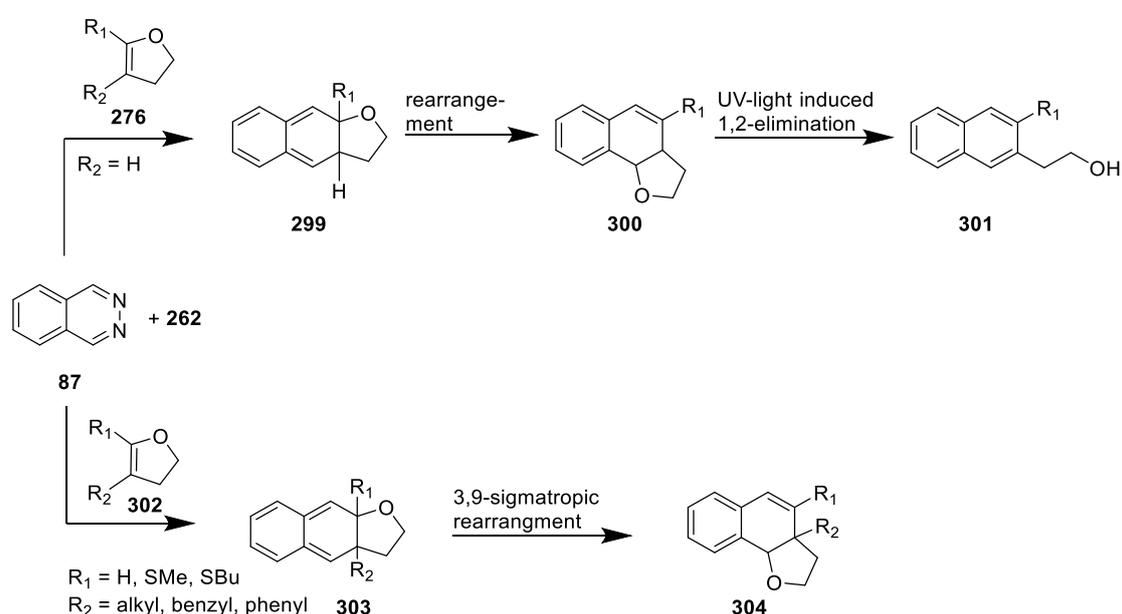
Scheme 100: Products of the domino/IEDDA reaction depending on the substitution pattern.

The first objective of this thesis consists in conducting an explorative study of 4-substituted-2,3-dihydrofurans in the bidentate IEDDA Lewis acid catalysed reaction with phthalazine. For the investigation of the domino/IEDDA reaction, phenyl, benzyl and alkyl chain substituted dihydrofurans were selected to explore the influence of sterical and electronical effects. A further sulphur substituent of R_1 on the enol ether **296** increases the sterical bulkiness of the dienophile, which kinetically hinders the IEDDA reaction. However, the IEDDA reaction is facilitated thermodynamically by an enlarged electron density due to the electron-donating effect of the sulphur substituent. Therefore, the influence of the sulphur substituent of R_1 of **302** should be investigated; the question is whether it thermodynamically enhances or kinetically hamper the IEDDA reaction. These studies require the synthesis of the catalyst **262** and substituted 2,3-dihydrofurans and phthalazines as starting materials.

3.2 Synthesis and Properties of the Redox Flow Battery material

The second objective of this thesis focuses on the synthesis and investigation of redox active compounds as prospective ORFB materials. To begin with, synthetic approaches to sustainable vanillin-based redox materials should be investigated. Retrosynthetic analysis and literature research result in quinone-based materials and indigo, well-known for redox properties, derivatives that constitute promising targets of vanillin derived redox materials.[167–171] These materials should by synthesized and the electrochemical properties should be investigated. Second, further ORFB materials should be synthesized, predominately via the bidentate boron Lewis acid catalysis of IEDDA reactions. Using this method according to Hong et al.[9], the 2,3-diazaanthraquinones should be synthesized from 1,2,4,5-tetrazine (**79**) and naphthoquinones **290**, and their electrochemical properties should be investigated by Jonas. D. Hofmann from Janek group (Scheme 101).
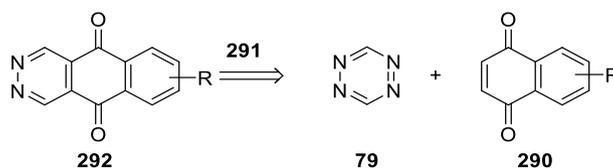
Scheme 101: Planned diazaanthraquinone synthesis.

Compared to other anthraquinone ORFB materials, the electron withdrawing diaza-unit might increase the potentials of the diazaanthraquinones. According to the results of Er et al.[118], the potentials are expected to increase even more by switching from the anthraquinone to the naphthoquinone moiety. Increased potentials are highly desirable for quinone-based catholyte materials because there is a need for a material that fulfils the criteria high potentials and stability during redox cycling.[172]
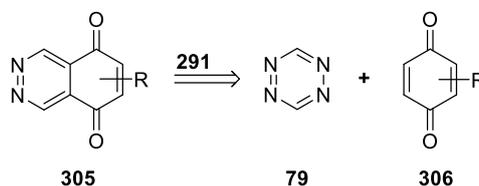
Scheme 102: Planned synthesis of 5,8-dihydroxyphthalazine.

Therefore, 2,3-diazanapthoquinones DNQ **305** should be synthesized via a bidentate boron Lewis acid catalysed IEDDA reaction by studying the catalysed reaction of 1,2,4,5-tetrazine (**79**) and 1,4-benzoquinones **306** (Scheme 102). This more versatile synthetic approach should extend the rare synthesis of 2,3-diazanaphthoquinones DNQ of Paige et al.[173] and Ryu et al.[174] The electrochemical properties of the targeted 2,3-diazanaphthoquinones should be

investigated by Jonas. D. Hofmann from Janek group. The substitution pattern of the tetrazine and quinones should be modified to explore the opportunities in synthesis for altering electrochemical potentials and for developing stable ORFB material, preferentially for catholyte materials with high potential.
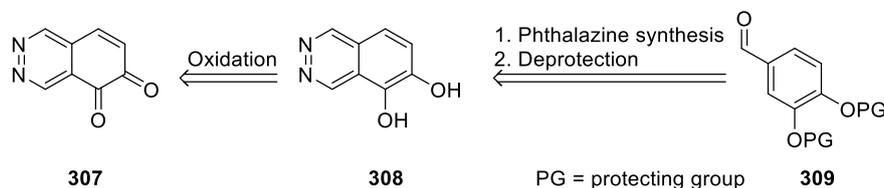
Scheme 103: Planned synthesis of dihydroxyphthalazines and oxidation to diazanaphthoquinones.[175]

According to the results of Er et al.[118], the 5,6-diazanaphthoquinone DNQ **307** was expected to have a higher potential than 5,8-DNQ **305**. Therefore, 5,6-dihydroxyphthalazine 5,6-DHP **308**, the reduced form of **307**, should be synthesized and the electrochemical properties should be compared to 5,8-DNQ/DHP (Scheme 103). The 5,6-DHP **308** should be accessible via Kessler et al.'s[161] phthalazine synthesis of protected protocatechualdehyde **309** and subsequent deprotection.

4. Results

4.1 IEDDA-Domino Reaction

4.1.1 Synthesis of Starting Material for IEDDA-Domino Reactions

The required catalyst **262** and phthalazines for the IEDDA-domino reaction were synthesized according to a procedure by Kessler et al.[3] The synthesis of the catalyst started with a *Grignard* reaction of 1,2-dibromobenzene (**259**) and trimethylsilyl chloride TMSCl to the 1,2-bis-(trimethylsilyl)benzene (**260**) (Scheme 104). After the treatment of **260** with boron trichloride, the 9,10-dichloro-9,10-dihydro-9,10-diboraanthracene (**261**) was obtained. The subsequent methylation with trimethylaluminium yielded the 9,10-dimethyl-9,10-dihydro-9,10-diboraanthracene (**262**).
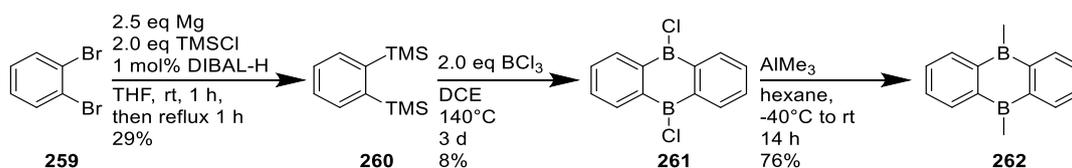
Scheme 104: Synthesis of the boron bidentate catalyst.[3]

The required phthalazines were synthesized via Kessler et al.'s[4] one-pot *ortho*-lithiation procedure. Substituted benzaldehydes **314** were treated with lithium amides **311** or **313** of

bis-(2-methoxyethyl)amine (**310**) or *N,N,N*-trimethylethylendiamine (**312**) to obtain a chelate complex which facilitated the *ortho*-lithiation with *n*-butyllithium BuLi (Scheme 105, 106). Adding DMF led to the *ortho*-dialdehydes which were transformed *in situ* with hydrazine into the phthalazines **315**. With this procedure, the 5,8-difluorophthalazine (**287**), the 5,8-dichlorophthalazine (**315**), the 5-fluorophthalazine (**315a**) and the 6-fluorophthalazine (**315c**) were obtained (Table 9, Entry 1-3).
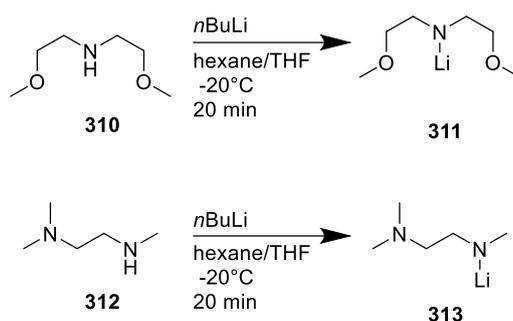
Scheme 105: Synthesis of the non-isolated lithiated amides.
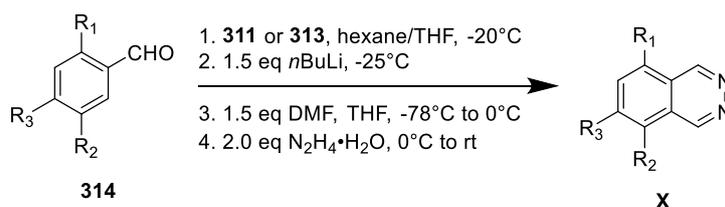
Scheme 106: Synthesis of phthalazines.[161]

Table 9: Yields of synthesized phthalazines.

Entry	Structure **X**	Amide	R_1	R_2	R_3	yield [%]
1	**287**	**311**	F	F	H	24
2	**315**	**311**	Cl	Cl	H	21
5	**315a**	**311**	F	H	H	24
4	**315b**	**311**	H	H	F	67
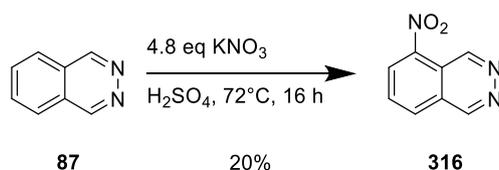
Scheme 107: Synthesis of 5-nitrophthalazine.[176]

Since 5-nitrophthalazine (**316**) was not accessible via Kessler et al.'s[161] phthalazine synthesis, a procedure by Shaikh et al.[176] was used (Scheme 107). Nitration with potassium nitrate in

sulfuric acid transformed phthalazine (**87**) into **316**. Alongside the catalyst and the phthalazines, the 2,3-dihydrofurans were synthesized as further starting material. Phenyl-, benzyl-, hexyl-, and methyl-substituted 2,3-dihydrofurans were envisaged to explore the influence of different degrees of steric bulkiness and electronic properties on the outcome of the reaction. The 4-phenyl-2,3-dihydrofuran was synthesized by Botteghi et al.[177] via a rhodium-catalysed carbon monoxide insertion in cinnamyl alcohol, and by de Felice et al.[178] via a Heck-type palladium arylation of 2,3-dihydrofuran on a small NMR-scale, respectively. The metal-catalysed cross-coupling was selected as the most suitable method because handling of toxic carbon monoxide gas under pressure was circumvented.
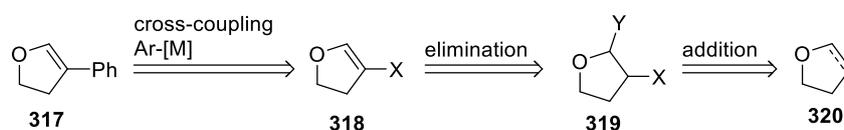
Scheme 108: Retrosynthesis of 4-phenyl-2,3-dihydrofurans.

Therefore, a metal-catalysed cross-coupling between an organometallic aryl compound and the 4-halogen-2,3-dihydrofuran **318** to obtain 4-phenyl-2,3-dihydrofuran (**317**) was planned according to a procedure of Czaplik et al.[179] (Scheme 109). The halogenation of dihydrofuran or tetrahydrofuran **320** and the subsequent elimination of dihalogen cmpound **319** should give access to **318**.
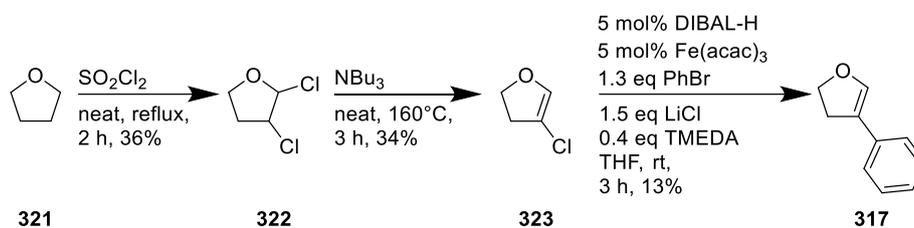
Scheme 109: Synthesis of 4-phenyl-2,3-dihydrofuran.

The synthesis of 4-phenyl-2,3-dihydyrofuran (**317**) started with the dichloronation of THF **321** with sulfuryl chloride to 2,3-dichlorotetrahydrofuran (**322**) according to a procedure of Nersasian.[180] The following elimination with tributylamine as base yielded the 4-chloro-2,3-dihydrofuran (**323**) as described by Schlosser et al.[181] (Scheme 109). After the iron(III)-acetylacetonate catalysed cross-coupling of **323** with in-situ generated phenyl magnesium bromide according to Czaplik et al.[179], **317** was obtained in a low yield of 13% due to not optimized reaction conditions. The benzyl, hexyl and methyl substituents should be installed according to a procedure of Zenk and Wiley[182] which was modified by Kessler et al.[160] (Scheme 110).

The target dihydrofurans **324** can be obtained by the reduction of *α*-substituted-*γ*-butyrolactones **325** with DIBAL-H and the subsequent elimination with methanesulfonyl chloride. Enolate substitution reactions of γ-butyrolactone GBL (**326**) should give access to **325**.
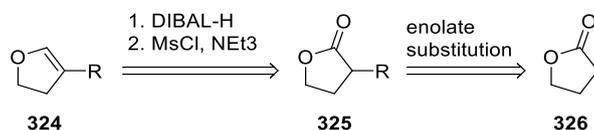
Scheme 110: Retrosynthesis of 2,3-dihydrofurans.
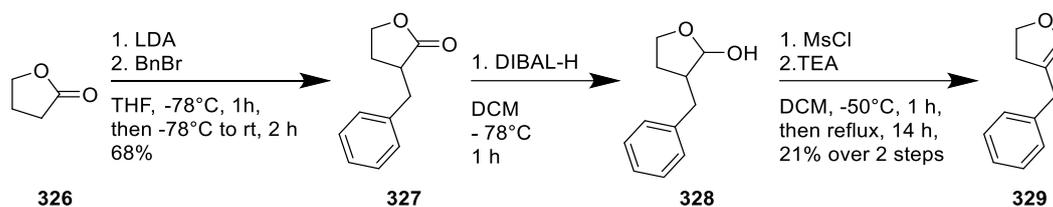
Scheme 111: Synthesis of 4-benzyl-2,3-dihydrofuran.

Analogous to Casavant et al.[183], the targeted enolate was obtained by the deprotonation of GBL (**326**) with lithium di*iso*propyl amide LDA (Scheme 111). The subsequent treatment with benzyl bromide yielded the *α*-benzyl-*γ*-butyrolactone (**327**). After the reduction of lactone **327** to lactol **328** with di*iso*butylaluminiumhydride DIBAL-H, mesylation and elimination with triethylamine TEA 4-benzyl-2,3-dihydrofuran (**329**) was obtained.
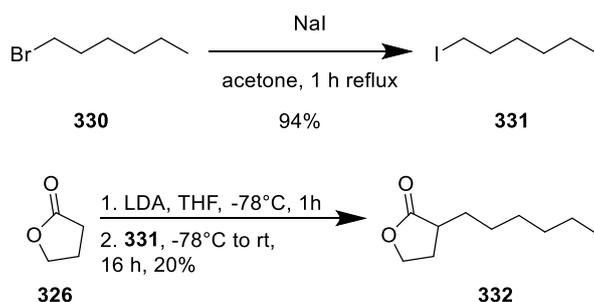
Scheme 112: Synthesis of 1-iodohexane and direct alkylation of GBL with 1-iodohexane.[184]

The synthesis of 4-hexyl-2,3-dihydrofuran was attempted analogous to the procedure of *α*-benzyl-GBL and Kessler et al.[160] Deprotonation of GBL **326** with LDA and treatment with 1-iodohexane (**331**), generated via a Finkelstein[184] reaction of 1-bromohexane (**330**) with sodium bromide, yielded *α*-hexyl-*γ*-butyrolactone (**332**) in low yield of 20% (Scheme 112). Moreover, this reaction could not be upscaled to over 20 mmol. Therefore, large amounts of starting material for IEDDA reaction were not synthesizable via this synthetic method. This experimental result of low yields in direct alkylation of GBL was confirmed by Posner et al.[185],

who also obtained poor yields with butyl iodide. Therefore, a new synthetic pathway was necessary. The procedure of Zenk and Wiley.[182] used *α*-ethylcarboxy-*γ*-butyrolactone (**338a**) instead of GBL. In this malonic ester synthesis-type approach, the *β*-dicarbonyl compound could be deprotonated with potassium carbonate and decarboxylated more easily, yielding the targeted *α*-alkylated GBL (Scheme 113). Therefore, this approach was chosen as the more suitable one for producing more starting material. Since the required *β*-dicarbonyl lactone compound was not commercially available, it was synthesized according to a modified procedure by Santra et al.[186] and Wilent et al.[187] The required *β*-dicarbonyl compound was synthesized via alkylation of diethylmalonate (**336**) with 2-(2-bromoethoxy)-tetrahydro-2*H*-pyran (**335**) and subsequent lactonization (Scheme 113). The THP-ether **335** was synthesized according to a procedure of Anzini et al.[188] by stirring 3,4-dihydropyran and 2-bromoethanol in DCM at room temperature with pyridinium tosylate as catalyst. The following toluene sulfonic acid catalysed deprotection and lactonization of **337** in the solvent methanol yielded an ethyl/methyl mixture of *α*-ethylcarboxy-*γ*-butyrolactone **338a** and *α*-methylcarboxy-*γ*-butyrolactone **338b** due to acid catalysed transesterification.

Scheme 113: Protecting as THP-ether.

Scheme 114: Synthesis of 4-hexyl-2,3-dihydrofuran via *α*-carboxy-GBL.

The lactone **338a/338b** was alkylated with 1-bromohexane, potassium carbonate as base and tetrabutylammonium bromide TBAB as catalyst to *α*-ethylcarboxy-*α-hexyl-γ*-butyrolactone *γ*-butyrolactone **339a** and *α*-methylcarboxy-*α-hexyl-γ*-butyrolactone **339b** according to a

71

procedure by Santra et al.[186] and Zieba et al.[189] Instead of Zenk's and Wiley's[182] base and acid catalysed decarboxylation of **338a**, a lithium chloride mediated elimination in DMSO according to Krapcho et al.[190] was used to obtain **332** in a yield of 64%. Lactone **332** was reduced with DIBAL-H to lactol **340**. After the subsequent mesylation and elimination, 4-hexyl-2,3-dihydrofuran (**285**) was obtained in a yield of 26%.[160,182] This seven-step synthesis successfully gave access to starting material **285**, but was time-consuming.
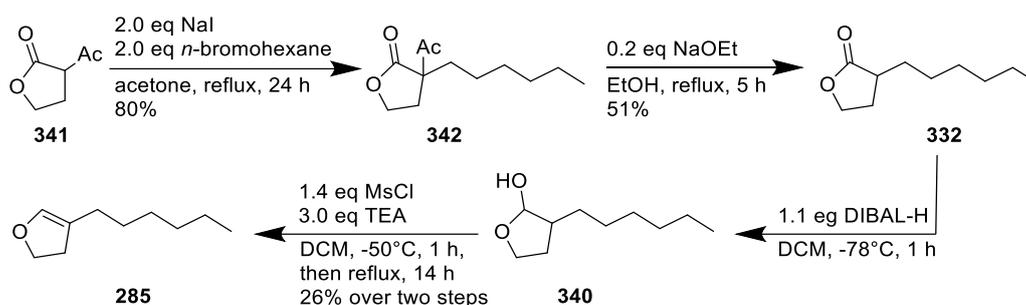
Scheme 115: From *α*-acetyl-GBL starting synthesis of 4-hexyl-2,3-dihydrofuran.

The whole synthesis of **285** was shortened to a four-step procedure using a retro-aldol reaction according to a modified synthesis by Brun and Baumgartner.[191] Instead of carboxy-GBL, commercially available *α*-acetyl-*γ*-butyrolactone (**341**), 1-bromohexane, and sodium iodide were used in a one-pot Finkelstein/alkylation to obtain *α*-acetyl-*α*-hexyl-GBL (**342**) in a yield of 80% (Scheme 115). Sub-stoichiometrical amounts of sodium ethanolate enabled a retro-Claisen condensation of **342** into **332**. After the reduction with DIBAL-H, mesylation, and elimination, **285** was obtained.
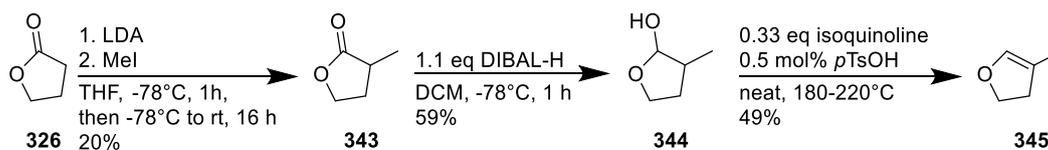
Scheme 116: Synthesis of 4-methyl-2,3-dihydrofuran.

The less sterically hindered 4-methyl-2,3-dihydrofuran was synthesized according to the procedure of by Posner et al.[185] and Zenk et al.[182] The deprotonation of **326** (Scheme 116) with LDA and alkylation with methyl iodide yielded the *α*-methyl- *γ*-butyrolactone (**342**). The lactone **342** was reduced with DIBAL-H to lactol 2-hydroxy-3-methyl-tetrahydrofuran **344**. Elimination to 4-methyl-2,3-dihydrofuran (**345**) was achieved via the treatment of **344** with catalytic amounts of *p*-toluenesulfonic acid and sub-stoichiometric amounts of isoquinoline at 180-220°C.
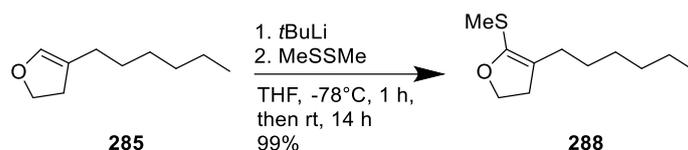
Scheme 117: Methylthiolation of 4-hexyl-2,3-dihydrofuran.

Since the IEDDA reactions required more electron-rich dihydrofurans, an electron-donating thiomethyl substituent was introduced according to an approach by Verkruijsse et al.[192] modified by Kessler et al.[160] In the case of the hexyl substituent, the 4-hexyl-5-methylthio-2,3-dihydrofuran (**288**) was obtained after lithiathon of **285** and further treatment with dimethyl disulphide (Scheme 117). Methylthiolation of methyl dihydrofuran **345** was also attempted by lithiation with *tert*-butyllithium *t*BuLi and subsequent treatment with dimethyl disulphide. Unfortunately, the high volatility of the product 4-methyl-5-methylthio-2,3-dihydrofuran (**346**) hindered its isolation in necessary the purity and amount necessary for further experiments (Scheme 118).
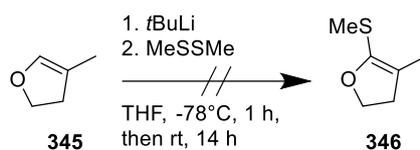
Scheme 118: Attempted methylthiolation of 4-methyl-2,3-dihydrofuran.

4.1.2 Catalysed IEDDA Reaction of 4-Alkyl-2,3-dihydrofurans with Phthalazines

After the synthesis of the starting material, the bidentate boron Lewis acid catalysed IEDDA reactions were conducted. The reaction of phthalazine (**87**) with phenyl- and benzyl-substituted dihydrofuran **317** and **329** was attempted (Scheme 119). Unfortunately, the expected rearrangement products **347** and **348** were not obtained, but starting material was recovered. The increased steric demand of the phenyl and benzyl substituents seemed to hinder the IEDDA reaction due to overcrowding the transition state.
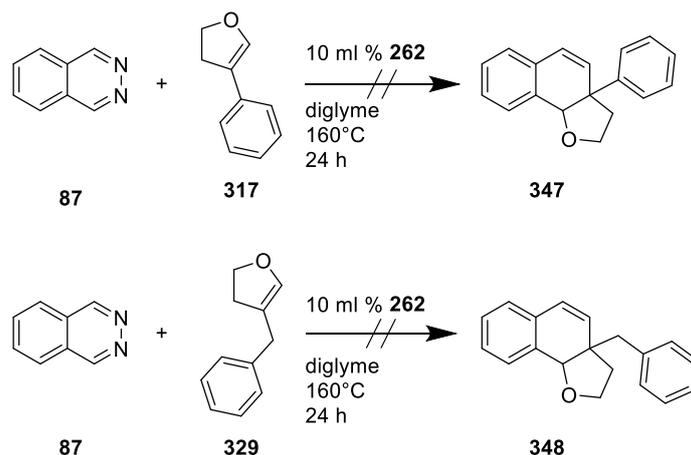
Scheme 119: Attempted domino IEDDA reactions with phenyl and benzyl dihydrofuran.
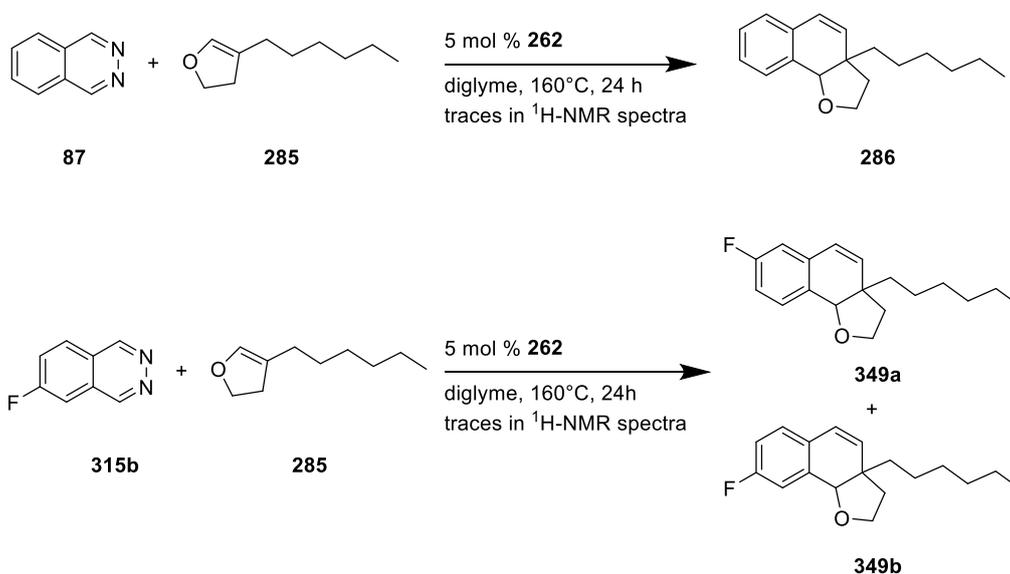
Scheme 120: Attempted domino IEDDA reactions with 4-hexyl-2,3-dihydrofuran.

Since the phenyl and benzyl substitutions were unsuccessful in the IEDDA reaction, the more flexible and less sterically demanding hexyl dihydrofuran **285** was attempted. After reacting with phthalazine and the catalyst, only traces of the IEDDA reaction product **286** were detected via an analysis of ^{1}H-NMR spectra (Scheme 120). The reaction mixture turned from a clear brown solution into a turbid, brown-coloured solution. Therefore, polymerization or degradation reactions of the starting material or the product were assumed. As side reactions may occur because of the high temperatures of 160°C, a decrease of the reaction temperature to 140°C and a more reactive electron-deficient diene 6-fluorophtalazine (**315b**) were tested. However, even these changed conditions only led to traces of the IEDDA products 2*H*,3*H*,9b*H*-7-fluoro-3a-hexyl-naptho-[1,2-*b*]-furan (**349a**) and 2*H*,3*H*,9b*H*-8-fluoro-3a-hexyl-naptho-[1,2-*b*]-furan (**349b**) confirmed via ^{1}H-NMR analysis. During the attempted isolation of the product, a dark-

coloured solid residue was found. This result indicated degradation and/or polymerization side or consecutive reactions of the starting material or the product. After these results in the IEDDA reactions, alternative conditions were explored by varying starting material and additives to improve the yield and to suppress side or consecutive reactions.
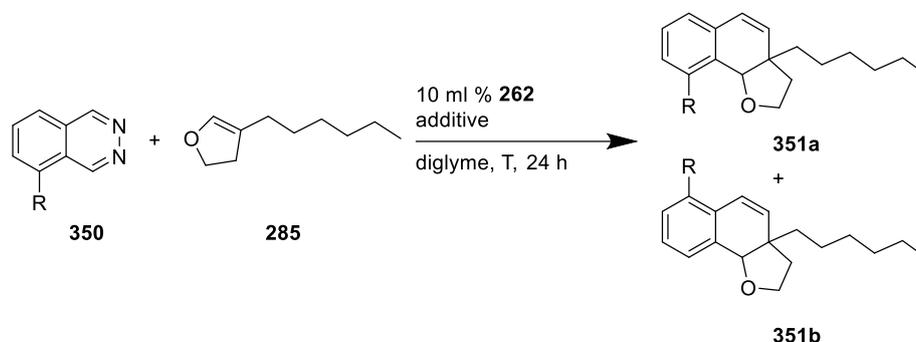
Scheme 121: Exploring domino IEDDA reactions of phthalazines and dihydrofurans with and without additives.

Table. 10: Conditions for the investigation of attempted domino IEDDA reactions.

Entry	R of 350	T [°C]	Additive	Result
1	F	100		s.m.r
2	F	140		Trace
3	Cl	120		s.m.r
4	Cl	160		s.m.r
5	NO_2	110		s.m.r
6	NO_2	130		s.m.r
7	H	160	iPr$_2$NEt	Trace
8	NO_2	100	iPr$_2$NEt	Trace
9	NO_2	100	Fumaronitrile	s.m.r.

s.m.r: starting material recovered.

Since styrenes and enol ethers are well-known in the pertinent literature for thermal or Lewis acid catalysed polymerisations, the enol ether dienophile and the styrene IEDDA product were assumed to polymerise. [193,194] Therefore, low temperatures at 100°C and 120°C for the 6-fluorophthalazine and 5-chlorophthalazine were attempted (Scheme 121, Table 10, Entry 1-4). During the reaction, a gas evolution was observed, which could be a hint at a successful IEDDA reaction according to results of Kessler et al.[160] These low reaction temperatures did not yield the targeted IEDDA product, and starting material was recovered, which was confirmed by the ^{1}H-NMR-spectral analysis of the reaction mixture. Since Kessler et al.[160]

described a gas evolution as a hint at a successful IEDDA reaction, a side or consecutive reaction of the starting material or the styrene product was assumed. Since the low temperatures were not successful, higher temperatures of 140°C (6-fluorophthalazine) and 160°C (5-chlorophthalazine) were tested to overcome the thermal threshold of the IEDDA reaction. In both cases, the starting material was recovered. A gas evolution and a darkening of the reaction mixture were observed. Moreover, a dark residue was obtained after the reaction. Since the starting material was recovered in all four cases, most of the material was assumed to not react to the IEDDA product at all. The gas evolution, the darkening of the reaction mixture and dark solid residues indicated occurring side or IEDDA reactions whose styrene products underwent consecutive reactions, for example as polymerisations. Since the used phthalazines did not lead to the styrene product, the more electron-poor 5-nitrophthalazine was chosen to enhance the IEDDA reaction (Table 10, Entry 5,6). Because experiments by Kessler et al.[4] showed that 100°C was sufficient to perform the IEDDA reactions of 2,3-dihydrofurans with 5-nitrophhalazine compared to 160°C and unsubstituted phthalazine, the reaction temperature was decreased to prevent side or consecutive reactions. Unfortunately, no reaction to the IEDDA product occurred at 100°C and 130°C, although a gas evolution was observed. The starting material was recovered after the reaction. A darkening of the reaction mixture and a dark black residue on the surface of the reaction vessel were observed. Therefore, a gas-expelling reaction, side reactions and the polymerisation of the styrene product were assumed. Those unwanted side reactions might have been induced by protons or acids as claimed by Kessler et al.[160] Therefore, *N,N*-di*iso*propylethylamine was added to prevent side reactions in the IEDDA reaction of phthalazine at 160°C and 5-nitrophthalazine at 100°C (Table 10, Entry 7,8). Unfortunately, only traces of the IEDDA product were determined via the ^{1}H-NMR analysis of crude reaction mixture. Therefore, a proton-catalysed side reaction can be excluded as a reason for side reactions. As an alternative, the highly reactive *o*-quinodimethane was suspected of undergoing side reactions. Because Schweighauser et al.[6] showed that *o*-quinodimethane intermediates of the IEDDA reaction underwent Diels-Alder reactions, a potential dienophile should trap these reactive compounds to prevent side reactions. Therefore, fumaronitrile was added as a scavenger of the *o*-quinodimethane intermediate. It was used with 5-nitrophthalazine in an IEDDA reaction at 100°C (Table 10, Entry 9). This low temperature was chosen to prevent side reactions and following reactions. After the reaction, only starting material was recovered, neither an IEDDA product nor a trapped intermolecular Diels-Alder product was observed via ^{1}H-NMR analysis. In summary, it can be stated that the IEDDA reaction of 4-hexyl-2,3-dihydrofuran with phthalazines did not occur even when electron deficient dienes were used. The observed or consecutive reactions can be explained by the chemical high reactivity of the enol ether, the *o*-quinodimethane or the styrene product which may undergo further reactions, for example

polymerisations. The chloro-, fluoro- and nitro-substituent might enhance further side reactions because their electron withdrawing effect could favour polymerisations of styrenes.[195,196] Therefore, an alternative approach was needed to overcome the threshold of the IEDDA reaction between phthalazines and dihydrofurans.

4.1.3 Catalysed IEDDA Reaction of 5-Thioalkyl-4-alkyl-2,3-dihydrofurans with Phthalazines

Thiomethylation and electron-deficient phthalazines were the key to higher yields and lower reaction temperatures according to Kessler et al.[160] Therefore, the influence of the more electron-rich but sterically bulkier thioalkyl-substituted dienophile on the IEDDA reaction was investigated. The higher electron density should increase the reactivity in the IEDDA reaction towards the phthalazines, but the increased sterical hindrance may hamper the necessary orbital overlap.
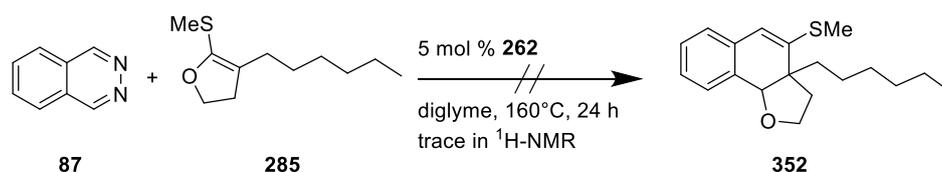
Scheme 122: Attempted reaction of phthalazine and 5-methylthio-4-hexyl-dihydrofuran.

Conducting the IEDDA reaction with phthalazine (**87**) and **285** at the high temperature of 160°C and with the electron-richer **288** did not lead to the styrene 2*H*,3*H*,9b*H*-3a-hexyl-4-methylthio-naptho-[1,2-*b*]-furan **352**, but starting material was recovered. (Scheme 122). Thus, the electron-donating effect of the thiomethyl substituent was not sufficient to enhance the IEDDA reaction. An additional electron-deficient phthalazine was necessary.
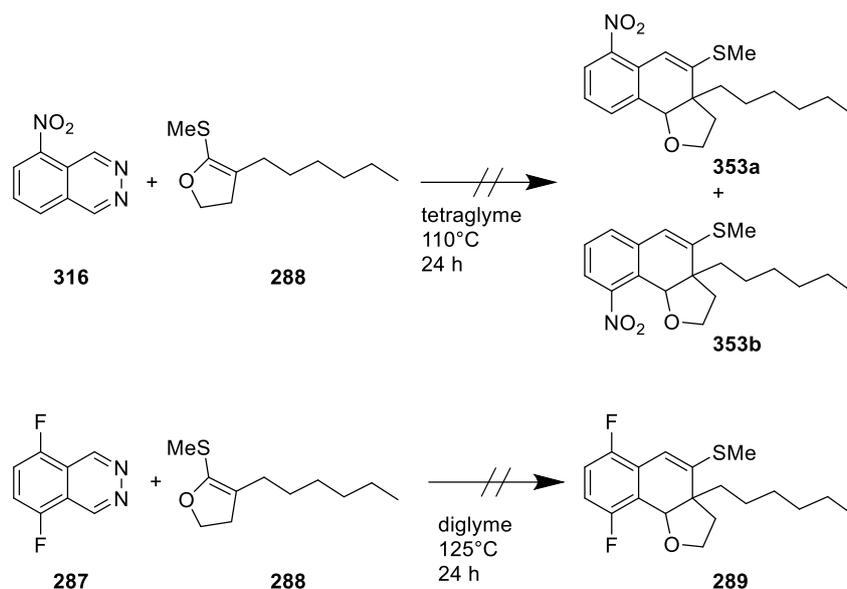
Scheme 123: Attempts to perform the IEDDA reaction without catalyst.

Combining an electron-deficient diene and an electron-rich dienophile increased the risk of the reaction occurring without the necessity of the catalyst.[72] The reaction was attempted with electron-deficient 5-nitrophthalazine (**316**) at 110°C, 5,8-difluorophthalazine (**287**) at 125°C, and **288** without catalyst. Solely the starting materials but not the rearrangement products **353a/353b** or **289** were obtained. (Scheme 123). Therefore, the catalyst was necessary for the IEDDA reaction.
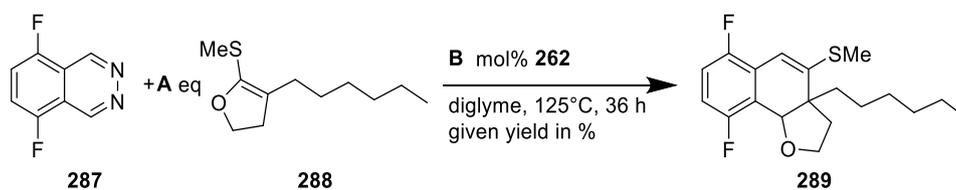
Scheme 124: Reactions of 5,8-difluorophthalazine with 5-methyltio-4-hexyl-dihydrofuran.

Table 11: Conditions for IEDDA reaction.

Entry	Equivalents **A**	Catalyst amount **B** [mol%]	Yield [%]
1	1	5	59
3	2	11	94

In contrast to the reaction of unsubstituted phthalazine and dihydrofuran, the **262**-catalysed IEDDA reaction of 5,8-difluorophthalazine (**287**) and **288** successfully yielded 2*H*,3*H*,9b*H*-6,9-difluoro-3a-hexyl-4-thiomethyl-naptho-[1,2-*b*]-furan (**289**) in 59%. The yield was optimized by increasing the amount of catalyst from 5 mol% to 10 mol% and by increasing the amount of dienophile from one equivalent to two equivalents.

Thus, yield **289** was optimized to a yield of 94% (Scheme 124, Table 11). On this basis, other electron-deficient phthalazines were explored to expand the scope.
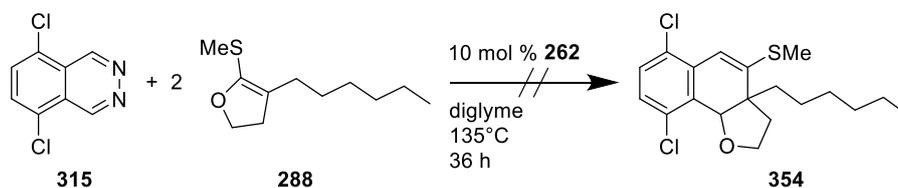
Scheme 125: Attempted IEDDA reaction of 5,8-dichlorophthalazine.
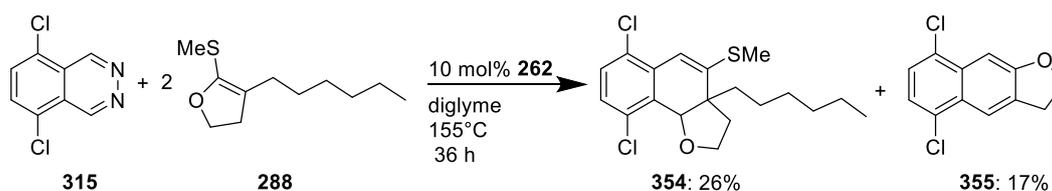
Scheme 126: Reaction of 5,8-dichlorophthalazine with 5-methyltio-4-hexyl-dihydrofuran.

At first, the 5,8-dichlorophthalazine was used, which is slightly less electron-deficient than the difluoro substituted one. At 135°C, **359** and **347** did not react because starting material was recovered (Scheme 125). The increase of the reaction temperature to 155°C led to the rearrangement product styrene 2*H*,3*H*,9b*H*-6,9-dichloro-3a-hexyl-4-thiomethyl-naptho-[1,2-*b*]-furan (**360**). Surprisingly, 2*H*,3*H*-5,8-dichloronaptho-[2,3-*b*]-furan (**361**) was obtained additionally, which was proved by ¹H⁻ and ¹³C-NMR and GC-MS analysis (Scheme 126).
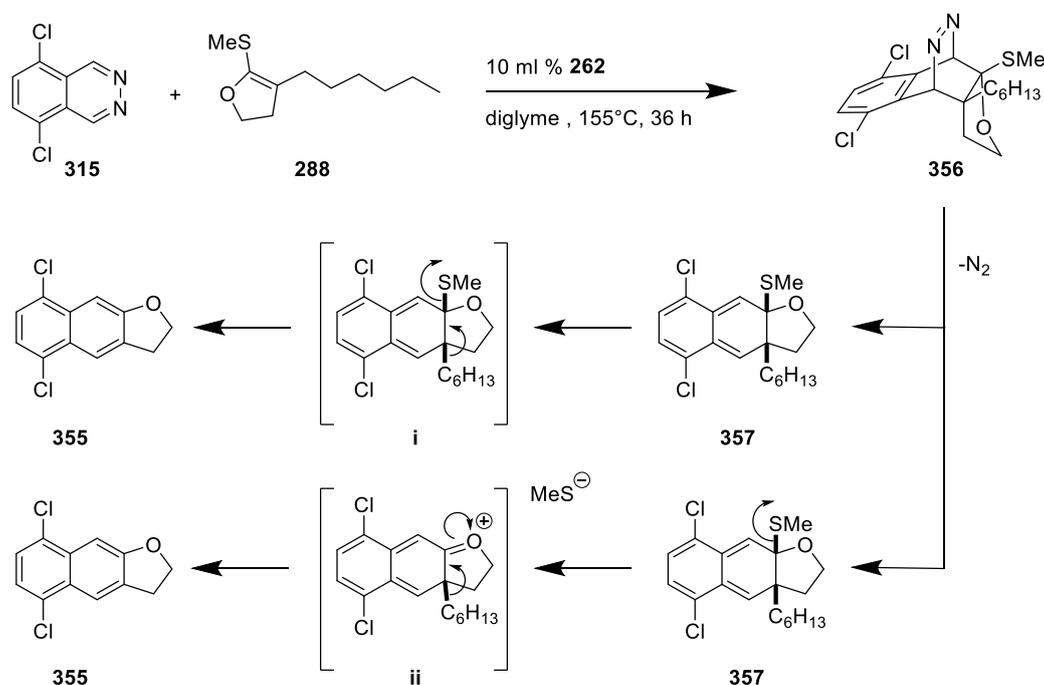
Scheme 127: Reaction of 5,8-dichlorophthalazine with 5-methyltio-4-hexyl-dihydrofuran.

This product indicated an elimination process of the thiomethyl and hexyl alkyl chain during the IEDDA reaction (Scheme 127). The high reaction temperatures enabled the elimination of the thiomethyl substituent of *o*-quinodimethane **357** to **355** to occur. Such a preferred S-substituent expulsion, in contrast to O-substituents elimination, can occur as confirmed by Sauer et al.'s[65] results of IEDDA reactions of mixed O-, N-, and S- acetals with 1,2,4,5-tetrazine. The elimination might occur via a concerted mechanism **357/i** or a stepwise **357/ii** mechanism (Scheme 126). It seems that the slightly lower electron deficiency of the 5,8-dichlorophthalazine compared to the 5,8-difluorophthalazine facilitated the elimination.
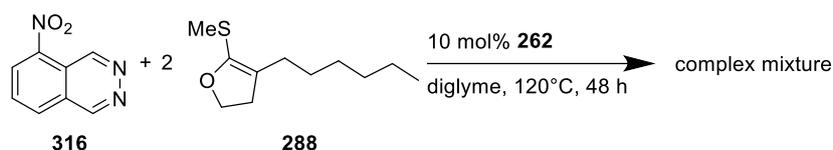
Scheme 128: Reaction of 5-nitrophthalazine with 4-hexyl-5-methyltio dihydrofuran.
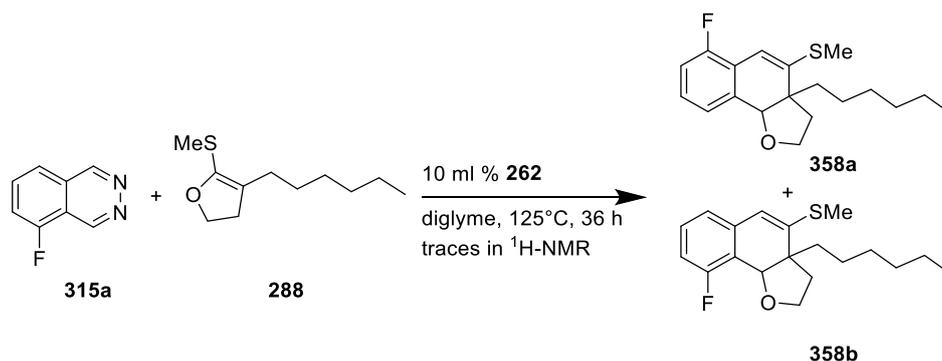
Scheme 129: Reaction of 5-fluorophthalazine with 4-hexyl-5-methyltio-dihydrofuran.

As electron-deficient phthalazines, 5-nitrophthalazine (**316**) and the less electron-deficient 5-fluorophthalazine (**315a**) were tested (Scheme 128, 129). Unfortunately, the catalysed IEDDA reaction of **316** with **288** yielded an inseparable, complex mixture. The high electron- withdrawing effect of the nitro group might cause side reactions of intermediates or products, such as polymerisations. With the mono-fluorinated phthalazine **315b,** the IEDDA reaction yielded only traces of the IEDDA product **358a/358b** confirmed by ^{1}H-NMR spectral analysis. Therefore, strongly electron-deficient phthalazines with a symmetric electron density distribution were necessary for obtaining high yields in IEDDA reactions.
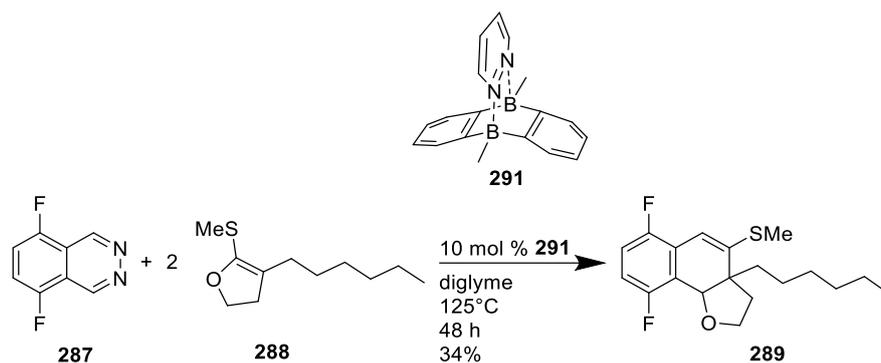
Scheme 130: Reaction of 5,8-difluorophthalazine with 5-methyltio-4-hexyl-dihydrofuran with the catalyst complex.

Table 12: Solvents and yields for reaction with the catalyst complex.

Entry	Solvent	Reaction temperature [°C]	Yield [%]
1	C_6H_5-CF_3	110	38
2	4-Cl-C_6H_4-CF_3	125	19

Because the preparation of the IEDDA experiments was very time-consuming due to fume hood Glovebox changes, the reaction conditions were modified to accelerate and simplify the experimental setup. Instead of the pure catalyst, the catalyst pyridazine complex was used because it allowed handling the catalyst outside of the glovebox.[197] Moreover, less polar solvents were investigated because the utilized polar ether solvents were suspected of decreasing the reactivity of the catalyst due to Lewis acid-base interactions.[198] The aromatic solvents benzotrifluoride and 4-chloro-benzotrifluoride do not provide oxygen Lewis bases and therefore might enhance the reactivity of the catalyst. The IEDDA reaction of **287** with **288** was catalysed by complex **291** (Scheme 130). In case of benzotrifluoride, **289** was obtained in a yield of 38%, and in the case of 4-chlorobenzotrifluoride in 19%, respectively (Table 12). One reason for these lower yields may be the use of the catalyst complex **291**, as Hong et al.[199] observed lower yields in IEDDA reactions of phthalazine with 2,3-dihydrofuran compared to non-complexed **262**. In the case of benzotrifluoride, the low reaction temperature of 110°C, restricted by the low boiling point of 100°C, compared to 125°C of diglyme, might reduce the yield. The lower temperatures decelerate the reaction rate and the starting materials overcoming the thermodynamic barriers of the IEDDA reaction. The low yield of 19% in the case of 4-chlorobenzotrifluoride, despite the reaction temperature of 125°C, might emerge from solvent effects and the non-dried and non-degassed solvent which might cause side reactions.
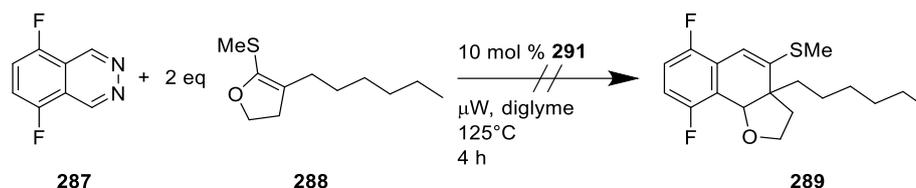
Scheme 131: Attempted reaction of 5,8-difluorophthalazine with 5-methyltio-4-hexyl-dihydrofuran with the catalyst complex in the microwave oven

The last attempt to speed up the IEDDA reaction took advantage of the accelerating effect of the microwave on chemical reactions.[200] Phthalazine **357** and **347** with the catalyst complex **291** in diglyme were subjected to the microwave oven (Scheme 131). Unfortunately, after a reaction time of 4 hours, only starting material was recovered. The gas-permeable sealing of the microwave reaction vessel might hamper the IEDDA reaction due to oxygen-induced side reactions. Therefore, the microwave was not sufficient to accelerate the IEDDA reaction. In summary, it can be stated that the IEDDA reaction of 5-methylthio-4-hexyl-2,3-dihydrofuran yielded a single product only with 5,8-difluorophthalazine. Other phthalazines caused side products and/or low yields. The reaction setup process was simplified and sped up by utilizing the catalyst complex **291**, but the yields decreased.

4.1.4 Catalysed IEDDA Reaction of 5-thioalkyl-2,3-dihydrofurans with Phthalazines

As the IEDDA reactions of phthalazines and the sterically bulky 4-alkyl-2,3-dihydrofurans and its 5-methylthio derivative suffered from low yields and side reactions, the less sterically hindered 5-thiolalkyl-2,3-dihydrofurans were investigated to facilitate the intramolecular orbital overlap. The synthesis according to Bodoky et al.[14] started with the lithiation of 2,3-dihydrofuran (**359**) with *tert*-butyllithium and further treatment with the dimethyl- or dibutyl-disulphide. Neat 5-thiomethyl-2,3-dihydrofuran (**360**) was obtained in a yield of 58%. A separable mixture of 5-thiobutyl-2,3-dihydrofuran and dibutyl sulphide was obtained. The calculated yield (**361**) was 19% (Scheme 132).
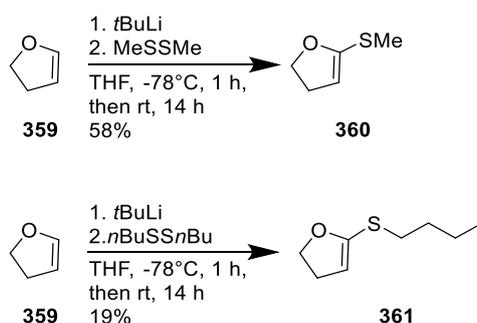
Scheme 132: Alkylthiolation of 2,3-dihydrofuran.
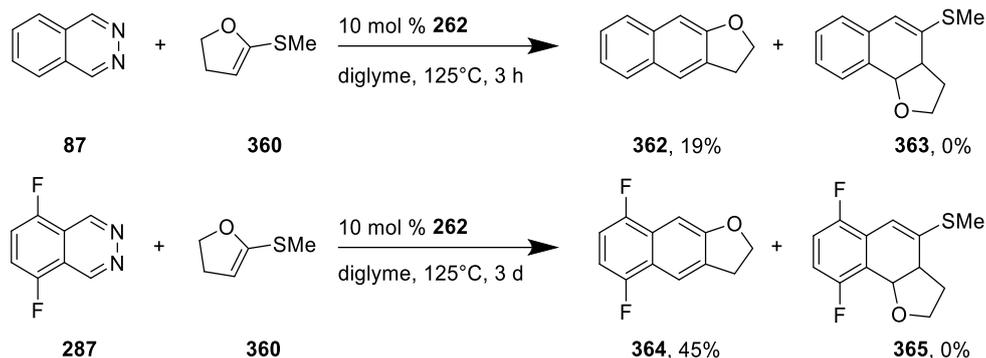
Scheme 133: IEDDA reaction with 5-methyllthio-dihydrofurans.
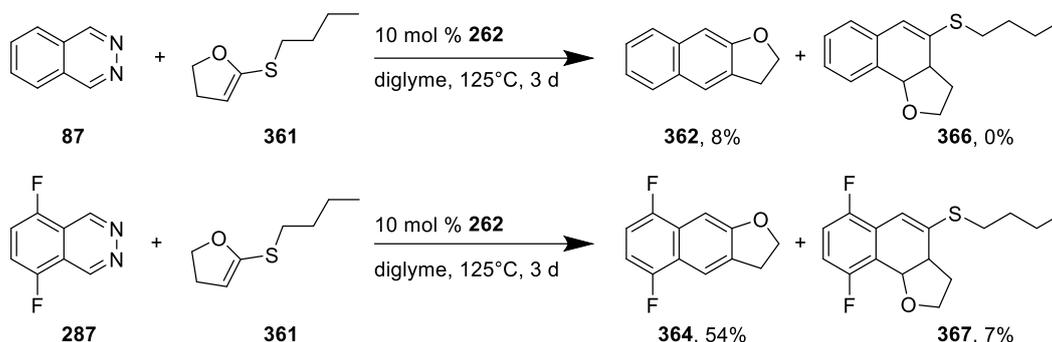
Scheme 134: IEDDA reaction with 5-butyl-2,3-dihydrofuran.

In the IEDDA reaction of 5-methylthio-2,3-dihydrofuran (**360**) with phthalazine (**87**) and 5,8-difluorophthalazine (**287**), only the elimination products 2*H*,3*H*-naphtho-[2,3-*b*]-furan (**362**) and 2*H*,3*H*-5,8-difluoronaphtho-[2,3-*b*]-furan (**364**) were obtained in yields of 9% and 45%, respectively (Scheme 133). The rearrangement products **363** and **365** were not observed. The same phthalazines were used in the IEDDA reaction of 5-butyl-2,3-dihydrofuran (**361**). The naphthofurans **362** and **364** were obtained. In the case of the 5,8-difluorophthalazine, the rearrangement product 2*H*,3*H*,3a*H*,9b*H*-6,9-difluoro-4-(butylthio)-naphtho-[1,2-*b*]-furan (**367**) was also found in a low yield of 7% (Scheme 134). The preferred elimination of the S-substituents in contrast to the O-substituents was confirmed by Sauer et al.[65] Since methanethiol is a gas, its expulsion from the reaction mixture irreversibly favours the elimination products **362** and **364** according to the principle of Le Chatelier.[201–203] By contrast, the butanethiol should have a lower tendency to leave the reaction mixture which should facilitate the rearrangement. Furthermore, the butyl substituent provides a higher electron density than the methyl substituent due to its larger +I effect. Thus, it may compete with the alkoxy substituent for elimination or rearrangement. The more electron-donating phthalazine facilitated the elimination of the thio substituent. However, the more electron-withdrawing 5,8-difluorophthalazine **287** substituent facilitated the rearrangement partially. With a lower temperature, more of the rearrangement product would be obtained, whereas with a higher temperature, more of the elimination product would be obtained.

In summary, it can be stated that in the bidentate boron Lewis acid catalysed IEDDA reaction of 4-alkyl-2,3-dihydrofurans and phthalazines, starting material was recovered and traces of the rearrangement product were obtained. Dark-coloured residues were observed. Therefore, side reactions or consecutive reactions of the styrene product probably inhibited the isolation of the product. Methylthiol-substitution, and thus an electron-richer dienophile, was not sufficient to enhance the IEDDA reaction with unsubstituted phthalazine. Electron-poor phthalazine and methylthiol-substitution were needed to enable the catalysed IEDDA reaction: difluorophthalazine yielded the rearrangement product. Less electron-poor dichlorophthalazine already needed higher temperatures to occur, which facilitated the elimination reaction to the naphthalene product. Less electron deficient phthalazines yielded only product traces or needed higher temperatures. Less sterically demanding 5-alkylthio-2,3-dihydrofurans facilitated the IEDDA to a major yield of the elimination products, but the rearrangement products were obtained only in a low yield or as traces.

4.2 Synthesis and Properties of Redox Flow Battery Material

4.2.1 Synthesis and Properties of Vanillin Derived Flow Battery Materials

After the retrosynthetic analysis and literature research, 1,4-quinones, 1,2-phenanthrenequinones and indigo were identified as redox active materials which were accessible from vanillin.[168–171] In the case of 1,4-quinones, the retrosynthesis was based on a Dakin reaction of vanillin or its derivative **368** to hydroquinone **369** and a subsequent oxidation to quinone **370** (Scheme 135).
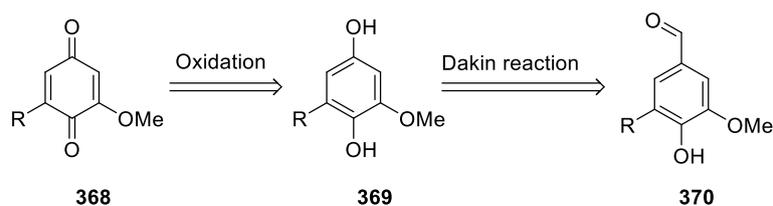
Scheme 135: Retrosynthesis of 1,4-quinones.
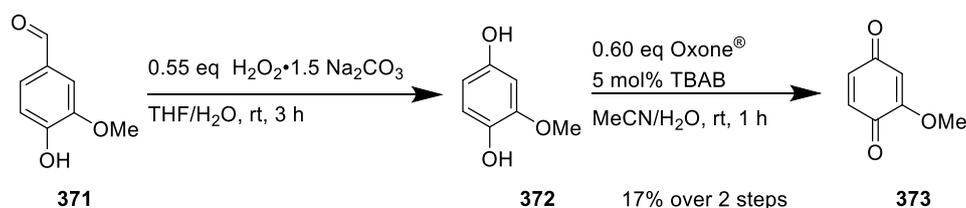
Scheme 136: Synthesis of 2-methoxy-1,4-benzoquinone.[171,204]

The synthesis of 2-methoxy-1,4-benzoquinone (**373**) started with a Dakin reaction of vanillin (**371**) with sodium percarbonate to impure 2-meththoxy-1,4-hydroquinone (**372**) according to a procedure of Fache et al.[171] For reasons of isolation and purification, **372** was directly oxidized with Oxone® and tetrabutylammonium bromide TBAB to 2-methoxy-1,4-benzoquinone (**373**) according to a method of Yakura et al.[204] (Scheme 136). The low yield of 17% was based on preoptimized conditions. Because an increased number of storable electrons would theoretically increase the storage capacity, the 6,6'-dimethoxy-2,2'-bis-(1,4-benzoquinoyl) (**376**) was targeted. Compared to simple benzoquinone, its capacity of storable electron should be doubled from two to four electrons. The synthesis of **376** started with Elbs et al.'s[205] persulfate dimerization of vanillin to dehydrodivanillin (**374**) with iron(II)-sulfate as catalyst and sodium persulfate as oxidant. The further synthesis was analogous to the 2-methoxy-1,4-benzoquinone synthesis. The dehydrodivanillin (**374**) was oxidized to bis-(hydroquinonyl) **375** via a Dakin reaction with sodium percarbonate. The oxidation with Oxone© and TBAB led to the 6,6'-dimethoxy-bis-2,2'-(1,4-benzoquinoyl) **376** (Scheme 137). The potentials of **373** with 384 mV vs. Ag/AgCl (~606 mV vs. SHE) and **376** with 393 mV vs. Ag/AgCl (~615 mV vs. SHE) were measured via cyclic voltammetry by Hofmann et al.[206] (Figure 3, Figure 4). These low potentials were surpassed by the catholyte materials BQDS with 1100 mV vs. SHE and DHDMBS with 720 mV vs. SHE. Therefore, the synthesis of **373** and **376** exemplified the opportunity to generate redox materials from vanillin, but their low positive potentials were disadvantageous for catholyte or anolyte applications.
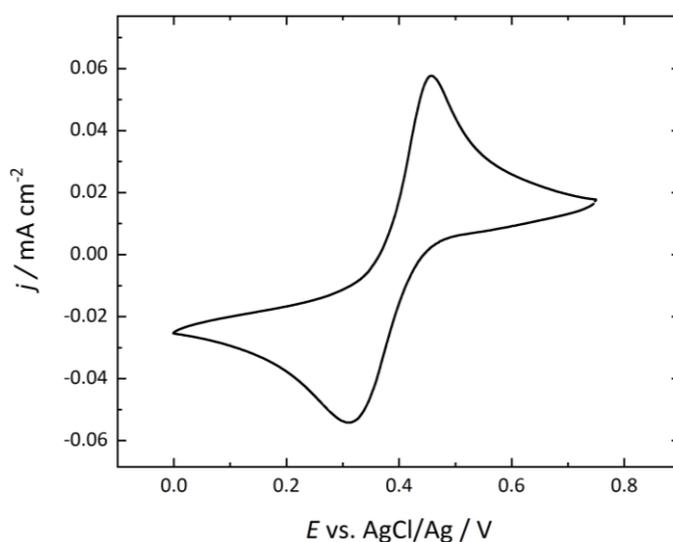
Figure 3: Cyclic voltammogram of 2-methoxy-1,4-benzoquinone (0.5 mM, 2 M HCl) measured by Hofmann et al.[206]
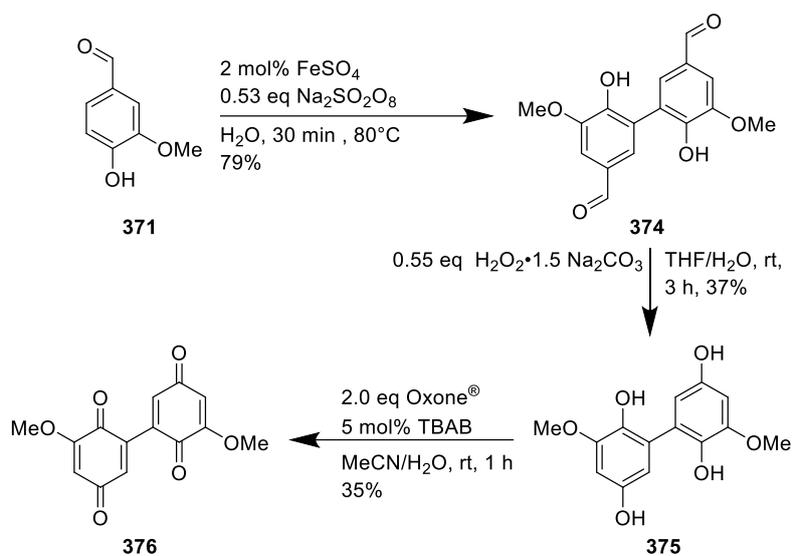
Scheme 137: Synthesis of 6,6'-dimethoxy-bis-2,2'-(1,4-benzoquinonyl).[90,171,204]
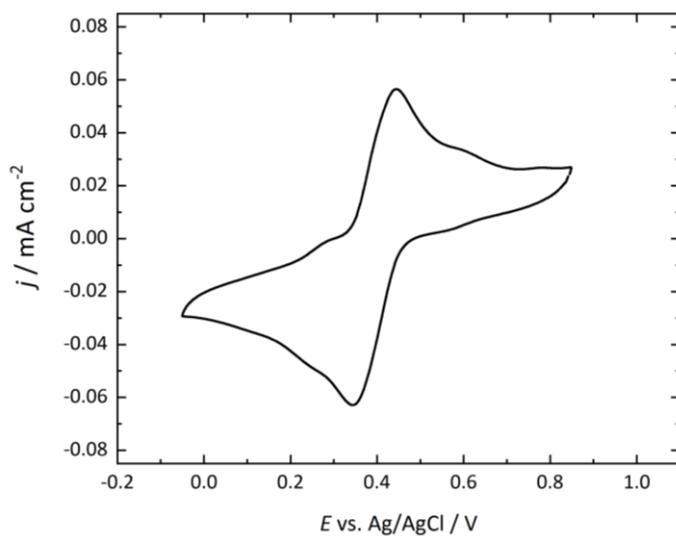
Figure 4: Cyclic voltammogram of 6,6'-dimethoxy-2,2'-(1,4-benzoquinoyl) (0.5 mM, 2 M H_2SO_4) measured by Hofmann et al.[206]
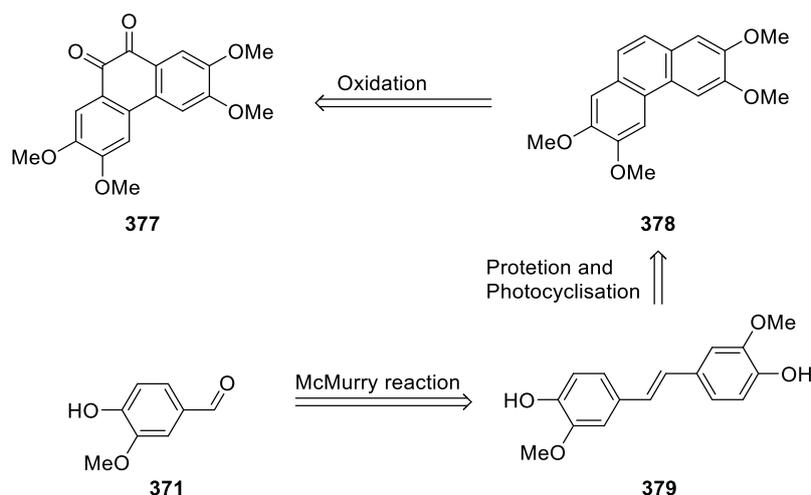
Scheme 138: Retrosynthesis to phenanthrenequinone via photocyclisation.

As a further redox active and vanillin-based compound, 2,3,6,7-tetramethoxy-9,10-phenanthrenequinone (**377**) was targeted. After the retrosynthetic analysis, two synthetic pathways were planned. First, a synthesis based on generating **377** via oxidation of 2,3,6,7-tetramethoxy phenanthrene (**378**), which is accessible via protection and photocyclization of 4,4'-dihydroxy-3,3'-dimethoxy stilbene **379**. A McMurry reaction of vanillin **371** should yield the necessary stilbene (Scheme 138).[207–209]
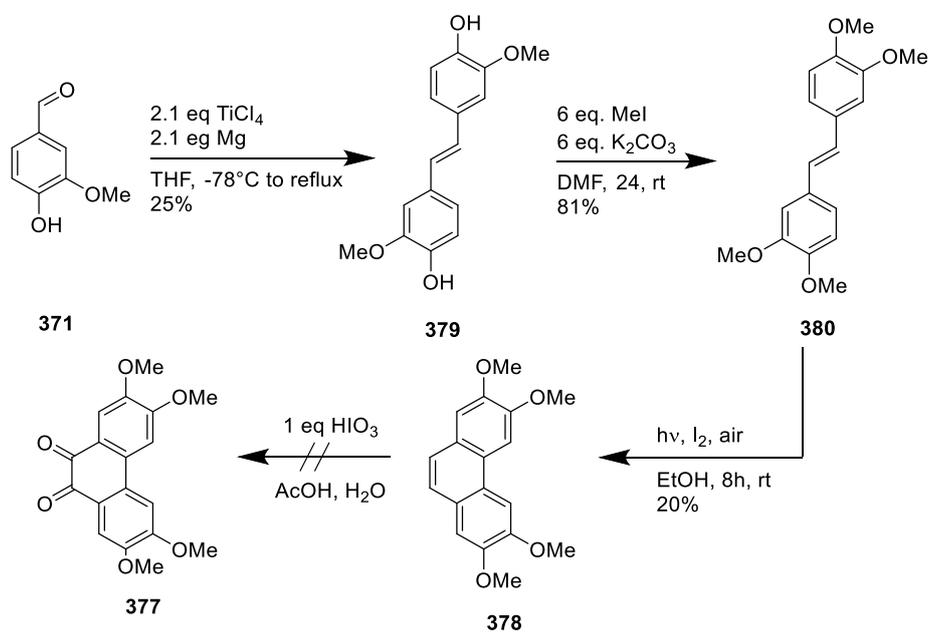
Scheme 139: Synthesis of Phenanthrenequinone via stilbene photocyclization.

The synthesis via photocyclization started with a McMurry coupling of vanillin (**371**) with magnesium and titanium(IV)-tetrachloride developed by Harvey et al.[208](Scheme 139). Stilbene **379** was obtained in a yield of 25%. To overcome possible photoredox issues, **379**

was protected by methylation to 3,3'4,4'-tetramethoxystilbene **380** with methyl iodide and potassium carbonate in a yield of 81% according to a modified procedure by Fang et al.[210] Phenanthrene **378** was obtained after photocyclization of **380** via UV-mercury lamp and iodine as oxidant under air in a yield of 20% according to a procedure by Mallory et al.[209] The yield was low because of non-optimized conditions. A further oxidation with iodic acid according to Fuson et al.[207] led to a complex mixture. The low yields and the oxidation step made another synthetic route necessary.
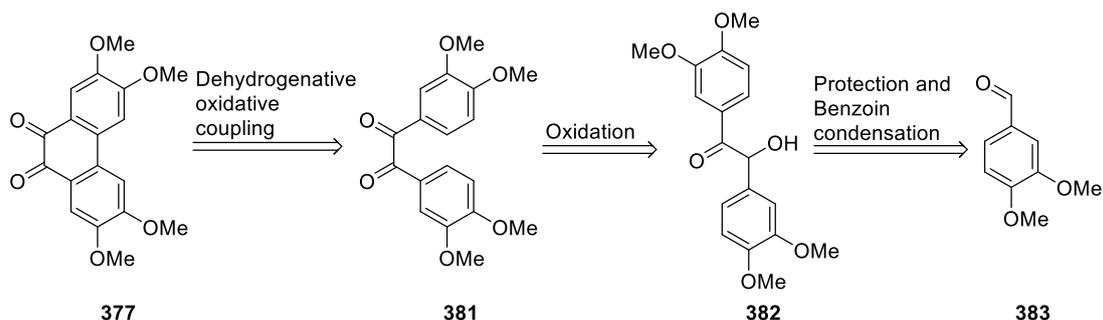
Scheme 140: Retrosynthesis of phenanthrenequinone via benzoin condensation.

In a second synthetic route, the targeted phenanthrenequinone **377** could be obtained via dehydrogenative coupling of a 3,3',4,4'-tetramethoxy benzil (**381**) (Scheme 140). This diketone might be accessible via oxidation of a 3,3',4,4'-tetramethoxy benzoin (**382**). A benzoin condensation of protected veratraldehyde (**383**), a methylated vanillin derivative, might yield benzoin **382**. For these benzoin condensation procedures, Miyashita et al.[211] were chosen because their approach offered a safer and organocatalytic reaction instead of the old approach with poisonous cyanide by Zinin et al.[212] The catalyst was synthesised by heating 1,2-phenylenediamine (**384**) and aqueous formic acid yielding benzimidazole (**385**) according to Soni et al.[213] After the alkylation with methyl iodide in acetonitrile and potassium carbonate as base, 1,3-dimethyl-benzimidazolium iodide (**386**) was obtained in a yield of 45% according to a synthesis by Rubbiani et al.[214] (Scheme 141).
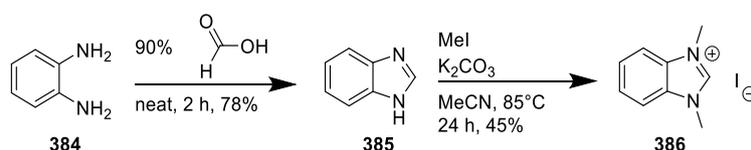
Scheme 141: Synthesis of imidazolium catalysts for benzoin condensation.[213,214]
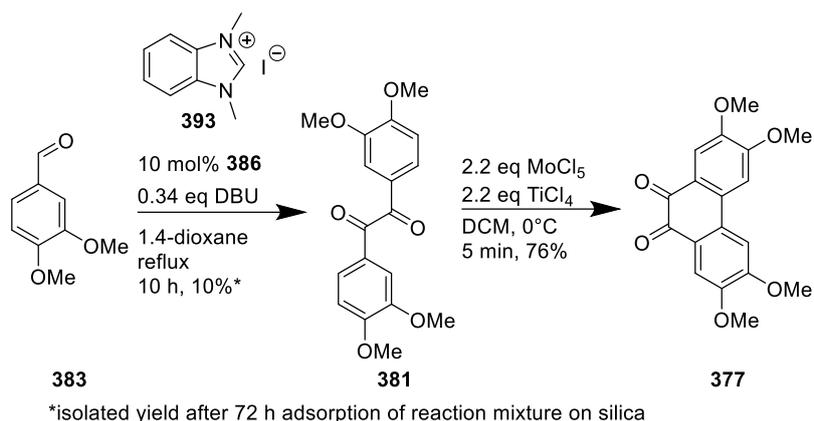
Scheme 142: Synthesis of 2,3,6,7-tetramethoxyphenanthrenequinone.

Veratraldehyde (**383**) was subjected to catalyst **386** in 1,4-dioxane with 1,8-Diaza-[5.4.0]bicycloundec-7-en DBU as base analogous to a procedure by Miyashita et al.[211] (Scheme 142). The reaction mixture was absorbed on silica for 72 h during isolation. After the column chromatography, the benzil **381** was found instead of the expected benzoin **382**. This observation can be rationalized by results of Shimakawa et al.[215], who reported the catalysing effect of DBU in oxidations of benzoins to benzils under air. Therefore, the combination of air and DBU oxidated the **382** to **381**. Further treatment with molybdenum(V)-pentachloride and titanium(IV)-tetrachloride according to Trosien and Waldvogel's[216] dehydrogenative oxidation successfully yielded to 2,3,6,7-tetramethoxy phenanthrenequinone (**377**) in 76%. The solubility of **377** was low in organic solvents and in water, the preferred less hazardous ORFB solvent with higher ion conductivity than organic solvents.[10] Water-solubility enhancing groups or bulky organic groups may increase the solubility.[217,218] Therefore, the synthesis was modified to implement a bulky protecting group on the 4'-hydroxyl function of vanillin, which enhances the solubility in organic solvents. After the synthesis of the protected phenanthrenequinone, deprotection followed by attaching a water-solubility enhancing group should increase the solubility in water. Tri*iso*propylsilyl TIPS was chosen as protecting group, because Kramer et al.[219] observed that TIPS-O-aryl ethers survived coupling reactions with molybdenum pentachloride.
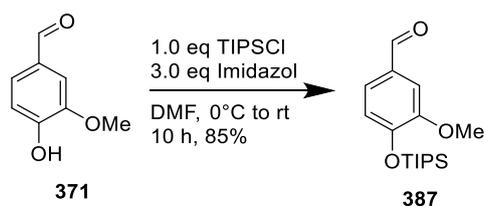
Scheme 143: Protection of vanillin with tri*iso*propyl chloride.

The TIPS protection of vanillin was analogous to Mulzer's[220] procedure (Scheme 143). A mixture of tri*iso*propylsilyl chloride, vanillin (**371**) and imidazole dissolved in DMF was stirred overnight and yielded 3-methoxy-4-tri*iso*propylsiloxy-benzaldehyde (**387**). The following benzoin condensation was modified, because the formerly used base DBU removed the TIPS group which was confirmed by results of Yeom et al.[221] Based on a modified procedure by Enders et al.[222], triethylamine as base, *t*BuOH as solvent and 3-ethyl-5-(2-hydroxyethyl)-4-methylthialzolium bromide (**388**) as catalyst were found as a suitable alternative for transforming **387** into benzoin **389** in a yield of 27% (Scheme 144).
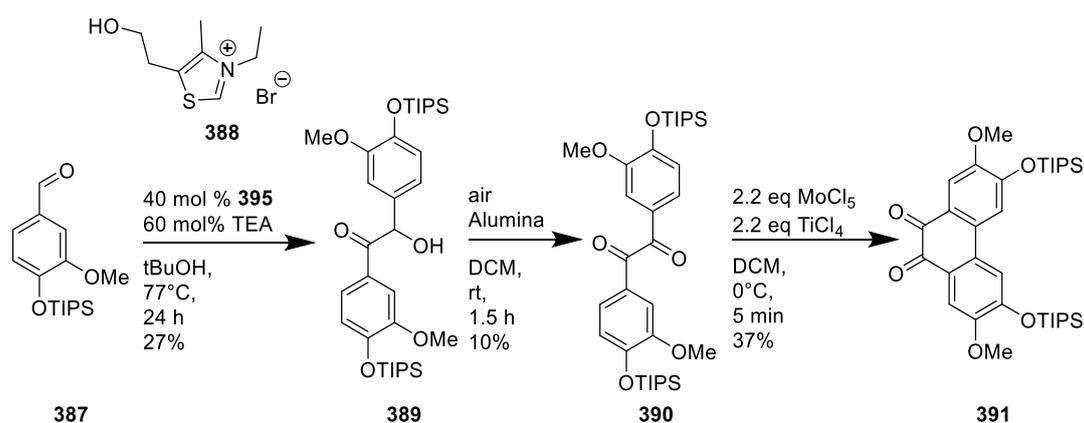
Scheme 144: Synthesis of 3,7-dimethoxy-2,6-bis (tri*iso*propsiloxy)-phenanthrenequinone.

Basic alumina catalysed oxidation of **379** with air yielded **390** in a low yield of 10%. After the oxidative dehydrogenative coupling of **390** with molybdenum(V)-pentachloride and titanium(IV)-tetrachloride, 3,6-dimethoxy-2,7-bis-(tri*iso*propylsiloxy)-9,10-phenanthrenequinone (**391**) was obtained in 37% yield. Cyclic voltammetry of 2,3,6,7-tetramethoxy phenanthrenequinone **377** by Hofmann et al.[206] revealed potentials of -1.830 mV and -1.248 mV vs. Fc/Fc$^+$ in acetonitrile. These low potentials exclude applications as catholyte material, but they offer opportunities for applications as anolyte material in non-aqueous ORBs.
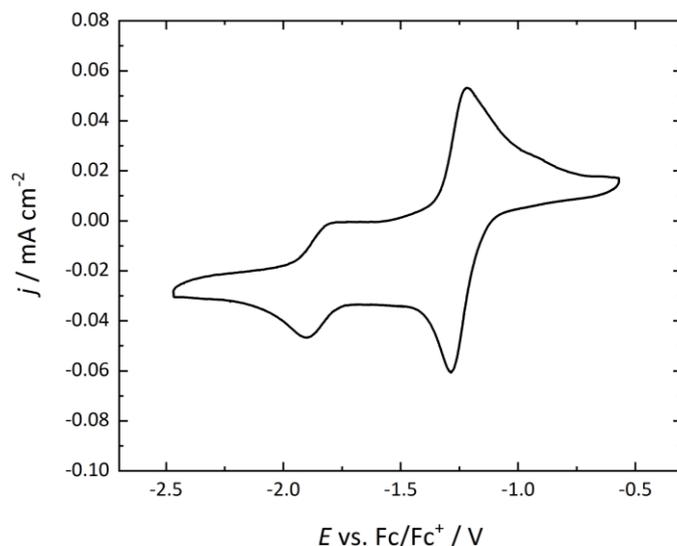
Figure 5: Cyclic voltammogram of to 2,3,6,7-tetramethoxy phenanthrenequinone (1 mM, MeCN, 0.1 M TBAP) measured by Hofmann et al.[206]

A third vanillin-derived redox material was reported by Kühlborn et al.[175] by synthesizing 5,5'6,6'-tetramethoxy indigo (**393**) (Scheme 145). Following this procedure, veratraldehyde (**383**) was nitrated with nitric acid in 61%. The obtained 6-nitro-veratraldehyde (**392**) was suspended in diluted sodium hydroxide/acetone mixture in a Baeyer-Drewson reaction yielding **393** in 23%. The very low solubility of **393** in water and organic solvents inhibited measuring the potential via cyclic voltammetry.
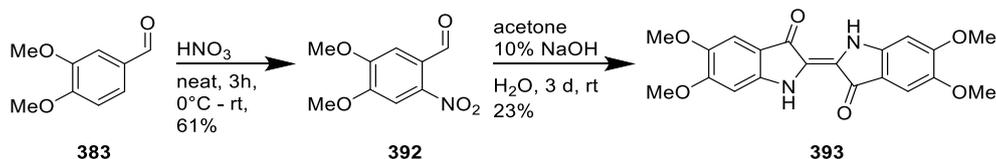
Scheme 145: Synthesis of tetramethoxyindigo.
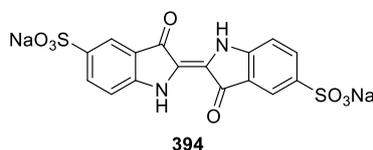
Scheme 146: indigo carmine.
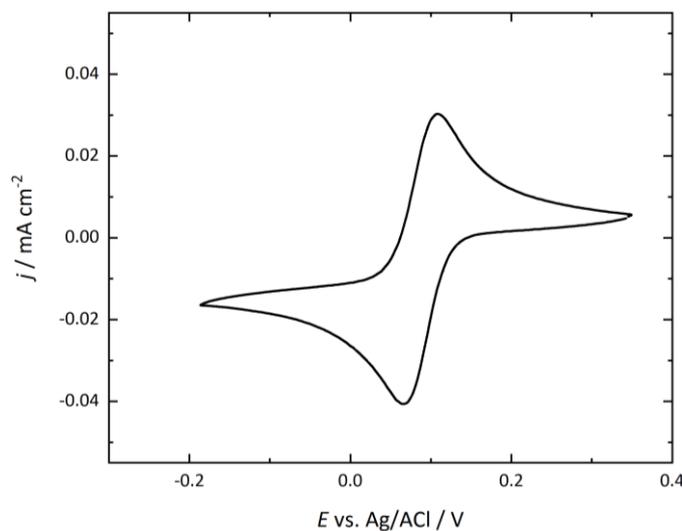
Figure 6: Cyclic voltammogram of indigo carmine (0.5 mM, 2 M H_2SO_4) measured by Hofmann et al.[206]

To get an impression of the potentials of indigo as redox material, the potential of indigo carmine (**394**) (Scheme 145) was measured by Hofmann et al.[206] via cyclic voltammetry. The measured low potential of **394** of 0.09 mV was inappropriate for applications as catholyte material (Figure 6). Methoxy substituents of **394** would decrease the potential even further due to the +M effect, which might encourage investigations as anolyte material. Moreover, indigo compounds are sparingly soluble in the targeted solvent water. Therefore, tetramethoxy indigo **394** offered another vanillin-derived redox material, but the low solubility hampered applications as ORFB material. In summary, it can be stated that vanillin can be a source for redox materials for quinone- and indigo-based redox systems. The 2-methoxy benzoquinone **373** and the bis-benzoquinone material **376** provide low positive potentials in the range of catholyte materials. Moreover, the unprotected quinone core made them susceptible to Michael-type degradation reactions with water. The negative potentials of the phenanthrenequinone derivative might fit in the range of anolyte materials. A drawback of all vanillin-derived quinone and indigo derivatives was their low water solubility. Therefore, further investigations on the potentials, stability and solubility are necessary.

4.2.2 Synthesis and Electrochemical Properties of Diazaanthraquinones

The unsubstituted diazaanthraquinone, the 6-methoxy-diazaanthaquinone and the 5,8-dihyrdroxy-diazaanthraquinone were synthesized and their electrochemical properties were investigated. The diazaanthraquinones were synthesized according to the procedure by Hong et al.[9] via the IEDDA reaction of 1,2,4,5-tetrazine and naphthoquinones catalysed by the bidentate boron Lewis acid. The necessary 1,2,4,5-tetrazine (**79**) was prepared according to a procedure by Domasevitch et al.[223]
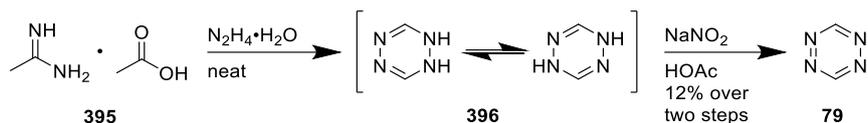
Scheme 147: Synthesis of tetrazine.[223]

After mixing formamidine acetate (**395**) with hydrazine hydrate and further oxidation with NaNO$_2$, 1,2,4,5-tetrazine (**79**) was obtained in a yield of 12% (Scheme 148). Low yields of **79** were also reported in the literature and resulted partially from its instability and high volatility.[65,223]
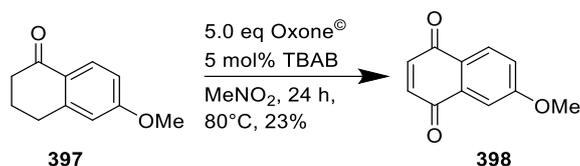
Scheme 148: Synthesis of 6-methoxynapthoquinone.[224]
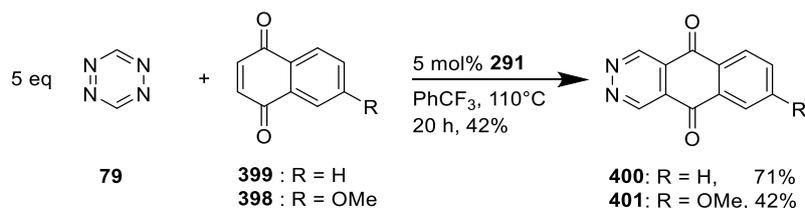
Scheme 149: IEDDA reaction of tetrazine and naphthoquinone.

Using the procedure of Hong et al.[9], the pyridazine catalyst complex **291**-catalysed IEDDA reaction of **79** and 1,4-naphthoquinone (**399**) in benzotrifluoride yielded 2,3-diazaanthraquinone (**400**) in 71% (Scheme 149). In the case of 6-methoxy-diazaanthraquinone, the required starting material 6-methoxy naphthoquinone (**398**) was prepared according to a procedure by Ren et al.[224] The 6-methoxy-1-tetralone (**397**) was oxidized in nitromethane by Oxone® and tetrabutylammonium bromide as phase transfer catalyst to the 6-methoxy-1,4-naphthoquinone (**398**) (Scheme 148). The IEDDA reaction of **79** and **399** with 5 mol% of the pyridazine catalyst complex **291** yielded 6-methoxy-diazaanthraquinone (**401**) in 42% yield (Scheme 149). The original synthesis of 5,8-dihydrodroxy-2,3-diazaanthraquinone of Hong et al.[9] was modified by protecting the hydroxy-functions of starting material naphtharazine (**402**) before the IEDDA reaction in order to the product isolation. The acetylation of **402** to 5,8-diacetoxy naphthoquinone (**403**) was accomplished by acetic anhydride and catalytic amounts of sulfuric anhydride according to a procedure by Paull et al.[225] (Scheme 150).
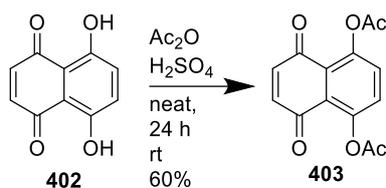
Scheme 150: Acetylation of naphtharazin.[225]
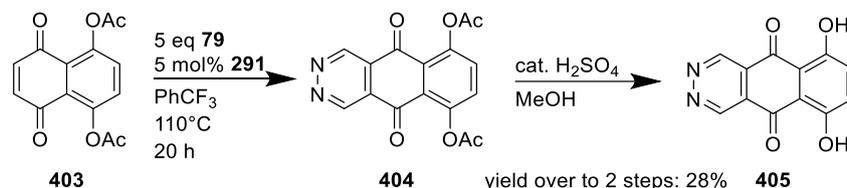
Scheme 151: Synthesis of dihydroxydiazaanthraquinone via IEDDA reaction.

The IEDDA reaction of **403** and **79**, catalysed by **291**, yielded 5,8-diacetoxy-2,3-diazaanthraquinone (**404**) (Scheme 151). Catalytic amounts of sulfuric acid in methanol deprotected **404** to 5,8-dihydroxy-2,3-diazaanthraquinone DAD(OH)$_2$ (**405**), which was obtained in a yield of 28% over two steps (Scheme 151). A sufficient isolation of **405** was achieved by using CHCl$_3$ + 1% HOAc as chromatography eluent. The overall yield from naphtharazine to **405** was 17%, which is 1% lower than Hong et al.'s[9] yield of 18% but circumvented a tedious aqueous extraction process in the product isolation.

The electrochemical properties of diazaanthraquinones were investigated via cyclic voltammetry by Hofmann et al.[199] Because the diaza-unit as potential organic Brønsted base might be susceptible to proton interactions, the measurements were conducted in acidic (2 M H$_2$SO$_4$, estimated pH = 0) and basic (1 M KOH, pH = 14) media. In acidic media, the DAD **400**, DAD(OMe) **401**, and DADdi(OH) **405** showed at a scan rate of 1 V/s potential of 328 mV, 328 mV, and 274 mV vs. Ag/AgCl, respectively (see Figure 3 in reference 198).[199] The electron-withdrawing effect of the diaza-unit caused a positive shift of the potential about by ~300 mV compared to AQDS.[127] The electron-donating effect of the hydroxy substituents of DADdi(OH) **405** decreased its potential about 54 mV. At lower scan rates of <1 V/s, decreased oxidation peaks and precipitates on the electrodes were observed in the case of DAD **400** and DADdi(OH) **405**. These results were attributed to side reactions, for example, a comproportionation reaction of reduced species and semiquinone radicals or with the sulfuric acid electrolyte. By contrast, in the case of DAD(OMe) **401**, precipitates and a decreased oxidation peak at slower scan rates were not detected. The radical stabilizing effect of the methoxy substituent was assumed to prevent such side reactions. In basic media, DAD **401**, DAD(OMe) **401**, and DADdi(OH) **405** provide a potential of -290 mV , -298 mV, -and -555 mV vs. Ag/AgCl, respectively.[199] Noteworthy was the peak splitting observed for DAD **400** and

DAD(OMe) **401**, which was attributed to stabilizing effects of the diaza-unit on the semiquinone radical. Such a peak splitting was not observed for DADdi(OH) **405**. The remarkable negative shift of the DADdi(OH) **405** potential was caused by the positive inducive effect of the deprotonated hydroxyl functions that occurred at that high *p*H level. In the basic media, the coulomb efficiencies for DAD **400** and DAD(OMe) **401** were 99.7% during 100 cycles. DADdi(OH) **405** showed an increase in the coulomb efficiency from 85% to 95% in the first 40 cycles and ~95% in the following 60 cycles.[199]

Table 13: Experimental and calculated potentials.[199]

Entry	Material	$E_{experimental}$ pH= 0, [V] vs. SHE	$E_{calculated}$ pH= 0 [V] vs. SHE	$E_{experimental}$ pH= 14 [V] vs. SHE	$E_{calculated}$ pH= 14 [V] vs. SHE
1	DAD	0.538	0.590 (0.328)[a]	-0.081	-0.448
2	DAD(OMe)	0.538	0.551 (0.295)[a]	-0.088	-0.505
3	DADdi(OH)	0.345	0.345 (0.073)[a]	-0.345	-1.804 (-0.439)[b]
4	AQ	0.077	0.120	-0.534	-0.915

[a] unprotonated species in brackets [b] one protonated hydroxyl group

The potentials of DAD **400**, DAD(OMe) **401**, and DADdi(OH) **405** were calculated with density functional theory DFT at the UBP86-D3/aug-cc-pVDZ level of theory to gain an insight into the electrochemical results by Mollenhauer et al.[199] Their geometric and electronical structures as well as their theoretical potentials were computed, considering an acidic or basic aqueous solvent (Table 13). In the case of acidic media, it was implied that the diaza-unit was protonated. In this case, the experimental results matched the calculated results for the potentials. The potential increasing effect of the electron withdrawing diaza-unit in all diazaanthraquinones and the potential decreasing effect of the hydroxyl functions were reflected by the calculations. Only the weak electron-donating effect of the methoxy substituent had a greater potential decreasing effect in the calculations which was not observed in the experimental results. In the case of the basic media, the DFT calculations overestimated the negative potential shift about 400 mV. In the case of DADdi(OH) **405**, the calculated potential for total deprotonated species exceeded the experimental value by about 1.5 V. The calculated potential for an assumed two-electron-one proton step with 439 mV was closer to the experimental result of 345 mV.[199] Therefore, the complex nature of the potential of the four hydroxyl functions bearing DADdi(OH) **405** required further studies.[199] In summary, it can be stated that the diaza-functionalisation caused a potential increase of about 300 mV in the diazaanthraquinones compared to anthraquinones. At a low pH value, DAD **400** and DADdi(OH) **405** showed side reactions. At a high pH value, an entirely electrochemically

95

reversible redox process was observed for all diazaanthraquinones. DAD **400** and DAD(OMe) **401** showed a peak-splitting, which occurred probably due to their stable semiquinones. DADdi(OH) **405** provided the lowest potential, which was therefore promising for anolyte applications. These results and the 300 mV positive potential shift predestined for catholyte material encouraged further studies in synthesizing naphthoquinones via IEDDA reaction and the investigation of their electrochemical properties.

4.2.3 Synthesis and Properties of Diazanaphthoquinones

Because Er et al.[118] calculated that the potential of the naphthoquinone core surpassed the potential of the anthraquinone core, the 2,3-diaza-5,8-naphthoquinone moiety was targeted as promising a ORFB material for prospective catholyte applications. The 2,3-diaza-naphthalene-5,8-quinone should be synthesized via the IEDDA reaction of 1,2,4,5-tetrazine and benzoquinone. Since Er et al.[118] pointed out that the 1,2-naphthoquinone achieved higher potentials than the 1,4-naphthoquinone, the 5,6-dihydroxyphthalazine 5,6-DHP (**308**), the reduced form of the 2,3-diaza-5,6-naphthoquinone, was synthesized to compare the potential with the 2,3-diaza-5,8-naphthoquinone. The precursor 2,2-dimethyl-phthalazinodioxole (**408**) was synthesized via Kessler et al.'s[161] established phthalazine synthesis.
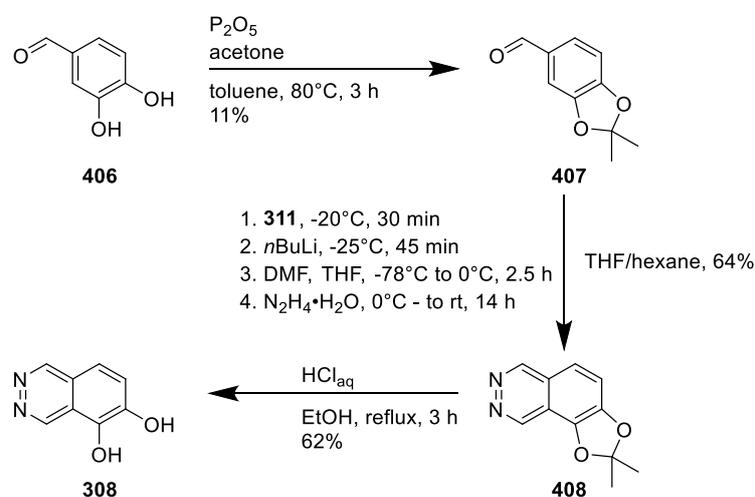
Scheme 152: Synthesis of 5,6-dihydroxyphthalazine.[161,226]

The synthesis of the 5,6-dihydroxy phthalazine 5,6-DHP (**308**) started with the protection of protocatechuic aldehyde (**413**) with acetone and phosphorous pentoxide as acid and water scavenger in toluene to 2,2-dimethyl-1,3-benzodioxole-5-carboxaldehyde (**414**) (Scheme 152). The low yield of 11% corresponds to the reported yield in the original procedure of Kotnik et al.[226] After the treatment with lithium amide **311**, *n*-butyllithium, DMF and hydrazine hydrate according to Kessler et al.'s[161] phthalazine synthesis, 2,2-dimethyl-phthalazinodioxole (**407**)

was obtained in a yield of 64%. The deprotection with hydrochloric acid in ethanol yielded 5,6-dihydroxy phthalazine (**308**) in a yield of 62%.
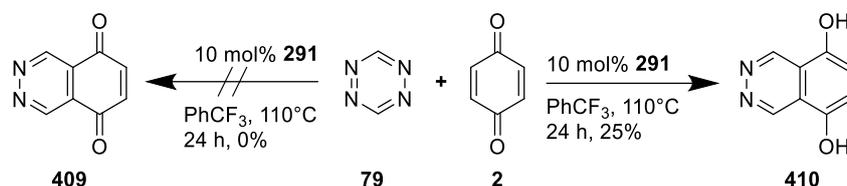
Scheme 153: Synthesis of Dihydroxyphthalazines.

The comparative compound 2,3-diazanaphthoquinone DNQ (**409**) was expected to be obtained from the IEDDA reaction between 1,2,4,5-tetrazine (**79**) and 1,4-quinone **2**. (Scheme 153). Both starting materials were exposed to the boron bidentate boron Lewis acid catalyst pyridazine complex **291** in benzotrifluoride at 100°C. Surprisingly, the 5,8-dihydroxy phthalazine DHP (**410**) was obtained instead of the predicted DNQ **409**.
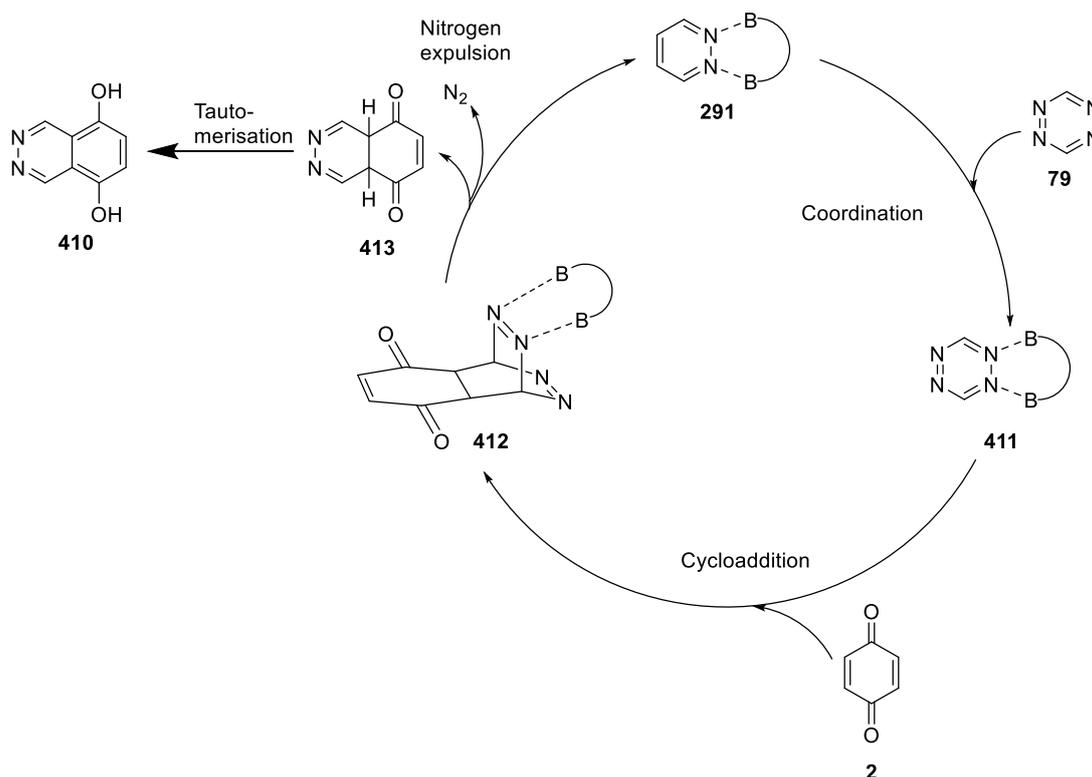
Scheme 154: Mechanism of the IEDDA reaction of tetrazine and 1,4-benzoquinone.

This result can be rationalized by an insight in the mechanism (Scheme 154). After 1,2,4,5-tetrazine (**79**) was coordinated by the bidentate boron Lewis acid **411**, the cycloaddition with benzoquinone (**2**) occurred to **412**. The thermodynamic driving force was the expulsion of nitrogen resulting in non-aromatic diaza-compound **413**. Because the aromatic enol form is

thermodynamically favoured in contrast to a non-aromatic keto structure, **413** tautomerized to phthalazine **410**. Such a thermal keto-enol tautomerism at around 120°C was also observed by Kündig et al.[227] in case of naphthalene-1,4-diol and 1,2,3,4-tetrahydronaphthalene. Moreover, the present boron Lewis acid might reinforce the tautomerism because boron Lewis acid facilitated enolization formation as observed by Banerjee et al.[228] Therefore, the phthalazine product was most likely caused by Lewis acid catalysed keto enol tautomerism driven by gaining the energy from aromatization. The electrochemical properties of 5,6-DHP **308** and 5,8-DHP **410** were investigated via cyclic voltammetry by Hofmann et al.[172,206] The measured potentials were in accordance with the computational studies of Er et al.[118]: the potential of *ortho*-quinone 5,6-DHP **308** with 666 mV (876 mV vs. SHE) vs. Ag/AgCl was higher than the potential of para-quinone DHP **410** with 586 mV vs. Ag/AgCl (796 mV vs. SHE) (Figure 7, 8).[172,206,229] The reduction peak of 5,6-DHP **308** was smaller than the oxidation peak, which indicated that side reactions occurred during the redox reaction. Because semiquinones were observed to undergo disproportionation reactions, the semiquinones of 5,6-DHP **308** could be disproportionate in the redox process.[230–232] The depopulation of the semiquinone amount might cause the increased oxidation peak and the decreased reduction peak. Moreover, the unsubstituted 8-position of 5,6-DHP **308** could be susceptible to Michael-type water attacks, such as in the BQDS degradation.[122] Thus, the presence of more oxidizable material might increase the oxidation peak.
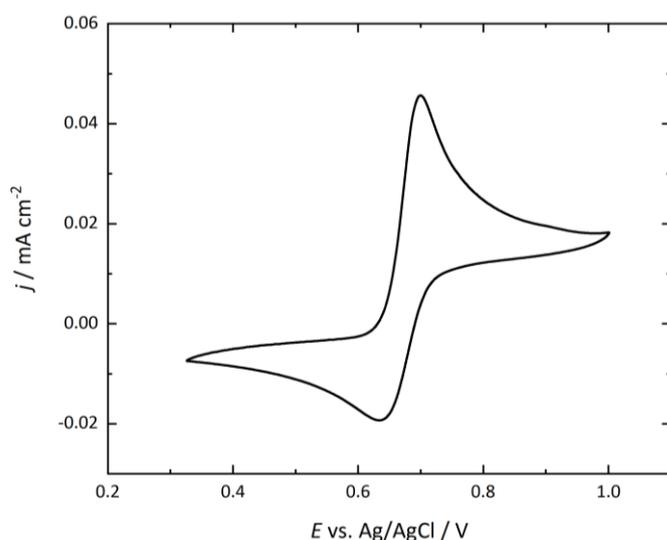
Figure 7: Cyclic voltammogram of 5,6-DHP ($E_{1/2}$ = 666 mV, 0.5 mM, 2 M HCl) measured by Hofmann et al.[206]
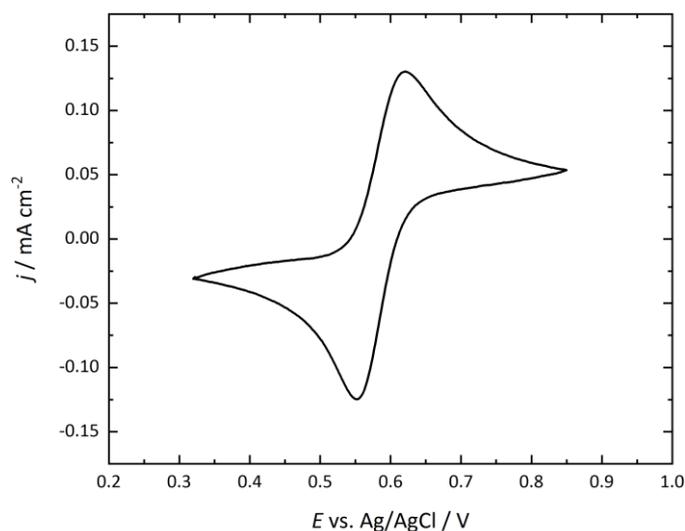
Figure 8: Cyclic voltammogram of 5,8-DHP ($E_{1/2}$ = 586 mV, 0.5 mM, 1 M H_2SO_4) measured by Hofmann et al.[172,229]

In contrast to 5,6-DHP **308**, the cyclic voltammogram of 5,8-DHP **410** showed a fully reversible redox process and, thus, a more stable material. Therefore, the investigation focused on the DHP **410** and the *ortho*-quinone 5,6-phthalazine **308** was not pursued.

Table 14: .Electrochemical half-cell potentials of quinone redox materials and DHP[121,122,172]

Entry	Material	$E_{1/2}$ [V] vs. SHE
1	1,4-BQ	693
2	1,2-BQ	782
3	BQDS	895
4	DHDMBS	553
5	DHP	796

Compared to the potentials of other quinone materials, the DHP **410** has a lower potential than BQDS, but a higher one than 1,4-benzoquinone, 1,2-benzoquinone and DHDMBS (Table 14, Entry 1-5). As a consequence of the successful synthesis of DHP **410** and its promising electrochemical properties, the substitution pattern was modified to alter the electrochemical potential. Therefore, the boron Lewis acid catalysed IEDDA reactions of electron-withdrawing and electron-donating substituted tetrazines and benzoquinones were explored.
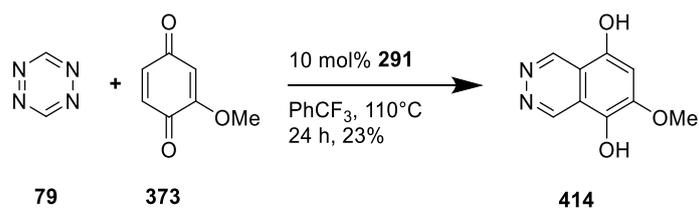
Scheme 155: Synthesis of 6-methoxy DHP.

This investigation offered the opportunity to combine the vanillin-derived materials with the catalysed IEDDA reaction: vanillin-derived 2-methoxybenzoquinone (**373**) was used as starting material in the bidentate boron catalysed IEDDA reaction with tetrazine (**79**) (Scheme 155). Dienophile **373** featured two potential reaction sites: The hydrogen-substituted, less sterically demanding alkene and a methoxy-substituted alkene, which was sterically more crowded, but more electron-rich due the electron donating effect of the methoxy group. As a result of the reaction, solely the 6-methoxy-5,8-dihydroxyphtalazine (**414**) was obtained in a yield of 23%. The unsubstituted DHP **410** was not detected. As Sauer et al.[118] pointed out, any other substituent instead of a hydrogen atom influences the reactivity of the dienophile referring to its steric and electronical properties. In this specific case, the lower steric demand of the unsubstituted alkene outcompeted the thermodynamically favoured electron-donating methoxy group substituted alkene.
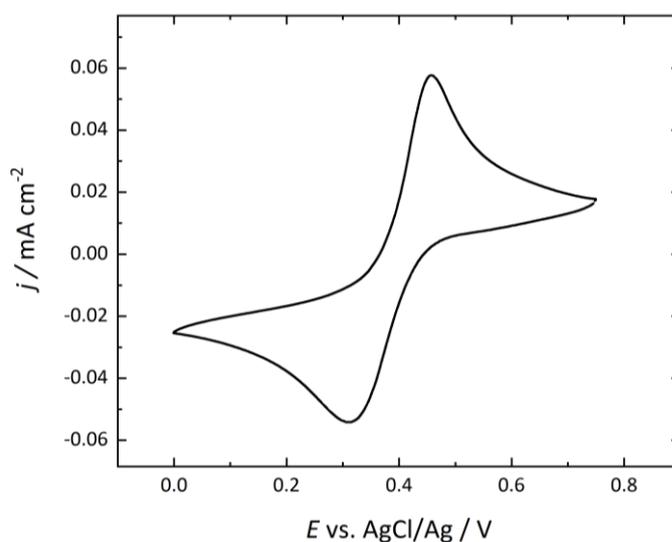
Figure 8: Cyclic voltammogram of DHP(OMe) ($E_{1/2}$ = 512 mV, 0.5 mM, 1 M H_2SO_4) measured by Hofmann et al.[172,229]

The potential of DHP(OMe) **414** was 512 mV vs. Ag/AgCl, which was investigated by Hofmann et al.[172,229] via cyclic voltammetry. The potential of **414** was lower than that of DHP **410** with 586 mV (Figure 8). This potential downshift was caused by the electron-donating effect of the

methoxy substituent as proposed by the computational studies of Er et al.[118] The same potential-decreasing effect was expected for electron-donating methyl substituents.
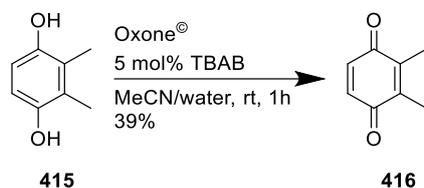
Scheme 156: Synthesis of 2,3-dimethylbenzoquinone.
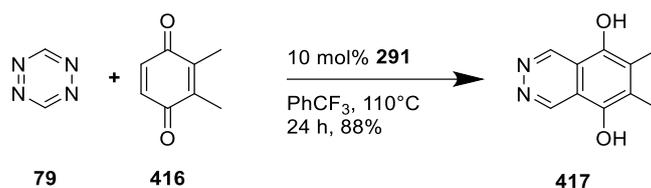
Scheme 156: Synthesis of DHP(Me)$_2$.

The synthesis of 6,7-dimethyl-5,6-dihydroxyphthalazine DHP(Me)$_2$ required 2,3-dimethyl-1,4-benzoquinone (**416**) as starting material which was obtained after oxidizing 2,3-dimethyl-1,4-hydroquinone (**415**) in a yield of 39% according to the procedure by Yakura et al.[204] (Scheme 156). The following bidentate boron Lewis acid catalysed IEDDA reaction with 1,2,4,5-tetrazine (**79**) and **416** yielded 6,7-dimethyl-5,6-dihydroxyphthalazine DHP(Me)$_2$ (**417**) in a yield 88% (Scheme 157).
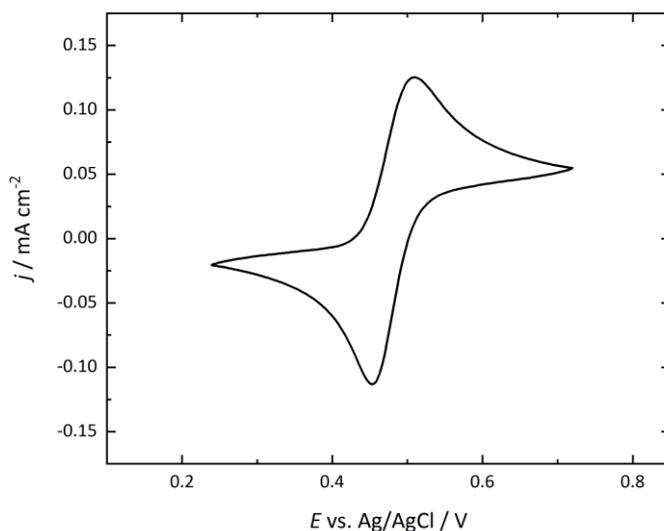
Figure 9: Cyclic voltammogram of DHP(Me)$_2$ ($E_{1/2}$ = 481 mV, 0.5 mM, 1 M H$_2$SO$_4$) measured by Hofmann et al.[172,229]

101

The potential of DHP(Me)$_2$ **417** with 481 mV vs. Ag/AgCl was investigated via cyclic voltammetry by Hofmann et al.[172,229] The electron-donating methyl substituents decreased the potential of DHP(Me)$_2$ **417** by about 105 mV to 481 mV vs. Ag/AgCl compared to 586 mV of DHP **410**, and thus, it was even lower than that of the single methoxy substituent **414** with 512 mV (Figure 9). By contrast, a potential upshift was expected for electron-withdrawing substituents, which was preferred for targeted catholyte ORFB material. Therefore, EWGs were attempted to add to the DHP structure. Moreover, attaching the EWGs at the diene or the dienophile of the catalysed IEDDA reaction enabled the investigation of the electronic and steric effect on the reaction outcome.
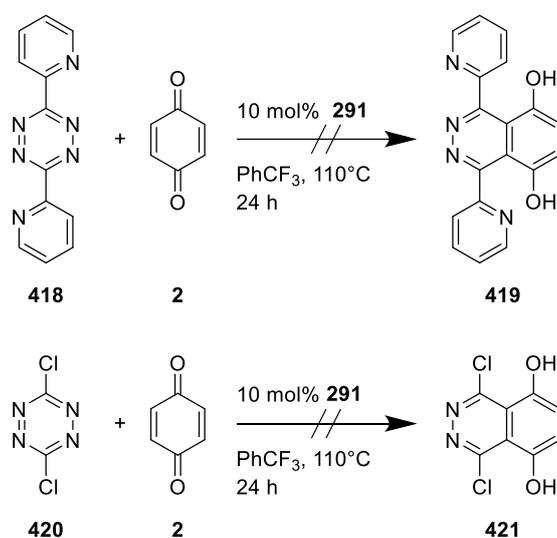
Scheme 158: Attempted IEDDA reactions of 2,6-substituted tetrazines.

The 1,2,4,5-tetrazines were substituted with EWGs because lowering its LUMO energy level should increase the reactivity of the dienophile. Chlorine-substituent was chosen because Er et al.[118] predicted their potential-decreasing effect via computational studies. The LUMO-lowering, and thus IEDDA reactivity-enhancing effect of pyridyl-substituent was shown by Xinyuan et al.[233] Moreover, protonation by acidic electrolytes or further methylation offered the opportunity for electron-withdrawing pyridinium ion, and thus higher potentials. Unfortunately, in the reactions of 3,6-dipyridyl-1,2,4,5-tetrazine (**418**) and 3,6-dichloro-1,2,4,5-tetrazine (**420**), benzoquinone (**2**), and the bidentate boron pyrazine complex **291**, the targeted phthalazines **419** and **421** were not obtained and the starting material was recovered (Scheme 158). The steric demand of the tetrazine substituents might have overcrowded the tetrazine catalyst complex and/or the transition state and prohibited the IEDDA reaction. As a consequence of the unsuccessful IEDDA reactions with substituted 1,2,4,5-tetrazines, the investigations were focused on introducing EWG-substituted benzoquinones.
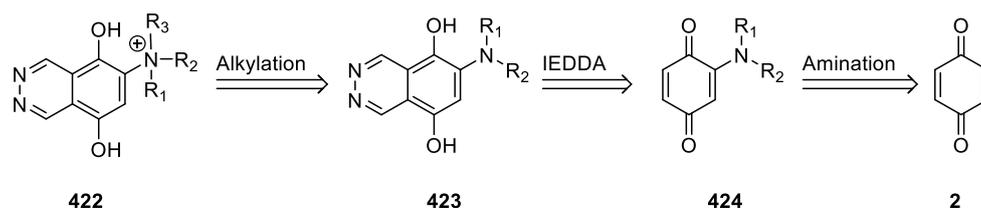
Scheme 159: Retrosynthesis trialkylammonium DHP synthesis.

A trialkylammonium substituent as EWG of the phthalazine was targeted to increase the potential and water-solubility because Janoschka et al.[132] observed both effects on the ORFB material TEMPTMA. Ammonium phthalazine **422** should be synthesized via the alkylation of an amine phthalazine **423**, which could be prepared via an IEDDA reaction of **79** and an amine benzoquinone **424** (Scheme 159). The amine benzoquinone **424** should be obtained from **2** according to the procedure of by Ott and Pinter.[234] The 2-pyrrolidino-benzoquinone (**426**) was obtained in 33% by mixing pyrrolidine (**425**) and benzoquinone (**2**) in CHCl$_3$/water mixture and potassium dihydrogenphosphate as pH buffer (Scheme 160).
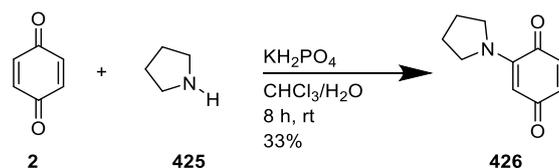
Scheme 160: Synthesis of 2-pyrrolidinyl-1,4-benzoquinone.
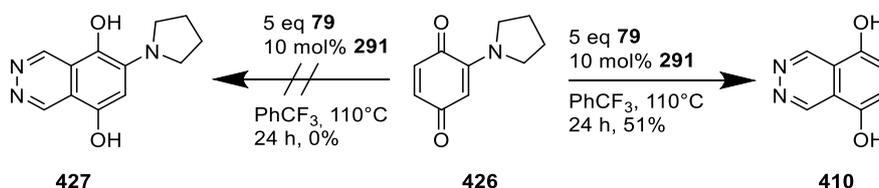
Scheme 161: Unexpected amine expulsion during IEDDA reaction.

Surprisingly, the IEDDA reaction of **426** and **79** yielded unsubstituted DHP **410** in a yield of 51% instead of the expected 6-pyrrolidino-5,8-dihydroxy-phthalazine (**427**) (Scheme 161). This result can be rationalized by the different substituent effects of bifunctional **428**: the amine as EDG increased the alkene reactivity in the IEDDA reaction compared to the hydrogen-substituted reaction site (Scheme 126).
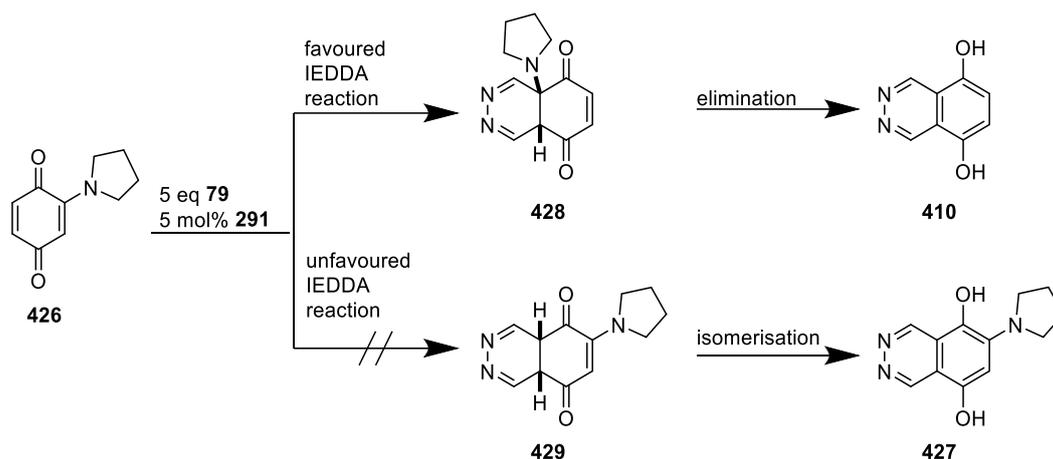
Scheme 162: Proposed mechanism for amine expulsion during IEDDA reaction.

Therefore, the **426** reacted to **428** and not to **429** (Scheme 162). The subsequent amine elimination yielded **410**. Contrary to the reaction of 2-methoxy-1,4-benzoquinone (**373**) and **79** to DHP(OMe) **414**, the effect of the amine EDG surpassed the steric demand its own steric demand and the sterically more accessible hydrogen-substituted reaction site (Scheme 162). These explanations were supported by the results IEDDA of the reactions of 1,2,4,5-tetrazine by Sauer et al.[65], in which amine substituted alkenes showed a higher reactivity and a higher tendency of amine elimination compared to alkoxy substituents. Therefore, the synthesis of amino-substituted DHP and the subsequent alkylation into an ammonium salt was not pursued further.

Alternatively, halogen substituents were investigated due to Er et al.'s[118] promising computational results of their potential-increasing effect. Moreover, the fluorine-, chloro- and bromo-substituents could be installed easily by reacting the achievable substituted benzoquinones in the IEDDA reaction with tetrazine.
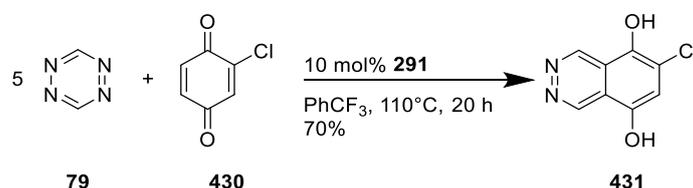
Scheme 163: Synthesis of 6-chloro-5,8-dihydroxyphthalazine
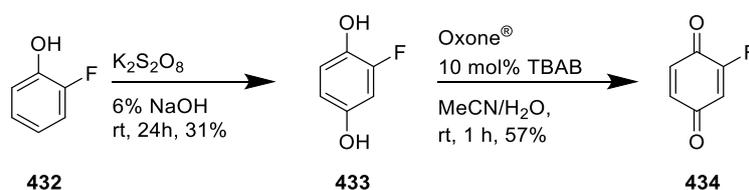
Scheme 164: Synthesis of 2-fluoro-1,4-benzoquinone.
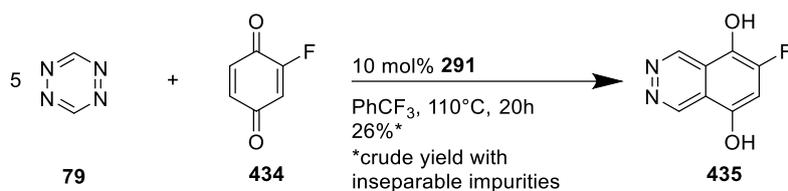
Scheme 165: Synthesis of 6-fluoro-5,8-dihydroxyphthalazine.

The 6-chloro-5,8-dihydroxy phthalazine DHP(Cl) (**431**) was obtained in a yield of 70% in the bidentate boron Lewis acid catalysed IEDDA reaction of 2-chloro-1,4-benzoquinone (**430**) and 1,2,4,5-tetrazine (**79**) (Scheme 163). Introducing the fluoro-substituent required the synthesis of the starting material 2-fluoro-1,4-benzoquinone (**434**) according to procedures by Essers et al.[235]: Elbs persulfate oxidation of 2-fluorophenol (**432**) yielded 2-fluoro-1,4-hydroquinone (**433**) in 31%, which was further oxidized with Oxone® to 2-fluoro-1,4-benzoquinone (**434**) in a yield of 57% (Scheme 164). The 6-fluoro-5,8-dihydroxy phthalazine DHP(F) (**435**) was obtained in a crude yield of 26% (Scheme 165). The impurities were not removable via column chromatography.
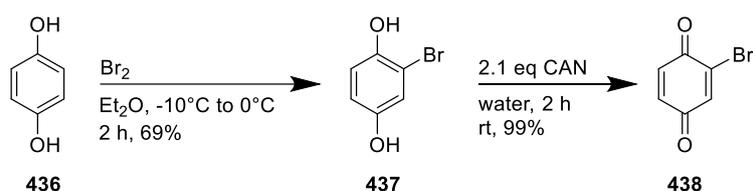
Scheme 166: Synthesis of 2-bromo-1,4-benzoquinone.
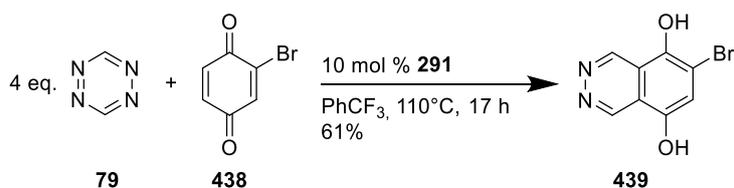
Scheme 167: Synthesis of 6-bromo-5,8-dihydrophthalazine.

The synthesis of the 6-bromo-DHP required 2-bromo-1,4-benzoquinone (**438**) as starting material. Bromination of 1,4-hydroquinone (**436**) with bromine led to 2-bromo-1,4-hydroquinone (**437**) in a yield of 69%, which was further oxidized by cerium ammonium nitrate to **438** in a yield of 99% (Scheme 166). After the **291**-catalysed IEDDA reaction of **79** with **438**, 6-bromo-5,8-dihydroxy phthalazine DHP(Br) (**439**) was obtained in a yield of 61% (Scheme 167).
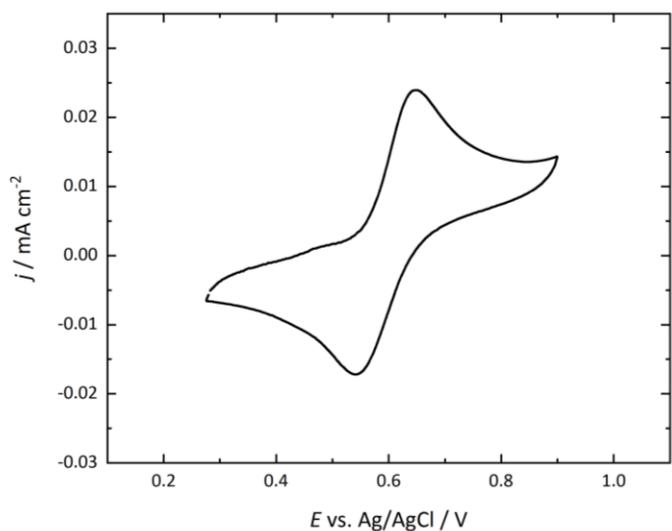
Figure 10: Cyclic voltammogram of DHP(F) ($E_{1/2}$ = 594 mV, 0.5 mM, 2 M HCl) measured by Hofmann et al.[206]
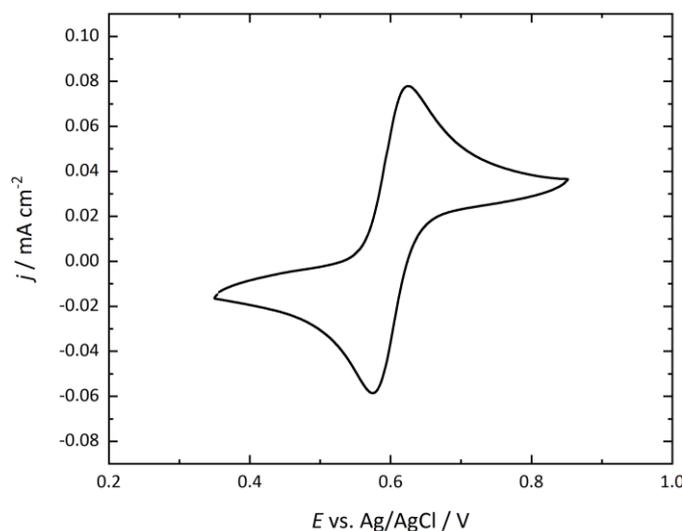
Figure 11: Cyclic voltammogram of DHP(Br) ($E_{1/2}$ = 599 mV, 0.5 mM, 2 M HCl) measured by Hofmann et al.[206]

The half-wave potentials of DHP(F) **435** with 594 mV and DHP(Br) **439** with 599 mV, which were slightly higher than that of DHP **410** with 586 mV, were measured via cyclic voltammetry by Hofmann et al.[206] (Figure 10, 11). The small potential increasing effect was confirmed by computations on PBE-D3/aug-cc-pVDZ level by Mollenhauer et al.[172,236] The higher potentials compared to DHP were caused by the negative inductive effect of both halogen substituents. However, the inherent positive resonance effect of the halogen substituents competed with their negative inductive effect. Compared to the bromo-substituent, the positive resonance

effect of the fluoro-substituent surpassed the negative inductive effect and caused the smaller half-wave potential.[235,237–241] In summary, it can be stated that halogen-substitution slightly increased the potential.

The electron-withdrawing sulfonic acid group, as applied by Yang et al.[121] and Hoober-Burkhardt et al.[122] on benzoquinones, combined an increasing effect on water-solubility and electrochemical potential. Moreover, computational studies on PBE-D3/aug-cc-pVDZ level by Mollenhauer et al.[172,236] demonstrated a positive potential shift about of 150-200 mV for DHPs substituted with methylsulfon/sulfonic acid functional group at 6-position compared to unsubstituted DHPs. Therefore, attaching the sulfonic acid group to the DHP was attempted. As an alternative to the sulfonic acid group, alkyl sulfon substituents should be tried because of their high electron-withdrawing effect.[240,241]
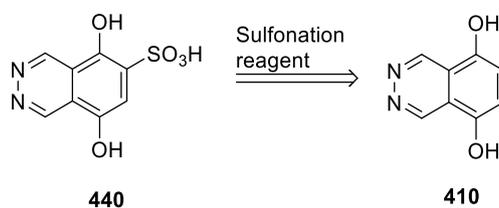
Scheme 168: Direct Sulfonation of DHP.
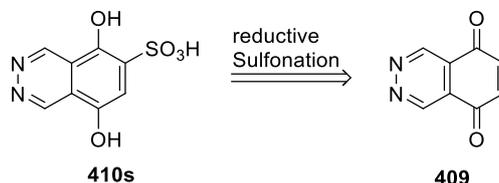
Scheme 169: Reductive Sulfonation of DNQ.
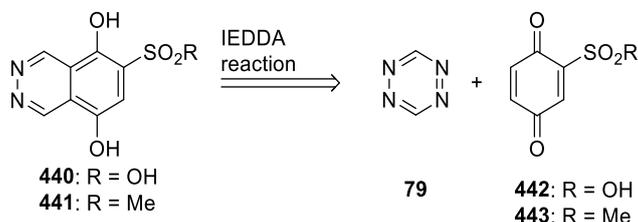
Scheme 170: IEDDA reaction of tetrazine and sulfonated benzoquinone.

Three strategies were considered to 5,8-dihydroxyphthalazine-6-sulfonic acid **440** or its derivative 5,8-dihydroxy-6-methylsulfonyl-phthalazine: the direct sulfonation of DHP **410** with a sulfonation reagent, the reductive sulfonation of DNQ **409** and the IEDDA reaction of 1,4-benzoquinone-2-sulfonic acid **442** and 2-methylsulfonyl-1,4-benzoquinone **443** and tetrazine (**79**) (Scheme 168-170).
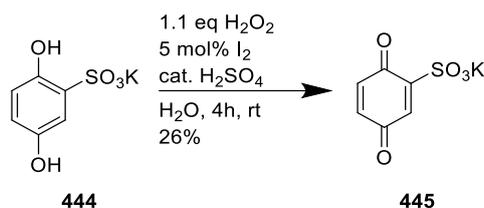
Scheme 171: Synthesis of 1,4-benzoquinone-2-sulfonic acid potassium salt.
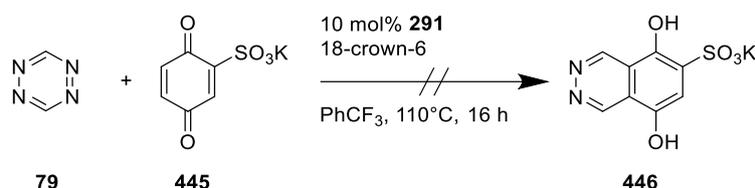
Scheme 172: Attempted synthesis of 5,8-dihydroxyphthalazine-6-sulfonic acid potassium salt.

The direct IEDDA reaction between 1,4-benzoquinone-2-sulfonate potassium salt (**445**) and tetrazine (**79**) to 5,8-dihydroxyphthalazine-6-sulfonic acid potassium salt (**446**) was attempted (Scheme 172). The required **445** was synthesized via the oxidation of 1,4-hydroquinone-2-sulfonate potassium salt (**444**) with hydrogen peroxide and iodine and sulfuric acid as catalyst in water as solvent according to a procedure by Minisci et al.[242] (Scheme 171). Potassium salt **445** was obtained in a yield of 26%. Crown ether 18-crown-6 was added to the reaction mixture of **79**, **445** and catalyst pyridazine complex **291** to exploit its solubility-increasing effect of potassium salts in organic solvents (Scheme 172).[243] Unfortunately, starting material was recovered after the attempted IEDDA reaction confirmed by crude spectra of ^{1}H-NMR spectroscopy and ESI-mass spectrometry. The sulfonate anion might coordinate strongly to the bidentate Lewis acid and might inhibit the catalyst. The synthesis of a protonated benzoquinone sulfonic acid species with a potentially higher solubility was neglected because of the high susceptibility of the benzoquinone core towards acid catalysed polymerisation and degradation reactions leading to self-destruction.[244] Additionally, the HOMO$_{dienophile}$-LUMO$_{diene}$ gap might be increased by the HOMO-level-decreasing electron-withdrawing sulfonate group of the diene **445**. Consequently, the thermodynamical barrier reached a level where the IEDDA reaction did not occur anymore. Since the synthesis of potassium salt via an IEDDA reaction failed, the alternative methods to introduce the sulfonic acid group were attempted.
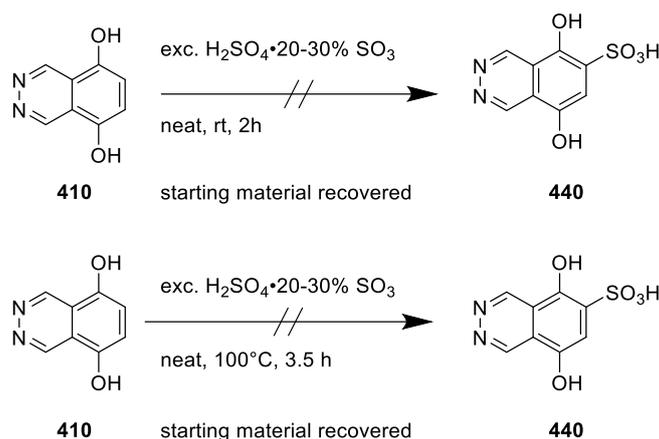
Scheme 173: Attempted direct sulfonations of DHP.

The direct sulfonation of DHP **410** to 5,8-dihydroxyphthalazine-6-sulfonic acid (**440**) was attempted with fuming sulfuric acid (20% - 30% SO_3 content) at room temperature and at 100°C (Scheme 173). Unfortunately, the starting material **410** was recovered. The low reactivity of hydroxy aza-naphthalenes in electrophilic sulfonations was also confirmed by the results of Andronova et al.[245]: the sulfonation of 3-hydroxyquinoline and 4-hydroxyquinoline required fuming sulfuric acid (20% SO_3 content) at 200°C. The electron-withdrawing 2,3-diaza unit might diminish the reactivity of DHP **410** towards electrophilic substitution reactions even more than the single nitrogen of hydroxyquinoline. Therefore, the direct sulfonation of DHP **410** was not pursued further.

The reductive method was attempted as the next method to synthesize a sulfonic acid DHP. The reductive sulfonation was based on the simultaneous reduction and sulfonation of naphthoquinone to 1,4-dihyhdroxy naphthalene with bisulfites by Fini et al.[246] (Scheme 174). Therefore, the oxidated DNQ species of DHP was required.
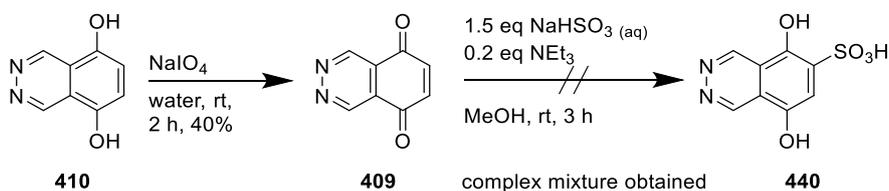
Scheme 174: Successful oxidation of DHP to DNQ and attempted reductive sulfonation.

Sodium iodide oxidized DHP **410** successfully to DNQ **409** in a yield of 40%. After the attempted reductive sulfonation to **440**, an inseparable complex mixture, including mainly **410**, was obtained. Therefore, the bisulphite reduced **409** back to **410** instead of the targeted substitution.
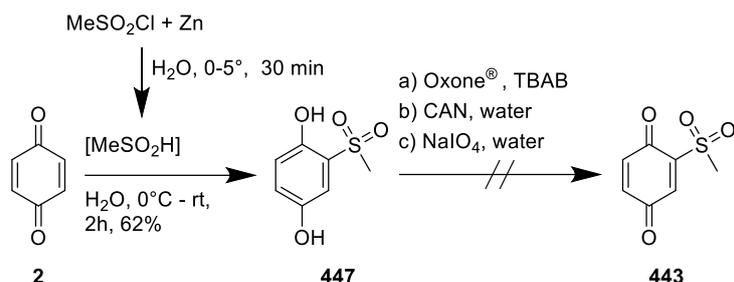
Scheme 175: Successful synthesis of 2-methylsulfonyl-1,4-benzoquinone and attempted IEDDA reaction with tetrazine.
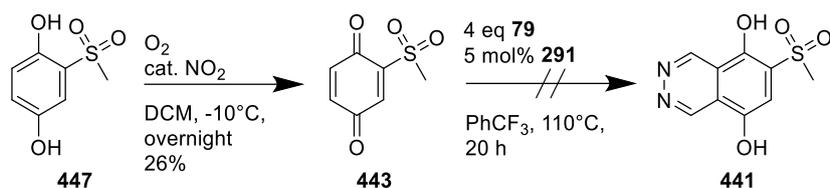
Scheme 176: Successful synthesis of 2-methylsulfonyl-1,4-benzoquinone and attempted IEDDA reaction with tetrazine.

As an alternative to the sulfonic acid group, it was attempted to introduce the methyl sulfon functional group via an IEDDA reaction of 2-methylsulfonyl-1,4-benzoquinone (**443**) (Scheme 175, 176). The synthesis of the required **443** was started by a reductive sulfonylation according to a procedure by Konieczny et al.[247] Benzoquinone (**2**) was reduced to 2-methylsulfonyl-1,4-hydroquinone (**447**) with sulfinic acid which was generated via the reduction of methansulfonyl chloride with zinc. Further oxidations of **447** with Oxone® and TBAB, cerium ammonium nitrate and sodium iodide did not lead to **443**. The probably high water-solubility of **443** hindered the isolation from the aqueous reaction mixture. After Rathore et al.'s[248] autocatalytic oxidation of **447** in oxygen atmosphere induced by traces of nitrogen dioxide in DCM, **443** was obtained in a yield of 26%. Unfortunately, the IEDDA reaction of **443** and tetrazine (**79**) catalysed by **291** did not lead to 6-methylsulfonyl-5,8-dihydroxyphthalazine (**441**). Instead of the targeted **441**, starting material was recovered. The strong electron-withdrawing effect of methylsulfonyl functional group decreased the HOMO level of **443** and thus increased the $HOMO_{dienophile}$-$LUMO_{diene}$ gap. This thermodynamic barrier inhibited the IEDDA reaction from occurring. Highly electron deficient benzoquinones did not undergo the IEDDA reaction. Because the installation of sulfonyl groups before the IEDDA reaction failed, a functionalisation after the IEDDA reaction was tried. The key method for this alternative approach was the reductive alkyl thiolation of the DNQ **409** to thioether **448** according to a modified procedure by Yadav et al.[249] (Scheme 177). Further oxidation should yield the targeted sulfone **449**.
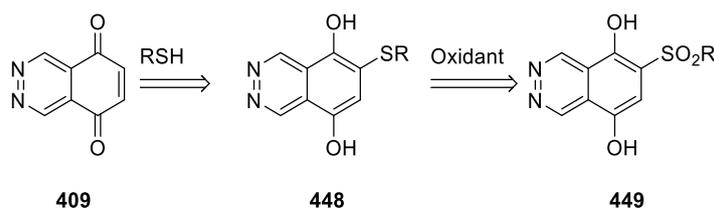
Scheme 177: Planned synthesis of 6-*iso*propylthio-DHP and attempted oxidation.
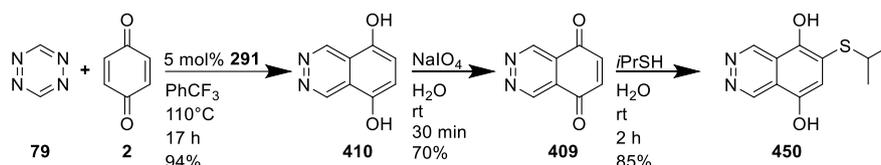
Scheme 178: Synthesis of 6-*iso*propylthio-DHP.
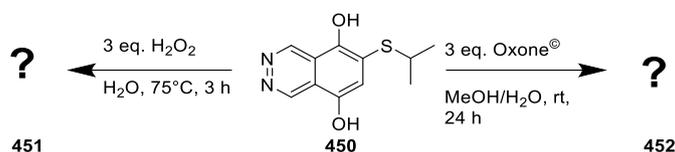
Scheme 179: Oxidation of 6-*iso*propylthio-DHP.
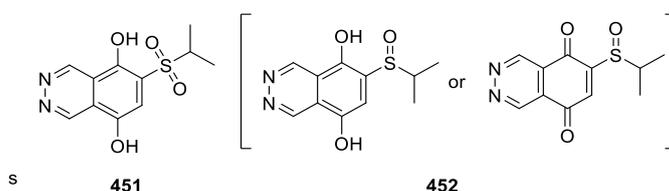
Scheme 180: Structure suggestions of the oxidated 6-*iso*propylthio-DHP species.

DHP **410** was obtained in a yield of 94% after the IEDDA reaction of **79** and **2**, catalysed by bidentate boron Lewis acid pyrazine complex **291**. Then, **410** was oxidized by sodium periodate, and **409** was obtained in 70% yield (Scheme 178). Less volatile propane-2-thiol was chosen for thio-alkylation because it was less volatile than methanethiol or ethanethiol. Stirring **417** with propane-2-thiol yielded thioether 5,8-dihydroxy-6-*iso*-propylthio-phthalazine DHP(S*i*Pr) (**450**). The following oxidation of **450** with hydrogen peroxide in water at 75°C was conducted according to a procedure for thiol oxidation by Jereb[250] yielding compound **451** (Scheme 179). The analysis of ^{1}H-NMR and ^{13}C-NMR spectra showed typical signals of a phthalazine. The signals of the shifts of methyl groups of the *iso*-propyl split into a doublet which indicated a stereogenic center. However, it cannot be excluded that **451** as probable oxidated thiol species provides a second order type of NMR spectra as described by Stevenson.[251] Therefore, the NMR analysis of **451** was not sufficient to distinguish between the assignment of a sulfone or a sulfoxide functional group. An alternative oxidation attempt of

450 with Oxone® described by Yu et al.[252] led to another compound **452** with different NMR-Spectra than **450** and **451**. It is important to note that all three thio-*iso*propyl compounds could not be identified via ESI- and GC-MS mass spectra because matching quasi-molecular ions were not found. The poor volatility might hinder the necessary evaporation in the gas phase. Moreover, the high redox potential and the multiple redox active functions of these compounds might interfere with the ionisation process. Sojo et al.[253] observed oxidation, rearrangements, and dimerization of the oxidative active catechol. Vessecchi et al.[254] studied the redox behaviour of 1,4-naphthoquinone derivatives during cyclic voltammetry and electrospray ionisation and found radical anions which underwent side reactions leading to complex the quasi-molecular ion spectra. Therefore, the *iso*propyl thio-compounds **450**, **451** and **452** were suspected of undergoing side reactions, e.g., oxidation, dimerization and rearrangements during the electrospray ionisation, which hindered the detection of suitable quasi-molecular ions. IR-spectroscopy was attempted as an alternative identification method. Unfortunately, a clear assignment of **451** and **452** to sulfoxide or sulfone based on the S=O IR-bands was hindered by interfering IR-bands of the aromatic naphthalene core structure. However, an oxidation of **451** to the quinoid form was excluded because the distinct carbonyl IR band was missing. Moreover, the IR-spectra of **451** did not include the distinct sulfoxide IR-band of 1070-1030 cm^{-1}. Therefore, **451** was assumed to be a sulfone: 6-methylsulfonyl-5,8-dihydroxyphthalazine (**451**) (Scheme 180). In the IR-spectra of **452** IR-bands of carbonyl and sulfoxide functionality at 1727 cm^{-1} and 1026 cm^{-1} were found. Moreover, the distinct sulfone IR-band of 1350-1300 cm^{-1} was not found. Therefore, **452** was assumed to be a DNQ species or a DNQ/DHP mixture with a sulfoxide functionality: 6-methylsulfinyl-5,8-dihydroxyphthalazine (**452**) (Scheme 180). The electrochemical potential of **450**, **451**, and **452** was measured via cyclic voltammetry by Hofmann et al.[206] The effect of the *iso*propyl-thio substituent on the electrochemical behaviour compared to DHP should be determined. Moreover, their electrochemical potential might indicate their sulfoxide or sulfon functional group because the higher electronic impact of the sulfoxide should generate a higher potential than sulfoxide with its lower electronic effect (Scheme 180).
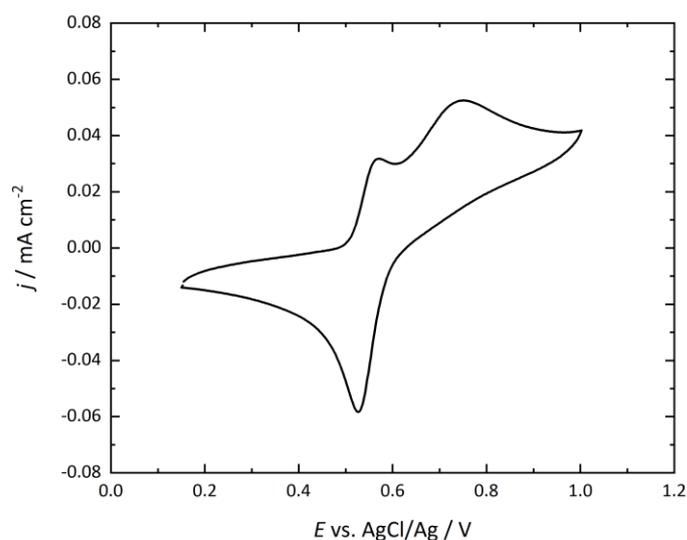
Figure 12: Cyclic voltammogram of DHP(S*i*Pr) (2 M HCl, scan rate 10 mV/s) measured by Hofmann et al.[206]

In the cyclic voltammogram of DHP(S*i*Pr) **450**, two oxidation peaks were observed by Hoffmann et al.[206] (Figure 12). Since thioethers can be oxidized electrochemically, the thioether substituent might be oxidized further to a sulfoxide or a sulfone. The two oxidation peaks hindered a definite potential assignment.
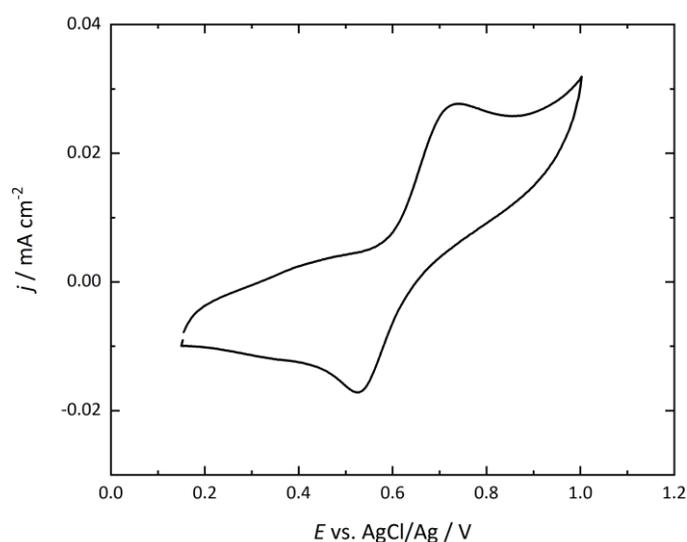
Figure 13: Cyclic voltammogram of **459** ($E_{1/2}$ = 655 mV, 2 M HCl, scan rate 10 mV/s) measured by Hofmann et al.[206]

The cyclic voltammogram curve of **451** showed a high oxidation peak and a smaller, more flattened reduction peak (Figure 13). This asymmetry might indicate some side reactions of the oxidized species of **451**. A half-wave potential of 655 mV was observed for **451** by Hoffman et al.[206] A slightly smaller half-wave potential was measured for compound **451** with 632 mV by Hofmann et al.[206] (Figure 14). A larger oxidation peak and a smaller and flattened reduction peak were also observed for **452** compared to **451**, which indicated side reactions of the oxidized species. The electron-withdrawing sulphur-oxo sulfoxide or sulfone functional groups **451** and **452** might make the quinone double bond of their oxidized species susceptible for irreversible nucleophilic Michael-type attacks of water.[122] Moreover, as mentioned before, side reactions of the semiquinone might occur as in the case of 5,6-DNQ. The potential difference of 23 mV between **451** and **452** might indicate different electron-withdrawing effects and thus different functional groups. Therefore, a stronger electron-withdrawing sulfone functional group of **451** and a less electron-withdrawing sulfoxide group of **452** might cause this potential difference.
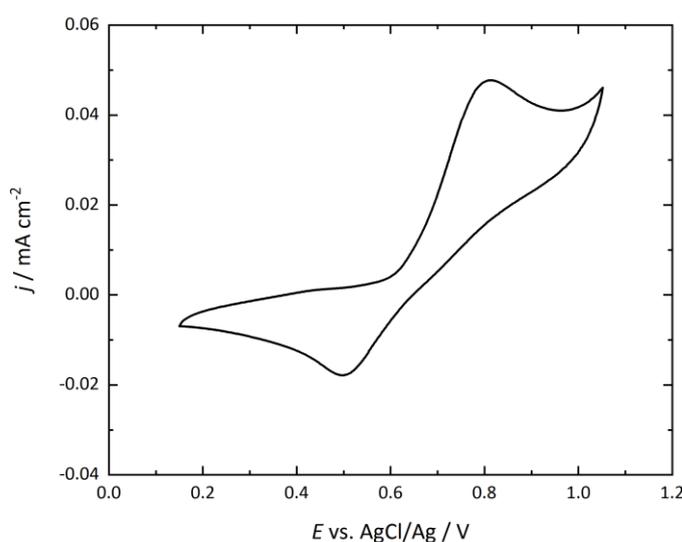
Figure 14: Cyclic voltammogram of **460** ($E_{1/2}$ =632 mV, 2 M HCl, scan rate 10 mV/s) measured by Hofmann et al.**[206]**

Compared to the computed potentials of methyl sulfon DHP, the potentials of the **451** and **452** were lower. This result can be rationalized by the increased electron density in the quinone due to the greater positive inductive effect of the *iso*-propyl substituent compared to the methyl one. In comparison to unsubstituted DHP, the potential was increased by about 69 mV for **451**, or 49 mV for **452,** respectively. The *iso*propyl sulphur-oxo substituents surpassed the halogen substituents in enlarging the potential. The fluoro- und bromo substituent caused only a shift of about 8 mV and 13 mV, respectively. Therefore, substituents with a strong negative

mesomeric effect had a strong impact on the enlargement of the electrochemical potential. The increased potentials of **451** and **452** would be beneficial for a larger overall cell voltage. However, the observed material instabilities contradict the ORFB material requirement for sufficient long-term stability. Thus, further research on increasing the stability of DHPs, especially of electron-withdrawing substituents bearing DHPs, is needed.
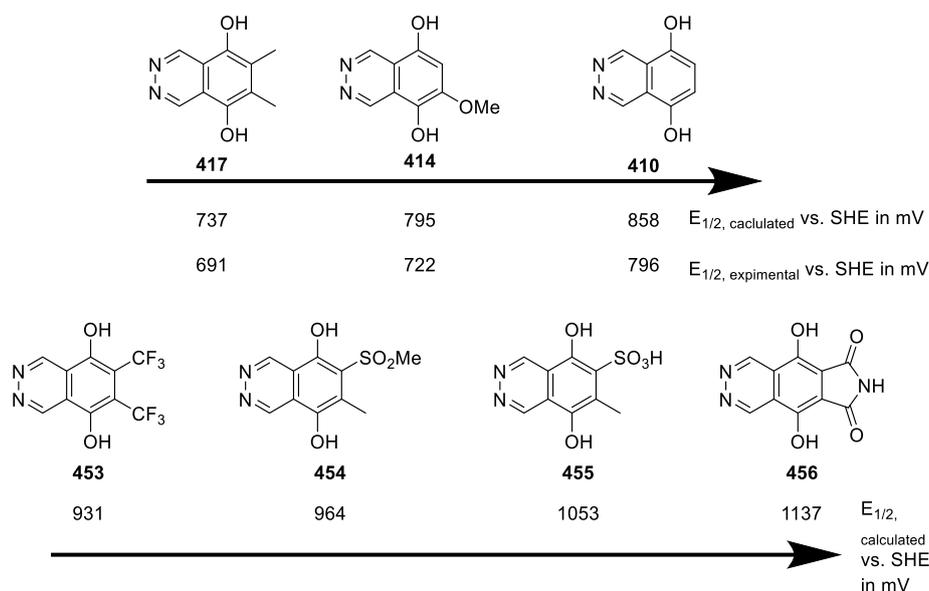
Scheme 181: Calculated potentials of DHPs based on computational studies of Mollenhauer et al. and experimental data measured by Hofmann et al.[172]

Computational studies on DFT PBE-D3/aug-cc-pVDZ(PCM) level of theory were performed by S. Schwan of the Mollenhauer group[172] to estimate the substituent effect of EWGs on the potential. The calculated potentials of DHP **410**, DHP(OMe) **414** and DHP(Me)$_2$ **417** were overestimated by this method, but within the range of the mean absolute deviation MAD of 30 mV (Scheme 181). The deviation was caused by the utilized simple polarizable continuum model. Therefore, this computational method was found suitable to estimate the effects of EWGs on the potential. A substituent dependent MAD of up to 194 mV were taken into account. Two electron-withdrawing trifluoromethyl substituents in 6,7-bis(trifluoromethyl)-5,8-dihydroxyphthalazine DHP(CF$_3$)$_2$ (**453**) would increase the potential, but the large distortion from ideal planarity of the oxidized species might destabilize the material. A higher potential was calculated for the methylated methylsulfon and the methylated sulfonic acid DHP derivatives 6-methyl-7-methylsulfonyl-5,8-dihydroxyphthalazine (**454**) and 6-methyl-5,8-dihydroxyphthalazine-7-sulfonic acid (**455**). The sulfonic acid group might be beneficial for the water solubility, but the calculated large distortion from ideal planarity in the molecule might destabilize **455**. Therefore, the methylsulfone **454** with less distortion might be the more stable alternative with lower potential. Moreover, the sulfonic acid or sulfonyl substituent might

decrease the rate of the charge transfer due to hydrogen bonding interactions with the carbonyl functionality.[121] Therefore, the succinimidyl DHP derivative **456** with the highest calculated potential might be a promising candidate with probable higher rate constants than **454** and **455**.[172]

Besides the enhancement of the potential of the DHP **410**, the stability of DHPs was investigated. Quinones were susceptible to Michael-type side reactions caused by the nucleophilic attack of water leading to material degradation and diminished battery capacity.[122] Since DNQ **409** was a quinone, a probable degradation in aqueous media and its prevention were studied by Hofmann et al.[172] The analytes were exposed to an increasing and measured current and time by a constant amount of DHP **410** for oxidation in water with hydrochloric acid as electrolyte. The charge to mol Q/n ratio indicated the number of electrons which were incorporated during oxidative reactions. Since the oxidation of DHP **410** to DNQ **409** was a two-electron process, an ideal Q/n ratio of 2 was expected. However, a Q/n ratio of 5.92 was observed by Hofmann et al.[172,206] for the oxidation of DHP **410** over 72 h (Figure 15). Therefore, more than twice the expected electrons oxidated the DHP **410**. Therefore, the DNQ **409** was overoxidized.
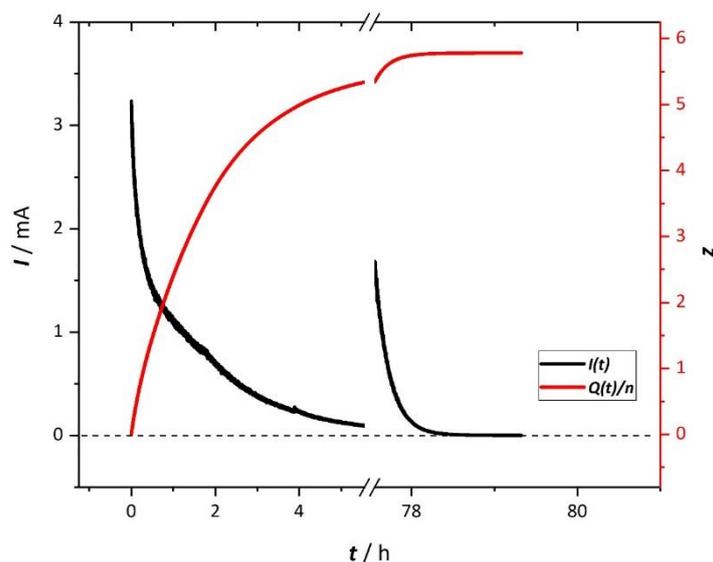
Figure 15: Overoxidation of DHP. Measured by Hofmann et al.[172] The gap in the curve was caused by pausing the experiment

This oxidized compound was analysed with ^{1}H-NMR spectroscopy and ESI-MS. Compared to the DNQ **409**, the signals of the 1,4-protons remained, but they shifted, as expected for a protonated species, and split off in several signals. These results might indicate the presence of more than one species. The proton signals of the quinone backbone protons vanished compared to the spectra of DHP. Thus, the quinone backbone protons must be substituted. According to the proposal by Hoober-Burkhardt et al.[122], a Michael-type attack of water on the quinone backbone led to dihydroxy species, which got oxidized further.[172] To prevent this overoxidation, the vulnerable quinone backbone needed to be protected. Therefore, methyl substituted DHP(Me)$_2$ was used.
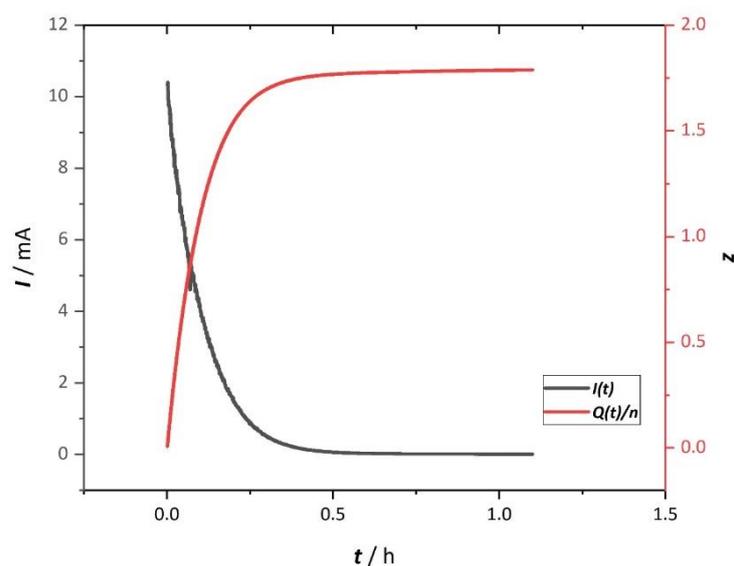
Figure 16: Overcharging of DHP(Me)$_2$ measured by Hofmann et al.[172]

In the case of the DHP(Me)$_2$ **417**, a Q/n ratio of under two was observed by Hofmann et al[172,206], which indicated that overoxidations did not occur (Figure 16). The observed difference to a Q/n ratio of two was caused by the purity of 92-94% of DHP(Me)$_2$ **417** diminishing the oxidizable material amount. The oxidized species was analysed via ^{1}H-NMR spectroscopy. The signals of the dihydroxy functionalities vanished due to the transformation into a quinone. The protons of the 1,4-hyrogen atoms shifted, but remained, and were thus not involved in the degradation process. Therefore, a two-electron oxidation process was assumed. As a consequence of the oxidation results of DHP **410** and DHP(Me)$_2$ **417**, it can be assumed that the degradation process solely occurred at the quinone backbone and not at the 1,4-position. Moreover, the double substitution of the quinone backbone stabilized the two-electron oxidation processes from DHP(Me)$_2$ **417**. In summary, it can be stated that DHP redox material was synthesizable via an IEDDA reaction. Altering the substitution pattern, and thus the potential and the stability,

succeeded at the quinone backbone. The potential of DHP was successfully enlarged via halogen, and it was increased even further by unidentified sulphur-oxo substituents. An oxidative degradation process of unsubstituted DHP/DNQ was discovered. This side reaction was successfully inhibited by a full substitution of the quinone backbone. Therefore, a more stable ORFB material than BQDS, DAAQ, and BQ was developed.

5. Conclusion and Outlook

In the first part of the thesis, the methodology of the bidentate boron Lewis acid catalysed IEDDA reaction was explored. The bidentate boron Lewis acid catalysed IEDDA reaction was tried on 4-alkyl-2,3-dihydrofurans and 5-alkylthio-4-alkyl-2,3-dihydrofurans. In the case of the 4-hexyl-2,3-dihydrofurans, only product traces were detected via ^{1}H-NMR spectral analysis, and mainly the starting material was recovered. Therefore, the combined sterical bulkiness and low electron density was not sufficient to obtain the IEDDA reaction product. Further experiments with more electron-rich dienophile 5-methylthio-4-hexyl-2,3-dihydrofuran revealed that only electron-poor 5,8-difluorophthalazine underwent a smooth IEDDA reaction to styrene **289**. The slightly less electron-poor 5,8-dichlorophthalazine needed higher reaction temperatures to undergo the IEDDA reaction. Surprisingly, the increased temperatures favoured also the unexpected thiomethyl- and hexyl-substituent elimination reaction to 2*H*,3*H*-6,7-dichloronaphtho-[2,3-*b*]-furan (**355**). More electron-rich phthalazines led only to observed traces of an IEDDA product and recovered starting material. Therefore, the dependency of the domino IEDDA reaction on temperatures and electronical properties of the phthalazine, which determines whether a subsequent elimination or rearrangement reaction occur, need to be investigated further. Less sterically demanding 5-thioalkyl-2,3-dihydrofurans applied in the bidentate boron catalysed IEDDA reaction led mainly to the elimination and the naphthofurans **362** and **364**. Further studies with protected thio-glycals or alkenes bearing thio-dihydrofurans might pave the way to hydroxylated naphthylfurans or to thio-multicycles, respectively. In the second part of this thesis, organic redox materials for RFBs were synthesized via the bidentate boron Lewis acid catalysed IEDDA reaction and the phthalazine synthesis. Moreover, vanillin was investigated as a starting material for organic redox material. Redox active 2-methoxy-benzoquinone (**373**), 6,6'-dimethoxy-2,2'-bis-(1,4-benzoquinone) (**376**), 2,3,6,7-tetramethoxy phenanthrenequinone (**377**) and 5,5',6,6'-tetramethoxyindigo (**393**) were synthesized successfully. Because the indigo derivative is poorly soluble in organic and aqueous solvents, electrochemical analysis was not pursued. The quinone materials were analysed via cyclic voltammetry. The lower potentials of 2-methoxy-1,4-benzoquinone (**370**) and 6,6'-dimethoxy-2,2'-bis-(1,4-benzoquinone) (**383**) compared to benzoquinone disqualified them for further catholyte applications. The low potential of 2,3,6,7-tetramethoxy phenanthrenequinone **384** might encourage further investigations as anolyte material. In summary, it can be stated that vanillin as renewable resource can be used as a precursor for redox material. The electron-donating, and thus, potential decreasing, methoxy- substituent might encourage the development of vanillin-derived anolyte material. Vanillin can be a starting material for phenothiazines. Derivatives of phenothiazines showed promising results as redox material for non-aqueous ORFBs.[255,256] Therefore, the synthetic access to vanillin-derived phenothiazines

and their electrochemical derivatives need to be investigated. Besides the vanillin redox material, applying the bidentate boron Lewis acid catalysed IEDDA reaction of 1,2,4,5-tetrazines and naphthoquinones yielded DAD **400**, DAD(OMe) **401** and DADdi(OH) **405**. Solely DAD(OMe) **401** showed reversible redox behaviour in acidic media with moderate positive potential. DADdi(OH)'s **405** fully reversible redox cycle and lowest potential in basic media predestined it for further investigations as anolyte material. In summary, it can be stated that DADs were demonstrated as potentially redox active ORFB material. The scope of the bidentate boron Lewis acid catalysis was successfully extended to the IEDDA reaction of 1,4-benzoquinones and 1,2,4,5-tetrazines. Surprisingly, instead of the DNQs, the 5,8-dihydroxyphthalazines DHPs were obtained, which probably indicated a proton shift during the reaction. Finally, DNQ was obtained by oxidizing DHP with $NaIO_4$. Bulky pyridyl- and chlorine-substituted tetrazines did not undergo an IEDDA reaction with benzoquinone, which is probably due to the preventing the coordination or the transition state by sterical overcrowding. The DHP(Me)$_2$, DHP(Br), DHP(Cl), DHP(F) were successfully synthesized from 1,2,4,5-tetrazine and the substituted benzoquinones. Noteworthy, the DHP(OMe) was synthesized from vanillin-derived 2-methoxy-1,4-benzoquinone (**373**). Amine substituted benzoquinone yielded DHP **410** because the IEDDA favoured the reaction with the enamine functionality, and the amine was expelled. The DHP **410** provide a smaller electrochemical potential than BQDS, but a higher one than DADs, DHDMBS and benzoquinone. The potential of the DHPs was decreased by the EDGs (MeO-, Me-), whereas the halogen substituents slightly increased the potential. Attempts at synthesizing DHPs with electron-withdrawing sulfonic acid potassium and methyl sulfonyl substituents, and thus with increased redox potential, were not successful. The strong electron-withdrawing effect of the substituents might inhibit the IEDDA reaction by diminishing the electron density of the dienophile, and thus enlarging the $HOMO_{dienophile}$-$LUMO_{diene}$ thermodynamical barrier to a level at which no reaction can occur. The alternative reductive substitution with *iso*propyl thiol successfully yielded DHP(S*i*Pr) **450**, and subsequent oxidations ted to the two unidentified DHPs **451** and **452**, probably a sulfoxide and a sulfone, with higher potentials but lower stability than DHP **410**. A degradation reaction during the electrochemical oxidation of DHP **410** to DNQ **409** was observed. The quinone backbone was identified as vulnerable to probable Michael-type water attacks and subsequent oxidation reactions. These side reactions can be prevented by the full substitution of the quinone backbone with DHP(Me)$_2$ **417**. In summary, it can be stated that the bidentate boron Lewis acid catalysed IEDDA reaction enabled the access to the new redox material DHP, which fulfilled the criteria of an ORFB material: a high potential and stability. In the future, quinone backbone protected DHPs with electron-withdrawing substituents, for instance 6-methyl-7-methylsulfonyl or succinimidyl, should pave the way towards stable redox materials with higher potentials, and thus, catholyte applications.[172]

6. Experimental Part

General Information

All reagents from Abcr, Alfa-Aesar, Fluorochem, Merck, Sigma-Aldrich, TCI and VWR were used as received or bulb-to-bulb distilled before usage. Dry solvents were obtained from ACROS/Fisher-Scientific with AcroSeal™ cap and were used without purification. Degassed solvents were obtained via freeze-bump-thaw cycling.

Reactions

Water-sensitive reactions were conducted with dried glassware. Air-sensitive reactions were set up in a nitrogen-filled glove-box or in a fume-hood with nitrogen as protecting gas. Multiple evacuate-refill cycles were performed to obtain dry and protecting gas-filled glassware before usage. Reactions with higher pressure were conducted in glass pressure tubes.

Chromatography

Silica gel 60 M (0.063 nm – 0.2 nm) or flash silica gel (0.04 nm - 0.063 nm) from Machery-Nagel was used for preparative column chromatography. For thin layer chromatography, POLYGRAM® SILG/UV$_{254}$ pre-coated polyester sheets with silica gel 60 with fluorescent indicator were used. Detection occurred via UV light at 254 nm or 365 nm with a GAMAG UV-light cabinet or development with potassium permanganate, iodine or phospomolybdic acid.

NMR

Spectra of ^{1}H, ^{13}C and ^{11}B were measured on Bruker Avance II 200 MHz Microbay, Bruker Avance II 400 MHz, Bruker Avance III 400 MHz HD, and Bruker Avance III HD 600 MHz spectrometers. The last two spectrometers were used for two-dimensional spectra. Deuterated solvents were purchased from Eurisotop and Deutero and were used without purification. Tetramethylsilane or the solvent signal were used as reference for chemical shifts, which were reported in ppm (parts per million). Coupling constants were listed in Hertz (Hz). Multiplets were reported as s = singlet, d = doublet, t = triplet, q = quartet and p = pentet, m = multiplet and as their combinations, for example dd as doublet x doublet.

Mass-spectrometry

On an ESI-MS Bruker Mikro-TOF and on an ESI-MS Finnigan LCQ –DUO, electrospray ionisation mass spectra were measured.

Elemental Analysis

All elemental analyses were performed on a Thermo Flash EA - 1112 Series CHN-analyser.

Infrared Spectroscopy

All IR spectra were measured on a VERTEX 70 / PMA50 or on a VERTEX 70 / Platinum ATR spectrometer.

Bis-trimethylsilyl-benzene 260
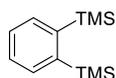
Mg powder (3.04 g, 125 mmol, 2.50 equiv) was dried under vacuum. After cooling down and flushing with nitrogen, 50 mL dry THF and DIBAL-H in (1.00 mL, 1.00 mmol, 2.00 mol%, 1.00 M solution in hexane) were added and refluxed for five minutes. After the addition of TMSCl (13.99 g, 16.30 ml, 125 mmol, 2.50 equiv), 1,2-dibromobenzene (11.80 g, 6.03 ml, 50 mmol, 1.00 equiv) was added dropwise within 30 min maintaining reflux. The mixture was refluxed for additional 1 h and stirred 30 min. The reaction mixture was poured into a mixture of 125 ml sat. $NaHCO_3$ and 60 ml ice, and 125 ml Et_2O was added. Solids were filtered off. The aqueous phase was extracted with Et_2O (1 × 125 ml, 1 × 100 ml, 1 × 60 ml), and the combined extract was dried over Na_2SO_4 and evaporated under reduced pressure. The crude product was purified by distillation over a Vigreux-column at 1.1 mbar and 72 – 81°C to yield a clear oil (2.29 g, 21%).

¹H NMR (200 MHz, Chloroform-*d*) δ 7.67 (dd, *J* = 5.6, 3.3 Hz, 2H), 7.32 (dd, *J* = 5.6, 3.4 Hz, 2H), 0.37 (s, 18H).

Analytical data are in accordance with the literature.[257]

9,10-Dichloro-9,10-diboraanthracene 261 and 9,10-Dimethyl-9,10-dihydro-9,10-diboraanthracene 262
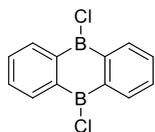
Borontrichloride (17.7 mL, 17.7 mmol, 2.05 equiv, 1.00 M in hexane) was added to degassed bis-1,2-(trimethyl)-silylbenzene (1.97 g, 8.85 mmol, 1.00 equiv) and 3.3 mL dry 1,2-dichloroethane in a dry pressure tube via septum cap. After sealing the tube, the reaction mixture was stirred for 4 d at 140°C. Then, the stirring of the mixture was stopped, and it was cooled to 0°C, decanted, washed 2 x 3 ml with hexane, and the precipitate was dried at high vacuum to yield white needles. (158 mg, 8%). Product was used without further purification.
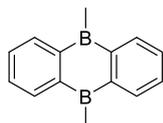
To a suspension of 9,10-dichloro-9,10-dihydro-9,10-boraanthracene (113 mg, 460 µmol, 1.00 equiv) in 15 ml dry hexane, AlMe$_3$ (230 µl, 460 µmol, 2 M in heptane, 1.00 equiv.) was added within 5 min at -40 °C. After stirring for 1 h at -40°C, the reaction mixture was allowed to warm to rt and stirred for 19 h. After sublimation at 120°C/0.2 mbar, a colourless solid was obtained (71.0 mg, 76%).

1H NMR (600 MHz, Chloroform-*d*) δ 8.15 (dd, *J* = 5.3, 3.3 Hz, 4H), 7.60 (dd, *J* = 5.4, 3.2 Hz, 4H), 1.43 (s, 6H).

Analytical data are in accordance with the literature.[7]

2,3-Dichlorotetrahydrofuran 322

Through a 100 mL three-necked flask with reflux condenser and dropping funnel, filled with dry THF (43.4 mL, 530 mmol, 1.00 equiv), nitrogen was bubbled via septum and pasteur pipette. To the refluxed THF, sulfuryl chloride (42.8 mL, 530 mmol, 1.00 equiv) was added via dropping funnel in 1 h. Afterwards the solution was bubbled with nitrogen for 30 min. After the distillation of the reaction mixture (5 mbar, 33°C), 2,3-Dichchloro-dihydrofuran was obtained as a colourless liquid (46.8 g, 36%).

¹H NMR (400 MHz, Chloroform-*d*) δ 4.64 (d, *J* = 5.5 Hz, 1H), 4.35 (dd, *J* = 9.1, 5.3 Hz, 2H), 2.87 (m, 1H), 2.33 – 2.13 (m, 2H).

¹³C NMR (101 MHz, Chloroform-*d*) δ 99.7, 68.8, 63.8, 31.9.

Analytical data are in accordance with the literature.[180,258]

4-Chloro-2,3-dihydrofuran 323

2,3-Dichlorodihydrofuran (36.4 ml, 345 mmol, 1.00 equiv) was added to tributylamine (82.0 ml, 345 mmol, 1.00 equiv) and stirred for 3. Afterwards, the product was distilled at 70 mbar and 30°C to 16 mbar and 70°C. The following fractional distillation (100 mbar, 53°C) yielded the product as a colourless liquid (12.9 g, 36%).

¹H NMR (400 MHz, Chloroform-*d*) δ 6.37 (t, *J* = 2.2 Hz, 1H), 4.43 (t, *J* = 9.6 Hz, 2H), 2.81 (td, *J* = 9.6, 2.2 Hz, 2H).

¹³C NMR (101 MHz, Chloroform-*d*) δ 142.17, 107.64, 70.32, 34.21.

Analytical data are in accordance with the literature.[181]

4-Phenyl-2,3-dihydrofuran 317
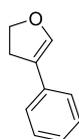
A 10 ml Schlenk tube charged with Mg powder (194 mg, 8.00 mmol, 8.00 equiv) and lithium chloride (254 mg, 6.00 mmol, 1.50 equiv) was heated under vacuum at 300°C and – after cooling – flushed with nitrogen. Then, 6 mL dry THF and DIBAL-H (200 µL, 100 µmol, 5 mol%, 1 M solution in hexane) was added and stirred for 10 min. Afterwards, bromobenzene (548 µL, 2.60 mmol, 1.30 equiv), 3-chloro-4,5-dihydrofuran (350 µL, 2.00 mmol, 1.00 equiv), TMEDA (120 µL, 0.80 mmol, 0.40 equiv) and Fe(acac)$_3$ (70.6 mg, 200 µmol, 5.00 mol%) were added. After 3 h, the reaction mixture was quenched with sat. Na$_2$CO$_3$ and extracted with 3 x 6 mL EtOAc. Combined organic phases were dried over Na$_2$CO$_3$, and the solvent was removed under reduced pressure. After column chromatography (silica pentane/EtOAc 99:1), the product was isolated as a colourless solid (47.0 mg, 13%).

¹H NMR (200 MHz, Chloroform-*d*) δ 7.43 – 6.91 (m, 5H), 6.80 (t, *J* = 2.1 Hz, 1H), 4.43 (t, *J* = 9.5 Hz, 2H), 2.89 (td, *J* = 9.6, 2.1 Hz, 2H).

¹³C NMR (50 MHz, Chloroform-*d*) δ 142.4, 134.3, 128.6, 125.8, 124.2, 115.6, 70.8, 30.6.

GC-EI-MS: m/z (%) calculated 146, found 146.

Analytical data are in accordance with the literature.[259]

α-Benzyl-*γ*-butyrolactone 327
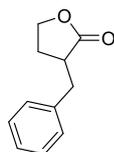
LDA (7.80 mL, 15.80 mol, 1.05 equiv, 2 M in ethylbenzene/hexane) was added dropwise to 12 ml THF in a 50 mL Schlenk tube. Afterwards, *γ*-butyrolactone (1.15 mL, 6.27 mmol, 1.00 equiv.) was added dropwise in 15 min., and the reaction mixture was stirred for 10 min. Then benzyl bromide (1.78 mL, 15.0 mol, 1.00 equiv.) was added. After 15 min., the reaction mixture was allowed to warm up to -40°C, stirred for one hour, allowed to warm up to room temperature and quenched with conc. 10 ml NH$_4$Cl solution. The mixture was extracted with 3 x 50 mL EtOAc and concentrated under reduced pressure. The crude product was purified via column chromatography cyclohexane/Et$_2$O 3:1 - cyclohexane/Et$_2$O/EtOAc 2:1:1 to yield the product as a colourless oil (1.78 g, 68%).

¹H-NMR (400 MHz, Chloroform-*d*) δ 7.43 – 7.06 (m, 5H), 4.22 (td, *J* = 8.8, 3.1 Hz, 1H), 4.14 (td, *J* = 9.3, 6.6 Hz, 1H), 3.25 (dd, *J* = 13.5, 4.0 Hz, 1H), 2.84 (qd, *J* = 9.4, 3.9 Hz, 1H), 2.76 (d, *J* = 13.6 Hz, 1H), 2.24 (ddt, *J* = 15.5, 9.4, 3.1 Hz, 1H), 1.99 (dq, *J* = 12.8, 9.4 Hz, 1H).

¹³C-NMR (101 MHz, Chloroform-*d*) δ 178.7, 138.4, 128.9, 128.7, 126.7, 66.6, 41.1, 36.1, 28.0.

HRMS (ESI-MS) m/z calculated [C$_{11}$H$_{12}$O]$^+$: [H]$^+$ 161.0691; found: 161.0658.

Analytical data are in accordance with the literature.[183]

4-Benzyl-2,3-dihydrofuran 329
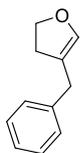
To a stirred solution of 2-benzyl-γ-butyrolactone (927 µL, 6.00 mmol, 1.00 equiv) in a 10 mL dry toluene in a Schlenk tube, DIBAL-H (6.60 mL, 6.60 mmol, 1.10 equiv, as a solution 1 M in hexane) was added at -78°C in 20 min. After stirring for 2 min. at -78°C, the reaction mixture was allowed to warm up to room temperature and quenched with saturated 7.5 mL NH$_4$Cl solution. The mixture was filtered through a Celite plug and was extracted with 3 x 20 mL EtOAc. Combined organic phases were washed with brine and dried over Na$_2$SO$_4$. After evaporation of the solvent under reduced pressure, the crude product was obtained. The product was used without further purification. To a solution of lactol (891 mg, 5.00 mmol, 1.00 equiv) in 50 mL dry THF in a 100 mL Schlenk flask, Et$_3$N (3.50 mL, 25.0 mmol, 5.00 equiv.) was added and cooled to -25°C. Afterwards, MeSO$_2$Cl (580 µL, 7.50 mmol, 1.50 equiv) was added dropwise while stirring. After 3 h, reaction mixture was heated to refluxed for 12 h at 80°C. After cooling down to room temperature, reaction mixture was filtered through a silica plug and eluted with 50 mL of a mixture of Et$_2$O and cyclohexane. Solvent was removed under reduced pressure. The crude product was distilled via bulb-tube apparatus. A colourless oil was obtained (52.0 mg, 16%).

^{1}H NMR (400 MHz, Chloroform-*d*) δ 7.44 − 7.01 (m, 5H), 6.11 (t, *J* = 1.8 Hz, 1H), 4.31 (t, *J* = 9.5 Hz, 2H), 3.36 (s, 2H), 2.64 − 2.30 (m, 2H).

^{13}C NMR (101 MHz, Chloroform-*d*) δ 141.2, 139.8, 128.7, 128.5, 126.2, 114.0, 70.2, 32.9, 32.2.

HRMS (ESI-MS) m/z calculated [C$_{11}$H$_{12}$O]$^+$: [H]$^+$ 199.0729; found: 199.0727.

Analytical data are in accordance with the literature.[260]

1-Iodohexane 331

1-bromohexane (14.0 mL, 100 mmol, 1.00 equiv) was added to a stirred 15% solution of sodium iodide (15.0 g, 100 mmol, 1.00 equiv) in 90 ml acetone. The reaction mixture was heated to reflux for 1 h and stirred for 1 h. After cooling down, the reaction mixture was concentrated under reduced pressure and the solid residue was filtered off. Filtrate was diluted with 100 mL Et$_2$O and washed with saturated sodium thiosulfate solution. The water phase was extracted with 3 x 100 mL Et$_2$O. Combined organic phases were washed with brine and

the solvent was removed under reduced pressure. 1-iodohexane was obtained as a pale oil (17.4 g, 82 %).

¹H NMR (200 MHz, Chloroform-*d*) δ 3.19 (t, *J* = 7.0 Hz, 2H), 1.96 – 1.68 (m, 2H), 1.58 – 1.15 (m, 6H), 1.01 – 0.63 (m, 3H).

¹³C NMR (50 MHz, Chloroform-*d*) δ 33.58, 30.78, 30.24, 22.52, 14.06, 7.32.

Analytical data are in accordance with the literature.[184,261]

2-Bromo-(tetrahydropyranyl) ethyl ether 335

THPO—⟋—Br
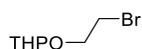
A 250 ml two-necked flask was charged with 100 ml DCM, 2-bromoethanol (3.50 ml, 50.0 mmol, 1.00 equiv), dihydropyran (7.00 mL, 75.0 mmol, 1.50 equiv) and pyridinium tosylate (10.0 ml, 5.00 mmol, 0.10 equiv, 0.5 M solution in DCM). The reaction mixture was stirred for 4 h at room temperature. The reaction was quenched with 75 ml NaHCO₃ solution and washed with saturated brine. Organic phases were dried over Na₂SO₄, and the solvent was removed under reduced pressure. The crude product was purified via column chromatography (300 g SiO₂, pentane/EtOAc 9.5:0.5 - 8:2). The product was obtained as a colourless liquid (8.60 g, 77%).

¹H NMR (200 MHz, Chloroform-*d*) δ 4.68 (t, *J* = 3.3 Hz, 1H), 4.12 – 3.68 (m, 2H), 3.64 – 3.41 (m, 4H), 2.00 – 1.32 (m, 6H).

Analytical data are in accordance with the literature.[188]

2-(Tetrahydropyranyloxy)-ethyl-diethylmalonate 337

EtOOC⟍⟋—OTHP
EtOOC
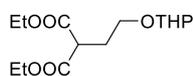
A three necked 500 mL flask was charged with potassium carbonate (25.0 g, 180 mmol, 1.50 equiv) and 60 ml acetonitril, diethyl malonate (24.0 mL, 150 mmol, 1.20 equiv) bromoethanol THP ether (27.0 g, 129 mmol, 1.00 equiv) and tetrabutylammonium bromide (977 mg, 3.00 mmol, 2 00 mol%). The reaction mixture was heated on 90°C for 48 h. After cooling down, 50 ml Et₂O was added, and potassium carbonate was filtered off. The mixture was concentrated under reduced pressure. After purification via column chromatography (600 g flash silica, gradient pentane/ EtOAc 9:1- 7.5:2.5), the product was obtained as a colourless oil (17.0 g, 47%).

¹H NMR (200 MHz, Chloroform-*d*) δ 4.54 (t, *J* = 3.1 Hz, 1H), 4.16 (q, *J* = 7.1 Hz, 4H), 3.87 − 3.67 (m, 2H), 3.60 − 3.32 (m, 3H), 2.17 (dt, *J* = 7.3, 6.1 Hz, 2H), 1.90 − 1.41 (m, 6H), 1.24 (t, *J* = 7.1 Hz, 6H)

¹³C DEPT NMR (50 MHz, Chloroform-*d*) δ 98.6, 64.6, 61.9, 61.3, 49.2, 30.5, 28.9, 25.4, 19.2, 14.0.

Analytical Data are in accordance with the literature.[262]

α-Ethylcarboxy-*γ*-butyrolactone 338a and *α*-Methylcarboxy-*γ*-butyrolactone 338b
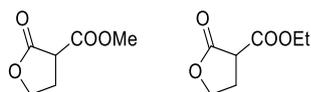
In a 100 ml flask, (2-Tetrahydropyranyl)-ethyl diethylmalonate (17.9 g, 56.0 mmol, 1.00 equiv) was dissolved in 55 ml MeOH, and toluenesulfonic acid (1.12 g, 5.88 mmol, 10.0 mol%) was added. The reaction mixture was stirred for 2 h at room temperature. The mixture was quenched with 150 µL pyridine and concentrated under reduced pressure. After purification via column chromatography (silica, pentane/acetone 9:1 - 7:3), the product mixture of *α*-methylcarboxy-*γ*-butyrolactone and *α*-ethylcarboxy-*γ*-butyrolactone was obtained as a colourless oil (6.70 g, 59% *α*-methylcarboxy-*γ*-butyrolactone, 19% *α*-ethylcarboxy-*γ*-butyrolactone).

α-Methylcarboxy-γ-butyrolactone:

¹H NMR (400 MHz, Chloroform-*d*) δ 4.51 − 4.42 (m, 1H), 4.36 − 4.28 (m, 2H), 3.80 (s, 3H), 3.52 (m, 1H), 2.82 − 2.60 (m, 1H), 2.58 − 2.40 (m, 1H).

¹³C NMR (101 MHz, Chloroform-*d*) δ 172.4, 168.3, 67.5, 53.2, 45.9, 26.5.

HRMS (ESI-MS) m/z calculated [$C_6H_8O_4$]⁺ : [Na]⁺ 167.0315; found: 167.0317.

α-Ethylcarboxy-γ-butyrolactone:

¹H NMR (400 MHz, Chloroform-*d*) δ 4.51 − 4.42 (m, 1H), 4.36 − 4.28 (m, 1H), 4.24 (q, *J* = 7.1 Hz, 2H), 3.53 (dd, *J* = 9.3, 7.6 Hz, 1H), 2.82 − 2.60 (m, 1H), 2.58 − 2.40 (m, 1H), 1.30 (t, *J* = 7.1 Hz, 3H).

¹³C NMR (101 MHz, Chloroform-*d*) δ 172.5, 167.9, 67.6, 67.5, 46.1, 26.5, 14.2.

HRMS (ESI-MS) m/z calculated [$C_7H_{10}O_4$]⁺ : [Na]⁺ 181.0471; found: 181.0468.

Analytical Data are in accordance with the literature.[263,182]

α-Ethylcarboxy-α-hexyl-γ-butyrolactone 339a and α-Methylcarboxy-α-hexyl-γ-butyrolactone 339b
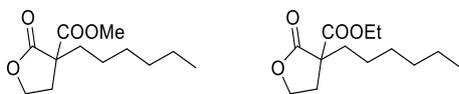
To a 100 ml flask charged with K_2CO_3 (7.26 g, 52.5 mmol, 1.50 equiv) and 20 ml dry DMF, a mixture of α-methylcarboxy-γ-lactone/α-ethylcarboxy-γ-lactone (6,97 g, 30.0 mmol, 1.00 equiv), 1-bomohexane (9.83 g, 70.0 mmol, 2.00 equiv) and sodium iodide (5.25 g, 35.0 mmol, 1.00 equiv) was added. The reaction mixture was stirred for 24 h at 70 °C. After cooling down to room temperature, the reaction mixture was diluted with 30 mL Et_2O and 20 mL EtOAc and filtered. The filtrate was concentrated under reduced pressure and purified via column chromatography (silica, pentane:acetone 9:1 - 8:2). The product was obtained as oil (6.30 g, Me: 34% over two steps, Et: 35% over two steps).

α-Methylcarboxy-α-hexyl-γ-butyrolactone:

¹H NMR (400 MHz, Chloroform-*d*) δ 4.36 – 4.28 (m, 2H), 3.76 (s, 3H), 2.21 (m, 1H), 2.15 – 2.01 (m, 1H), 1.37 – 1.21 (m, 10H), 0.90 – 0.81 (m, 3H).

¹³C NMR (101 MHz, Chloroform-*d*) δ 175.0, 170.6, 66.3, 54.3, 53.2, 34.4, 31.8, 31.6, 29.3, 24.9, 22.6, 14.1.

HRMS (ESI-MS) m/z calculated $[C_{13}H_{22}O_4]^+$: $[Na]^+$ 251.1254; found: 251.1257.

α-Ethylcarboxy-α-hexyl-γ-butyrolactone:

¹H NMR (400 MHz, Chloroform-*d*) δ 4.36 – 4.28 (m, 2H), 4.22 (m, 2H), 2.21 (m, 1H), 2.15 – 2.01 (m, 2H), 1.37 – 1.21 (m, 13H), 0.90 – 0.81 (m, 3H).

¹³C NMR (101 MHz, Chloroform-*d*) δ 175.1, 169.7, 63.2, 62.2, 54.3, 34.2, 31.8, 31.6, 29.4, 24.8, 22.6, 14.4, 14.1.

HRMS (ESI-MS) m/z calculated $[C_{13}H_{20}O_4]^+$: $[Na]^+$ 265.1410; found: 265.1411.

Analytical data are in accordance with the literature.[182]

α-Acetyl-*α*-hexyl-*γ*-butyrolactone 342
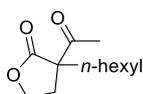
To a solution of α-acetylbutyrolactone (11.0 mL,102 mmol, 1.00 equiv) in acetone (100 mL) in a 500 ml two-necked flask, dry sodium iodide, 1-bromohexane and dry potassium carbonate

(28.2 g, 204 mmol, 2.00 equiv) were added. The reaction mixture was refluxed for 24 h. Then, the reaction mixture was diluted with 80 ml pentane, filtered and concentrated in under reduced pressure. After purification via column chromatography (flash silica 300 ml, pentane:acetone 8:2), the product was obtained as oil (19.2 g, 89%).

¹H NMR (400 MHz, Chloroform-*d*) δ 4.27 (td, *J* = 8.9, 3.1 Hz, 1H), 4.13 (td, *J* = 9.1, 7.1 Hz, 1H), 2.91 (ddd, *J* = 12.9, 7.2, 3.1 Hz, 1H), 2.31 (s, 3H), 2.11 (ddd, *J* = 13.9, 11.9, 5.0 Hz, 1H), 2.01 (dt, *J* = 12.9, 9.0 Hz, 1H), 1.76 (ddd, *J* = 13.9, 12.0, 4.8 Hz, 1H), 1.36 – 1.05 (m, 8H), 0.96 – 0.77 (m, 3H).

¹³C NMR (101 MHz, Chloroform-*d*) δ 202.7, 175.7, 66.3, 61.7, 35.1, 31.4, 29.3, 29.1, 25.5, 22.5, 14.0.

HRMS (ESI-MS) m/z calculated [$C_{12}H_{20}O_3$]⁺ : [Na]⁺ 235.1304; found: 235.1302.

Analytical data are in accordance with the literature.[264]

α-Hexyl-*γ*-butyrolactone 332
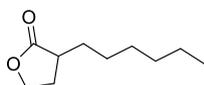
Starting from γ-butyrolactone: LDA (15.8 mL, 31.5 mmol, 1.10 equiv, 2 M in ethylbenzene/hexane) was added dropwise to 15 ml THF in a 250 mL Schlenk tube. Afterwards, γ-butyrolactone (2.31 mL, 30.0 mmol, 1.00 equiv) was added dropwise for 15 min. and the reaction mixture was stirred for 10 min. Then, 3.90 mL 1,3-dimethyl-2-imidazolidinone and hexyl iodide (4.41 mL, 30.0 mmol, 1.00 equiv.) were added. After 15 min., the reaction mixture was allowed to warm up to -30°C, stirred for 12 h, allowed to warm up to 0°C and quenched with conc. 50 ml NH₄Cl solution. The mixture was extracted with 3 x 80 mL Et₂O. The combined organic phases were washed with 25 mL brine and concentrated under reduced pressure. The crude product was purified with column chromatography (silica, pentane/EtOAc 9:1-8:2) to yield the product as a colourless oil (650 mg, 3%).

Starting from a-methylcarboxy-a-hexyl-γ-butyrolactone/a-ethylcarboxy-a-hexyl-γ-butyrolactone: To a solution of a-methylcarboxy-a-hexyl-γ-butyrolactone/a-ethylcarboxy-a-hexyl-γ-butyrolactone in 53 mL DMSO and 2 mL water, lithium chloride (8.99 g, 212 mmol, 4.00 equiv) was added. Reaction mixture was stirred and heated for 24 h on 140°C under nitrogen. After cooling down to room temperature, the reaction mixture was quenched with 200 mL cold water and the mixture was extracted with 5 x 100 mL Et₂O. Combined organic phases were washed with 100 mL brine. Combined organic phases were dried over Na₂SO₄ and were concentrated under reduced pressure. After purification via column chromatography (silica, pentane/EtOAc 8:2), the product was obtained as a colourless oil (6.90 g, 77%).

Starting from a-acetyl-a-hexyl-γ-butyrolactone: Sodium metal pieces (500 mg, 22.1 mmol, 0.25 equiv) were added in portions to 100 mL anhydrous EtOH until a clear solution was obtained. Then, *α*-Acetyl-*α*-Hexylbutyrolactone (17.2 g, 121 mmol, 1.00 equiv) was added and the mixture was refluxed for 5 h. After cooling down to room temperature, 7.50 g Ammonium chloride was added to the mixture. Volatile compounds were removed under reduced pressure. The residue was dissolved in as little water as possible and extracted with diethylether 3 x 100 mL. Combined organic phases were dried over sodium sulfate and were concentrated under reduced pressure. After column chromatography (silica, pentane/EtOAc 8:2), the product was obtained as liquid (7.7 g, 51%).

^{1}H NMR (400 MHz, Chloroform-*d*) δ 4.34 (td, *J* = 8.7, 3.0 Hz, 1H), 4.27 – 4.15 (m, 1H), 2.52 (qd, *J* = 9.0, 4.8 Hz, 1H), 2.47 – 2.32 (m, 1H), 2.05 – 1.81 (m, 2H), 1.46 – 1.18 (m, 9H), 0.89 (t, *J* = 6.7 Hz, 3H).

HRMS (ESI-MS) m/z calculated $[C_{10}H_{18}O_2]^+$: $[H]^+$ 193.1199 found: 193.1196.

Analytical data are in accordance with the literature.[182]

4-*n*-Hexyl-2,3-dihydrofuran 285
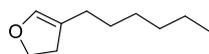
To a stirred solution of alpha-hexyl-γ-butyrolactone (6.81 g, 46.0 mmol, 1.00 equiv) in 100 mL dry DCM in a 250 mL flask, DIBAL-H (49.5 mL, 49.5 mmol, 1.10 equiv, as a solution 1 M in hexane) was added at -78°C. After the TLC-controlled consumption of the starting material, the reaction was allowed to warm up to -30°C and quenched with 4 ml EtOAc and stirred for 30 min. Then, saturated 80 mL potassium sodium tartrate solution was added, and the reaction mixture was stirred overnight. Solid residues were filtered off and the organic phases were dried over Na$_2$SO$_4$. After concentration of the mixture under reduced pressure, crude product was used without further purification. To a solution of lactol (6.33 g) in 80 mL dry DCM in a 250 mL Schlenk flask, TEA (16.7 mL, 120 mmol, 3.00 equiv) was added and cooled to -50°C. Afterwards, MeSO$_2$Cl (4.04 mL, 52.0 mmol, 1.40 equiv) was added dropwise while stirring. After 20 min, the reaction mixture was heated on 50°C. After 12 h, reaction mixture was cooled to room temperature and filtered through a 3 cm silica plug with cyclohexane/EtOAc +1% TEA. Solvent was removed under reduced pressure. Then, crude product was distilled via bulb tube apparatus (55°C, 1-2 mbar). The product was obtained as a clear, colourless liquid (1.76 g, 26% over two steps)

^{1}H NMR (400 MHz, Chloroform-*d*) δ 6.05 (s, 1H), 4.29 (t, *J* = 9.4 Hz, 2H), 2.52 (dddd, *J* = 10.4, 8.2, 2.1, 1.0 Hz, 2H), 2.03 (ddd, *J* = 7.7, 6.7, 1.3 Hz, 2H), 1.47 – 1.20 (m, 8H), 0.93 – 0.82 (m, 3H).

^{13}C NMR (101 MHz, Chloroform-*d*) δ 139.5, 114.9, 69.8, 32.5, 31.8, 29.1, 28.1, 26.3, 22.8, 14.2.

HRMS (ESI-MS) m/z calculated $[C_{10}H_{18}O]^+$: $[H]^+$ 155.1431 found: 155.1431.

Analytical data are in accordance with the literature.[182]

α-Methyl-*γ*-butyrolactone 343

To a 250 mL three-necked flask charged with 40 mL anhydrous THF, LDA (30.0 mL, 60.0 mmol, 1.20 equiv, 2.0 M in THF/heptane/ethylbenzene) was added at -78°C. Then, GBL (3.84 ml, 50.0 mml, 1.00 equiv) as solution in 5 ml dry THF was added dropwise. After 1 h, iodomethane (9.34 mL, 150 mmol, 3.00 equiv) was added, and the temperature was allowed to rise to -30°C. After 3 h at -30°C, the reaction mixture was quenched with saturated ammonium chloride solution and extracted with 3 x 75 mL EtOAc. Combined organic phases were dried over MgSO$_4$ and concentrated under reduced pressure. After purification via column chromatography (silica, pentane/EtOAc 8: 2 - 7:3), the product was obtained as a light-yellow liquid (2.26 g, 45%).

¹H NMR (400 MHz, Chloroform-d) δ 4.35 (td, J = 8.7, 2.7 Hz, 1H), 4.19 (ddd, J = 9.9, 9.0, 6.6 Hz, 1H), 2.61 (ddd, J = 10.4, 8.8, 7.1 Hz, 1H), 2.44 (dddd, J = 12.5, 8.9, 6.5, 2.7 Hz, 1H), 2.00 – 1.86 (m, 1H), 1.29 (d, J = 7.1 Hz, 3H).

HRMS (ESI-MS) m/z calculated $[C_5H_8O_2]^+$: $[Na]^+$ 123.0416 found: 123.0418.

Analytical data are in accordance with the literature.[265]

4-Methyl-2,3-dihydrofuran 345

To a solution of a-methyl-γ-butyrolactone (4.51 g, 45.0 mmol, 1.00 equiv) in 125 mL anhydrous DCM, DIBAL-H (44.0 ml, 44.0 mmol, 1.10 equiv, 1 M solution in hexane) was added dropwise at -78°C. After 1 h, the reaction mixture was quenched at -78°C with EtOAc and allowed to warm to 0°C (ice bath). Then, 80 ml potassium sodium tartrate solution was added, and the mixture was stirred overnight. The mixture was filtered over celite and extracted with 3 x 80 mL DCM. Combined organic phases were dried over Na$_2$SO$_4$ and solvent was removed under reduced pressure (2.42 g, 59%). The crude product was used without further purification.

A 50 mL flask with female outer mantle was charged with 2-hydroxy-3-methyltetrahydrofuran (2.35 g, 23.0 mmol, 1.00 equiv), isoquinoline (910 µL, 7.60 mmol, 0.33 equiv) and p-toluenesulfonic acid hydrate (21.0 mg, 115 µmol, 0.005 equiv). The flask was connected via a connector (14.5 inner male -14.5 inner male, bented by 130 degrees), to an Schlenk tube with open valve, which was cooled to -78°C. The flask was then heated to 175°C to 200°C via heating mantle. The product was co-distilled with water and trapped in the Schlenk tube. The crude product was taken off from frozen water via Pasteur pipette and filtered through a Pasteur pipette filled with a 1 cm plug of dry Na_2SO_4. The product was obtained as a clear colourless liquid (952 mg, 49%).

¹H NMR (400 MHz, Chloroform-*d*) δ 6.04 (d, *J* = 1.8 Hz, 1H), 4.30 (t, *J* = 9.5 Hz, 2H), 2.52 (tdd, *J* = 9.4, 2.2, 1.2 Hz, 2H), 1.67 (q, *J* = 1.4 Hz, 3H).

Analytical data are in accordance with the literature.[182,266]

4-hexyl-5-methylthio-2,3-dihydrofuran 288
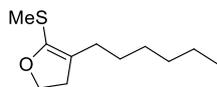
To a solution of 4-hexyl-2,3-dihydrofuran (386 mg, 2.50 mmol, 1.00 equiv) in 2.5 mL dry THF, *t*BuLi (1.76 mL, 3.00 mmol, 1.20 equiv) was added dropwise at -78°C and stirred for 35 min. The suspension was allowed to warm up to 0°C over 10 min and stirred for another 30 min. The mixture was cooled to -50°C, and dimethyl disulphide was added dropwise over 15 min. After 15 min., the mixture was allowed to slowly warm to rt overnight under stirring. The next day, the solvent was removed under reduced pressure via canula and septum. After bulb-to-bulb tube distillation directly from the residue, the product was obtained as a colourless oil (501 mg, >99%).

¹H NMR (400 MHz, Chloroform-*d*) δ 4.29 (t, *J* = 9.2 Hz, 1H), 2.62 (t, *J* = 9.3 Hz, 1H), 2.21 (s, 3H), 2.17 (t, *J* = 7.3 Hz, 1H), 1.50 – 1.22 (m, 8H), 0.98 – 0.68 (m, 3H).

Analytical data are in accordance with the literature.[160]

5,8-Difluorophthalazine 287
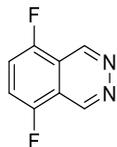
First, *n*-Butyllithium (6.00 ml, 9.63 mmol, 1.6 M in hexane, 1.07 equiv) was added drop-wise to a stirred solution of bis-(2-methoxyethyl)amine (1.74 g, 7.36 mmol, 1.00 equiv) in a mixture of 15 mL hexane and 3.75 mL THF at -20°C. After stirring the reaction mixture at -20°C for 30 min, 2,5-difluorobenzaldehyde (978 µL, 9.00 mmol, 1.00 equiv) was added in portions. Then *n*-BuLi (8.44 ml, 13.5 mmol, 1.60 M in hexane, 1.50 equiv) was added dropwise at -20°C. The reaction mixture is warmed to 0°C. After 2 h, the reaction mixture was cooled to -78°C. THF (7.5 mL) DMF (2.50 ml, 27.0 mmol, 3.00 equiv) was added and the mixture was stirred at –78°C for 20 min and then allowed to warm to 0°C. After 1.5 h, the reaction was quenched with a solution of NH$_4$Cl (1.44 g, 27.0 mmol, 3.00 equiv) and N$_2$H$_4$·H$_2$O (900 µl, 18.0 mmol, 80% in H$_2$O, 2.00 equiv) in H$_2$O (7.5 ml). The reaction mixture was allowed to warm to rt, stirred for 14 h, extracted with DCM (3 × 30 ml) and dried over Na$_2$SO$_4$. After concentration, the solid residue was dissolved in a mixture of Cyclohexane/acetone. The mixture was concentrated under reduced pressure until solid residues precipitated. Solid residues were filtered off, dissolved in DCM and adsorbed on silica. After purification twice via column chromatography (50 g, acetone/cyclohexane 1:1), the product was obtained as colourless solid (352 mg, 24%).

¹H NMR (200 MHz, Chloroform-d) δ 9.80 (s, 2H), 7.55 (dd, *J* = 6.4, 5.9 Hz, 2H).

Analytical data are in accordance to the literature.[160,267]

5,8-Dichlorophthalazine 315
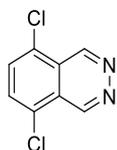
First, *n*-Butyllithium (6.00 ml, 9.63 mmol, 1.6 M in hexane, 1.07 equiv) was added dropwise to a stirred solution of bis-(2-methoxyethyl)amine (1.74 g, 7.36 mmol, 1.00 equiv) in a mixture of 15 mL hexane and 3.75 mL THF at -20 °C. After stirring the reaction mixture at -20°C for 30 min, 2,5-Chlorobenzaldehyde was added portion wise. Then *n*-BuLi (8.44 ml, 13.5 mmol, 1.60 M in hexane, 1.50 equiv) was added dropwise at –20°C°C. The reaction mixture was warmed to 0°C (ice bath). After 2 h, reaction mixture was cooled to -78°C. THF (7.5 mL), DMF (2.50 ml, 27.0 mmol, 3.00 equiv) was added, and the mixture was stirred at –78°C for 20 min

and then allowed to warm to 0°C. After 1.5 h, the reaction was quenched with a solution of NH_4Cl (1.44 g, 27.0 mmol, 3.00 equiv) and $N_2H_4 \cdot H_2O$ (2.33 ml, 45.0 mmol, 80% in H_2O, 5.00 equiv) in H_2O (7.5 ml). The reaction mixture was allowed to warm to rt, stirred for 14 h, extracted with DCM (3 × 30 ml) and dried over Na_2SO_4. After concentration of the mixture under reduced pressure, the solid residues were dissolved in Cyclohexane/acetone and the mixture was concentrated until solids residues precipitated. Solid residues were filtered off, dissolved in DCM and adsorbed on silica and purified via column chromatography (50 g silica, acetone/cyclohexane 1:1). Product was obtained as a light-yellow solid (760 mg, 21%).

¹H NMR (400 MHz, Chloroform-*d*) δ 9.84 (s, 2H), 7.80 (s, 2H).

MP: 213.0°C.

Analytical data are in accordance to the literature.[160,267]

5-Fluorophthalazine 315a
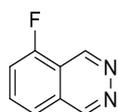
First, *n*-Butyllithium (6 ml, 9.63 mmol, 1.6 M in hexane, 1.07 equiv) was added drop-wise to a stirred solution of bis-(2-methoxyethyl)amine (1.74 g, 7.36 mmol, 1.00 equiv) in a mixture of 15 mL hexane and 3.75 mL THF at -20 °C. After stirring the reaction mixture at -20°C for 30 min, 2-fluorobenzaldehyde was added in portions. Then, *n*-BuLi (8.44 ml, 13.5 mmol, 1.60 M in hexane, 1.50 equiv) was added dropwise at –20°C °C. The reaction mixture was warmed to 0°C. After 2 h, the reaction mixture was cooled to -78°C. THF (7.5 mL) and DMF (2.50 ml, 27.0 mmol, 3.00 equiv) was added, and the mixture was stirred at –78°C for 20 min and then allowed to warm to 0°C. After 1.5 h, the reaction was quenched with a solution of NH_4Cl (1.44 g, 27.0 mmol, 3.00 equiv) and $N_2H_4 \cdot H_2O$ (2.33 ml, 45.0 mmol, 80% in H_2O, 5.00 equiv) in H_2O (7.5 ml). The reaction mixture was allowed to warm to rt, stirred for 14 h, extracted with DCM (3 × 30 ml) and dried over Na_2SO_4. After concentration, the solid residues were dissolved in Cyclohexane/acetone. The mixture was concentrated under reduced pressure until solids precipitated. The precipitate was filtered off, dissolved in DCM and adsorbed in silica and purified twice via column chromatography (50 g silica, acetone/cyclohexane 1:1). The product was obtained as colourless solid (453 mg, 24%).

¹H NMR (400 MHz, Chloroform-*d*) δ 9.73 (s, 1H), 9.51 (s, 1H), 7.84 (td, *J* = 8.0, 5.1 Hz, 1H),

7.72 (d, *J* = 8.1 Hz, 1H), 7.57 – 7.47 (m, 1H).

HRMS (ESI-MS) m/z calculated $[C_8H_5FN_2]^+$: $[Na]^+$ 171.0329; found: 171.0330.

Analytical data are in accordance with the literature.[160]

6-Fluorophthalazine 315b
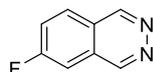
To a 100 mL three-necked flask charged with a stirred mixture of dry hexane (10 ml), dry THF (2.5 ml) and to a stirred solution of bis(2-methoxyethyl)amine (177 µL, 12.0 mmol, 1.10 equiv), *n*-BuLi (6.88 ml, 10.88 mmol, 1.6 M in hexane, 1.07 equiv) was added dropwise under nitrogen at -25°C. After the addition, the mixture was stirred at -20°C for 30 min to form the lithium amide. Then 4-fluorobenzaldehyde (1.07 mL, 10.0 mmol, 1.00 equiv.) was added at -20°C and the mixture was stirred for 45 min at –20 °C. Then, more n-BuLi (9.38 ml, 15.0 mmol, 1.6 M in hexane, 1.50 equiv.) was added drop wise at –20 °C. The mixture was allowed to warm to 0°C for 10 min and stirred for 2 h. After cooling to –78°C, 8.35 ml dry THF and dry DMF (2.34 ml, 20.0 mmol, 3.00 equiv.) were added and stirred for 10 minutes before the mixture was allowed to warm to 0°C and stirred for 1.5 h. The reaction was quenched with a mixture of N_2H_4 H_2O (640 µL, 20.0 mmol, 80% in H_2O, 2.00 equiv) in water, stirred for 14 h, extracted with 3 x 30 mL EtOAc, and dried over Na_2SO_4. The reaction mixture was concentrated and adsorbed on silica. After purification via column chromatography (silica 50 g, acetone/cyclohexane 1:1), the product was obtained as a beige solid (598 mg, 40%).

¹H NMR (400 MHz, Chloroform-*d*) δ 9.50 (dd, *J* = 9.8, 1.7 Hz, 2H), 8.01 (dd, *J* = 8.9, 5.1 Hz, 1H), 7.66 (td, *J* = 8.7, 2.5 Hz, 1H), 7.57 (dd, *J* = 8.1, 2.5 Hz, 1H).

¹³C NMR (101 MHz, Chloroform-*d*) δ 165.4, 162.9, 150.8, 150.8, 150.3, 150.3, 129.8, 129.7, 128.1, 128.0, 123.7, 123.7, 123.2, 122.9, 110.4, 110.2.

Analytical data are in accordance with the literature.[161]

5-Nitrophthalazine 316
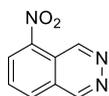
To a solution of phthalazine (5.10 g, 38.4 mmol, 1.00 equiv) in concentrated 35 mL H_2SO_4, potassium nitrate (18.7 g, 185 mmol, 4.80 equiv) was added in small portions at 0°C. The reaction mixture was heated to 70-80°C for 16 h. After cooling the reaction mixture with an ice bath down to 0-5°C, 84 mL 25% aq. NH_3 solution was added until the mixture was slightly basic. After extraction of the mixture with 3 x 50 mL EtOAc, sodium chloride was added to the aqueous phase which was further extracted with 2 x 50 mL EtOAc. Combined organic phases

were dried over Na$_2$SO$_4$, and the solvent was removed under reduced pressure. Recrystallisation from EtOH give the pure product as dark red crystals (805 mg, 20%).

¹H NMR (200 MHz, DMSO-d_6) δ 10.20 (dd, J = 1.6, 0.8 Hz, 1H), 9.91 (d, J = 1.5 Hz, 1H), 8.83 (dd, J = 7.8, 1.1 Hz, 1H), 8.63 (dt, J = 8.1, 1.0 Hz, 1H), 8.25 (t, J = 8.0 Hz, 1H).

HRMS (ESI-MS) m/z calculated [C$_8$H$_5$O$_2$N$_2$]$^+$: [Na]$^+$ 198.0275; found: 198.0278.

MP: 192.1°C.

Analytical data are in accordance with the literature.[176]

2*H*,3*H*,9b*H*-6,9-Difluoro-3a-hexyl-4-(methylthio)-naphtho-[1,2-*b*]-furan 289
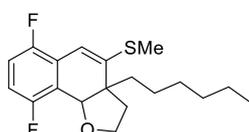
The 5,8-difluorophthalazine (44.3 mg, 266 μmol, 1.00 equiv) and the bidentate boron catalyst (5.50 mg, 27.0 μmol, 10 mol%) were mixed with 0.5 mL diglyme, and methyl-4-hexyl-2,3-dihydrofuran (106 mg, 532 μmol, 2.00 equiv) was added. The reaction mixture was stirred and heated for 23 h at 125°C. After 23 h, the reaction mixture was cooled down and the solvent was removed under reduced pressure. The residues were absorbed on silica, and, after column chromatography, the product was obtained as an oil (63.0 mg, 70%).

¹H NMR (400 MHz, Chloroform-d) δ 6.96 (td, J = 9.1, 4.4 Hz, 1H), 6.83 (td, J = 8.8, 4.1 Hz, 1H), 6.34 (d, J = 1.9 Hz, 1H), 4.82 (t, J = 1.1 Hz, 1H), 3.94 (td, J = 8.2, 3.6 Hz, 1H), 3.72 (ddd, J = 9.3, 8.1, 6.4 Hz, 1H), 2.64 (ddd, J = 12.7, 6.4, 3.6 Hz, 1H), 2.42 (s, 3H), 2.16 (dt, J = 12.7, 8.7 Hz, 1H), 1.94 – 1.81 (m, 1H), 1.45 (ddd, J = 13.6, 11.5, 4.7 Hz, 1H), 1.26 – 1.08 (m, 9H), 0.82 (t, J = 6.9 Hz, 3H).

¹³C NMR (101 MHz, Chloroform-d) δ 157.2 (dd, J = 243.3, 2.0 Hz), 153.7 (dd, J = 244.2, 2.0 Hz), 147.76 – 144.09 (m), 122.4 (dd, J = 15.5, 4.6 Hz), 119.4 (dd, J = 18.3, 3.7 Hz), 116.4 (dd, J = 24.2, 9.0 Hz), 113.5 (dd, J = 25.1, 8.3 Hz), 108.9 (dd, J = 4.8, 2.9 Hz), 76.4, 66.5, 51.3, 39.9, 39.3, 31.6, 29.8, 24.6, 22.7, 14.6, 14.1.

HRMS (ESI-MS) m/z calculated [C$_{19}$H$_{24}$F$_2$OS]$^+$: [Na]$^+$ 361.1406; found: 361.1406.

Analytical data are in accordance with the literature.[160]

2*H*,3*H*,9b*H*-6,9-Dichloro-3a-hexyl-4-(methylthio)-naphtho-[1,2-*b*]-furan 354 and 2*H*,3*H*-6,9-Dichloronaphtho-[1,2-*b*]-furan 355
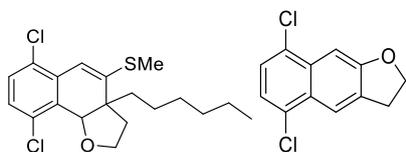
5,8-dichlorophthalazine (50.0 mg, 250 µmol, 1.00 equiv) and the bidentate boron catalyst (5.10 mg, 25.0 µmol, 10 mol%) were mixed with 0.5 mL diglyme, and 5-methylthio-4-hexyl-2,3-dihydrofuran (100 mg, 500 µmol, 2.00 equiv) was added. The reaction mixture was stirred and heated at 155°C for 48 h. After 48 h, the reaction mixture was cooled down, and solvent was removed under reduced pressure. After the purification of the residue via column chromatography, a mixture of 2*H*,3*H*,9b*H*-6,9-Dichloro-3a-hexyl-4-(methylthio)-2,3,3a,9b-naptho-[1,2b]-furan (24 mg, 26%) and 5,8-dichloro naphtho-1,2-furan (10.3 mg, 17%) was obtained.

2*H*,3*H*,3a*H*,9b*H*-6,9-Dichloro-3a-hexyl-4-(methylthio)-naphtho-[1,2b]-furan

¹H NMR (600 MHz, Chloroform-*d*) δ 8.08 (t, *J* = 1.6 Hz, 1H), 7.52 (s, 1H), 7.37 (d, *J* = 8.0 Hz, 1H), 7.27 (d, *J* = 8.0 Hz, 1H), 7.25 (d, *J* = 8.6 Hz, 2H), 7.11 (d, *J* = 8.6 Hz, 2H), 6.53 (s, 11H), 4.90 (s, 3H), 3.97 (td, *J* = 8.3, 2.9 Hz, 3H), 3.69 (ddd, *J* = 9.9, 8.0, 6.2 Hz, 3H), 2.66 (ddd, *J* = 12.7, 6.2, 2.9 Hz, 3H), 2.44 (s, 8H), 2.18 (ddd, *J* = 12.8, 10.0, 8.5 Hz, 3H), 1.84 (ddd, *J* = 13.7, 12.4, 4.2 Hz, 3H), 1.50 – 1.45 (m, 2H), 1.35 – 1.11 (m, 6H), 0.82 (t, *J* = 7.1 Hz, 8H).

¹³C NMR (101 MHz, Chloroform-*d*) δ 147.6, 133.6, 133.2, 130.6, 128.9, 127.6, 113.2, 80.1, 66.7, 51.7, 39.4, 38.9, 31.5, 29.7, 24.7, 22.7, 14.7, 14.1.

HRMS (ESI-MS) m/z calculated [C₁₉H₂₄Cl₂OS]⁺ : [Na]⁺ 393.0817; found: 393.0777.

2*H*,3*H*-5,8-Dichloronaphtho-[2,3-b]-furan

¹H NMR (600 MHz, Chloroform-*d*) δ 8.08 (t, *J* = 1.6 Hz, 1H), 7.52 (s, 1H), 7.37 (d, *J* = 8.0 Hz, 1H), 7.27 (d, *J* = 8.0 Hz, 1H), 4.69 (t, *J* = 8.4 Hz, 2H), 3.41 (td, *J* = 8.3, 1.6 Hz, 2H).

¹³C NMR (101 MHz, Chloroform-*d*) δ 160.6, 133.3, 133.1, 130.6, 130.5, 129.7, 125.6, 123.4, 121.1, 101.3, 71.9, 29.5.

GC-EI-MS: m/z (%) calculated 238, found 238.

Analytical data are in accordance with the literature.[160]

5-Thiomethyl-2,3-dihydrofuran 360
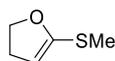
To a solution of 2,3-dihydrofuran (1.48 ml, 19.6 mmoL, 1.40 equiv) in 7 mL anhydrous THF (big bulb tube flask 50 mL), *t*BuLi (9.88 ml, 16.8 mmol, 1.20 equiv, 1.7 M solution in pentane) was added dropwise at -78°C. The reaction mixture was stirred for 35 min. The suspension was allowed to warm to 0°C and stirred for another 30 min. The mixture was cooled to -78°C, and dimethyldisulfide (1.24 ml; 14.0 mmol, 1.00 equiv) was added dropwise over 20 min. The mixture was allowed to slowly warm to rt overnight and stirred for 15 h. Solvent was removed via N_2-stream for 15 min. and the residue was bulb-tube distilled (50 mbar and 50°C – 13 mbar and 60°C). The product was obtained as a colourless liquid (949 mg, 58%).

^{1}H-NMR (400 MHz, Chloroform-*d*) δ 4.80 (t, *J* = 2.6 Hz, 1H), 4.40 (t, *J* = 9.2 Hz, 2H), 2.67 (td, *J* = 9.2, 2.6 Hz, 2H), 2.28 (s, 3H).

^{13}C-NMR (101 MHz, Chloroform-*d*) δ 152.8, 97.3, 71.2, 30.5, 14.9.

Analytical data are in accordance with the literature.[14]

5-Thiobutyl-2,3-dihydrofuran 361
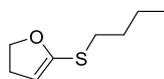
To a solution of 2,3-dihydrofuran (1.48 mL, 19.6 mmol, 1.40 equiv) in 7 mL dry THF in a 50 mL bulb-tube flask, *t*BuLi (9.88 mL, 16.8 mmol, 1.20 equiv, 1.7 M solution in pentane) was added dropwise at -78°C. The reaction mixture was stirred for 35 min. The suspension was allowed to warm to 0°C and stirred for another 30 min. The mixture was cooled to -78°C and dibutyl disulphide (2.74 mL, 14.0 mmol, 1.00 equiv) was added dropwise over 20 min. The mixture was allowed to slowly warm to rt overnight and stirred for 15 h. Then, solvent was removed via N_2-stream for 10-15 min. The residue was bulb-tube distilled (500 mbar to 5 mbar and rt - 3.0-1.5-0.9 mbar and 55-75°C). A mixture of product and dibutyl disulphide (497 mg, Product: 437 mg, 19%, 60.0 mg dibutyl disulphide) was obtained.

^{1}H NMR (400 MHz, Chloroform-*d*) δ 4.94 (t, *J* = 2.6 Hz, 1H), 4.39 (t, *J* = 9.2 Hz, 2H), 2.76 – 2.71 (m, 2H), 2.68 (td, *J* = 9.3, 2.6 Hz, 2H), 1.68 – 1.49 (m, 2H), 1.50 – 1.31 (m, 2H), 0.92 (td, *J* = 7.3, 4.6 Hz, 3H).

^{13}C NMR (101 MHz, Chloroform-*d*) δ 151.3, 100.3, 70.9, 66.9, 39.3, 31.6, 21.8, 13.7.

Analytical data are in accordance with the literature.[14]

2*H*,3*H*-5,8-Naphtho-[2,3-*b*]-furan 362
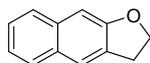
The reaction was prepared in a nitrogen-filled glove box. A Schlenk-tube was charged with phthalazine (33.0 mg, 250 µmol,1.00 equiv) and the bidentate boron catalyst (1.30 mg, 6.30 µmol, 2.00 mol%). Diglyme was added. After stirring for 1 min, 5-butylthio-2,3-dihydrofuran (60.0 mg, 375 µmol, 1.50 equiv) was added. The reaction mixture was stirred and heated at 125 °C outside of the glove box. After 72 h, the reaction mixture was cooled down, and the solvent was removed under reduced pressure. After purification via column chromatography, 2*H*,3*H*-5,8-Naphtho-[2,3-*b*]-furan was obtained as a solid (8.00 mg, 19%).

The reaction was prepared in a nitrogen-filled glove box. A Schlenk-tube was charged with phthalazine (33.0 mg, 250 µmol, 1.00 equiv) and catalyst (1.30 mg, 6.30 µmol, 2 mol%). Diglyme was added. After stirring for 1 min, 5-methylthio-2,3-dihydrofuran (43.6 mg, 375 µmol, 1.50 equiv) was added. The reaction mixture was stirred and heated at 125 °C outside of the glove box. After 72 h, reaction mixture was cooled down, and the solvent was removed under reduced pressure. After purification via column chromatography, 2*H*,3*H*-5,8-Naphtho-[2,3-*b*]-furan was obtained as a solid (24.0 mg, 24%).

1H NMR (400 MHz, Chloroform-*d*) δ 7.69 (dd, *J* = 12.1, 8.2 Hz, 1H), 7.62 (s, 1H), 7.40 – 7.32 (m, 1H), 7.32 – 7.23 (m, 1H), 7.09 (s, 1H), 4.63 (t, *J* = 8.3 Hz, 2H), 3.36 (td, *J* = 8.4, 1.3 Hz, 2H).

13C NMR (101 MHz, Chloroform-*d*) δ 158.8, 134.6, 129.7, 129.7, 127.7, 126.9, 125.9, 123.7, 123.3, 103.7, 71.5, 29.6.

HRMS (ESI-MS) m/z calculated $[C_{12}H_{10}O]^+$: $[H]^+$ 171.0805; found: 171.0806.

Analytical data are in accordance with the literature.[14,268]

2*H*,3*H*-5,8-Difluoronaphtho-[2,3-*b*]-furan 364 and 2*H*,3*H*,3a*H*,9b*H*-6,9-Difluoro-4-(butylthio)-naphtho-[1,2-*b*]-furan 367
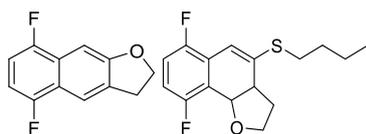
The reaction was prepared in a nitrogen-filled glove box. A Schlenk tube was charged with 5,8-difluorophthalazine (41.5 mg, 250 µmol, 1.00 equiv) and the bidentate boron catalyst (1.30 mg, 6.20 µmol, 2.00 mol%) and 250 µl diglyme. After stirring for 1 min, 5-butylthio-2,3-dihydrofuran (59.3 mg, 375 µmol, 1.50 equiv) was added. The reaction mixture was stirred and heated at 125°C outside of the glove box. After 72 h, reaction mixture was cooled down, and volatile

compounds were removed under reduced pressure. After purification via column chromatography, a mixture of 2*H*,3*H*-5,8-Difluoronaphtho-[2,3-*b*]-furan and 2*H*,3*H*,3a*H*,9b*H*-6,9-Difluoro-4-(butylthio)-naphtho-[1,2-*b*]-furan was obtained (2*H*,3*H*-5,8-Difluoronaphtho-[2,3-*b*]-furan: 27.7 mg, 54%; 2*H*,3*H*,3a*H*,9b*H*-6,9-Difluoro-4-(butylthio)-naphtho-[1,2-*b*]-furan: 5.30 mg, 7%).

The reaction was prepared in a nitrogen-filled glove box. A Schlenk tube was charged with 5,8-difluorophthalazine (41.5 mg, 250 µmol, 1.00 equiv), the bidentate boron catalyst (1.30 mg, 6.20 µmol, 2.00 mol%) and 250 µl diglyme. After stirring for 1 min, 5-methylthio-2,3-dihydrofuran (42.6 mg, 375 µmol, 1.50 equiv) was added. The reaction mixture was stirred and heated at 125 °C outside of the glove box. After 72 h, reaction mixture was cooled down, and volatile compounds were removed under reduced pressure. After purification via column chromatography 2*H*,3*H*-5,8-Difluoronaphtho-[2,3-*b*]-furan was obtained (23.2 mg, 45%).

2*H*,3*H*-5,8-Difluoronaphtho-[2,3-b]-furan

¹H NMR (400 MHz, Chloroform-*d*) δ 7.84 (s, 1H), 7.25 (s, 1H), 6.94 (ddd, *J* = 10.1, 8.4, 4.2 Hz, 1H), 6.83 (ddd, *J* = 10.1, 8.4, 4.0 Hz, 1H), 4.67 (t, *J* = 8.4 Hz, 2H), 3.37 (t, *J* = 8.3 Hz, 2H).

¹³C NMR (101 MHz, Chloroform-*d*) δ 159.84, 156.42 – 155.08 (m), 153.86 – 152.82 (m), 131.31, 125.66 (dd, *J* = 19.0, 5.3 Hz), 120.37 (dd, *J* = 18.9, 5.9 Hz), 116.73 (dd, *J* = 5.0, 2.1 Hz), 108.72 (dd, *J* = 22.9, 9.2 Hz), 105.87 (dd, *J* = 23.2, 8.6 Hz), 97.08 (dd, *J* = 5.3, 1.8 Hz), 71.65, 29.36.

GC-EI-MS: m/z (%) calculated 206, found 206.

2*H*,3*H*,3a*H*,9b*H*-6,9-Difluoro-4-(butylthio)-naphtho-[1,2b]-furan

¹H NMR (400 MHz, Chloroform-*d*) δ 6.94 (ddd, *J* = 10.1, 8.4, 4.1 Hz, 1H), 6.83 (ddd, *J* = 10.0, 8.4, 4.0 Hz, 1H), 4.67 (t, *J* = 8.3 Hz, 1H), 3.38 (td, *J* = 8.4, 1.5 Hz, 1H).

¹³C NMR (101 MHz, Chloroform-*d*) δ 160.0, 156.2 (t, *J* = 10.6 Hz), 155.6, 153.8 (t, *J* = 10.6 Hz), 153.2, 131.4, 131.4, 125.8 (dd, *J* = 19.0, 5.6 Hz), 120.5 (dd, *J* = 19.0, 5.9 Hz), 116.9 (dd, *J* = 5.1, 2.2 Hz), 108.8 (dd, *J* = 22.8, 8.9 Hz), 106.0 (dd, *J* = 23.1, 8.5 Hz), 97.2 (dd, *J* = 5.3, 1.8 Hz), 71.8, 28.3 (d, *J* = 244.5 Hz).

HRMS (ESI-MS) m/z calculated $[C_{15}H_{18}OS]^+$: $[Na]^+$ 319.0940; found: 319.0938.

Analytical data are in accordance with the literature.[14]

4,4'-Dihydroxy-3,3'-dimethoxystilbene 379
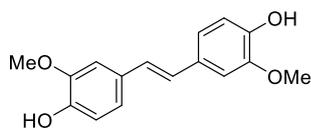
A flask was charged with Mg powder (2.35 g, 96.7 mmol, 2.10 equiv) and 100 mL anhydrous THF. The mixture was chilled to −78 °C, and then, TiCl$_4$ (10.6 mL, 96.5 mmol, 2.10 equiv) was added dropwise through an addition funnel. The flask was allowed to slowly warm up to room temperature and the mixture transitioned to a green slurry and finally a black solution. After stirring at room temperature for 30 min, a solution of vanillin (7.01 g, 46.1 mmol, 1.00 equiv) in 50 mL anhydrous THF was added dropwise. The reaction was mildly exothermic and resulted in a dark brown mixture. The mixture was heated at reflux for 3 h and was then cooled to room temperature. The solvent was removed under reduced pressure, and the residue was treated with 100 mL 2 M HCl to yield a dark solution with pale brown suspended solid. The mixture was filtered, and the isolated solid was washed with 3 × 50 mL water and 3 × 25 mL chilled (0°C) ethanol. The solid was dried in a vacuum overnight to yield a dark green solid. Product was purified via column chromatography (silica 100 g, cyclohexane/EtOAc 2:1 to 1:1, then DCM. The product was isolated as a solid, coloured white to pink. (1.55 g, 25%).

¹H NMR (400 MHz, DMSO-d_6) δ 9.03 (s, 2H), 7.1 (d, J = 1.8 Hz, 2H), 6.95 (d, J = 2.0 Hz, 2H), 6.93 (d, J = 1.9 Hz, 2H), 6.80 (d, J = 8.1 Hz, 2H), 3.89 (s, 6H).

¹³C NMR (101 MHz, DMSO-d_6) δ 148.3, 146.6, 129.7, 126.2, 120.0, 116.1, 110.0, 56.1.

MP: 212.6°C.

The Analytical data are in accordance with the literature.[208]

3,3',4,4'-Tetramethoxystilbene 380
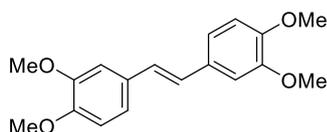
In a 50 mL flask, 4,4'-hydroxy-3,3'-dimethoxystilbene (8.17 g, 3.00 mmol, 1.00 equiv) was dissolved in 10 mL DMF, and K$_2$CO$_3$ (2.49 g, 6.00 mmol, 6.00 equiv) was added in a single portion at 25°C. After stirring the resultant slurry for 5 min at 25°C, iodomethane (2.55 mL, 60.0 mmol, 6.00 equiv) was added slowly over the course of 5 min via syringe. The reaction mixture was stirred for 12 h at 25 °C. Upon completion, the reaction contents were quenched with 20 mL saturated aqueous NH$_4$Cl, poured into 7.5 mL water, and extracted with 4 × 20 mL

EtOAc. The combined organic extracts were then washed with 20 mL water and 20 mL brine, dried over MgSO$_4$, filtered, and concentrated under reduced pressure. The resultant crude, yellow oil was purified by flash column chromatography (silica gel, hexanes/EtOAc, 3:1) to obtain the product (731 mg, 81%) as a colourless solid.

¹H NMR (200 MHz, Chloroform-*d*) δ 7.12 – 6.98 (m, 2H), 6.93 (s, 2H), 6.86 (d, *J* = 8.5 Hz, 2H), 3.95 (s, 6H), 3.90 (s, 6H).

HRMS (ESI-MS) m/z calculated [C$_{18}$H$_{20}$O$_4$]$^+$: [Na]+ 323.1254; found: 321.1254.

Analytical data are in accordance with the literature.[269]

2,3,6,7-Tetramethoxyphenanthrene 378
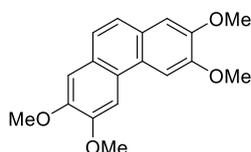
Tetramethoxystilbene (8.17 g, 3.00 mmol, 1.00 equiv) and iodine (5.00 mg, 20.0 µmol, 1.00 mol%) were dissolved in 400 mL absolute ethanol and irradiated with a mercury lamp for 7 h. The solvent was removed under reduced pressure. After recrystallization of the residue from toluene/hexane (1:1), the product was obtained as a colourless solid (120 mg, 20%).

¹H NMR (200 MHz, Chloroform-*d*) δ 7.80 (s, 2H), 7.56 (s, 2H), 7.23 (s, 2H), 4.13 (s, 6H), 4.04 (s, 6H).

HRMS (ESI-MS) m/z calculated [C$_{18}$H$_{18}$O$_4$]$^+$: [Na]$^+$ 321.1097; found: 321.1099.

Analytical data are in accordance with the literature.[209,270]

6-Nitroveratraldehyde 392
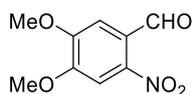
In a 250 mL flask, 100 mL of 65% nitric acid was cooled to 0°C, and powdered (grounded in mortar) veratraldehyde (10.1 g, 60.0 mmol, 1.00 equiv) was added under stirring. The mixture was brought to room temperature, stirred for 3 h and then poured into ice-water (200 mL). The resulting yellow precipitate was collected by filtration and washed with cold water and ethanol. The crude material was recrystallized from ethanol. The product was obtained as a yellow solid (7.31 g, 58%).

¹H NMR (400 MHz, Chloroform-*d*) δ 10.44 (s, 1H), 7.61 (s, 1H), 7.42 (s, 1H), 4.03 (s, 3H), 4.02 (s, 3H).

MP: 130.6.

Analytical data in accordance with the literature.[175]

5,5'6,6'-Tetramethoxyindigo 393
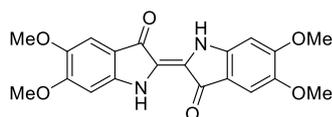
To a suspension of 3,4-dimethoxy-2-nitrobenzaldehyde (2.01 g, 9.50 mmol, 1.00 equiv) in 5 mL acetone, 5 drops of 10% NaOH were added under exclusion of light. After 1 h, 30 mL water and 5 mL 10% NaOH were added. The reaction mixture was stirred for 24 h, then it was left standing for 2 days without stirring. A precipitate was collected by filtration and washed with boiling EtOH. For further purification, the solid was mixed with 1.7 mL EtOH, heated to boiling and filtered over a silica frit and washed with 5.15 mL EtOH and 2 x 1.5 mL Et₂O. After drying, the product was obtained as a dark green-blue solid (256 mg, 7%).

¹H NMR (400 MHz, DMSO-*d*₆) δ 10.08 (s, 2H), 7.11 (s, 2H), 7.05 (s, 2H), 3.94 (s, 6H), 3.85 (s, 6H).

¹³C NMR (101 MHz, DMSO-*d*₆) δ 186.3, 157.2, 150.8, 144.6, 122.0, 110.9, 104.9, 96.7, 56.3.

HRMS (ESI-MS) m/z calculated [$C_{20}H_{18}N_2O_6$]⁺ : [H]⁺ 383.1238; found: 383.1238.

Analytical data in accordance with the literature.[175]

Dehydrodivanillin 374
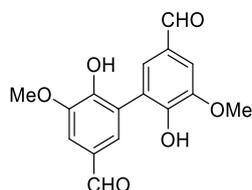
Vanillin (2.07 g, 20.0 mmol, 1.00 equiv) was dissolved in 200 mL 80°C hot deionized water, and iron(II) sulphate (112 mg, 400 μmol, 2.00 mol%) was added. Then, sodium peroxodisulfate (2.52 g, 10.6 mmol, 0.55 equiv) was added at once, and reaction mixture was stirred for 30 min without additional heating. Reaction mixture turned dark, and a brown precipitate was formed. Afterwards, the reaction mixture was filtered. The filter cake was dissolved in 12.5% NaOH solution and was precipitated again with 6 M HCl solution. After filtration via Buchner funnel,

the solid residues are dried at high vacuum overnight. Dehydrodivanillin was obtained as a light brown solid which was used without further purification.

^{1}H NMR (400 MHz, DMSO-d_6) δ 9.81 (s, 2H), 7.43 (m, 4H), 3.93 (s, 6H).

^{13}C NMR (101 MHz, DMSO-d_6) δ 191.7, 150.9, 148.7, 128.6, 128.2, 125.1, 109.7, 56.5.

MP: 306.5°C (decomposition).

Analytical data are in accordance with the literature.[205,271]

Bis-(2-methoxy-1,4-hydroquinone) 375
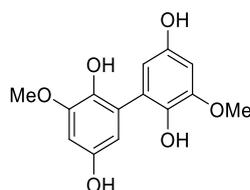
Dehydrodivanillin (1.51 g, 5.00 mmol, 1.00 equiv) was suspended in a mixture of 20 ml THF and 7 mL water. The mixture was degassed via a nitrogen stream into solution for 30 min. The following reaction was performed under nitrogen stream. Then, sodium percarbonate (1.73 g, 5.50 mmol, 1.10 equiv) was added in portions. The reaction mixture was stirred for 3 h at room temperature. The reaction mixture was quenched with 0.1 M diluted hydrochloric acid until pH = 3. The reaction mixture was extracted with EtOAc. The combined organic phases were washed with brine and dried over Na_2SO_4. The solvent was removed under reduced pressure. A thick dark brown oily residue was obtained. After adding chloroform, a slurry precipitated. Removing of $CHCl_3$ under reduced pressure led to a red foam. The residue was dissolved in EtOAc and adsorbed on silica. After purification via column chromatography ($CHCl_3$/MeOH 95:5), the product was obtained as an off-white solid and was used without further purification.

^{1}H NMR (200 MHz, DMSO-d_6) δ 8.82 (s, 2H), 7.78 (s, 2H), 6.38 (d, J = 2.7 Hz, 2H), 6.15 (d, J = 2.7 Hz, 2H), 3.75 (s, 6H).

HRMS (ESI-MS) m/z calculated [$C_{14}H_{14}O_6$]$^+$: [Na]$^+$ 301.0682; found: 301.0681.

Analytical data are in accordance with the literature.[272]

6,6'-Dimethoxy-2,2'-bis-(1,4-benzoquinoyl) 376
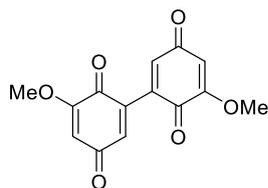
To a suspension of 2,2-bis-(1,4-dihydroxy-2-methoxybenzene) (779 mg, 2.80 mmol, 1.00 equiv) in a mixture of 11 ml acetonitrile and 5 mL water, TBAB (45.6 mg, 140 µmol, 5.00 mol%) and Oxone® (3.44 g, 4.60 mmol, 2.00 equiv) were added, and the reaction mixture was stirred at room temperature. The reaction mixture turned from brown to dark brown, and a precipitate was formed. After 10 min., the reaction mixture was filtered and washed with water. More of the product precipitated in the filtrate and was collected via filtration. After purification twice via column chromatography (70 g silica, first DCM/MeOH 98:2, second pure DCM), the product was obtained as a yellow solid (266 mg, 35%).

^{1}H NMR (400 MHz, DMSO-d_6) δ 6.85 (d, J = 2.4 Hz, 2H), 6.21 (d, J = 2.4 Hz, 2H), 3.83 (s, 6H).

^{13}C NMR (101 MHz, DMSO-d_6) δ 187.1, 159.2, 138.8, 136.5, 108.2, 57.2.

HRMS (ESI-MS) m/z calculated [$C_{14}H_{10}O_6$]$^+$: [Na]$^+$ 297.0370 found: 297.0372.

MP: (decomposition).

EA: (%) for $C_{14}H_{10}O_6$: calcd C, 61.32; H, 3.68; N, 0; found C, 59.26; H, 3.69; N, 0.32.

Benzimidazole 385
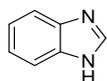
In a 100 mL flask, *o*-phenylenediamine (11.0 g, 100 mmol, 1.00 equiv) was added to a mixture of 8 mL formic acid in 1 mL water. The reaction mixture was stirred and heated at 100°C for 2 h. Then, 10% NaOH was added until the mixture was basic. The precipitate was filtered and washed with ice-cooled water. Crude product was recrystallised from hot water. Product was obtained as colourless solid (9.23 g, 78%).

^{1}H NMR (400 MHz, DMSO-d_6) δ 12.51 (s, 1H), 8.24 (s, 1H), 7.61 (m, 3H), 7.20 (dd J = 6.0, 3.2 Hz).

Analytical data are in accordance with the literature.[213]

1,3-dimethyl benzimidazolium iodide 386
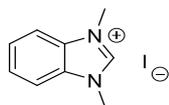
A 100 mL flask was charged with K_2CO_3 (8.29 g, 60.0 mmol, 2.00 equiv), 30 mL acetonitrile, benzimidazole (3.54 g, 30.0 mmol, 1.00 equiv) and iodomethane (5.60 mL, 90.0 mmol, 3.00 equiv). The reaction mixture was stirred and heated at 85°C for 24 h. After cooling to room temperature, the mixture was concentrated under reduced pressure. Then, DCM was added to precipitate potassium iodide. The solid residues were filtered off and the filtrate was concentrated under reduced pressure to obtain a solid. This solid was resuspended in THF and filtered for further purification. The product was obtained as colourless solid (3,70 g, 45%).

¹H NMR (400 MHz, DMSO-d_6) δ 9.65 (s, 1H), 8.03 (dd, J = 6.3, 3.2 Hz, 2H), 7.72 (dd, J = 6.3, 31 Hz), 4.06 (s, 6H).

HRMS (ESI-MS) m/z calculated $[C_9H_{11}N_2]^+$: 147.0917 found: 147.0919

Analytical data are in accordance with the literature.[214]

3,3'4,4'-Tetramethoxybenzil 381
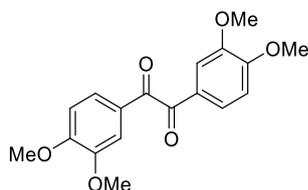
A 500 mL flask was charged with veratraldehyde (16.8 g, 100 mmol, 1.00 equiv) and 1,3-dimethyl benzimidazolium iodide (1.14 g, 5.00 mmol, 5.00 mol%). Then, 250 mL dioxane and DBU (5.00 mL, 34.0 mmol, 0.34 equiv) were added. Reaction mixture was stirred and heated on reflux for 12 h. The solvent was removed under reduced pressure. Reaction mixture was concentrated and adsorbed on silica gel. The reaction mixture-silica was left stranding over the weekend. Afterwards, the mixture was purified via column chromatography (silica, first toluene, which eluted starting material veratraldehyde, then chloroform, which eluted product). Product was obtained as a yellow solid (3.43 g, 10%).

¹H NMR (200 MHz, Chloroform-d) δ 7.60 (d, J = 2.0 Hz, 2H), 7.48 (dd, J = 8.4, 2.0 Hz, 2H), 6.89 (d, J = 8.4 Hz, 2H), 3.96 (d, J = 0.7 Hz, 6H).

MP: 225.2°C.

Analytical data are in accordance with the literature.[211,216,273]

2,3,6,7-tetramethoxy-9,10-phenanthrenequinone 377
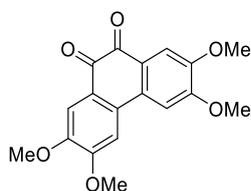
Tetramethoxybenzil (661 mg, 2.00 mmol, 1.00 equiv) was dissolved in 40 mL anhydrous DCM in a Schlenk tube under nitrogen. Reaction mixture was cooled down to 0°C. Then, TiCl$_4$ (500 µL, 4.40 mmol, 2.20 equiv) was added as 10% solution in 6 mL anhydrous DCM. Afterwards, MoCl$_5$ (1.20 g, 4.40 mmol, 2.20 equiv) was added. The reaction mixture was stirred for 15 min. The reaction mixture was quenched with an ice cooled NaHCO$_3$ solution. The slurry was filtered, and the residual solid was washed thoroughly with chloroform (800 ml). The aqueous phase was extracted 5 x 40 mL with chloroform. The combined organic layers were separated, dried over MgSO$_4$, and the solvent was removed under reduced pressure. The crude product was recrystallized from 1,4-dioxane. The product was obtained as a golden coloured solid (500 mg, 76%).

^{1}H NMR (200 MHz, Chloroform-*d*) δ 7.54 (s, 2H), 7.12 (s, 2H), 4.09 (s, 6H), 3.97 (s, 6H).

MP: 260.5°C.

Analytical data are in accordance with the literature.[216,273]

3-Methoxy-4-(tri*iso*propylsiloxy) benzaldehyde 387
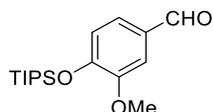
In a 100 mL flask, 32mL anhydrous DMF was added to a mixture of vanillin (6.15 g, 40.0 mmol, 1.00 equiv.) and imidazole (8.17 g, 120 mmol, 3 equiv.) under N$_2$. At 0°C, tri*iso*propylsilyl chloride (8.60 mL, 40.0 mmol, 1.00 equiv.) was added dropwise via syringe. After 5 min, the ice bath was removed, and the reaction mixture was stirred at room temperature for 2 h. The reaction mixture was poured into 200 mL water and was extracted with 3 x 200 mL and 1 x 100 mL DCM. Combined organic phases were washed with 1 x 200 mL brine and were dried over Na$_2$SO$_4$. The solvent was removed under reduced pressure. The crude product was purified via flash column chromatography (silica 150 g, cyclohexane/EtOAc 9:1). The product was obtained as a colourless oil (10.5 g, 85%).

¹H NMR (400 MHz, Chloroform-*d*) δ 9.76 (s, 1H), 7.32 (d, *J* = 1.9 Hz, 1H), 7.28 (dd, *J* = 8.0, 2.0 Hz, 1H), 6.91 (d, *J* = 8.0 Hz, 1H), 3.79 (s, 3H), 1.26 – 1.14 (m, 3H), 1.02 (d, *J* = 7.4 Hz, 18H).

¹³C NMR (101 MHz, Chloroform-*d*) δ 191.0, 151.9, 151.6, 130.6, 126.2, 120.2, 110.1, 55.4, 17.8, 12.9.

HRMS (ESI-MS) m/z calculated $[C_{10}H_{10}N_2O_2]^+$: $[Na]^+$ 331.1699; found: 331.1700.

Analytical data are in accordance with the literature.[220]

3,3'-Dimethoxy 4,4'-bis (tri*iso*propylsiloxy) benzoin 389
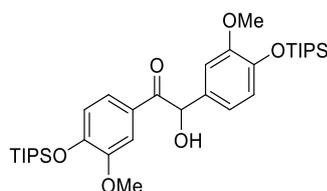
To a Schlenk tube charged with TIPS-protected-vanillin (6.30 g, 20.5 mmol, 1.00 equiv) and thiazolium bromide (1.43 g, 8.30 mmol, 40.0 mol%), 20 mL *t*BuOH were added. Then, triethylamine (1.80 mL, 12.3 mmol, 0.60 equiv) was added, and reaction mixture was stirred and heated on 70°C for 17 h under nitrogen. The solvent was removed under reduced pressure and residue was dissolved in DCM and adsorbed on silica. After purification via column chromatography (75 g silica, cyclohexane: EtOAc 95:5 - 8:2), the product was obtained as oil (2.04 g, 27%).

¹H NMR (400 MHz, Chloroform-*d*) δ 7.39 (d, *J* = 2.1 Hz, 2H), 7.31 (dd, *J* = 8.4, 2.1 Hz, 2H), 6.76 – 6.63 (m, 2H), 5.71 (s, 1H), 3.71 (s, 3H), 3.67 (s, 3H), 1.25 – 1.07 (m, 6H), 1.02 – 0.93 (m, 36H).

¹³C NMR (101 MHz, Chloroform-*d*) δ 197.7, 151.5, 151.3, 151.0, 145.9, 133.1, 127.1, 124.0, 120.8, 120.7, 119.8, 112.4, 111.4, 76.0, 55.6, 55.6, 18.0, 17.9, 13.0, 13.0.

HRMS (ESI-MS) m/z calculated $[C_{10}H_{10}N_2O_2]^+$: $[Na]^+$ 639.3507; found: 639.3503.

EA: (%) for $C_{34}H_{56}O_6Si_2$: calcd C, 66.19; H, 9.15; N, 0; found C, 65.44; H, 9.17; N, 0.40.

3,3'-Dimethoxy 4,4'-bis (triisopropylsiloxy) benzil 390
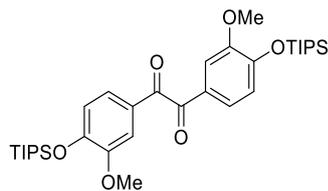
To a solution of 3,3'-Dimethoxy-4,4'-bis-(tri*iso*propylsiloxy) benzoin (2.04 g, 3.30 mmol, 1.00 equiv) in 64 mL DCM in an open (non-sealed) flask, aluminium oxide (16.0 g, basic, 50-200 µm) was added and stirred for 2 h at room temperature. The reaction mixture was filtered, and the solvent was removed under reduced pressure. After purification via column chromatography (silica, 120 g, cyclohexane/EtOAc 98:2), the product was obtained as a yellow sticky oil (200 mg, 10%).

^{1}H NMR (400 MHz, Chloroform-*d*) δ 7.56 (d, *J* = 2.0 Hz, 2H), 7.37 (dd, *J* = 8.3, 2.1 Hz, 2H), 6.88 (d, *J* = 8.3 Hz, 2H), 3.87 (s, 6H), 1.33 – 1.19 (m, 3H), 1.09 (d, *J* = 7.4 Hz, 36H).

^{13}C NMR (101 MHz, Chloroform-*d*) δ 193.8, 152.3, 151.4, 126.9, 125.8, 120.0, 111.4, 55.6, 17.8, 13.0.

HRMS (ESI-MS) m/z calculated $[C_{34}H_{54}O_6Si_2]^+$: $[Na]^+$ 637.3351; found: 637.3351.

2,3-Dimethoxy 6,7-bis (tri*iso*propylsiloxy) phenanthrenequinone 391
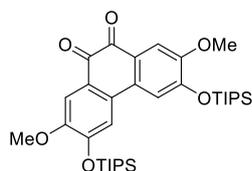
TIPS protected-benzil (154 mg, 250 µmol, 1.00 equiv) was dissolved in 5 mL anhydrous DCM and cooled down to 0°C. Then, $TiCl_4$ (60.0 µL, 550 µmol, 2.00 equiv) was added as 10% solution in 750 µL anhydrous DCM. Afterwards, $MoCl_5$ (150 mg, 55.0 µmol, 2.20 equiv) was added. The reaction mixture was stirred for 15 min. Then, reaction mixture was quenched with an ice cooled $NaHCO_3$ solution. The slurry was filtered, and the residual solid was washed thoroughly with chloroform (100 ml). The aqueous phase was extracted with 5 x 5 mL chloroform. The combined organic layers were separated, dried over $MgSO_4$, and the solvent was removed under reduced pressure. The crude product was purified via column chromatography (silica 30 g, cyclohexane/EtOAc 8:2). The product was obtained as a violet solid (54 mg, 37%).

^{1}H NMR (400 MHz, Chloroform-*d*) δ 7.56 (s, 2H), 7.13 (s, 2H), 3.89 (s, 6H), 1.33 (m, 6H), 1.14 (d, *J* = 7.4 Hz, 36H).

13C NMR (101 MHz, Chloroform-*d*) δ 179.2, 151.5, 131.1, 125.1, 114.8, 112.6, 55.8, 17.8, 13.0.

HRMS (ESI-MS) m/z calculated $[C_{34}H_{52}O_6Si_2]^+$: $[Na]^+$ 635.3194; found: 635.3198.

MP: 233.4°C.

EA: (%) for $C_{34}H_{52}O_6Si_2$: calcd C, 66.52; H, 8.55; N, 0; found C, 66.48; H, 8.51; N, 0.19.

6-Methoxy-1,4-naphthoquinone 398
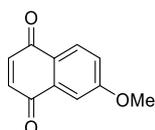
In a dried Schlenk tube, 6-Methoxy-1-tetralone (534 mg, 3.00 mmol, 1.00 equiv) was dissolved in 30 mL $MeNO_2$ under N_2. Then, 2-iodobenzoic acid (152 mg, 600 μmol, 0.20 equiv), TBAB (48.8 mg, 150 μmol, 5 mol%), and Oxone® (9.3 g, 15.0 mmol, 5.00 equiv) were added at room temperature. The reaction mixture was stirred at 80°C for 24 h. After cooling down to room temperature, the solvent was removed under reduced pressure. The residue was extracted with 3 × 60 mL EtOAc. The combined organic layers were washed with 2 ×20 mL H_2O and 10 mL brine and dried over Na_2SO_4. After filtration, the solvent was removed under reduced pressure. The residue was purified via column chromatography (silica, pentane/EtOAc 8:2). The product was obtained as yellow solid (131 mg, 23%).

1H NMR (400 MHz, Chloroform-*d*) δ 8.03 (d, *J* = 8.7 Hz, 1H), 7.51 (d, *J* = 2.7 Hz, 1H), 7.22 (dd, *J* = 8.6, 2.7 Hz, 1H), 6.93 (d, *J* = 1.0 Hz, 2H), 3.95 (s, 3H).

HRMS (ESI-MS) m/z calculated $[C_{11}H_8N_2O_3]^+$: $[Na]^+$ 211.0365; found: 211.0367.

Analytical data are in accordance with the literature.[224]

6-Methoxy-2,3-diazaanthraquinone 401
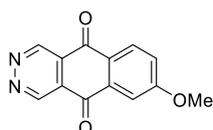
In a Schlenk tube, bidentate boron catalyst pyridazine complex (3.98 mg, 14.0 μmol, 5.00 mol%), tetrazine (115 mg, 1.4 mmol, 5.00 equiv) and 6-methoxy-1,4-naphthoquinone (52.7 mg, 280 μmol, 1.00 equiv) were suspended in anhydrous benzotrifluoride under N_2 atmosphere. The reaction mixture was stirred and heated to 55°C, sealed and stirred at 110°C

for 24 h. The reaction mixture was cooled down and the solvent and the excess tetrazine were removed under reduced pressure. The solid residue was purified via column chromatography (silica, cyclohexane/EtOAc 6:4 - 1:1). The product was obtained as a yellow-green solid (28.0 mg, 42%).

^{1}H NMR (400 MHz, Chloroform-*d*) δ 10.00 (d, *J* = 1.3 Hz, 1H), 9.97 (d, *J* = 1.2 Hz, 2H), 8.29 (d, *J* = 8.7 Hz, 1H), 7.72 (d, *J* = 2.7 Hz, 1H), 7.39 (dd, *J* = 8.8, 2.7 Hz, 1H), 4.03 (s, 3H), 1.55 (s, H$_2$O).

^{13}C NMR (101 MHz, Chloroform-*d*) δ 182.5, 180.9, 165.5, 147.3, 146.8, 134.5, 130.2, 125.5, 122.5, 110.3, 56.3.

HRMS (ESI-MS) m/z calculated [C$_{13}$H$_8$N$_2$O$_3$]$^+$: [H]$^+$ 241.0608; found: 241.0611.

EA: (%) for C$_{13}$H$_8$N$_2$O$_3$: calcd C, 65.00; H, 3.36; N, 11.66; found C, 60.21; H, 2.87; N, 9.96.

Analytical data are in accordance with the literature.[9]

2,3-Diazaanthraquinone 400
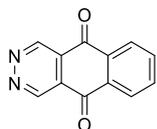
In a Schlenk tube, bidentate boron catalyst pyridazine complex (3.55 mg, 1.00 µmol, 5.00 mol%), tetrazine (103 mg, 1.25 mmol, 5.00 equiv) and 6-methoxy-1,4-naphthoquinone (40.8 mg, 250 µmol, 1.00 equiv) were suspended in 3 mL anhydrous benzotrifluoride under N$_2$. The reaction mixture was stirred and heated to 55°C, sealed and stirred at 110°C for 24 h. The reaction mixture was cooled down and the solvent and the excess tetrazine were removed via reduced pressure. The solid residue was purified via column chromatography (silica, cyclohexane/EtOAc 1:1). The product was obtained as a yellow-green solid (39.0 mg, 74%).

^{1}H NMR (400 MHz, Chloroform-*d*) δ 10.01 (s, 2H), 8.34 (dd, *J* = 5.8, 3.3 Hz, 2H), 7.95 (dd, *J* = 5.8, 3.3 Hz, 2H), 2.30 – 0.44 (silicon grease).

MP: decomposition >390°C.

Analytical data are in accordance with the literature.[9]

Diacetyl naphtharazin 403
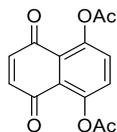
To a 10 mL flask charged with naphtharazin (114 mg, 0.60 mmol, 1.00 equiv), a mixture of 1.5 mL acetic anhydride and sulfuric acid (Ac_2O: 1.50 mL, 15.8 mmol, 26.30 equiv + 1/3 drop of concentrated sulfuric acid) was added. The reaction mixture was shortly warmed to 40°C for better solubility. Then stirred at room temperature overnight (100 mg, 61%). Afterwards, 15 mL ice-water were added, and the reaction mixture was filtered. The filter residue was washed twice with 1 ml cold water. The product was obtained as yellow solid (99.0 mg, 60%)

^{1}H NMR (200 MHz, Chloroform-*d*) δ 7.40 (s, 2H), 6.81 (s, 2H), 2.44 (s, 6H).

HRMS (ESI-MS) m/z calculated $[C_{14}H_{10}O_6]^+$: $[Na]^+$ 297.0369; found: 297.0368.

Analytical data are in accordance with the literature.[225]

5,8-Dihydroxy-2,3-díazaanthraquinone 405
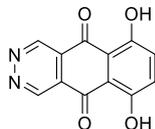
A Schlenk tube was charged with the bidentate boron catalyst pyridazine complex (5.00 mg, 18.0 µmol, 5.00 mol%), tetrazine (144 mg, 1.75 mmol, 5.00 equiv) and 5,8-acetoxy-1,4-naphthoquinone (96.0 mg, 350 µmol, 1.00 equiv) and 3.00 mL anhydrous benzotrifluoride were added. The reaction mixture was stirred and heated at 55°C, sealed from N_2, and heated at 110°C for 24 h. After cooling down to room temperature, the solvent and the excess tetrazine were removed via reduced pressure. The solid residue was purified via column chromatography (15 g, silica, cyclohexane/EtOAc 1:1). For the deprotection, the acetylated product was suspended in 5 mL Methanol and two drops of concentrated HCl were added. The reaction mixture was heated at reflux for 1 h. Volatile compounds were removed under reduced pressure. The crude product was purified twice via column chromatography (40 g silica, $CHCl_3$). Product was obtained as a dark red solid (24.0 mg, 28% over two steps).

^{1}H NMR (400 MHz, Chloroform-*d*) δ 12.62 (s, 2H), 10.06 (s, 2H), 7.46 (s, 2H), 1.25 (s, cyclohexane), 0.88 (silicon grease).

HRMS (ESI-MS) m/z calculated $[C_{12}H_6N_2O_4]^+$: $[Na]^+$ 265.0220; found: 265.0221.

MP: >390°C decomposition.

Analytical data are in accordance with the literature.[9]

2-Bromo-1,4-hydroquinone 437
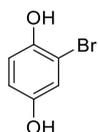
Hydroquinone (4.92 g, 45 mmol, 1.00 equiv.) was dissolved/suspended in Et_2O in a two-necked flask with thermometer and cooled to 0°C. Then, bromine (7.91 g, 45 mmol, 1.00 equiv.) was added dropwise. The reaction mixture was stirred for 2 h at room temperature and quenched with 20 mL saturated thiosulfate solution. After the extraction with 3 x 60 mL Et_2O, combined organic phases were dried over $MgSO_4$. The solvent was removed under reduced pressure. The crude product was adsorbed on celite and purified twice via column chromatography (flash silica 175 g, pentane : EtOAc 8:2, then flash silica 175 g, pentane : EtOAc 9:1). Product was obtained as a colourless solid (2.88 g, 34%)

¹H NMR (200 MHz, DMSO-d_6) δ 9.36 (s, 1H), 9.05 (s, 1H), 6.86 (d, J = 2.8 Hz, 1H), 6.76 (d, J = 8.7 Hz, 1H), 6.59 (dd, J = 8.7, 2.8 Hz, 1H).

MP: 111°C (lit. 112-116°C).

Analytical data are in accordance with the literature.[274]

2-Methoxy-1,4-hydroquinone 372
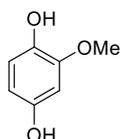
Vanillin (7.68 g, 50.0 mmol, 1.00 equiv) was suspended in a mixture of 200 mL THF and 80 mL water. The solvent was degassed via a nitrogen stream for 30 min. The further reaction was performed under N_2-atmosphere. Then, sodium percarbonate (8.64 g, 27.5 mmol, 0.55 equiv) was added in portions. The reaction mixture was stirred for 3 h at room temperature. The reaction mixture was quenched by adding 0.1 M diluted hydrochloric acid until a pH value of 3 was reached. The reaction mixture was extracted with Ethyl acetate. The Combined organic phases were washed with brine and dried over Na_2SO_4. The mixture was concentrated under

154

reduced pressure. The residue was directly used in the oxidation step to 2-methoxy-1,4-benzoquinone without further purification.

¹H NMR (400 MHz, DMSO-d_6) δ 8.75 (s, 1H), 8.39 (s, 1H), 6.57 (s, 1H), 6.48 (s, 1H), 3.73 (s, 3H).

MP: 83.3°C.[275]

Analytical data are in accordance with the literature.[171]

2-Methoxy-1,4-benzoquinone 373
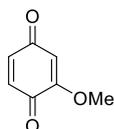
To a suspension of 1,4-dihydroxy-2-methoxybenzene (3.50 g, 25.0 mmol, 1.00 equiv) in a mixture of 40 ml acetonitrile and 20 ml water, TBAB (407 mg, 1.25 mmol, 5.00 mol%) and Oxone® (9.92 g, 15.0 mmol, 0.60 equiv) were added and the reaction mixture was stirred at room temperature. The reaction mixture turned form brown to dark brown and a precipitate was formed. After 45 min, reaction mixture was diluted with 200 mL EtOAc and washed with 100 mL water and 75 mL brine. The combined aqueous phases were extracted with 100 mL EtOAc. Combined organic phases were dried over MgSO₄ and the solvent was removed under reduced pressure. The crude Product was obtained as a yellow solid. After further purification via column chromatography (200 g silica, DCM/MeOH 95:5), the product was obtained as a yellow solid (1.19 g, 35%)

¹H NMR (400 MHz, DMSO-d_6) δ 6.77 (d, J = 2.2 Hz, 1H), 6.74 (d, J = 2.2 Hz, 1H), 6.12 (d, J = 2.2 Hz, 1H), 3.78 (s, 3H).

MP: 136.2°C.

Analytical data are in accordance with the literature.[276,277]

2,3-Dimethyl-1,4-benzoquinone 416
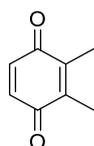
To a suspension of 2,3-dimethyl-1,4-hydroquinone (2.10 g, 15.2 ml, 1.00 equiv) in a mixture of 30 mL acetonitrile and 15 mL water, TBAB (247 mg, 760 μmol, 5.00 mol%) and Oxone® (5.61 g, 9.12 mmol, 0.60 equiv) were added and the reaction mixture was stirred at room temperature. The reaction mixture turned from brown to dark brown and a precipitate was

formed. After 45 min, the reaction mixture was diluted with 100 mL EtOAc and 100 mL water. Combined organic phases were washed with 75 mL water and 75 mL brine. The solvent was removed under reduced pressure. The crude product was recrystallized from hot cyclohexane. The product 2,3-dimethyl-1,4-benzoquinone was obtained as a yellow solid (800 mg, 39%).

¹H NMR (400 MHz, Chloroform-*d*) δ 6.71 (s, 2H), 2.02 (s, 6H).

¹³C NMR (101 MHz, Chloroform-*d*) δ 187.5, 141.4, 136.4, 12.3.

MP: 57.6°C (lit. 55-57°C)

Analytical data are in accordance with the literature.[278]

2-(Pyrrolidino) benzoquinone 426
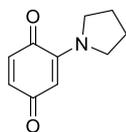
To a solution of *p*-benzoquinone (1.20 g, 11.0 mmol, 1.10 equiv) in 30 mL CHCl₃, a second solution consisting of pyrrolidine (830 µL, 10.0 mmol, 1.00 equiv), KH₂PO₄ (1.36 g, 10.0 mmol, 1.00 equiv) in 15 mL water was added. The reaction mixture was stirred for 16 h at room temperature. After the separation of the two phases, the aqueous phase was extracted with 3 x 30 mL chloroform. The combined organic phases were dried over Na₂SO₄ and the solvent was removed under reduced pressure. The residue was purified via column chromatography (silica, 150 g, CHCl₃ - CHCl3/MeOH 98:2). The product was obtained as a dark violet solid (589 g, 33%)

¹H NMR (200 MHz, Chloroform-*d*) δ 6.57 (dd, *J* = 10, 2.4 Hz, 1H), 6.42 (d, *J* = 10.0 Hz), 5.42 (m, 4H), 1.91 (m, 4H).

HRMS (ESI-MS) m/z calculated [C₁₀H₁₁NO₂]⁺ : [Na]⁺ 200.0682; found: 200.0683.

MP: sublimation before melting according to literature.[234]

Analytical data are in accordance to the literature.[234]

2-Fluorohydroquinone 433
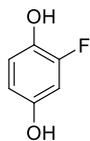
To 2-fluorophenol (5.60 g, 50.0 mmol, 1.00 equiv), dissolved in 6% aqueous NaOH (200 mL), solid potassium persulfate (13.5 g, 50.0 mmol, 1.00 equiv) was added in portions over 10 min to result in a dark solution. This dark solution was stirred overnight at room temperature, then it was concentrated to one third of its original volume under reduced pressure. The solution was cooled to 0°C, neutralized to pH 6.5 with concentrated HCl and extracted once with diethyl ether (100 mL). The aqueous solution was acidified with 50 mL concentrated HCl, refluxed for 1 h, then concentrated to ca. 50 mL under reduced pressure. The addition of 100 mL acetone precipitated the inorganic salts, which were removed by filtration. The solvent was removed under reduced pressure, and the residue was dissolved in acetone and adsorbed on silica gel (10 g). After purification via column chromatography (hexane/ethylacetate 3:1), the product was obtained as an off-white solid (2.00 g, 31%).

^{1}H NMR (200 MHz, DMSO-d_6) δ 9.09 (d, J = 0.9 Hz, 1H), 8.97 (s, 1H), 6.73 (dd, J = 10.3, 8.7 Hz, 1H), 6.51 (dd, J = 12.8, 2.8 Hz, 1H), 6.39 (ddd, J = 8.7, 2.8, 1.3 Hz, 1H).

MP: 122.3°C.

Analytical data are in accordance with the literature.[235]

2-Fluoro-1,4-benzoquinone 434
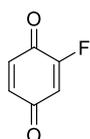
To a suspension of 1,4-dihydroxy-2-fluorobenzene (1.01 g, 7.90 mmol, 1.00 equiv) in 14 mL acetonitrile and 6 mL water, TBAB (129 mg, 395 µmol, 5 mol%) and Oxone® (2.91 g, 4.74 mmol, 0.60 equiv) were added, and the reaction mixture was stirred at room temperature. After 1 h, the reaction mixture was extracted with 50 mL EtOAc and washed with 50 mL water and 50 mL brine. Organic phase was dried over MgSO$_4$. After filtration, the solvent was removed under reduced pressure. The crude product was dissolved in Et$_2$O and filtered through a silica plug. Product was obtained as yellow-green solid (566 mg, 57%).

^{1}H NMR (200 MHz, Chloroform-d) δ 6.75 (m, 2H), 6.74 (m, 1H),

MP: 76.5°C (lit. 77-78°C)[235].

Analytical data are in accordance with the literature.[235]

2-bromo-1,4-benzoquinone 438
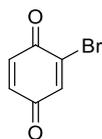
Cerium ammonium nitrate (5,70 g, 10.4 mmol, 1.00 equiv) was dissolved in 60 mL water and 2-bromo-1,4-hydroquinone (1.96 g, 10.4 mmol, 1.00 equiv) was added in portions under stirring. After 1.5 hour stirring at room temperature, reaction mixture was extracted with 3 x 50 mL diethyl ether. The combined organic phases were dried over $MgSO_4$. The filtrate was passed through a silica column (Ø 3 cm x 9 cm) and eluted with Et_2O. After removing the solvent under reduced pressure, the product was obtained as a yellow solid (1.92 g, 99%).

¹H NMR (200 MHz, DMSO-d_6) δ 7.53 (d, J = 2.4 Hz, 1H), 7.08 (d, J = 10.1 Hz, 1H), 6.92 (dd, J = 10.1, 2.4 Hz, 1H).

MP: 53.1°C.

Analytical data are in accordance to the literature.[278]

1,4-Benzoquinone potassium 2-sulfonate 445
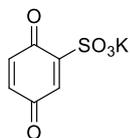
Potassium 1,4-hydroxybenzo-2-sulfonate (2.28 g, 10.0 mmol, 1.00 equiv) was dissolved in 30 mL water and Iodine (127 mg, 500 µmol, 5.00 mol%) and H_2SO_4 (0.5 mL) were added. Then, hydrogen peroxide (890 µL, 11 mmol, 1.10 equiv) was added dropwise via syringe. The reaction mixture was stirred for 4 h at room temperature. The crude product precipitated which was filtered off, washed with water and dried under vacuum. The product was obtained as a yellow solid (581 mg, 26%).

¹H NMR (400 MHz, Deuterium Oxide) δ 7.30 (d, J = 2.3 Hz, 1H), 6.96 (d, J = 2.3 Hz, 1H), 6.94 (s, 1H).

¹³C NMR (101 MHz, Deuterium Oxide) δ 189.1, 184.2, 145.1, 137.3, 136.7, 134.2.

MP: decomposition

2-Methylsulfonyl 1,4-hydroquinone 447
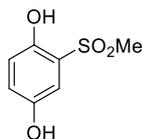
A suspension of Zn (2.80 g, 42.8 mmol, 2.14 equiv) in H_2O (7.2 mL) was cooled to 0°C, and methanesulfonyl chloride (2.20 mL, 28.2 mmol, 1.42 equiv) was added dropwise to the stirred suspension. The mixture was stirred for 30 min with cooling, acidified with 7.2 mL conc. HCl at 0–5°C, stirred for 5 min, and filtered. 1,4-Benzoquinone (2.16 g, 10.0 mmol, 1.00 equiv) was added to the filtrate at the low temperature, and the mixture was stirred for 2 h, while the temperature was allowed to rise to room temperature. The solid residue was filtered off. The reaction mixture was diluted with 10 mL water and extracted with 2 x 30 mL Et_2O. The ethereal phases were dried over Na_2SO_4. After filtration and concentration under reduced pressure, solvent was removed under reduced pressure. The crude product was recrystallized from MeOH/CHCl$_3$. A crystallin solid was obtained at -20°C in a freezer (2.29 g, 61%, corrected yield because of 2% remaining hydroquinone according to ^{1}H-NMR analysis).

^{1}**H-NMR** (200 MHz, DMSO-d_6) δ 10.23 (s, 1H), 9.34 (s, 1H), 7.12 (d, *J* = 2.7 Hz, 1H), 6.90 (d, *J* = 2.7 Hz, 1H), 6.88 (d, *J* = 0.5 Hz, 1H), 3.20 (s, 3H).

MP: 141.6°C (lit. 139-142°C).

Analytical data are in accordance with the literature.[247]

2-Methylsulfonyl benzoquinone 443
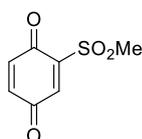
Methyl-(2-hydroquinonyl)-sulfon (76.2 mg, 405 µmol, 1.00 equiv) was dissolved/suspended in 1.6 mL DCM and cooled to -10°C. The flask and the solution were purged with oxygen (balloon) and nitrogen oxide was added via syringe (nitrogen oxide was produced via reaction of copper with nitric acid). The reaction mixture was stirred at -10°C overnight. The solvent was removed under reduced pressure. The product was obtained as an orange solid (26%).

^{1}**H-NMR** (400 MHz, DMSO-d_6) δ 7.23 (d, *J* = 2.1 Hz, 1H), 7.04 (d, *J* = 2.1 Hz, 1H), 7.03 (s, 1H), 3.29 (s, 3H).

^{13}**C-NMR** (101 MHz, DMSO-d_6) δ 186.60, 182.64, 144.12, 137.70, 137.52, 137.14, 43.15.

The use of MeOH as solvent in ESI-MS led to the detection of the methoxylated hydroquinone due to addition:
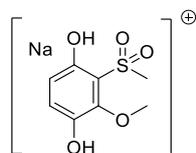
HRMS (ESI-MS) m/z calculated [$C_8H_{10}O_5S$]$^+$: [Na]$^+$ 441.0142; found: 241.014.

2,2-Dimethyl-1,3-benzodioxole-5-carboxaldehyde 407
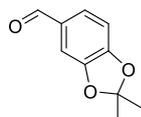
A mixture of 3,4-dihydroxybenzaldehyde (13.8 g, 100 mmol, 1.00 equiv), P_2O_5 (2.80 g, 20.0 mmol, 0.20 equiv) and 50 mL toluene was heated to 75°C. To this suspension, 15 mL acetone over 3 h was added dropwise. After the addition was started, four portions of P_2O_5 (2.80 g, 20 mmol, 0.20 equiv) were added to the reaction mixture every 30 min. (total amount 100 mmol). After the addition of acetone, the reaction mixture was heated for further 1 h. After removing the oily compound (lower layer), 15 mL 25% NaOH solution was added. The organic layer was separated, washed with water and concentrated under reduced pressure. After purification via column chromatography (silica 175 g, cyclohexane/EtOAc 9:1), a colourless oil was obtained (1.97 g, 11%).

^{1}H NMR (400 MHz, Chloroform-*d*) δ 9.71 (s, 1H), 7.29 (dd, *J* = 7.9, 1.4 Hz, 1H), 7.18 (d, *J* = 1.3 Hz, 1H), 6.76 (d, *J* = 7.9 Hz, 1H), 1.64 (s, 6H).

^{13}C NMR (101 MHz, Chloroform-*d*) δ 190.4, 153.0, 148.5, 131.4, 128.4, 119.8, 108.2, 106.7, 25.9.

Analytical data are in accordance with the literature.[226]

2,2-Dimethyl-1,3-phthalazinodioxol 408
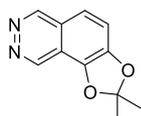
First, *n*-Butyllithium (7.80 ml, 11.8 mmol, 1.6 M in hexane, 1.07 equiv) was added drop-wise to a stirred solution of *N,N,N*-trimethyldiamine (1.47 mL, 11.0 mmol, 1.00 equiv) in a mixture of 18.3 mL hexane and 4.8 mL THF at -20°C. After stirring the reaction mixture at -25°C for 30 min., aldehyde was added in portions and the reaction mixture was stirred for 45 min. Then, *n*-BuLi (16.5 mL, 16.5 mmol, 1.60 M in hexane, 1.50 equiv) was added dropwise at -20 °C. The

reaction mixture was warmed to 0°C (ice bath). After 2.5 h, the reaction mixture was cooled to -78°C. THF (9.12 mL) and DMF (2.60 ml, 33.0 mmol, 3.00 equiv) were added, and the mixture was stirred at –78 °C for further 20 min. and then allowed to warm to 0°C. After 1.5 h, the reaction was quenched with a solution of NH_4Cl (1.76 g, 27.0 mmol, 3.00 equiv) and $N_2H_4 \cdot H_2O$ (1.30 ml, 22.0 mmol, 80% in H_2O, 2.00 equiv) in 9 mL H_2O. The reaction mixture was allowed to warm to rt and stirred for 14 h. The reaction mixture was extracted with DCM (3 × 40 ml). Combined organic phases were dried over Na_2SO_4. After filtration and concentration under reduced pressure, the residue was further purified via column chromatography (75 g, cyclohexane/acetone 1:1). The Crude product was recrystallized from toluene. The product and was obtained as beige solid (1.43 g, 64%).

^{1}H-NMR (400 MHz, Chloroform-d) δ 9.49 (s, 1H), 9.32 (d, J = 1.6 Hz, 1H), 7.50 (d, J = 8.4 Hz, 1H), 7.43 (d, J = 8.4 Hz, 1H), 1.83 (s, 6H).

^{13}C-NMR (101 MHz, Chloroform-d) δ 150.6, 149.0, 144.9, 140.6, 121.9, 121.3, 120.6, 115.9, 112.2, 26.1

HRMS (ESI-MS) m/z calculated $[C_{11}H_{10}N_2O_2]^+$: $[H]^+$ 203.0815.0408; found: 203.814.

MP: 162.3°C.

EA: (%) for $C_{11}H_{10}N_2O_2$: calcd C, 65.34; H, 4.98; N, 13.85; found C 65.14; H, 4.97; N, 13.96.

5,6-Dihydroxyphthalazine 308
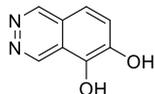
Phthalazine acetonide (101 mg, 500 µmol, 1.00 equiv) was dissolved in 1 mL EtOH, and 12 drops of concentrated HCl were added. Then, the reaction mixture was heated to reflux and the reaction progress was observed via TLC. After the consumption of the starting material detected via TLC (3 h), volatile compounds were removed under reduced pressure. After washing with $CHCl_3$, the pure product was obtained as colourless solid (53 mg, 62%).

^{1}H NMR (400 MHz, DMSO-d_6) δ 9.97 (s, 1H), 9.91 (s, 1H), 8.04 – 7.93 (m, 2H).

^{13}C NMR (101 MHz, DMSO-d_6) δ 153.1, 149.3, 147.7, 141.6, 127.3, 122.9, 120.5, 118.9.

HRMS (ESI-MS) m/z calculated $[C_8H_6N_2O_2]^+$: $[H]^+$ 163.0502; found: 163.0502.

EA: (%) for $C_8H_6N_2O_2$: calcd C, 59.26; H, 3.73; N, 17.28; found C, 44.02; H, 3.07; N, 11.68.

1,2,4,5-Tetrazine 79

Cold hydrazine hydrate (100 mL, 2.00 mol, 2.78 equiv) was added for 10 min at 0°C and with stirring to solid formamidinium acetate (77.9 g, 726 mmol, 1.00 equiv) in a 1 L flask. The initially formed clear solution solidified after stirring for 8 min and it was left for 1 h at room temperature. Then 50 mL ice water was added, and the mixture was stirred for 1 h in an ice bath. The solid was filtered via a Buchner funnel with suction and was made as dry as possible by pressing. The solid was dissolved in 250 mL of cold glacial acetic acid and $NaNO_2$ (25.8 g, 374 mmol, 0.51 equiv) was added in small portions for 2 h at 0°C (ice bath cooling) under stirring. After additional 1.5 h of stirring, the mixture was pre-cooled to -18°C (necessary for high yield), and 375 mL of ice water were added at once. The solution was extracted with 2 x 5 × 200 mL (2 x 1 L separatory funnels were used at the same time) of cold CH_2Cl_2. The combined organic phases were washed with 830 mL of saturated $NaHCO_3$ solution and with 664 mL water, and then dried overnight over $CaCl_2$ in a refrigerator. The red-violet solution was gently evaporated to a volume of 30-40 mL by distillation of the solvent from a 500 mL flask through a 30 cm Vigreux column. The residual liquid was transferred into a Schlenk tube. The remaining solvent was evaporated under reduced pressure (-40°C, 0.2 mbar) and the residual solid was sublimed at room temperature and 1.0 Torr directly on a cooling finger (-40°C, acetone/liquid N_2). The product was obtained as a deep red, very volatile solid (3.50 g, 12%, storable at -20°C).

¹H NMR (200 MHz, Chloroform-*d*) δ 10.40 (s, 1H).

MP: Compound evaporated at room temperature.

Analytical data are in accordance with the literature.[223]

5,8-Dihydroxy-2,3-phthalazin 410
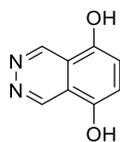
A dried Schlenk tube equipped with stirring bar was charged with catalyst pyridazine complex (42.6 mg, 150 µmol, 5.00 mol%), benzoquinone (360 mg, 3.00 mol, 1.00 equiv) and tetrazine (948 mg, 11.5 mmol, 3.50 equiv) under nitrogen. Then, 23 mL benzotrifluoride was added. The reaction mixture was heated under stirring to 55°C, then sealed from N_2, and heated at 110°C overnight. After cooling down to room temperature, the solvent and the excess tetrazine were removed in vacuum via a cooling trap. The solid residue was dissolved/suspended in

DCM/MeOH 1:1 mixture and adsorbed on silica. After purification via column chromatography (150 g silica, DCM/MeOH 8:2), product was obtained as a dark green solid (505 mg, 94%).

¹H-NMR (400 MHz, DMSO-*d₆*) δ 10.27 (s, 2H), 9.57 (s, 2H), 7.16 (s, 2H).

¹³C-NMR (101 MHz, DMSO-*d₆*) δ 145.4, 144.9, 116.4, 116.3.

HRMS (ESI-MS) m/z calculated $[C_8H_6N_2O_2]^+$: $[H]^+$ 163.0502; found: 163.0502.

EA: (%) for $C_8H_6N_2O_2$: calcd C,59.26; H, 3.73; N, 17.28; found C 58.58; H, 3.31; N, 17.47.

IR (*v*/cm⁻¹): 2922(w), 2826(w), 2655(w), 1561(m), 1503(m), 1354(s), 1315(s), 1302 (s), 1238, 1106(s), 942(m), 884(m), 810(s), 746(s), 586(m).

MP: > 300°C

Analytical data are in accordance with the literature.[172]

5,8-Dihydroxy-6,7-dimethyl-2,3-phthalazin 417
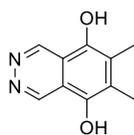
A dried Schlenk tube equipped with stirring bar was charged with catalyst pyridazine complex (14.2 mg, 50.0 μmol, 5.00 mol%), fresh recrystallized (from cyclohexane) 2,3-dimethylbenzoquinone (136 mg, 1.00 mol, 1.00 equiv) and tetrazine (287 mg, 3.5 mmol, 3.50 equiv) under nitrogen. Then, 6 mL benzotrifluoride was added. The reaction mixture was heated under stirring to 55°C, then sealed from N₂, and heated at 110°C overnight. After cooling down to room temperature, the solvent and the excess tetrazine were removed in vacuum via a cooling trap. The solid residue was dried in high vacuum and then dissolved in MeOH/DCM and adsorbed on silica for chromatography. After purification via column chromatography (75 g silica, DCM/MeOH 8:2), product was obtained as a yellow-brown solid (168 mg, 88%).

¹H-NMR (400 MHz, DMSO-*d₆*) δ 9.62 (s, 2H), 9.33 (s, 2H), 2.33 (s, 6H).

¹³C-NMR (101 MHz, DMSO-*d₆*) δ 146.0, 142.9, 129.5, 116.1, 13.9.

HRMS (ESI-MS) m/z calculated $[C_{10}H_{10}N_2O_2]^+$: $[H]^+$ 191.0815; found: 191.0818.

EA: (%) for $C_{10}H_{10}N_2O_2$: calcd C, 63.15; H, 5.30; N, 14.73; found C 61.58; H, 5.02; N, 15.49.

MP: > 300°C

Analytical data are in accordance with the literature.[172]

6-Chloro-5,8-dihydroxy-2,3-phthalazine 431
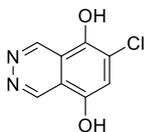
A dried Schlenk tube equipped with stirring bar was charged with catalyst pyridazine complex (20.0 mg, 70.0 µmol, 10.0 mol%), 2-chloro-1,4-benzoquinone (88.0 mg, 700 µmol, 1.00 equiv) and tetrazine (230 mg, 2.80 mmol, 4.00 equiv) under nitrogen. Then, 7 mL benzotrifluoride was added. The reaction mixture was heated under stirring to 55°C, then sealed from N_2 and heated at 110°C overnight. After cooling to room temperature, the solvent and the excess tetrazine were removed in vacuum via a cooling trap. The solid residue was adsorbed on silica (solvent DCM/MeOH 1:1) and purified via column chromatography (53 g silica, DCM/MeOH 8:2 - 6:4). 6-chloro-5,8-dihydroxyphthalazine was obtained as a dark red solid (43.0 mg, 31%).

¹H NMR (400 MHz, DMSO-d_6) δ 10.89 (s, 1H), 10.28 (s, 1H), 9.71 (d, J = 1.5 Hz, 1H), 9.59 (d, J = 1.5 Hz, 1H), 7.22 (s, 1H).

¹³C NMR (101 MHz, DMSO-d_6) δ 146.8, 145.6, 144.3, 140.6, 122.4, 118.4, 116.6, 116.0.

HRMS (ESI-MS) m/z calculated [$C_8H_5ClN_2O_2$]⁺ : [H]⁺ 197.0113; found: 197.0117.

EA: (%) for $C_8H_5N_2O_2Cl$: calcd C,48.88; H, 2.56; N, 18.03; found C 44.45; H, 2.56; N, 13.11.

MP: > 300°C

5,8-Dihydroxy-6-methoxy-2,3-phthalazine 414
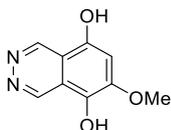
A dried Schlenk tube equipped with stirring bar was charged with catalyst pyridazine complex (21.3 mg, 75.0 µmol, 10.0 mol%), 2-methoxy-1,4-benzoquinone (105 mg, 750 µmol, 1.00 equiv) and tetrazine (308 mg, 3.75 mmol, 5.00 equiv) under nitrogen. Then, 6 mL benzotrifluoride was added. The reaction mixture was heated under stirring to 55°C, then sealed from N_2 and heated at 110°C overnight. After cooling down to room temperature, the solvent and the excess tetrazine were removed in vacuum via a cooling trap. The solid residue was dissolved/suspended in DCM/MeOH 1:1 and adsorbed on silica. After purification via column chromatography (silica, 75 g DCM/MeOH 8:2 – 7:3), product was obtained as solid. After further recrystallization/heating from CHCl₃/MeOH (9:1) pure product was obtained as a brown-yellow solid (33.0 mg, 23%).

¹H NMR (400 MHz, DMSO-d_6) δ 10.61 (s, 1H), 9.53 (d, J = 1.4 Hz, 1H), 9.41 (d, J = 1.4 Hz, 1H), 9.36 (s, 1H), 7.14 (s, 1H), 3.92 (s, 3H).

¹³C NMR (101 MHz, DMSO-d_6) δ 149.0, 147.3, 145.5, 145.03,132.01, 116.8, 110.5, 103.9, 56.3.

HRMS (ESI-MS) m/z calculated for $[C_9H_8N_2O_2]^+$: $[H]^+$ 163.0502 ; found: 163.0503.

MP: > 300°C

Analytical data are in accordance with the literature.[172]

5,8-Dihydroxy-6-fluoro-2,3-phthalazine 435
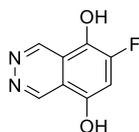
A dried Schlenk tube equipped with stirring bar was charged with catalyst pyridazine complex (20.0 mg, 70.0 µmol, 10.0 mol%), 2-fluoro-1,4-benzoquinone (88.0 mg, 700 µmol, 1.00 equiv) and tetrazine (230 mg, 2.80 mmol, 4.00 equiv) under nitrogen. Then, 7 mL benzotrifluoride was added. Reaction mixture was heated under stirring to 55°C, then sealed (from N2), and heated at 110°C overnight. After cooling down to room temperature and settlement of all solid residues, the solvent and the excess tetrazine were removed via filtration. The solid residue was dissolved/suspended in DCM/MeOH and adsorbed on silica. After purification via column chromatography (DCM/MeOH 8:2), crude product was obtained as a dark purple solid (33.0 mg, 26%).

¹H NMR (400 MHz, DMSO-d_6) δ 9.68 (d, J = 1.4 Hz, 1H), 9.54 (d, J = 1.4 Hz, 1H), 7.15 (d, J = 12.7 Hz, 1H), 6.6-7.4 (m, unidentified impurity).

¹³C NMR (101 MHz, DMSO-d6) δ 145.6, 135.2.*

*The C-F coupling decreased the intensity of the signals of the ¹³C-shifts, which were mainly on the level of the background noise. Therefore, a distinct assignment of signals to ¹³C-shifts was impossible.

HRMS (ESI-MS) m/z calculated $[C_8H_5FN_2O_2]^+$: $[H]^+$ 180.0408; found: 181.0406.

6-Bromo-5,8-dihydroxy-2,3-phthalazine 439
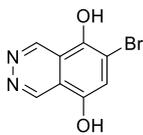
A dried Schlenk tube equipped with stirring bar was charged with catalyst pyridazine complex (42.6 mg, 150 µmol, 10.0 mol%), 2-bromo-1,4-benzoquinone (280 mg, 1.50 mmol, 1.00 equiv) and tetrazine (492 mg, 6.00 mmol, 4.00 equiv) under nitrogen. Then, 10 mL benzotrifluoride was added. Reaction mixture was heated under stirring to 55°C, then sealed from N_2, and heated at 110°C overnight (17 h). After cooling to room temperature, the solvent and the excess tetrazine were removed in vacuum via liquid nitrogen filled cooling trap and high vacuum. The reaction mixture was dissolved/suspended in DCM/MeOH and adsorbed on silica. After purification via column chromatography (silica 125 g, DCM/MeOH 8:2), product was obtained as a dark red solid (158 mg, 44%).

¹H NMR (400 MHz, DMSO-d6) δ 10.88 (s, 1H), 10.22 (s, 1H), 9.72 (d, J = 1.4 Hz, 1H), 9.59 (d, J = 1.4 Hz, 1H), 9.42 (m, unidentified impurity), 7.69 (m, unidentified impurity) 7.41 (s, 1H).

¹³C NMR (101 MHz, DMSO-d6) δ 146.0, 145.9, 119.9, 119.8, 116.8, 113.6.

HRMS (ESI-MS) m/z calculated for $[C_8H_5BrN_2O_2]^+$: $[H]^+$ 240.9607 ; found: 240.9609.

Phthalazine-5,8-dione 409
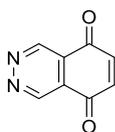
In a 5 mL flask equipped with a stirring bar, 5,8-dihydroxyphthalazine (40.5 mg, 250 µmol, 1.00 equiv) was suspended in 3 mL water. Then, sodium periodate (56.1 mg, 263 µmol, 1.05 equiv) was added. The reaction mixture was stirred for 1 h at room temperature. Then, the reaction mixture was concentrated under reduced pressure. The residues were thoroughly extracted/suspended with DCM and filtered through a cotton pad in a Pasteur pipette. Then, volatile compounds were removed under reduced pressure. The product was obtained as dark orange solid (16 mg, 40%).

¹H NMR (400 MHz, DMSO-d6) δ 9.73 (s, 2H), 7.23 (s, 2H).

¹³C NMR (101 MHz, DMSO-d6) δ 184.7, 145.9, 138.3, 124.4.

HRMS (ESI-MS) m/z calculated for $[C_8H_4N_2O_2]^+$: $[H]^+$ 183.0165 ; found: 183.0166.

IR (v/cm^{-1}): 3038(w), 2923(w), 1669(s, C=O), 1596(m), 1312(s), 1164(m), 1057(m), 961(s), 862(s), 571(s).

Analytical data are in accordance with the literature.[173]

6-*iso*-Propyl-thio-5,8-dihydroxyphthalazine 450
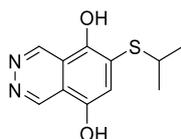
In a 10 mL flask equipped with a stirring bar, 5,8-diazanaphthoquinone (64.1 mg, 400 µmol, 1.00 equiv) was suspended in water and propane-2-thiol was added. The reaction mixture was stirred for 1 h at room temperature. Then, volatile compounds were removed under reduced pressure. The product was obtained as dark violet solid (80.1 mg, 85%).

¹H NMR (400 MHz, DMSO-d6) δ 10.36 (s, 1H), 9.75 (s, 2H), 9.66 (s, 1H), 7.25 (s, 1H), 3.72 (p, *J* = 6.6 Hz, 1H), 1.26 (d, J = 6.7 Hz, 6H).

¹³C NMR (101 MHz, DMSO-d6) δ 147.8, 146.2, 146.1, 145.7, 127.4, 117.3, 117.1, 117.1, 23.1.

IR (v/cm^{-1}): 3050(w), 2962(m), 2924(w), 2862(w), 2653(w), 1564(w), 1377(s), 1317(s), 1295(s), 1234(m), 1190(m), 1106(s), 1051(w), 950(s), 929(m), 852(m), 809(m), 748(s), 669(m), 588(m).

Oxidation of 6-*iso*-Propyl-thio-5,8-dihydroxyphthalazine with hydrogen peroxide 451

In a 5 mL vial, 6-(*iso*-propylthio)-5,8-dihydroxyphthalazine (94.5 mg, 400 µmol, 1.00 equiv) was suspended in a mixture of hydrogen peroxide (100 µL, 1.2 mmol, 3 00 equiv, 70% in water) and 200 µL water. The reaction mixture was heated at 75°C for 3 h. Then, the reaction mixture was diluted with water and the solid residues were allowed to settle at the bottom of the vial. Overstanding liquid was decanted. Volatile compounds were evaporated via air stream of the fume hood. A brown solid was obtained (47 mg).

¹H NMR (400 MHz, DMSO-d6) δ 10.41 (s, 1H), 9.75 (s, 2H), 9.62 (s, 1H), 7.22 (s, 1H), 3.83 (m, 1H), 1.38 (d, *J* = 7.0 Hz, 3H), 1.31 (d, *J* = 7.0 Hz, 3H).

¹³C NMR (101 MHz, DMSO-d6) δ 146.3, 146.2, 146.1, 145.3, 120.3, 120.3, 117.9, 117.1, 54.83, 17.1, 14.3.

IR (v/cm⁻¹): 2928(m), 2857(m), 2664(m), 2361(m), 1367(s), 1295(s), 1242(s), 995(s), 928(s), 799(s), 750(s), 663(s), 503(s).

Oxidation of 6-*iso*-Propyl-thio-5,8-dihydroxyphthalazine with Oxone® 452

In a 5 mL vial, 6-(*iso*-propylthio)-5,8-dihydroxyphthalazine (47.3 mg, 200 µmol, 1.00 equiv) was suspended in a mixture of Oxone® (369 mg, 600 µmol, 3.00 equiv) and 1 mL water. The reaction mixture was heated at 85°C for 1 h. Then, the reaction mixture was diluted with water and the solid residues were allowed to settle at the bottom of the vial. Overstanding liquid was decanted. Volatile compounds were evaporated via air stream of the fume hood. A brown solid was obtained (151 mg, product and potassium sulfate salts).

¹H NMR (400 MHz, DMSO-d6) δ 9.95 (s, 1H), 7.64 (s, 1H), 2.58 (m, 1H), 1.10 (d, J = 7.0 Hz, 6H).

¹³C NMR (101 MHz, DMSO-d6) δ 148.3, 147.3, 116.4, 117.1, 49.51, 18.0.

IR (*v*/cm⁻¹): 3436(w), 1138(s), 1026(s), 1000(s), 873(s), 782(s), 567(s).

7. References

(1) Poliakoff, M.; Licence, P.; *Nature* **2007**, *450*, 810.

(2) Garcia Martinez, J.; *Chem. Int.* **2016**, *38.*

(3) Kessler, S. N.; Wegner, H. A.; *Org. Lett.* **2010**, *12*, 4062–4065.

(4) Kessler, S. N.; Neuburger, M.; Wegner, H. A.; *Eur. J. Org. Chem.* **2011**, *2011*, 3238–3245.

(5) Kessler, S. N.; Neuburger, M.; Wegner, H. A.; *J. Am. Chem. Soc.* **2012**, *134*, 17885–17888.

(6) Schweighauser, L.; Bodoky, I.; Kessler, S. N.; Häussinger, D.; Donsbach, C.; Wegner, H. A.; *Org. Lett.* **2016**, *18*, 1330–1333.

(7) Ahles, S.; Götz, S.; Schweighauser, L.; Brodsky, M.; Kessler, S. N.; Heindl, A. H.; Wegner, H. A.; *Org. Lett.* **2018**, *20*, 7034–7038.

(8) Ahles, S.; Ruhl, J.; Strauss, M. A.; Wegner, H. A.; *Org. Lett.* **2019**, *21*, 3927–3930.

(9) Hong, L.; Ahles, S.; Strauss, M. A.; Logemann, C.; Wegner, H. A.; *Org. Chem. Front.* **2017**, *4*, 871–875.

(10) Winsberg, J.; Hagemann, T.; Janoschka, T.; Hager, M. D.; Schubert, U. S.; *Angew. Chem. Int. Ed.* **2017**, *56*, 686–711.

(11) Zhang, X.; Yang, L.; Li, Y.; Li, H.; Wang, W.; Ye, B.; *Environ. Model. Assess.* **2012**, *184*, 2261–2273.

(12) Leung, P. K.; Ponce-de-León, C.; Low, C.; Walsh, F. C.; *Electrochim. Acta* **2011**, *56*, 6536–6546.

(13) Fache, M.; Boutevin, B.; Caillol, S.; *ACS Sustain. Chem. Eng.* **2016**, *4*, 35–46.

(14) Bodoky, I.; Wegner, H. A. Structural Diversity by Lewis acid Catalyzed Domino-type Inverse Electron Demand Diels-Alder reactions: Master Thesis, University of Basel, Basel, **2012**.

(15) Albrecht, W.; *Justus Liebigs Ann. Chem.* **1906**, *348*, 31–49.

(16) v. Euler, H.; Josephson, K. O.; *Ber. dtsch. Chem. Ges. A/B* **1920**, *53*, 822–826.

(17) Diels, O.; Alder, K.; *Justus Liebigs Ann. Chem.* **1928**, *460*, 98–122.

(18) Nobel Price Commitee. Otto Diels – Facts. NobelPrize.org. <https://www.nobelprize.org/prizes/chemistry/1950/diels/facts/> (22.05.2020)) (accessed May 22, 2020).

(19) Houk, K. N.; Gonzalez, J.; Li, Y.; *Acc. Chem. Res.* **1995**, *28*, 81–90.

(20) Wassermann, A.; *J. Chem. Soc.* **1935**, 828.

(21) Fukui, K.; Yonezawa, T.; Shingu, H.; *J. Chem. Phys.* **1952**, *20*, 722–725.

(22) Woodward, R. B.; Hoffmann, R.; *Angew. Chem. Int. Ed. Engl.* **1969**, *8*, 781–853.

(23) Hoffmann, R.; Woodward, R. B.; *J. Am. Chem. Soc.* **1965**, *87*, 4389–4390.

(24) Houk, K. N.; *Acc. Chem. Res.* **1975**, *8*, 361–369.

(25) Sauer, J.; Sustmann, R.; *Angew. Chem. Int. Ed. Engl.* **1980**, *19*, 779–807.

(26) Houk, K. N.; *J. Am. Chem. Soc.* **1973**, *95*, 4092–4094.

(27) Sauer, J.; Wiest, H.; *Angew. Chem.* **1962**, *74*, 353.

(28) Alder, K.; *Justus Liebigs Ann. Chem.* **1951**, *571*, 157–166.

(29) Sauer, J.; *Angew. Chem. Int. Ed. Engl.* **1966**, *5*, 211–230.

(30) Alder, K.; Stein, G.; *Justus Liebigs Ann. Chem.* **1934**, *514*, 211–227.

(31) Wannere, C. S.; Paul, A.; Herges, R.; Houk, K. N.; Schaefer, H. F.; Ragué Schleyer, P. von; *J. Comput. Chem.* **2007**, *28*, 344–361.

(32) Berson, J. A.; Hamlet, Z.; Mueller, W. A.; *J. Am. Chem. Soc.* **1962**, *84*, 297–304.

(33) Woodward, R. B.; Sondheimer, F.; Taub, D.; Heusler, K.; McLamore, W. M.; *J. Am. Chem. Soc.* **1952**, *74*, 4223–4251.

(34) Funel, J.-A.; Abele, S.; *Angew. Chem. Int. Ed.* **2013**, *52*, 3822–3863.

(35) Wilhelm, M.; Schmidt, P.; *Helv. Chim. Acta* **1969**, *52*, 1385–1395.

(36) Wilhelm, M.; Schmidt, P.; Eichenberger, K., CH448069, **1968**.

(37) Ikeda, N.; Sugishima, N.; Fujii, Y.; Ikuta, S.; Nakanishi, Y.; Nippon Shokubai Kagaku Kogyo Co., Ltd., US4840749, **1987**.

(38) Weissermel, K.; Arpe, H. J. *Industrial Organic Chemistry 3rd ed.*; WILEY-VCH Verlag: Weinheim, **1997**.

(39) Szmant, H. *Organic Building Blocks of the Chemical Industry*; Wiley: New York, **1989**.

(40) Schenk, N.; Krekel, J.; Losacker, P.; Swdenk, W., DE2532398A1, **1977**.

(41) Diels, O.; Alder, K.; *Ber. dtsch. Chem. Ges. A/B* **1929**, *62*, 2337–2372.

(42) Rüttimann, A.; Lorenz, P.; *Helv. Chim. Acta* **1990**, *73*, 790–796.

(43) Diels, O.; Blom, J. H.; Koll, W.; *Justus Liebigs Ann. Chem.* **1925**, *443*, 242–262.

(44) Jørgensen, K. A.; *Angew. Chem.* **2000**, *39*, 3558–3588.

(45) Needleman, S. B.; Chang Kuo, M. C.; *Chem. Rev.* **1962**, *62*, 405–431.

(46) Arbuzov, Y. A.; *Russ. Chem. Rev.* **1964**, *33*, 407–424.

(47) McCarrick, M. A.; Wu, Y. D.; Houk, K. N.; *J. Org. Chem.* **1993**, *58*, 3330–3343.

(48) Günther; Schenck, O.; Ziegler, K.; *Naturwissenschaften* **1944**, *32*, 157.

(49) Esser, P.; Pohlmann, B.; Scharf, H.-D.; *Angew. Chem. Int. Ed. Engl.* **1994**, *33*, 2009–2023.

(50) Watkins, H.; Liu, O. C.; Krivda, J. A., US5219836A, **1993**.

(51) Newman, C. P.; Aggarwal, V. K.; Quest international, EP854143A1, **1998**.

(52) Scognamiglio, J.; Jones, L.; Letizia, C. S.; Api, A. M.; *Food Chem. Toxicol.* **2012**, *50*, S224-S239.

(53) Fischesser, J.; Fritsch, H.; Gum, A. G.; Krage, R.; Keuper, R. D., WO2005049618A1, **2005**.

(54) Griffiths, G. J.; Previdoli, F. E.; *J. Org. Chem.* **1993**, *58*, 6129–6131.

(55) Sullivan, B.; Carrera, I.; Drouin, M.; Hudlicky, T.; *Angew. Chem. Int. Ed.* **2009**, *48*, 4229–4231.

(56) Legentil, L.; Bastide, J.; Delfourne, E.; *Tetrahedron Lett.* **2003**, *44*, 2473–2475.

(57) Schwartz, M. M., WO2001070760A1, **2001**.

(58) Kubodera, N.; Miyamoto, K.; Watanabe, H.; Kato, M.; Sasahara, K.; Ochi, K.; *J. Org. Chem.* **1992**, *57*, 5019–5020.

(59) Jacobi, P. A.; Blum, C. A.; DeSimone, R. W.; Udodong, U. E. S.; *J. Am. Chem. Soc.* **1991**, *113*, 5384–5392.

(60) Bachmann, W. E.; Deno, N. C.; *J. Am. Chem. Soc.* **1949**, *71*, 3062–3072.

(61) Carboni, R. A.; Lindsey, R. V.; *J. Am. Chem. Soc.* **1959**, *81*, 4342–4346.

(62) Boger, D. L.; Robarge, K. D.; *J. Org. Chem.* **1988**, *53*, 5793–5796.

(63) Boger, D. L.; Mullican, M. D.; *J. Org. Chem.* **1984**, *49*, 4045–4050.

(64) Boger, D. L.; Mullican, M. D.; *J. Org. Chem.* **1984**, *49*, 4045–4050.

(65) Sauer, J.; Heldmann, D. K.; Hetzenegger, J.; Krauthan, J.; Sichert, H.; Schuster, J.; *Eur. J. Org. Chem.* **1998**, *1998*, 2885–2896.

(66) Boger, D. L.; Schaum, R. P.; Garbaccio, R. M.; *J. Org. Chem.* **1998**, *63*, 6329–6337.

(67) Soenen, D. R.; Zimpleman, J. M.; Boger, D. L.; *J. Org. Chem.* **2003**, *68*, 3593–3598.

(68) Oliveira, B. L.; Guo, Z.; Bernardes, G. J. L.; *Chem. Soc. Rev.* **2017**, *46*, 4895–4950.

(69) Balcar, J.; Chrisam, G.; Huber, F. X.; Sauer, J.; *Tetrahedron Lett.* **1983**, *24*, 1481–1484.

(70) Müller, K.; Sauer, J.; *Tetrahedron Lett.* **1984**, *25*, 2541–2544.

(71) Kamber, D. N.; Liang, Y.; Blizzard, R. J.; Liu, F.; Mehl, R. A.; Houk, K. N.; Prescher, J. A.; *J. Am. Chem. Soc.* **2015**, *137*, 8388–8391.

(72) Gruseck, U.; Heuschmann, M.; *Tetrahedron Lett.* **1987**, *28*, 6027–6030.

(73) Horner, K. A.; Valette, N. M.; Webb, M. E.; *Chemistry (Weinheim an der Bergstrasse, Germany)* **2015**, *21*, 14376–14381.

(74) Oishi, E.; Taido, N.; Iwamoto, K.; Miyashita, A.; Higashino, T.; *Chem. Pharm. Bull.* **1990**, *38*, 3268–3272.

(75) Glinkerman, C. M.; Boger, D. L.; *J. Am. Chem. Soc.* **2016**, *138*, 12408–12413.

(76) Ishikawa, H.; Elliott, G. I.; Velcicky, J.; Choi, Y.; Boger, D. L.; *J. Am. Chem. Soc.* **2006**, *128*, 10596–10612.

(77) Plass, T.; Milles, S.; Koehler, C.; Szymański, J.; Mueller, R.; Wiessler, M.; Schultz, C.; Lemke, E. A.; *Angew. Chem. Int. Ed.* **2012**, *51*, 4166–4170.

(78) Uttamapinant, C.; Howe, J. D.; Lang, K.; Beránek, V.; Davis, L.; Mahesh, M.; Barry, N. P.; Chin, J. W.; *J. Am. Chem. Soc.* **2015**, *137*, 4602–4605.

(79) Lewis, G. N. *Valence and the Structure of Atoms and Molecules*; Chemical Catalog Company: New York, New York, U.S.A, **1923**.

(80) Yamamoto, H. *Lewis acids in organic synthesis*; Wiley-VCH: Weinheim, New York, **2000**.

(81) Yates, P.; Eaton, P.; *J. Am. Chem. Soc.* **1960**, *82*, 4436–4437.

(82) Allen, C. F. H.; Ryan, R. W.; van Allan, J. A.; *J. Org. Chem.* **1962**, *27*, 778–779.

(83) Corey, E. J.; Weinshenker, N. M.; Schaaf, T. K.; Huber, W.; *J. Am. Chem. Soc.* **1969**, *91*, 5675–5677.

(84) Kishi, Y.; Nakatsubo, F.; Aratani, M.; Goto, T.; Inoue, S.; Kakoi, H.; Sugiura, S.; *Tetrahedron Lett.* **1970**, *11*, 5127–5128.

(85) Kishi, Y.; Fukuyama, T.; Aratani, M.; Nakatsubo, F.; Goto, T.; *J. Am. Chem. Soc.* **1972**, *94*, 9219–9221.

(86) Corey, E. J.; Imwinkelried, R.; Pikul, S.; Xiang, Y. B.; *J. Am. Chem. Soc.* **1989**, *111*, 5493–5495.

(87) Gatzenmeier, T.; van Gemmeren, M.; Xie, Y.; Höfler, D.; Leutzsch, M.; List, B.; *Science* **2016**, *351*, 949–952.

(88) Cookson, R. C.; Tuddenham, R. M.; *J. Chem. Soc. D* **1973**, 742.

(89) Li, P.; Yamamoto, H.; *J. Am. Chem. Soc.* **2009**, *131*, 16628–16629.

(90) Abraham, C. J.; Paull, D. H.; Scerba, M. T.; Grebinski, J. W.; Lectka, T.; *J. Am. Chem. Soc.* **2006**, *128*, 13370–13371.

(91) Türkmen, Y. E.; Montavon, T. J.; Kozmin, S. A.; Rawal, V. H.; *J. Am. Chem. Soc.* **2012**, *134*, 9062–9065.

(92) Xue, J.; Gao, E.; Wang, X.-N.; Chang, J.; *Org. Lett.* **2018**, *20*, 6055–6058.

(93) Maruoka, K.; *Catal. Today* **2001**, *66*, 33–45.

(94) Shriver, D. F.; Biallas, M. J.; *J. Am. Chem. Soc.* **1967**, *89*, 1078–1081.

(95) Beauchamp, A. L.; Olivier, M. J.; Wuest, J. D.; Zacharie, B.; *J. Am. Chem. Soc.* **1986**, *108*, 73–77.

(96) Beauchamp, A. L.; Olivier, M. J.; Wuest, J. D.; Zacharie, B.; *Organometallics* **1987**, *6*, 153–156.

(97) Wuest, J. D.; *Acc. Chem. Res.* **1999**, *32*, 81–89.

(98) Reilly, M.; Oh, T.; *Tetrahedron Lett.* **1994**, *35*, 7209–7212.

(99) Kwabi, D. G.; Ji, Y.; Aziz, M. J.; *Chem. Rev.* **2020**, *120*, 6467–6489.

(100) Kangro, W., DE1006479, **1957**.

(101) Kangro, W., DE914264, **1949**.

(102) Kangro, W.; Pieper, H.; *Electrochim. Acta* **1962**, *7*, 435–448.

(103) Hagedorn, N., NASA-TM_83677, **1976**.

(104) Skyllas-Kazacos, M.; Robins, R. G., AU575247, **1968**.

(105) Skyllas-Kazacos, M.; *J. Electrochem. Soc.* **1986**, *133*, 1057.

(106) Bradly, C. S., US312802, **1885**.

(107) Lim, H. S.; *J. Electrochem. Soc.* **1977**, *124*, 1154.

(108) Wei, X.; Pan, W.; Duan, W.; Hollas, A.; Yang, Z.; Li, B.; Nie, Z.; Liu, J.; Reed, D.; Wang, W.; Sprenkle, V.; *ACS Energy Lett.* **2017**, *2*, 2187–2204.

(109) Leung, P.; Shah, A. A.; Sanz, L.; Flox, C.; Morante, J. R.; Xu, Q.; Mohamed, M. R.; Ponce de León, C.; Walsh, F. C.; *J. Power Sources* **2017**, *360*, 243–283.

(110) Liu, T.; Wei, X.; Nie, Z.; Sprenkle, V.; Wang, W.; *Adv. Energy Mater.* **2016**, *6*, 1501449.

(111) Li, Z.; Li, S.; Liu, S.; Huang, K.; Fang, D.; Wang, F.; Peng, S.; *Electrochem. Solid-State Lett.* **2011**, *14*, A171.

(112) Park, S.-K.; Shim, J.; Yang, J.; Shin, K.-H.; Jin, C.-S.; Lee, B. S.; Lee, Y.-S.; Jeon, J.-D.; *Electrochem. Commun.* **2015**, *59*, 68–71.

(113) Brushett, F. R.; Jansen, A. N.; Vaughey, J. T.; Su, L.; Milshtein, J. D., US 0236543 A1, **2015**.

(114) Brushett, F. R.; Vaughey, J. T.; Jansen, A. N.; *Adv. Energy Mater.* **2012**, *2*, 1390–1396.

(115) Kaur, A. P.; Holubowitch, N. E.; Ergun, S.; Elliott, C. F.; Odom, S. A.; *Energy Technol.* **2015**, *3*, 476–480.

(116) Chen, W.; Park, S. K.; Yu, W.; Xiong, A.; Sanders, B. G.; Kline, K.; *Eur. J. Med. Chem.* **2012**, *58*, 72–83.

(117) Wei, X.; Duan, W.; Huang, J.; Zhang, L.; Li, B.; Reed, D.; Xu, W.; Sprenkle, V.; Wang, W.; *ACS Energy Lett.* **2016**, *1*, 705–711.

(118) Er, S.; Suh, C.; Marshak, M. P.; Aspuru-Guzik, A.; *Chem. Sci.* **2015**, *6*, 885–893.

(119) Xu, Y.; Wen, Y.; Cheng, J.; Cao, G.; Yang, Y.; *Electrochem. Commun.* **2009**, *11*, 1422–1424.

(120) Xu, Y.; Wen, Y.-H.; Cheng, J.; Cao, G.-P.; Yang, Y.-S.; *Electrochim. Acta* **2010**, *55*, 715–720.

(121) Yang, B.; Hobber-Burkhardt, L.; Wang, F.; Surya Prakash, G. K.; Narayanan, S. R.; *J. Electrochem. Soc.* **2014**, *161*, A1371-A1380.

(122) Hoober-Burkhardt, L.; Krishnamoorthy, S.; Yang, B.; Murali, A.; Nirmalchandar, A.; Prakash, G. K. S.; Narayanan, S. R.; *J. Electrochem. Soc.* **2017**, *164*, A600-A607.

(123) Yang, Z.; Tong, L.; Tabor, D. P.; Beh, E. S.; Goulet, M.-A.; Porcellinis, D. de; Aspuru-Guzik, A.; Gordon, R. G.; Aziz, M. J.; *Adv. Energy Mater.* **2018**, *8*, 1702056.

(124) Murali, A.; Nirmalchandar, A.; Krishnamoorthy, S.; Hoober-Burkhardt, L.; Yang, B.; Soloveichik, G.; Prakash, G. K. S.; Narayanan, S. R.; *J. Electrochem. Soc.* **2018**, *165*, A1193-A1203.

(125) Singh, V.; Kim, S.; Kang, J.; Byon, H. R.; *Nano Res.* **2019**, *12*, 1988–2001.

(126) Lin, K.; Chen, Q.; Gerhardt, M. R.; Tong, L.; Kim, S. B.; Eisenach, L.; Valle, A. W.; Hardee, D.; Gordon, R. G.; Aziz, M. J.; Marshak, M. P.; *Science* **2015**, *349*, 1529–1532.

(127) Huskinson, B.; Marshak, M. P.; Suh, C.; Er, S.; Gerhardt, M. R.; Galvin, C. J.; Chen, X.; Aspuru-Guzik, A.; Gordon, R. G.; Aziz, M. J.; *Nature* **2014**, *505*, 195–198.

(128) Kwabi, D. G.; Lin, K.; Ji, Y.; Kerr, E. F.; Goulet, M.-A.; Porcellinis, D. de; Tabor, D. P.; Pollack, D. A.; Aspuru-Guzik, A.; Gordon, R. G.; Aziz, M. J.; *Joule* **2018**, *2*, 1894–1906.

(129) Goulet, M.-A.; Tong, L.; Pollack, D. A.; Tabor, D. P.; Odom, S. A.; Aspuru-Guzik, A.; Kwan, E. E.; Gordon, R. G.; Aziz, M. J.; *J. Am. Chem. Soc.* **2019**, *141*, 8014–8019.

(130) Bird, C. L.; Kuhn, A. T.; *Chem. Soc. Rev.* **1981**, *10*, 49.

(131) Janoschka, T.; Martin, N.; Martin, U.; Friebe, C.; Morgenstern, S.; Hiller, H.; Hager, M. D.; Schubert, U. S.; *Nature* **2015**, *527*, 78.

(132) Janoschka, T.; Martin, N.; Hager, M. D.; Schubert, U. S.; *Angew. Chem. Int. Ed. Engl.* **2016**, *55*, 14427–14430.

(133) DeBruler, C.; Hu, B.; Moss, J.; Liu, X.; Luo, J.; Sun, Y.; Liu, T. L.; *Chem* **2017**, *3*, 961–978.

(134) Winsberg, J.; Stolze, C.; Schwenke, A.; Muench, S.; Hager, M. D.; Schubert, U. S.; *ACS Energy Lett.* **2017**, *2*, 411–416.

(135) Hu, B.; DeBruler, C.; Rhodes, Z.; Liu, T. L.; *J. Am. Chem. Soc.* **2017**, *139*, 1207–1214.

(136) Beh, E. S.; Porcellinis, D. de; Gracia, R. L.; Xia, K. T.; Gordon, R. G.; Aziz, M. J.; *ACS Energy Lett.* **2017**, *2*, 639–644.

(137) DeBruler, C.; Hu, B.; Moss, J.; Luo, J.; Liu, T. L.; *ACS Energy Lett.* **2018**, *3*, 663–668.

(138) Winsberg, J.; Janoschka, T.; Morgenstern, S.; Hagemann, T.; Muench, S.; Hauffman, G.; Gohy, J.-F.; Hager, M. D.; Schubert, U. S.; *Adv. Mater.* **2016**, *28*, 2238–2243.

(139) Yang, C.; Wang, M.-S.; Cai, L.-Z.; Jiang, X.-M.; Wu, M.-F.; Guo, G.-C.; Huang, J.-S.; *Inorg. Chem. Commun.* **2010**, *13*, 1021–1024.

(140) Hu, B.; Tang, Y.; Luo, J.; Grove, G.; Guo, Y.; Liu, T. L.; *Chem. Commun.* **2018**, *54*, 6871–6874.

(141) Nutting, J. E.; Rafiee, M.; Stahl, S. S.; *Chem. Rev.* **2018**, *118*, 4834–4885.

(142) Orita, A.; Verde, M. G.; Sakai, M.; Meng, Y. S.; *Nat. Commun.* **2016**, *7*, 13230.

(143) Lin, K.; Gómez-Bombarelli, R.; Beh, E. S.; Tong, L.; Chen, Q.; Valle, A.; Aspuru-Guzik, A.; Aziz, M. J.; Gordon, R. G.; *Nat. Energy* **2016**, *1*, 928.

(144) Leung, P.; Aili, D.; Xu, Q.; Rodchanarowan, A.; Shah, A. A.; *Sustain. Energy Fuels* **2018**, *2*, 2252–2259.

(145) Hollas, A.; Wei, X.; Murugesan, V.; Nie, Z.; Li, B.; Reed, D.; Liu, J.; Sprenkle, V.; Wang, W.; *Nat. Energy* **2018**, *3*, 508–514.

(146) Milshtein, J. D.; Su, L.; Liou, C.; Badel, A. F.; Brushett, F. R.; *Electrochim. Acta* **2015**, *180*, 695–704.

(147) Oh, S. H.; Lee, C.-W.; Chun, D. H.; Jeon, J.-D.; Shim, J.; Shin, K. H.; Yang, J. H.; *J. Mater. Chem. A* **2014**, *2*, 19994–19998.

(148) Potash, R. A.; McKone, J. R.; Conte, S.; Abruña, H. D.; *J. Electrochem. Soc.* **2015**, *163*, A338-A344.

(149) Duan, W.; Vemuri, R. S.; Milshtein, J. D.; Laramie, S.; Dmello, R. D.; Huang, J.; Zhang, L.; Hu, D.; Vijayakumar, M.; Wang, W.; Liu, J.; Darling, R. M.; Thompson, L.; Smith, K.; Moore, J. S.; Brushett, F. R.; Wei, X.; *J. Mater. Chem. A* **2016**, *4*, 5448–5456.

(150) Hagemann, T.; Winsberg, J.; Häupler, B.; Janoschka, T.; Gruber, J. J.; Wild, A.; Schubert, U. S.; *NPG Asia Mater.* **2017**, *9*, e340-e340.

(151) Winsberg, J.; Hagemann, T.; Muench, S.; Friebe, C.; Häupler, B.; Janoschka, T.; Morgenstern, S.; Hager, M. D.; Schubert, U. S.; *Chem. Mater.* **2016**, *28*, 3401–3405.

(152) Winsberg, J.; Stolze, C.; Muench, S.; Liedl, F.; Hager, M. D.; Schubert, U. S.; *ACS Energy Lett.* **2016**, *1*, 976–980.

(153) Janoschka, T.; Friebe, C.; Hager, M. D.; Martin, N.; Schubert, U. S.; *ChemistryOpen* **2017**, *6*, 216–220.

(154) Wohl, A.; Aue, W.; *Ber. Dtsch. Chem. Ges.* **1901**, *34*, 2442–2450.

(155) Asgarouladi, B.; Full, R.; Schaper, K.-J.; Siebert, W.; *Ber.* **1974**, *107*, 34–47.

(156) Schulz, H.; Pritzkow, H.; Siebert, W.; *Ber.* **1991**, *124*, 2203–2207.

(157) Müller, P.; Pritzkow, H.; Siebert, W.; *J. Organomet. Chem.* **1996**, *524*, 41–47.

(158) Kaufmann, D.; *Ber.* **1987**, *120*, 901–905.

(159) Schacht, W.; Kaufmann, D.; *J. Organomet. Chem.* **1987**, *331*, 139–152.

(160) Kessler, S. N.; Wegner, H.; Pfaltz, A. Development of a Bidentate Lewis Acid Catalyzed Inverse Electron Demand Diels-Alder Reaction of 1,2-diazines for the Synthesis of Substituted Arenes: Dissertation, University of Basel, Basel, **2013**.

(161) Kessler, S. N.; Wegner, H. A.; *Org. Lett.* **2012**, *14*, 3268–3271.

(162) Fouillaud, M.; Venkatachalam, M.; Girard-Valenciennes, E.; Caro, Y.; Dufossé, L.; *Marine drugs* **2016**, *14*.

(163) Malik, E. M.; Müller, C. E.; *Med. Res. Rev.* **2016**, *36*, 705–748.

(164) Bechtold, T., Ed. *Handbook of Natural Colorants*, Repr; Wiley series in renewable resources; Wiley: Chichester, **2010**.

(165) Krapcho, A. P.; Maresch, M. J.; Helgason, A. L.; Rosner, K. E.; Hacker, M. P.; Spinelli, S.; Menta, E.; Oliva, A.; *J. Heterocycl. Chem.* **1993**, *30*, 1597–1606.

(166) Hassan, A. A.; Mourad, A. F. E.; Zied, A. H. A.; *ARKIVOC* **2007**, 222–235.

(167) Conant, J. B.; Fieser, L. F.; *J. Am. Chem. Soc.* **1924**, *46*, 1858–1881.

(168) Clark, W. M.; *J. Wash. Acad. Sci.* **1920**, *10*, 255–270.

(169) Sullivan, M. X.; Cohen, B.; Clark, W. M.; *Public Health Rep.* **1923**, *38*, 1669.

(170) Fieser, L. F.; *J. Am. Chem. Soc.* **1929**, *51*, 3101–3111.

(171) Fache, M.; Auvergne, R.; Boutevin, B.; Caillol, S.; *Eur. Polym. J.* **2015**, *67*, 527–538.

(172) Hofmann, J. D.; Schmalisch, S.; Schwan, S.; Hong, L.; Wegner, H. A.; Mollenhauer, D.; Janek, J.; Schröder, D.; *Chem. Mater.* **2020**, *32*, 3427–3438.

(173) Paige, M.; Kosturko, G.; Bulut, G.; Miessau, M.; Rahim, S.; Toretsky, J. A.; Brown, M. L.; Üren, A.; *Bioorg. Med. Chem. Lett.* **2014**, *22*, 478–487.

(174) Ryu, C.-K.; Park, R.-E.; Ma, M.-Y.; Nho, J.-H.; *Bioorg. Med. Chem. Lett.* **2007**, *17*, 2577–2580.

(175) Kühlborn, J.; Danner, A.-K.; Frey, H.; Iyer, R.; Arduengo, A. J.; Opatz, T.; *Green Chem.* **2017**, *19*, 3780–3786.

(176) Shaikh, I. A.; Johnson, F.; Grollman, A. P.; *J. Med. Chem.* **1986**, *29*, 1329–1340.

(177) Botteghi, C.; *Gazz. Chim. Ital.* **1975**, 235–245.

(178) Felice, V. de; Renzi, A. de; Fraldi, N.; Panunzi, B.; *Inorg. Chim. Acta* **2009**, *362*, 2015–2019.

(179) Czaplik, W. M.; Schmlaz, H. G.; Bergkessel, A.; Bolm, C. Neue Aspekte Eisen- und Kobalt-katalysierter Kreuzkupplungsreaktionen. Dissertation, University of Cologne, Cologne, **2009**.

(180) Nersasian, A.; *Ind. Eng. Chem. Res.* **1963**, *2*, 138–139.

(181) Schlosser, M.; Schaub, B.; Spahic, B.; Sleiter, G.; *Helv. Chim. Acta* **1973**, *56*, 2166–2170.

(182) Zenk, P. C.; Wiley, R. A.; *Synthesis* **1984**, *1984*, 695–697.

(183) Casavant, B. J.; Khoder, Z. M.; Berhane, I. A.; Chemler, S. R.; *Org. Lett.* **2015**, *17*, 5958–5961.

(184) Finkelstein, H.; *Ber. Dtsch. Chem. Ges.* **1910**, *43*, 1528–1532.

(185) Posner, G. H.; Loomis, G. L.; *J. Chem. Soc., Chem. Commun.* **1972**, 892–893.

(186) Santra, S.; Kaittanis, C.; Perez, J. M.; *Langmuir* **2010**, *26*, 5364–5373.

(187) Wilent, J.; Petersen, K. S.; *J. Org. Chem.* **2014**, *79*, 2303–2307.

(188) Anzini, M.; Di Capua, A.; Valenti, S.; Brogi, S.; Rovini, M.; Giuliani, G.; Cappelli, A.; Vomero, S.; Chiasserini, L.; Sega, A.; Poce, G.; Giorgi, G.; Calderone, V.; Martelli, A.; Testai, L.; Sautebin, L.; Rossi,

A.; Pace, S.; Ghelardini, C.; Di Cesare Mannelli, L.; Benetti, V.; Giordani, A.; Anzellotti, P.; Dovizio, M.; Patrignani, P.; Biava, M.; *J. Med. Chem.* **2013**, *56*, 4821.

(189) Zięba, G.; Rojkiewicz, M.; Kozik, V.; Jarzembek, K.; Jarczyk, A.; Sochanik, A.; Kuś, P.; *Monatsh. Chem.* **2012**, *143*, 153–159.

(190) Krapcho, A. P.; Weimaster, J. F.; Eldridge, J. M.; Jahngen, E. G. E.; Lovey, A. J.; Stephens, W. P.; *J. Org. Chem.* **1978**, *43*, 138–147.

(191) Brun, K. A.; Heimgartner, H.; *Helv. Chim. Acta* **2005**, *88*, 2951–2959.

(192) Verkruijsse, H. D.; Brandsma, L.; R. Schleyer, P. von; *J. Organomet. Chem.* **1987**, *332*, 99–103.

(193) Khuong, K. S.; Jones, W. H.; Pryor, W. A.; Houk, K. N.; *J. Am. Chem. Soc.* **2005**, *127*, 1265–1277.

(194) Schildknecht, C. E.; Zoss, A. O.; McKinley, C.; *Ind. Eng. Chem.* **1947**, *39*, 180–186.

(195) Imoto, M.; Kinoshita, M.; Nishigaki, M.; *Makromol. Chem.* **1965**, *86*, 217–230.

(196) Qiu, J.; Matyjaszewski, K.; *Macromolecules* **1997**, *30*, 5643–5648.

(197) Hong, L.; Ahles, S.; Heindl, A. H.; Tiétcha, G.; Petrov, A.; Lu, Z.; Logemann, C.; Wegner, H. A.; *Beilstein J. Org. Chem.* **2018**, *14*, 618–625.

(198) Engberts, J. B. F. N.; Feringa, B. L.; Keller, E.; Otto, S.; *Recl. Trav. Chim. Pays-Bas* **1996**, *115*, 457–464.

(199) Hofmann, J. D.; Pfanschilling, F. L.; Krawczyk, N.; Geigle, P.; Hong, L.; Schmalisch, S.; Wegner, H. A.; Mollenhauer, D.; Janek, J.; Schröder, D.; *Chem. Mater.* **2018**, *30*, 762–774.

(200) Chen, P.-K.; Rosana, M. R.; Dudley, G. B.; Stiegman, A. E.; *J. Org. Chem.* **2014**, *79*, 7425–7436.

(201) Le Chatelier, H. L.; *C. R. Acad. Sci. Paris* **1884**, 786–789.

(202) Treptow, R. S.; *J. Chem. Educ.* **1980**, *57*, 417.

(203) Braun, F.; *Z. Phys. Chem.* **1887**, *1*, 259–272.

(204) Yakura, T.; Ozono, A.; Morimoto, K.; *Chem. Pharm. Bull.* **2011**, *59*, 132–134.

(205) Elbs, K.; Lerch, H.; *J. Prakt. Chem.* **1916**, *93*, 1–9.

(206) Hofmann, J. D.; et al. *Unpublished results*.

(207) Fuson, R. C.; Tomboulian, P.; *J. Am. Chem. Soc.* **1957**, *79*, 956–960.

(208) Harvey, B. G.; Guenthner, A. J.; Meylemans, H. A.; Haines, S. R. L.; Lamison, K. R.; Groshens, T. J.; Cambrea, L. R.; Davis, M. C.; Lai, W. W.; *Green Chem.* **2015**, *17*, 1249–1258.

(209) Mallory, F. B.; Wood, C. S.; Gordon, J. T.; *J. Am. Chem. Soc.* **1964**, *86*, 3094–3102.

(210) Fang, X.; Zhang, Y.-M.; Chang, K.; Liu, Z.; Su, X.; Chen, H.; Zhang, S. X.-A.; Liu, Y.; Wu, C.; *Chem. Mater.* **2016**, *28*, 6628–6636.

(211) Miyashita, A.; Suzuki, Y.; Iwamoto, K.; Higashino, T.; *Chem. Pharm. Bull.* **1994**, *42*, 2633–2635.

(212) Zinin, N.; *Ann. Pharm.* **1839**, *31*, 329–332.

(213) Soni, N.; Soni, N.; Gupta, P.; *Der Pharma Chem.* **216**, *8*, 77–82.

(214) Rubbiani, R.; Kitanovic, I.; Alborzinia, H.; Can, S.; Kitanovic, A.; Onambele, L. A.; Stefanopoulou, M.; Geldmacher, Y.; Sheldrick, W. S.; Wolber, G.; Prokop, A.; Wölfl, S.; Ott, I.; *J. Med. Chem.* **2010**, *53*, 8608–8618.

(215) Shimakawa, Y.; Morikawa, T.; Sakaguchi, S.; *Tetrahedron Lett.* **2010**, *51*, 1786–1789.

(216) Trosien, S.; Waldvogel, S. R.; *Org. Lett.* **2012**, *14*, 2976–2979.

(217) Itami, K.; Yoshida, J.-I.; *Chem. Rec.* **2002**, *2*, 213–224.

(218) Risse, W.; Sogah, D. Y.; *Macromolecules* **1990**, *23*, 4029–4033.

(219) Kramer, B.; Fröhlich, R.; Bergander, K.; Waldvogel, S. R.; *Synthesis* **2003**, *1*, 91–96.

(220) Mulzer, J. *Synthetic efforts towards a synthesis of the tetracyclic core of (-)-lemonomycin: Diploma Thesis*; Wien, **2009**.

(221) Yeom, C.-E.; Kim, H.; Lee, S.; Kim, B.; *Synlett* **2007**, *2007*, 146–150.

(222) Enders, D.; Niemeier, O.; *Synlett* **2004**, *2004*, 2111–2114.

(223) Domasevitch, K. V.; Gural'skiy, I. A.; Solntsev, P. V.; Rusanov, E. B.; Krautscheid, H.; Howard, J. A. K.; Chernega, A. N.; *Dalton Trans.* **2007**, 3140–3148.

(224) Ren, J.; Lu, L.; Xu, J.; Yu, T.; Zeng, B.-B.; *Synthesis* **2015**, *47*, 2270–2280.

(225) Paull, K. D.; Zee-Cheng, R. K.; Cheng, C. C.; *J. Med. Chem.* **1976**, *19*, 337–339.

(226) Kotnik, M.; Oblak, M.; Anderluh, P. S.; Prezelj, A.; Humiljan, J.; Plantan, I.; Uros, U.; Solmajer, T., US0247516A1, **2009**.

(227) Kündig, E. P.; Enríquez García, A.; Lomberget, T.; Bernardinelli, G.; *Angew. Chem. Int. Ed.* **2005**, *45*, 98–101.

(228) Banerjee, A. K.; Bedoya, L.; Vera, W. J.; Melean, C.; Mora, H.; Laya, M. S.; Alonso, M.; *Synth. Commun.* **2004**, *34*, 3399–3408.

(229) Wegner, H. A.; Janek, J.; Schröder, D.; Hong, L.; Hofmann, J. D.; Schmalisch, S., EP3691011A1, **2019**.

(230) Armitage, B.; Yu, C.; Devadoss, C.; Schuster, G. B.; *J. Am. Chem. Soc.* **1994**, *116*, 9847–9859.

(231) Pezzella, A.; Crescenzi, O.; Panzella, L.; Napolitano, A.; Land, E. J.; Barone, V.; d'Ischia, M.; *J. Am. Chem. Soc.* **2013**, *135*, 12142–12149.

(232) Song, Y.; Buettner, G. R.; *Free Radical Biol. Med.* **2010**, *49*, 919–962.

(233) Xinyuan Fan; Yun Ge; Feng Lin; Yi Yang; Gong Zhang; William Shu Ching Ngai; Zhi Lin; Siqi Zheng; Jie Wang; Jingyi Zhao; Jie Li; Peng R. Chen; *Angew. Chem. Int. Ed.* **2016**, *55*, 14046–14050.

(234) Ott, R.; Pinter, E.; *Monatsh. Chem.* **1997**, *128*, 901–909.

(235) Essers, M.; Haufe, G.; *J. Chem. Soc., Perkin Trans. 1* **2002**, 2719–2728.

(236) Mollenhauer, D.; et al. *Unpublished Results*.

(237) Castillo, N.; Boyd, R. J.; *J. Chem. Theory Comput.* **2006**, *2*, 271–280.

(238) Essers, M.; Mück-Lichtenfeld, C.; Haufe, G.; *J. Org. Chem.* **2002**, *67*, 4715–4721.

(239) Olthoff, J. K.; Tossell, J. A.; Moore, J. H.; *J. Chem. Phys.* **1985**, *83*, 5627–5634.

(240) Shorter, J.; *Chemie Unserer Zeit* **1985**, *19*, 197–208.

(241) Aslam, M. H.; Chapman, N. B.; Shorter, J.; Charton, M.; *J. Chem. Soc., Perkin Trans. 2* **1981**, 720.

(242) Minisci, F.; Citterio, A.; Vismara, E.; Fontana, F.; Bernardinis, S. de; Correale, M.; *J. Org. Chem.* **1989**, *54*, 728–731.

(243) Sam, D. J.; Simmons, H. E.; *J. Am. Chem. Soc.* **1972**, *94*, 4024–4025.

(244) Erdtman, H.; Högberg, H.-E.; *Tetrahedron* **1979**, *35*, 535–540.

(245) Andronova, N. A.; Smirnov, L. D.; Lezina, V. P.; Dyumaev, K. M.; *Bull. Acad. Sci. USSR, Div. Chem. Sci.* **1972**, *21*, 404–405.

(246) Fini, F.; Nagabelli, M.; Adamo, M. F. A.; *Adv. Synth. Catal.* **2010**, *352*, 3163–3168.

(247) Konieczny, M. T.; Horowska, B.; Kunikowski, A.; Konopa, J.; Wierzba, K.; Yamada, Y.; Asao, T.; *Synthesis* **2001**, *2001*, 1363–1367.

(248) Rathore, R.; Bosch, E.; Kochi, J. K.; *Tetrahedron Lett.* **1994**, *35*, 1335–1338.

(249) Yadav, J. S.; Swamy, T.; Reddy, B. S.; Rao, D. K.; *J. Mol. Catal. A: Chem.* **2007**, *274*, 116–119.

(250) Jereb, M.; *Green Chem.* **2012**, *14*, 3047–3052.

(251) Stevenson, P. J.; *Org. Biomol. Chem.* **2011**, *9*, 2078–2084.

(252) Yu, B.; Liu, A.-H.; He, L.-N.; Li, B.; Diao, Z.-F.; Li, Y.-N.; *Green Chem.* **2012**, *14*, 957.

(253) Sojo, L. E.; Chahal, N.; Keller, B. O.; *Rapid Commun. Mass Spectrom.* **2014**, *28*, 2181–2190.

(254) Vessecchi, R.; Naal, Z.; Lopes, J. N. C.; Galembeck, S. E.; Lopes, N. P.; *J. Phys. Chem. A* **2011**, *115*, 5453–5460.

(255) S. R. Prakash; R. L. Ellsworth; H. E. Mertel; *J. Labelled Compd. Radiopharm.* **1987**, *24*, 97–105.

(256) Attanayake, N. H.; Kowalski, J. A.; Greco, K. V.; Casselman, M. D.; Milshtein, J. D.; Chapman, S. J.; Parkin, S. R.; Brushett, F. R.; Odom, S. A.; *Chem. Mater.* **2019**, *31*, 4353–4363.

(257) Bettinger, H. F.; Filthaus, M.; *J. Org. Chem.* **2007**, *72*, 9750–9752.

(258) Spectral Database for Organic Compounds SDBS. 2,3-dichlorotetrahydrofuran. https://sdbs.db.aist.go.jp/sdbs/cgi-bin/landingpage?sdbsno=5314 (accessed April 22, 2021).

(259) Baumann, M.; Togni, A.; Pregosin, P. S. Asymmetrische Heck-Reaktion mit chiralen P,N-Ferrocenyl-Liganden, ETH Zurich, **2000**.

(260) Temme, O.; Taj, S.-A.; Andersson, P. G.; *J. Org. Chem.* **1998**, *63*, 6007–6015.

(261) Spectral Database of Organic Compounds SDBS. NMR 1-Iodohexane. https://sdbs.db.aist.go.jp/sdbs/cgi-bin/landingpage?sdbsno=10281 (accessed April 19, 2021).

(262) Ziyanak, F.; Kuş, M.; Artok, L.; *Adv. Synth. Catal.* **2011**, *353*, 897–902.

(263) Ishida, A.; Yamashita, S.; Takamuku, S.; *Bull. Chem. Soc. Jpn.* **1988**, *61*, 2229–2231.

(264) Inaba, T.; Sakamoto, M.; Jujita, T.; Watanabe, S.; *Int. J. Mater. Prod. Technol.* **1989**, *4*, 151–158.

(265) Caretto, A.; Noè, M.; Selva, M.; Perosa, A.; *ACS Sustain. Chem. Eng.* **2014**, *2*, 2131–2141.

(266) Borrajo-Calleja, G. M.; Bizet, V.; Mazet, C.; *J. Am. Chem. Soc.* **2016**, *138*, 4014–4017.

(267) Götz, S. Investigation on Domino-Type Lewis Acid Catalyzed Inverse Electron-Demand Diels-Alder Reactions of Phthalazines. Master Thesis, University of Basel, Basel, **2013**.

(268) Liu, L.-P.; Hammond, G. B.; *Org. Lett.* **2010**, *12*, 4640–4643.

(269) Talipov, M. R.; Navale, T. S.; Hossain, M. M.; Shukla, R.; Ivanov, M. V.; Rathore, R.; *Angew. Chem. Int. Ed. Engl.* **2017**, *56*, 266–269.

(270) Barrett, T. N.; Braddock, D. C.; Monta, A.; Webb, M. R.; White, A. J. P.; *J. Nat. Prod.* **2011**, *74*, 1980–1984.

(271) Mouterde, L. M. M.; Flourat, A. L.; Cannet, M. M. M.; Ducrot, P.-H.; Allais, F.; *Eur. J. Org. Chem.* **2013**, *2013*, 173–179.

(272) Savonnet, E.; Defoort, b.; Cramail, H.; Grélier, S.; Grau, E., WO2019092359A1, **2017**.

(273) Mohr, B.; Enkelmann, V.; Wegner, G.; *J. Org. Chem.* **1994**, *59*, 635–638.

(274) Viault, G.; Grée, D.; Das, S.; Yadav, J. S.; Grée, R.; *Eur. J. Org. Chem.* **2011**, *2011*, 1233–1241.

(275) Seka, R.; Kallir, P.; *Ber. dtsch. Chem. Ges. A/B* **1931**, *64*, 622–627.

(276) Teuber, H.-J.; Jellinek, G.; *Chem. Ber.* **1952**, *85*, 95–103.

(277) Pratt, D. V.; Ruan, F.; Hopkins, P. B.; *J. Org. Chem.* **1987**, *52*, 5053–5055.

(278) Ali, M. H.; Welker, A.; York, C.; *Synthesis* **2015**, *47*, 3207–3211.

8. Appendix and Acknowledgement

8.1 Abbreviations

Ac	acetyl	DBMMB	2,5-di-*tert*-butyl-1-methoxy-4-(2-methoxyethoxy)-benzene
ACA	7,8-carboxy alloxazine	DCE	dichloroethane
AORFB	aqueous organic redox flow battery	DCM	dichloromethane
AQDS	anthraquinone-2,7-disulfonic acid	DFT	density functional theory
AQS	anthraquinone-2-sulfonic acid	DHAQ	2,6-dihydroxyanthraquinone
BCF3EPT	3,7-*bis*(trifluoromethyl)-*N*-ethylphenazine	DHP	dihydroxyphthalazine
BQ	benzoquinone	DIBAL-H	di*iso*butylaluminium hydride
BQDS	*ortho*-quinone-4,5-dihydroxybenzene-1,3-disulfonic acid	DMF	*N,N*-dimethylformamide
BTMAP	1,1-b*is*-((trimethylammonio)propyl)-	DNQ	diazanaphthoquinone
DAD	diazaanthraquinone	EA	elemental analysis
DBBB	2,5-di-*tert*-butyl-1,4-bis(4-methoxyethoxy)	EDG	electron donating group
DBEAQ	4,4'-((9,10-anthraquinone-2,6-diyl)-dioxy)dibutyrate	EI	electron impact
		equiv	equivalents

ESI	electro spray ionisation	MO	molecular orbital
Et$_2$O	diethylether	MP	melting point
EtOAc	ethyl acetate	MePhth	*N*-methylphthalimide
EtOH	Ethanol	MS	mass spectrometry
EWG	electron withdrawing group	m/z	Mass to charge ratio
FL	9-flourenone	*n*BuLi	*N*-butyllithium
FMN	flavin mononucleotide	NHE	normal hydrogen electrode
FMO	frontier molecular orbital	NMR	nuclear magnetic resonance
GBL	*γ*-butyrolactone	PC	propylene carbonate
HOMO	highest occupied molecular orbital	PG	protecting group
HRFB	hybrid redox flow battery	PPTS	pyridinium *p*-toluenesulfonate
IEDDA	Inverse electron-demand Diels-Alder reaction	PTIO	2-phenyl-4,4,5,5-tetramethyl-imidazolin-1-oxyl-3-oxide
LDA	Lithium di*iso*propylamide	*p*TsOH	*para*-toluenesulfonic acid
LUMO	lowest occupied molecular orbital	RFB	redox flow battery
MAD	mean absolute deviation	SHE	standard hydrogen electrode
MeCN	Acetonitrile	TBAB	tetrabutylammonium bromide
MeOH	Methanol	*t*BuLi	*tert*-butyllithium

TEA	Triethylamine	THF	Tetrahydrofuran
TEATFSI	tetraethylammonium bis-(Trifluormethanesulfonyl)imide	THP	Tetrahydropyranyl
TEG	triethylene glycol	TIPS	Tri*iso*propyl
TEMPO	(2,2,6,6-Tetramethylpiperidin-1-yl)-oxyl	TLC	thin layer chromatography
TEMPOL	(4-Hydroxy-2,2,6,6-tetramethylpiperidin-1-yl)-oxyl	TMeQ	2,3,6-trimethylquinoxaline
TEMPTMA	(4-(trimethylammonio)-2,2,6,6-tetramethylpiperidin-1-yl)-oxyl	TMS	Trimethylsilane
TFSI	*bis*-(trifluormethanesulfonyl)-imide	VIOTEMP	1-(4-(((1-oxyl-2,2,6,6-tetramethylpiperidin-4-yl)oxy)carbonyl)benzyl)-1′-methyl-[4,4′-bipyridine]-1,1′-diium-chloride

8.2 Publication list

Parts of this work have been previously published:

Hofmann, J. D.; Pfanschilling, F. L.; Krawczyk, N.; Geigle, P.; Hong, L.; Schmalisch, S.; Wegner, H. A.; Mollenhauer, D.; Janek, J.; Schröder, D.; *Chem. Mater.* **2018**, *30*, 762–774.

Wegner, H. A.; Janek, J.; Schröder, D.; Hong, L.; Hofmann, J. D.; Schmalisch, S., EP3691011A1, **2019**.

Hofmann, J. D.; Schmalisch, S.; Schwan, S.; Hong, L.; Wegner, H. A.; Mollenhauer, D.; Janek, J.; Schröder, D.; *Chem. Mater.* **2020**, *32*, 3427–3438.

Acknowledgement